



**HAL**  
open science

# Distribution et partitionnement de la biodiversité hydrothermale dans un système discontinu de dorsales : le cas des bassins arrière-arc de l'ouest Pacifique

Camille Poitrimol

► **To cite this version:**

Camille Poitrimol. Distribution et partitionnement de la biodiversité hydrothermale dans un système discontinu de dorsales : le cas des bassins arrière-arc de l'ouest Pacifique. Biodiversité. Sorbonne Université, 2022. Français. NNT : 2022SORUS314 . tel-03900421

**HAL Id: tel-03900421**

**<https://theses.hal.science/tel-03900421>**

Submitted on 15 Dec 2022

**HAL** is a multi-disciplinary open access archive for the deposit and dissemination of scientific research documents, whether they are published or not. The documents may come from teaching and research institutions in France or abroad, or from public or private research centers.

L'archive ouverte pluridisciplinaire **HAL**, est destinée au dépôt et à la diffusion de documents scientifiques de niveau recherche, publiés ou non, émanant des établissements d'enseignement et de recherche français ou étrangers, des laboratoires publics ou privés.



**SORBONNE  
UNIVERSITÉ**



CNRS • SORBONNE UNIVERSITÉ  
**Station Biologique  
de Roscoff**



**Ifremer**



## **Thèse de doctorat Sorbonne Université**

*Ecole doctorale 227 : Science de la nature et des l'Homme : Ecologie et Evolution*

présentée pour obtenir le titre de  
DOCTEUR DE SORBONNE UNIVERSITÉ

Spécialité : ÉCOLOGIE MARINE

# **Distribution et partitionnement de la biodiversité hydrothermale dans un système discontinu de dorsales : le cas des bassins arrière-arc de l'ouest Pacifique**

---

**Camille Poitrimol**

*CNRS - SU, Station Biologique de Roscoff, UMR7144 - Centre Ifremer de Brest, UMR6197*

Soutenue le 23 septembre 2022 devant le jury composé de :

Ana COLAÇO	Investigadora Principal, Universidade dos Açores	Rapporteure
Mathieu CUSSON	Professeur, Université du Québec à Chicoutimi	Rapporteur
Nicolas DESROY	Cadre de recherche, Ifremer Dinard	Examinateur
Didier JOLLIVET	Directeur de recherche, CNRS	Examinateur
Florence PRADILLON	Cadre de recherche, Ifremer Brest	Invitée
Eric THIÉBAUT	Professeur, Sorbonne Université	Directeur
Marjolaine MATABOS	Cadre de recherche, Ifremer Brest	Directrice



## Remerciements

Nous y voilà, il était grand temps d'écrire mes remerciements ! Ce travail de thèse n'aurait jamais été tel qu'il est sans les échanges, collaborations, l'aide et le soutien de nombreuses personnes que je tiens à remercier ici.

Pour commencer, un énorme merci à mes deux directeurs de thèse Éric Thiébaud et Marjolaine Matabos. Merci à vous deux de m'avoir fait confiance pour ce projet et permis de découvrir toute cette belle faune hydrothermale ! Merci pour votre bienveillance, pédagogie et soutien tout au long de ma thèse, malgré la distance et les différentes périodes de confinements. Vous avez vraiment été super, merci beaucoup !

Je remercie également les membres de mon jury, mes rapporteurs Ana Colaço et Mathieu Cusson et tous les examinateurs, Nicolas Desroy, Didier Jollivet et Florence Pradillon pour avoir accepté de lire et évaluer mon manuscrit. Merci à tous d'être venus à Roscoff m'écouter et pour vos retours. Merci aux membres de mon comité de thèse, Olivier Gauthier, Stéphane Hourdez et Frédéric Partensky pour votre temps, discussions et conseils lors des différents comités.

Un très grand merci également à Didier et Stéphane d'avoir porté le projet Cerberus et la mission Chubacarc. Grâce à vous j'ai pu vivre une expérience formidable que je n'oublierai pas : la mission d'échantillonnage dans le Pacifique. Nos échanges m'ont beaucoup servi durant la thèse. Merci pour vos conseils et votre aide précieuse sur les analyses de la partie génétique. Merci Stéphane pour ton accueil à l'observatoire de Banyuls et ton aide énorme pour l'identification des polychètes.

Évidemment la campagne Chubacarc n'aurait pas été un succès sans tous les membres des deux legs. Un grand merci aux capitaines de l'*Atalante* et leurs équipages, aux pilotes et responsables du ROV et à toute l'équipe scientifique qui ont tous fait un travail formidable. Je tiens particulièrement à remercier tous ceux qui nous ont aidé, Marjo, Éric et moi au tri de la faune à bord, notamment Thierry Comtet, Thomas Broquet, Stéphane l'Haridon, Loïc Michel et Stéphane qui y ont passé beaucoup de temps, mais aussi tous les autres, que ce soit de l'équipe scientifique ou ROV, qui sont venus nous apporter leur aide, sur des périodes plus ou moins longues certes (la patience étant nécessaire pour le tri ahah), mais qui m'ont permis de gagner un temps précieux pour la suite, merci ! Merci également à Sophie Arnaud-Haond, François Bonhomme et Pierre-Alexandre Gagnaire pour votre travail d'extraction d'ADN sur les *L. schrolli* et *S. tollmanni*. Et merci beaucoup aux chimistes, Cécile Cathalot, Nicolas Gayet, Olivier Rouxel et Cédric Boulart pour votre travail et toutes les mesures qui accompagnent nos échantillons de communautés. Et mention spéciale aux autres étudiants en thèse de la mission avec qui j'ai passé de beaux moments, Jade, Victor et Adrien !

Bien sûr il y a toutes celles et ceux qui ont fourni un travail important au laboratoire. Les stagiaires de master, Alicia Veillot, Annah Ramière et Mathilde Le Pans, alternante au LEP, qui ont travaillé avec moi et qui ont toutes les trois généré beaucoup beaucoup de données pour le chapitre 2. Merci beaucoup à vous trois, c'était un plaisir de travailler avec vous. J'en profite d'ailleurs pour remercier Christine Dubreuil et Virgile Quillien de nous avoir formées aux techniques d'histologie et permis d'utiliser votre matériel. Merci encore une fois à Mathilde mais aussi à Ève-Julie Pernet pour l'aide sur le tri aux centob. Merci beaucoup Ève pour tout

ton travail sur les refus d'*Alviniconcha* et tous les copépodes que tu as triés et comptés !! Merci aussi à tous ceux qui m'ont aidé à un moment ou un autre pour l'identification de la faune, évidemment Stéphane, mais aussi Céline Houbin et Caroline Broudin à Roscoff. Merci aussi à Jade Castel, Valérie Cueff-Gauchard et Ambre Chabert d'avoir partagé vos données de barcode. Merci à tous ceux qui m'ont formé et aidé pour les techniques de biologie moléculaire, Guillaume Lannuzel et Sandra Fuchs au LEP puis Anne-Sophie Le Port, Marion Ballenghien et Claire Daguin-Thiébaud à DYDIV. Merci encore Claire pour toute ton aide, expertise et travail pour la partie barcode. Enfin, merci à Ewan Pelleter et surtout Anne-Sophie Alix pour votre aide avec les cartes.

Je tiens également à remercier Pierre-Marie Sarradin et Fabrice Not pour votre accueil au sein des unités BEEP à Ifremer et AD2M à la station biologique de Roscoff, et tous les membres des équipes du LEP, d'EDYCO et des services administratifs et d'accueil. Merci à tous ceux d'Ifremer ou de la station avec qui j'ai pu échanger et partager des moments autour d'un repas, café ou d'une bière. Merci à Florian, Lydia, Robin et à la « Éric dream team » : Sylvie, Nicolas, Laurie-Anne et Maéva qui ont partagé mon bureau à Roscoff. Un grand merci à Sylvie et Annabelle pour votre soutien et aide apportée ces derniers mois.

Merci à tous les copains de Brest et Roscoff, avec qui j'ai passé de superbes moments surf/paddle/yoga/course/baignade/soirées qui m'ont permis de décompresser, Mel, Julien, Mathilde, Alicia, Loïc, Adriana, Joan, Fanny, Élodie, Malo et toute la bande des Roscovites Aurélie, Lisa, Mathilde, Yasmine, Louison, Jana, Sam, Jeremy, Lucie, Erwan, Guillaume, Bertille, Damien, Sylvie et Seb, Aurélien, Roman, Charlotte, Emma, Aline et bien d'autres... Merci aussi aux copains qui me suivent depuis plus longtemps. Les "gros potes" de La Rochelle, Momo et Axou, les copains de fac retrouvés à Dinard/Vannes/La Rochelle et toute la bande des LST pour ces superbes vacances et weekends. Petite dédicace à Félix et Mel toujours partants pour des répétitions tardives et à Léo pour ton énorme soutien dans les grosses périodes de stress. Merci infiniment !

Pour finir, j'embrasse très fort ma famille, mes parents et mes deux sœurs, Aurore et Magali. Merci d'être toujours là pour moi, de me soutenir depuis toujours et dans tous mes projets ! Et puis évidemment Ben, en première ligne pour recevoir tout mon stress ... Merci de de nous avoir supportées, ma charge émotionnelle et moi, surtout cette année, et de toujours savoir me redonner le sourire. Merci du fond du cœur.

Et puis, à tous ceux qui auront lu ces pages et à ceux qui liront celles qui suivent, merci beaucoup !





---

## Table des matières

---

<b>Introduction</b>	<b>1</b>
L'étude de la biodiversité . . . . .	1
Environnement profonds et sources hydrothermales . . . . .	8
Organisation spatiale de la biodiversité hydrothermale . . . . .	17
Objectifs de la thèse . . . . .	27
<b>1 Phylogéographie comparée de gastéropodes hydrothermaux</b>	<b>29</b>
1.1 Introduction . . . . .	30
1.2 Materials and Methods . . . . .	33
1.2.1 Ethics statement . . . . .	33
1.2.2 Sampling . . . . .	40
1.2.3 Molecular methods . . . . .	40
1.2.4 Phylogenetic analysis . . . . .	44
1.3 Results . . . . .	45
1.3.1 Lepetodrilidae . . . . .	48
1.3.2 Neomphalidae . . . . .	52
1.3.3 Phenacolepadidae . . . . .	54
1.3.4 Provannidae . . . . .	57
1.4 Discussion . . . . .	60
<b>2 Biologie de la reproduction de gastéropodes hydrothermaux</b>	<b>69</b>
2.1 Introduction . . . . .	70
2.2 Materials and Methods . . . . .	73



2.2.1	Sampling . . . . .	73
2.2.2	Population structure . . . . .	74
2.2.3	Sex ratio and reproductive biology . . . . .	78
2.3	Results . . . . .	82
2.3.1	Environmental conditions . . . . .	82
2.3.2	<i>Lepetodrilus schrolli</i> . . . . .	82
2.3.3	<i>Shinkailepas tollmanni</i> . . . . .	90
2.4	Discussion . . . . .	93
2.4.1	Recruitment patterns . . . . .	93
2.4.2	Reproductive biology . . . . .	95
<b>3</b>	<b>Structure des communautés hydrothermales et biogéographie</b>	<b>101</b>
3.1	Introduction . . . . .	102
3.2	Materials and Methods . . . . .	106
3.2.1	Study area and data collection . . . . .	106
3.2.2	Diversity analysis . . . . .	112
3.2.3	Link with the environment . . . . .	114
3.3	Results . . . . .	116
3.3.1	Diversity analysis . . . . .	117
3.3.2	Environmental and spatial drivers of faunal composition . . . . .	133
3.4	Discussion . . . . .	141
3.4.1	Regional scale diversity and taxonomic issues . . . . .	143
3.4.2	Community structure through habitat type . . . . .	144
3.4.3	Biogeography . . . . .	150
	<b>Discussion générale et perspectives</b>	<b>153</b>
<b>A</b>	<b>Annexes du chapitre 1</b>	<b>189</b>
A.1	<i>Cox1</i> Maximum Likelihood trees inferred from <i>Cox1</i> sequences from <i>Lepetodrilus</i> (A), <i>Symmetromphalus</i> and <i>Lamellomphalus</i> (B), <i>Shinkailepas</i> (C) and <i>Desbruyeresia</i> and <i>Provanna</i> (D) within their genus or family . . . . .	189
<b>B</b>	<b>Annexes du chapitre 2</b>	<b>195</b>
B.1	Illustrations of <i>Lepetodrilus schrolli</i> and <i>Shinkailepas tollmanni</i> and the different shell measurements . . . . .	195
B.2	Size-frequency histograms of <i>Lepetodrilus schrolli</i> . . . . .	195
B.3	Oocytes size-frequency histograms of <i>Lepetodrilus schrolli</i> . . . . .	195
B.4	Size-frequency histograms of <i>Shinkailepas tollmanni</i> . . . . .	195

*TABLE DES MATIÈRES*

<b>C Annexes du chapitre 3</b>	<b>201</b>
C.1 PCA based on scaled physico-chemical datas (without Methane) . . . . .	201
C.2 dbRDA and variance partitioning . . . . .	201
<b>D Annexes générales</b>	<b>205</b>
D.1 Description du champ hydrothermal La Scala . . . . .	205
D.2 Cartes des champs échantillonnées . . . . .	231
D.3 Photos des habitats échantillonnées . . . . .	234
D.4 Numéros de plongée, de boîte et d'aspirateur pour chaque échantillon . . . . .	245



---

## Table des figures

---

1	Schéma illustrant les différentes composantes des coefficients de dissimilarité de Jaccard et Sorensen (i.e. a, b et c) et comment ces composantes sont utilisées pour estimer la similarité (carrés gris) et la dissimilarité et ses deux composantes, le remplacement d'espèces (carrés rouges mouchetés) et la différence de richesse (carrés bleu rayés) entre deux échantillons. D'après Podani et Schmera (2011) et Legendre (2014) . . . . .	6
2	Diagramme ternaire (ou SDR-simplex) : concept (a) et mesures des différentes composantes (b) proposé par Podani et Schmera (2011). . . . .	7
3	Carte mondiale répertoriant les sources hydrothermales connues (en rouge), inférées (en jaune) et supposées (en bleu). Tiré de Beaulieu et Szafranski (2020) . .	9
4	Schéma illustrant différents contextes géologiques dans lesquels on observe des sources hydrothermales. Tiré de Le Bris <i>et al.</i> (2019). . . . .	9
5	Carte présentant les différentes vitesses d'expansion des dorsales classées en cinq catégories : Dorsales très lentes (bleu foncé; < 20 mm.an <sup>-1</sup> ), lentes (bleu; 20-50 mm.an <sup>-1</sup> ), intermédiaires (vert; 50-80 mm.an <sup>-1</sup> ), rapides (orange; 80-140 mm.an <sup>-1</sup> ) et très rapides (rouge; > 140 mm.an <sup>-1</sup> ). Tiré de Dick (2019). . . . .	10
6	Schéma simplifié de la circulation hydrothermale et des différents fluides qu'il en résulte. Tiré de Koschinsky (2014). . . . .	11
7	Schéma de la formation d'un bassin arrière-arc. Extrait du site web <a href="https://www.geologynorth.uk/ballantrae-ophiolite-complex/">https://www.geologynorth.uk/ballantrae-ophiolite-complex/</a> . . . . .	13
8	Carte mondiale des bassins arrière-arc (BAB). Tirée de Guinot et Segonzac (2018).	13

9	Carte des bassins arrière-arc du Pacifique Sud-Ouest. BM : Bassin de Manus; NB : Nouvelle Bretagne, FNB : Fosse de la Nouvelle Bretagne. Vanuatu (ex-Nouvelles Hébrides). Adaptée de Ruellan et Lagabrielle (2005). . . . .	14
10	Exemples de la mégafaune symbiotique dominant les sources hydrothermales selon la province biogéographique . . . . .	19
11	Illustrations de la mégafaune des bassins arrière-arc (A) : les agrégations de gastéropodes <i>Alviniconcha</i> (B) et <i>Ifremeria</i> (C), et moulières à <i>Bathymodiolus</i> (D). . . . .	20
12	Distribution globale des 11 provinces biogéographiques identifiées à ce jour. Tiré de Thaler et Amon (2019). . . . .	21
13	Schéma simplifié de la structuration spatiale de différents habitats le long du gradient de dilution du fluide hydrothermal sur l'horizontal (A) et la verticale (B). Tiré de Marsh <i>et al.</i> (2012). . . . .	23
14	Illustration de l'exploitation de sulfures polymétalliques issus de l'activité hydrothermale d'un site inactif. ©Capsule graphik . . . . .	26
1.1	Illustrations of a <i>Lepetodrilus shcrolli</i> individual concerned in ethanol. White scalebar : 1 mm. . . . .	33
1.2	Illustrations of <i>Symmetromphalus</i> individuals from Woodlark (A), Manus (B-C) and Lau Basins (D). A and C are concerned in ethanol, B and D were pictured alive. White scalebar : 1 mm. . . . .	34
1.3	Illustrations of <i>Lamellomphalus</i> individuals from Manus Basin (A) and Futuna Volcanic Arc (B). A and C are concerned in ethanol, B was pictured alive. White scalebar : 1 mm. . . . .	35
1.4	Illustrations of <i>Shinkailepas 'tufari'</i> individuals from Woodlark (A), Manus (B) and Lau Basins (C). A and B are concerned in ethanol, C was pictured alive. White scalebar : 1 mm. . . . .	36
1.5	Illustrations of <i>Shinkailepas tollmanni</i> individuals from the Futuna Volcanic Arc (A), the Manus (B) and Lau Basins (C). A and B are concerned in ethanol, C was pictured alive. White scalebar : 1 mm. . . . .	37
1.6	Illustrations of <i>Desbruyeresia</i> individuals concerned in ethanol: <i>D. cancellata</i> (A), <i>D. melanioides</i> (B) and <i>D. costata</i> (C). White scalebar : 1 mm. . . . .	38
1.7	Illustrations of <i>Provanna</i> individuals concerned in ethanol from the Lau (A), Manus (B-E) and Woodlark Basins (F). White scalebar : 1 mm. . . . .	39
1.8	Back-arc-basins sampling area in the South West Pacific (A) and sampling location of the various gastropod species from the Lepetodrilidae (B1), Neomphaloidae (B2), Phenacolepadidae (B3) and Provannidae (B4) families. Red dots represent sampled fields. . . . .	41

TABLE DES FIGURES

1.9 *Cox1* Neighbor-Joining trees inferred from *Cox1* sequences from *Lepetodrilus* (A) and *Symmetromphalus* and *Lamellomphalus* (B) within their family. Number at nodes indicates the proportion of occurrences in 1000 bootstraps; percentages below 50% are not shown. Genbank accession numbers of the present study and published sequences are indicated. Published sequences are in brackets. Sequence lengths: (A) = 496 bp, (B) = 541 bp. . . . . 49

1.10 Minimum Spanning Networks based of *Cox1* haplotypes from each taxon. Circles represent the different haplotypes; their diameter indicates the number of individuals with the same haplotype and colour their location. Mutational steps are symbolised by dashes. n = number of sequences within each lineage. Grey numbers represent the divergence between the different lineages (mean K2P% ± Sd). . . . . 50

1.11 Distribution of pairwise differences obtained from ABGD analyses of *L. schrolli* complex (A) and *Provanna* (B) *Cox1* sequences. . . . . 51

1.12 Observed and simulated match-mismatch curves. The chi-square goodness of fit test results presented compare the observed distribution to the expected under an expanding population one. Results of Chi-squared test comparing the observed distribution to the expected under a constant population one (not shown in the figure) always indicated that observed distribution did not fit the expected one ( $p < 0.001$ ). . . . . 53

1.13 *Cox1* Neighbor-Joining trees showing the position of individuals from *Shinkailepas* within their genus. Numbers at nodes indicate the proportion of occurrences in 1000 bootstraps; percentages below 50% are not shown. Genbank accession numbers of the present study and published sequences are indicated. Published sequences are in brackets. Sequence lengths: 281 bp. . . . . 56

1.14 *Cox1* Neighbor-Joining trees showing the position of individuals from *Desbruyeresia* and *Provanna* within their family. Number at nodes indicates the proportion of occurrences in 1000 bootstraps; percentages below 50% are not shown. Genbank accession numbers of the present study and published sequences are indicated. Published sequences are in brackets. Sequence lengths: 469 bp. . . . . 58

2.1 Back-arc-basins sampling area in the South West Pacific. Red dots represent sampled vent field. . . . . 75

2.2 *Lepetodrilus schrolli* female and male reproductive structures. . . . . 79

2.3 *Shinkailepas tollmanni* female and male reproductive structures. . . . . 80

2.4 Example of size-frequency histograms of *Lepetodrilus schrolli* collected in *Ifremeria* and *Bathymodiolus* habitats. . . . . 84

2.5	Examples of mean oocyte size-frequency distribution histograms for females of <i>Lepetodrilus shcrolli</i> (A) and <i>Shinkailepas tollmanni</i> (B). . . . .	88
2.6	Proportion of vitellogenic oocyte according to females' size for <i>Lepetodrilus schrolli</i> (A) and <i>Shinkailepas tollmanni</i> (B). . . . .	89
2.7	Example of size-frequency histograms of <i>Shinkailepas tollmanni</i> collected in <i>Ifremeria</i> and <i>Bathymodiolus</i> habitats . . . . .	91
3.1	Back-arc-basins sampling area in the South West Pacific. Red dots represent sampled vent field. The sites sampled are listed in italics. . . . .	107
3.2	Sampling procedure . . . . .	110
3.3	Phylum proportion by habitat (A) and at the South West Pacific scale (B) and phylum abundance by habitat (C) and at the South West Pacific scale (D). . . . .	118
3.4	Number of species from biobox only and biobox plus suction collector. . . . .	122
3.5	Samples rarefaction curves computed based on the total number of individuals: colored per habitat (A) and per basins (B). . . . .	123
3.6	Diversity indices: Species richness, ES50, total number of individuals, Shannon index and Pielou's evenness . . . . .	125
3.7	Accumulation curves (A) and venn diagramm showing the number of shared and specific to one habitat species (B). . . . .	128
3.8	Principal Coordinate Analysis (PCoA) based on the square root of the Jaccard dissimilarities . . . . .	129
3.9	SDR-simplex by habitat . . . . .	132
3.10	SDR-simplex for the Manus and Lau Basins . . . . .	134
3.11	Before and after sampling average temperature (°C) for each sample. Bars indicate the mininal and maximal values. . . . .	135
3.12	Before and after sampling average $\Sigma S$ ( $\mu M$ ) for each sample. Bars indicate the mininal and maximal values. . . . .	136
3.13	Physico-chemical measures by habitat: Temperature max and min (A-B), $H_2S$ mean (C), pH (D), $CH_4$ (E), $S$ and $P$ (F-G). White rhombus indicates the average. Kruskal-Wallis test results and level of significance of the post-hoc Nemenyi and Dunn test: * $p$ value <0.05; ** $p$ value <0.01; *** $p$ value <0.001. . . . .	138
3.14	PCA based on scaled physico-chemical data. The fist three graphs show axes one and two with ellipses constructed by habitat (A), basin (B) and field (C). The fourth graph displays axes one and three with ellipses produced by field (D). . . . .	140
3.15	dbRDA axes 1 and 2 (A) and 1 and 3 (B) and variance partitioning (C) based on square root of Jaccard dissimilarities and environmental data without methane. . .	142

TABLE DES FIGURES

B.1 Illustrations of *Lepetodrilus schrolli* and *Shinkailepas tollmanni* inhabiting the complex three-dimensional habitat formed by *Bathymodiolus* and *Ifremeria* and the different shell measurements (in pink). . . . . 196

B.2 Size-frequency histograms of the curvilinear shell length of *Lepetodrilus schrolli* for each sample from the Manus (in black) and Lau Basins (in grey). . . . . 197

B.3 Mean oocytes size-frequency histograms of *Lepetodrilus shcrolli* females for each sample. . . . . 198

B.4 Size-frequency histograms of the maximal shell length of *Shinkailepas tollmanni* for each sample. . . . . 199

C.1 PCA based on scaled physico-chemical datas (without Methane). Graphs show axes one and two with ellipses constructed by habitat (A), basin (B) and field (C). . 202

C.2 dbRDA (A) and variance partitioning (B) based on square root of Jaccard dissimilarities and environmental datas with methane. . . . . 203





---

## Liste des tableaux

---

1.1	Location of gastropods sampled along the South West Pacific back-arc basins and number of individuals used for DNA barcoding. . . . .	42
1.2	Primers used in the present study for each taxon. . . . .	44
1.3	List of accession numbers from gastropod individuals used for phylogenetic trees. . . . .	46
1.4	Variation among <i>Cox1</i> nucleotides sequences for each taxon and lineages. . . . .	47
2.1	<i>Lepetodrilus schrolli</i> and <i>Shinkailepas tollmanni</i> sampling locations at the southwestern Pacific back-arc basins . . . . .	76
2.2	Number, shell length range, mean and median (mm) of individuals of <i>L. schrolli</i> and <i>S. tollmanni</i> used for demographic analysis within each sample collected in the South West Pacific back-arc basins. . . . .	85
2.3	Number and characteristics of individuals of <i>Lepetodrilus schrolli</i> and <i>Shinkailepas tollmanni</i> used for the sex ratio, gametogenesis and fecundity analysis within each sample from the South West Pacific. . . . .	87
3.1	Sampling locations at the southwestern Pacific back-arc basins . . . . .	108
3.2	Inventory of taxa collected from the <i>Alviniconcha</i> , <i>Bathymodiolus</i> and <i>Ifremeria</i> habitats in southwestern Pacific back-arc basins. . . . .	119
3.3	Species richness (SR), Expected number of Species (ES50), total number of individuals (Nb. ind.), Shannon index (H') and Pielou's evenness (J') measures among the different samples from the southwestern Pacific back-arc basins. . . . .	126

3.4 Results of the PERMANOVA analysis based on the square root of Jaccard dissimilarities to test for differences in vent macrofaunal assemblages between basins and habitats (fixed factors), and fields within a basin and sites within a field (nested random factors)(A) and results of the post-hoc pairwise basins comparison (B). Df: degrees of freedom, SS: sum of squares, *F*: pseudo-F value by permutation, *P*: *p* values based on 9999 permutations. PERMANOVA and post-hoc test level of significance: \* *p* value <0.05; \*\* *p* value <0.01; \*\*\* *p* value <0.001. . . . . 130

D.4 Chubacarc dive, box and suction numbers for each sample. . . . . 246





---

## Introduction

---

### **L'étude de la biodiversité**

#### **Biodiversité marine et pressions anthropiques**

Les écosystèmes marins sont soumis à de fortes pressions liées aux activités humaines qui incluent en particulier les pollutions, l'exploitation des ressources biologiques ou minérales, la dégradation et la fragmentation des habitats, l'introduction d'espèces non indigènes, ou plus récemment les modifications des conditions environnementales issues du changement climatique (e.g. élévation des températures, désoxygénation et acidification des océans)(Halpern *et al.*, 2008, 2015; IPBES, 2019). À cela s'ajoutent également des pressions naturelles comprenant des évènements extrêmes, d'ordre climatique (e.g. tempêtes, ouragans, vagues de chaleur) et géologiques (i.e. séismes et éruptions volcaniques). Ces pressions multiples entraînent la dégradation et l'appauvrissement des écosystèmes et une perte conséquente de la biodiversité, essentielle à leur bon fonctionnement (Cardinale *et al.*, 2012; Gamfeldt *et al.*, 2015). L'effondrement de la biodiversité a des répercussions importantes sur l'ensemble des écosystèmes qui seront potentiellement moins résilients et plus vulnérables (Loreau *et al.*, 2001;

Ives et Carpenter, 2007; Strong *et al.*, 2015).

Les progrès technologiques au cours des dernières décennies ont rendu accessibles des environnements jusqu'alors moins soumis aux pressions anthropiques, comme l'océan profond par exemple. Ces progrès ont permis aux scientifiques d'accéder à l'étude des écosystèmes de l'océan profond, mais aussi aux industriels de concevoir des projets d'exploitation des ressources biologiques et minérales qu'ils contiennent. Si les impacts sur la biodiversité des environnements profonds demeurent spéculatifs en ce qui concerne les activités minières, elles ont été largement documentées pour les impacts de la pêche (Clark *et al.*, 2016). Au-delà des effets de l'exploitation des ressources, les environnements profonds sont également exposés aux effets de la pollution et du changement climatique (Sweetman *et al.*, 2017; Levin et Le Bris, 2015) et il demeure de profondes incertitudes sur leur résilience aux pressions anthropiques (Paulus, 2021). Préserver la biodiversité marine, des milieux côtiers comme des milieux profonds, est ainsi un enjeu majeur du XXI<sup>e</sup> siècle.

## **Les différentes facettes de la biodiversité**

La biodiversité s'organise autour de trois niveaux d'organisation du vivant : la diversité génétique (i.e. au sein des espèces), la diversité spécifique (i.e. entre les espèces) et la diversité écosystémique (i.e. entre les écosystèmes). Si ces trois niveaux sont très largement reconnus, la très grande majorité des études se concentre aujourd'hui sur la diversité spécifique, faisant de l'espèce l'unité de base de toutes les mesures de la diversité. Les mesures de la diversité spécifique peuvent toutefois se heurter aux difficultés associées à la notion d'espèce (De Queiroz, 2007), et à la présence dans le milieu marin d'un nombre très élevé d'espèces cryptiques (Knowlton, 1993).

La biodiversité peut par ailleurs être mesurée à plusieurs échelles spatiales : la diversité locale (i.e. diversité  $\alpha$ ), la diversité régionale (i.e. diversité  $\gamma$ ) et la variation de la diversité (i.e. diversité  $\beta$ ; Whittaker, 1960, 1972). La diversité  $\alpha$  peut être déterminée à l'échelle d'un site de prélèvement ou peut être considérée comme une propriété d'un habitat ou d'une

communauté (Gray, 2000). Alors que la mesure la plus simple de la diversité  $\alpha$  consiste à mesurer la richesse spécifique, c'est-à-dire le nombre d'espèces présentes dans un prélèvement ou un habitat, plusieurs auteurs ont également proposé de prendre en considération non seulement le nombre d'espèces mais également les proportions relatives de ces espèces (Whittaker, 1972; Hill, 1973; Magurran, 1988). De nombreux indices ont ainsi été proposés dont les plus célèbres sont l'indice de Shannon ou l'indice de Simpson. La diversité  $\gamma$  mesure la diversité en combinant différentes communautés ou différentes unités géographiques. Certains auteurs comme Rosenzweig (1995) ont suggéré que la diversité  $\gamma$  devait être déterminée à l'échelle d'une province biogéographique. Mesurer la diversité  $\alpha$  comme la diversité  $\gamma$  pose la question de notre capacité à mesurer la richesse spécifique aux différentes échelles spatiales concernées afin de pouvoir faire des comparaisons entre habitats ou entre régions (Gotelli et Colwell, 2001). En dépit de l'apparente simplicité de cette mesure, elle demeure un défi car elle est très sensible à l'effort d'échantillonnage et repose sur le calcul de courbes d'accumulation d'espèces ou de courbes de raréfaction.

Historiquement, les écologistes se sont concentrés dans un premier temps sur les facteurs qui structurent la biodiversité à l'échelle locale. Mais depuis plusieurs années, un nombre croissant d'études s'est intéressé aux liens entre les différentes communautés et aux règles d'assemblages des communautés dans un contexte spatialisé. Il s'agit ainsi d'identifier les mécanismes qui structurent ces métacommunautés à différentes échelles spatiales et temporelles, qu'il s'agisse de processus évolutifs (i.e. spéciation, dispersion), de processus écologiques (e.g. filtres environnementaux et biologiques) ou de processus stochastiques (Leibold *et al.*, 2004; Chase et Myers, 2011).

La diversité  $\beta$  représente le changement de la biodiversité d'un site à l'autre. Originellement décrite comme le ratio entre la diversité  $\alpha$  et  $\gamma$  (Whittaker, 1960, 1972), elle est désormais définie de deux manières distinctes : (1) la variabilité entre unités d'échantillonnage dans une aire géographique donnée; (2) la variabilité entre unités d'échantillonnage le long d'un gradient spatial, temporel ou environnemental (Anderson *et al.*, 2011). On parle alors



de turn-over de la diversité. Quelle que soit la forme qu'elle prend, elle peut être mesurée d'une multitude de manières différentes. Ces méthodes incluent des métriques qui lient les diversités  $\alpha$ ,  $\beta$  et  $\gamma$  (Lande, 1996; Crist *et al.*, 2003; Josefson, 2009) ou des méthodes d'analyses multivariées qui reposent le plus souvent sur une mesure de la dissimilarité entre les échantillons (Clarke et Warwick, 2001; Legendre et Gallagher, 2001; Legendre et Legendre, 2012). Les mesures de la dissimilarité entre échantillons s'établissent à partir d'une matrice espèce  $\times$  stations, soit sur des données de présence-absence, soit sur des données d'abondances ou de biomasses.

Alors que le déclin de la diversité locale en réponse aux pressions anthropiques à fait l'objet de nombreuses études depuis plusieurs décennies (e.g. Magurran *et al.*, 2010), une attention particulière est désormais portée aux effets des pressions sur la diversité  $\beta$ . En effet, une relative stabilité de la diversité  $\alpha$  peut s'accompagner d'importants changements de la composition en espèces et de la structure des communautés. Dans plusieurs écosystèmes côtiers, une baisse de la diversité  $\beta$  se traduisant par une homogénéisation biotique a été observée sans que les conséquences sur le fonctionnement et la résilience de ces écosystèmes soient totalement appréhendées (Thrush *et al.*, 2008; Socolar *et al.*, 2016; Primack *et al.*, 2018).

## La partition de la diversité $\beta$

La dissimilarité entre échantillons est la conséquence de deux processus distincts : (1) le remplacement ou renouvellement des espèces entre deux échantillons (i.e. des espèces sont remplacées par d'autres), et (2) la différence de richesse spécifique entre deux échantillons (i.e. des espèces sont perdues ou gagnées) (Legendre, 2014). Ces deux processus sont liés à des phénomènes différents. Les espèces sont remplacées par d'autres le long d'un gradient géographique, environnemental ou biologique en réponse à des événements historiques, à un filtre environnemental ou à des interactions biotiques (Leprieur *et al.*, 2011). Le remplacement d'espèces implique le gain ou la perte simultanée d'espèces. A l'inverse, une différence de richesse spécifique entre des échantillons peut être due à des barrières physiques, à un plus petit

nombre de niches disponibles localement ou à l'absence d'espèces dispersant sur de faibles distances. Si la composition des espèces d'un échantillon est un simple sous-ensemble de celle d'un autre site, on parle alors de "nestedness" (Legendre, 2014).

Plusieurs méthodes ont été développées pour réaliser une partition de la diversité  $\beta$  en remplacement d'espèces et différence de richesse spécifique (Podani et Schmera, 2011; Baselga, 2010, 2012; Podani *et al.*, 2013; Legendre, 2014). Legendre (2014) a regroupé ces différentes méthodes en deux familles d'indices en fonction des auteurs qui en sont à l'origine (i.e. les indices de Podani et les indices de Baselga). Indépendamment de la famille, le calcul des indices utilisent les composantes  $a$ ,  $b$  et  $c$  qui servent dans le calcul des coefficients de dissimilarité entre échantillons dans le cas d'indices de dissimilarité basés sur des données de présence-absence, comme ceux de Jaccard et de Sorensen par exemple. En considérant deux échantillons 1 et 2, ( $a$ ) correspond au nombre d'espèces en commun aux deux échantillons (i.e. la similarité), ( $b$ ) au nombre d'espèces présentes seulement dans l'échantillon 1 et ( $c$ ) au nombre d'espèces présentes seulement dans l'échantillon 2 (Figure 1). La somme de  $b$  et  $c$  représente la dissimilarité et correspond au numérateur dans le calcul des coefficients de dissimilarité (i.e. Jaccard ou Sorensen). La dissimilarité est donc composée de deux dimensions : le remplacement d'espèces égale à  $2 \times \min(b, c)$  et la différence de richesse  $|b - c|$ . Ces valeurs représentent les numérateurs utilisés dans le calcul des indices de Podani et Baselga. Seul le dénominateur change entre les deux familles d'indices. La famille des indices de Podani utilise le même dénominateur que ceux des coefficients de dissimilarité (i.e.  $a + b + c$  pour le coefficient de Jaccard et  $2a + b + c$  pour le coefficient de Sorensen). Celle des indices de Baselga utilise au dénominateur  $a + 2 \times \min(b, c)$  dans le calcul du remplacement d'espèces.

En prenant l'exemple du coefficient de Jaccard, les indices de remplacement (Repl) et de différence de richesse (RichDiff) de Podani sont calculés selon les formules suivantes :

$$Repl = \frac{2 \times \min(b, c)}{a + b + c} \quad \text{et} \quad RichDiff = \frac{|b - c|}{a + b + c}$$

Dans les indices de Baselga, la différence de richesse est appelée "nestedness" ce qui peut prêter

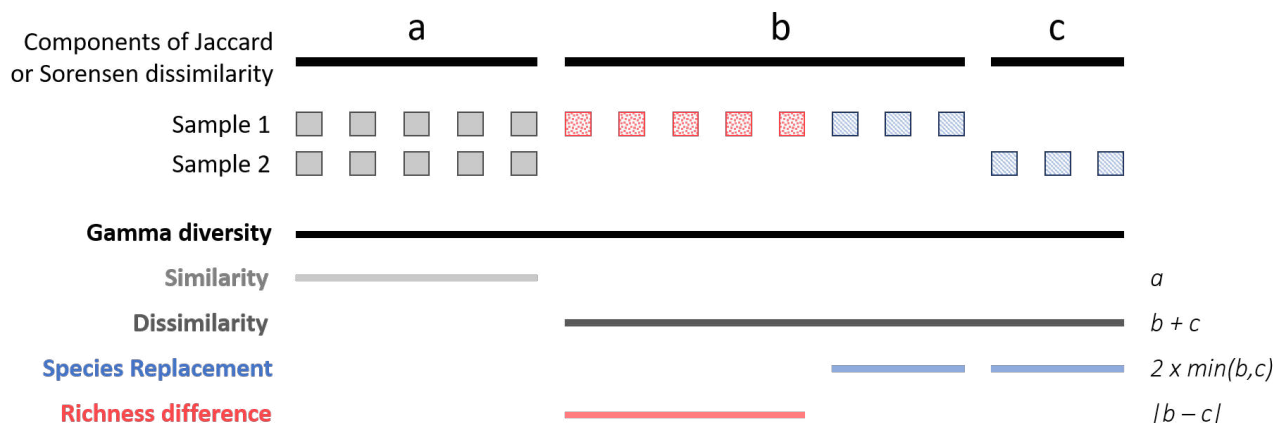


FIGURE 1 – Schéma illustrant les différentes composantes des coefficients de dissimilarité de Jaccard et Sorensen (i.e. a, b et c) et comment ces composantes sont utilisées pour estimer la similarité (carrés gris) et la dissimilarité et ses deux composantes, le remplacement d'espèces (carrés rouges mouchetés) et la différence de richesse (carrés bleu rayés) entre deux échantillons. D'après Podani et Schmera (2011) et Legendre (2014)

à confusion au regard de la définition précédemment fournie. Elle correspond à la différence de richesse calculée par Podani multiplié par  $\frac{a}{a+2 \times \min(b,c)}$  ou  $\frac{a}{a+\min(b,c)}$  selon le coefficient de dissimilarité utilisé. Dans le cas du coefficient de Jaccard, les indices de remplacement ( $Repl_B$ ) et de "nestedness" ( $Nes_B$ ) de Baselga sont :

$$Repl_B = \frac{2 \times \min(b,c)}{a + 2 \times \min(b,c)} \quad \text{et} \quad Nes_B = \frac{|b-c|}{a+b+c} \times \frac{a}{a+2 \times \min(b,c)}$$

La définition de la "nestedness" est donc aussi une des différences entre les deux familles d'indices. Podani considère qu'il s'agit d'un cas particulier de la différence de richesse. Podani et Schmera (2011) ont donc proposé de la calculer de la manière suivante :

$$Nes_P = \frac{a + |b-c|}{a+b+c} \quad \text{lorsque } a > 0, \quad \text{si } a = 0 \quad \text{alors } Nes_P = 0$$

La différence de richesse de Podani n'est donc pas égale à la « nestedness » de Baselga. Dans les deux familles, les indices sont construits de sorte que la somme du remplacement et de la différence de richesse soient égales au coefficient de dissimilarité utilisé. Le remplacement

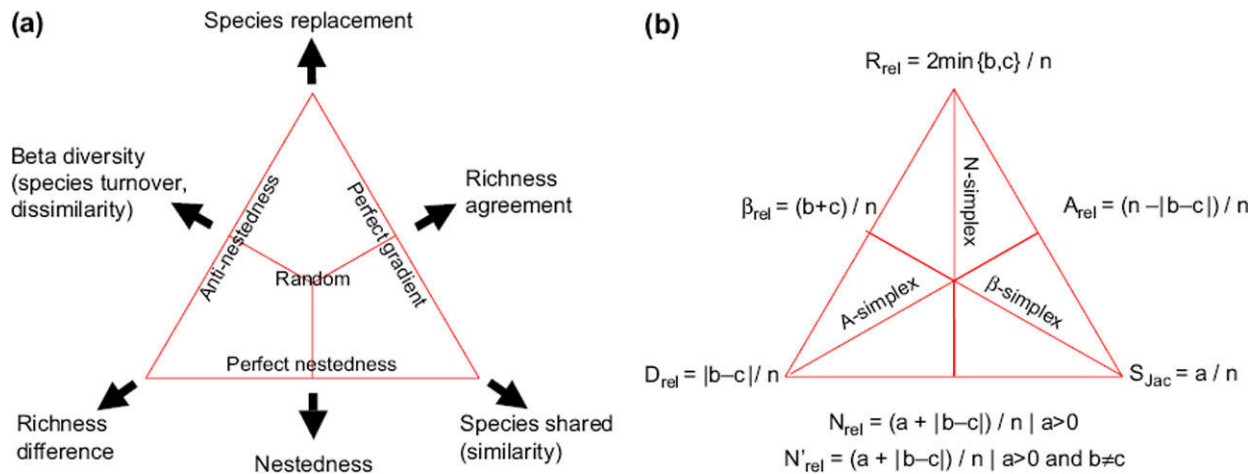


FIGURE 2 – Diagramme ternaire (ou SDR-simplex) : concept (a) et mesures des différentes composantes (b) proposé par Podani et Schmera (2011).

calculé par Podani à partir du coefficient de Jaccard aurait tendance à être sous-estimé (Baselga, 2012), alors que l'indice de remplacement de Baselga serait surestimé pour le coefficient de Sorensen (Carvalho *et al.*, 2012).

Dans la mesure où la dissimilarité ( $D$ ) est composée du remplacement des espèces et de la différence de richesse entre échantillons et que la similarité ( $S$ ) est égale à  $1 - D$ , Podani et Schmera (2011) et Podani *et al.* (2013) ont suggéré d'illustrer ces valeurs dans un diagramme ternaire (i.e. SDR-simplex, Figure 2). Cette représentation permet de visualiser l'importance relative de la similarité et des deux composantes de la dissimilarité parmi toutes les paires d'échantillons, et donc de voir quelle composante façonne le plus la diversité  $\beta$ . L'analyse de ces diagrammes permet de déduire les processus qui structurent la distribution de la biodiversité. En raison de leur logique de construction, les indices de la famille Podani sont écologiquement plus faciles à interpréter (Legendre, 2014).

Les processus structurant la biodiversité varient selon l'échelle considérée. Alors que les conditions physico-chimiques de l'environnement local structurent la biodiversité essentiellement à de petites échelles spatiales, les processus historiques vont influencer la biodiversité aux échelles les plus grandes. Comprendre les processus qui se produisent à ces différentes échelles est important pour mieux appréhender les schémas de distribution

de la biodiversité. Cette connaissance est essentielle pour établir des mesures optimales de gestion des écosystèmes, ce qui est d'autant plus important dans un contexte où les pressions anthropiques sur les écosystèmes sont ou sont amenées à être de plus en plus fortes.

## **Environnements profonds et sources hydrothermales**

La surface de notre planète est majoritairement recouverte par les océans (70,8%). Leur profondeur moyenne est autour de 4 000 m et environ la moitié des eaux marines se trouve à plus de 3 000 m de profondeur. Constituant ainsi 90% de l'espace habitable de la planète, l'océan profond représente l'écosystème le plus étendu mais reste toujours très peu connu (Ramirez-Llodra *et al.*, 2010). Le terme d'environnements profonds regroupe tous les environnements marins se situant au-delà de 200 m de profondeur - limite de pénétration de la lumière nécessaire à la photosynthèse. Le plancher océanique y est majoritairement constitué de grandes étendues relativement plates, les plaines abyssales. On y trouve également une grande diversité de paysages incluant le talus continental, des monts et canyons sous-marins, des arcs-volcaniques, les fosses hadales ou bien encore les dorsales médio-océaniques. L'océan profond abrite ainsi de nombreux écosystèmes benthiques, dont les sources hydrothermales.

### **Les sources hydrothermales**

Les sources hydrothermales ont été découvertes il y a moins de 50 ans, en 1977, au niveau la dorsale des Galápagos dans le Pacifique oriental (Lonsdale, 1977). Depuis, 666 zones actives ont été répertoriées dans des contextes géophysiques et géologiques variés, le long de dorsales médio-océaniques, le long des arcs volcaniques, dans les bassins arrière-arc ou encore au niveau de zones de subduction ou de points chauds (Figure 3 et 4) (Beaulieu *et al.*, 2013; Beaulieu et Szafranski, 2020). La morphologie des sites hydrothermaux varie en fonction de la vitesse d'expansion des rides océaniques que l'on peut classer en cinq catégories allant de très lentes (i.e.  $< 20 \text{ mm.an}^{-1}$ ) à très rapides (i.e.  $> 140 \text{ mm.an}^{-1}$ ) en passant par lentes (i.e. 20-

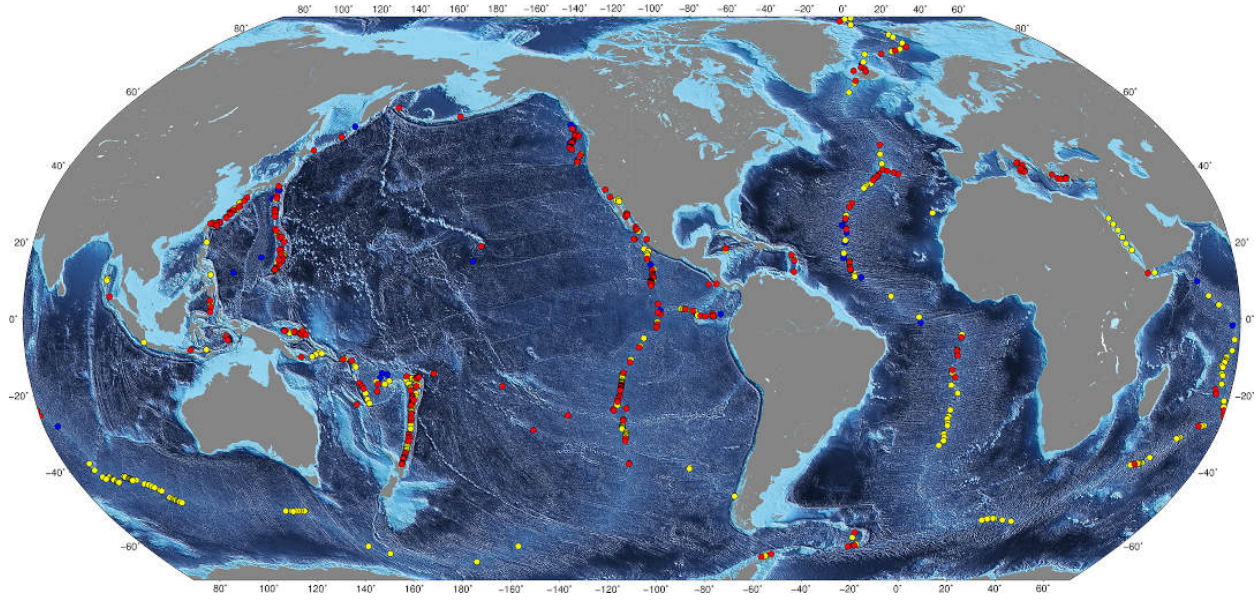


FIGURE 3 – Carte mondiale répertoriant les sources hydrothermales connues (en rouge), inférées (en jaune) et supposées (en bleu). Tiré de Beaulieu et Szafranski (2020)

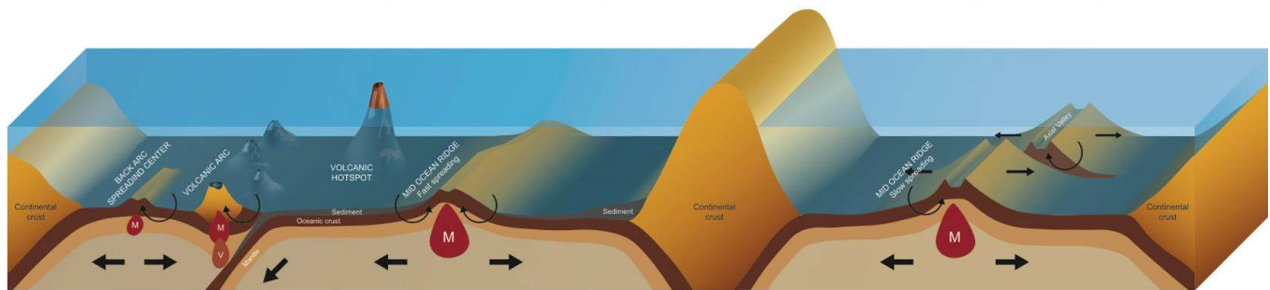


FIGURE 4 – Schéma illustrant différents contextes géologiques dans lesquels on observe des sources hydrothermales. Tiré de Le Bris *et al.* (2019).

50 mm.an<sup>-1</sup>), intermédiaires (i.e. 50-80 mm.an<sup>-1</sup>) et rapides (i.e. 80-140 mm.an<sup>-1</sup>) (Figure 5). L'activité volcanique façonne en grande partie la morphologie des sites au niveau des rides à vitesses d'expansion rapides et très rapides comme la dorsale Est-Pacifique par exemple. Dans les systèmes lents à très lents, tels que la dorsale médio-Atlantique ou Arctique, l'activité tectonique impacte davantage la structure des sites, les apports magmatiques et les éruptions y étant moins importants (Perfit et Chadwick, 1998; Kelley *et al.*, 2002).

Ces sources hydrothermales se forment donc dans les zones à forte activité volcanique et/ou tectonique où le magma remonte dans la lithosphère océanique. L'eau de mer s'infiltré dans les fissures de la croûte océanique où sa composition va subir une série de

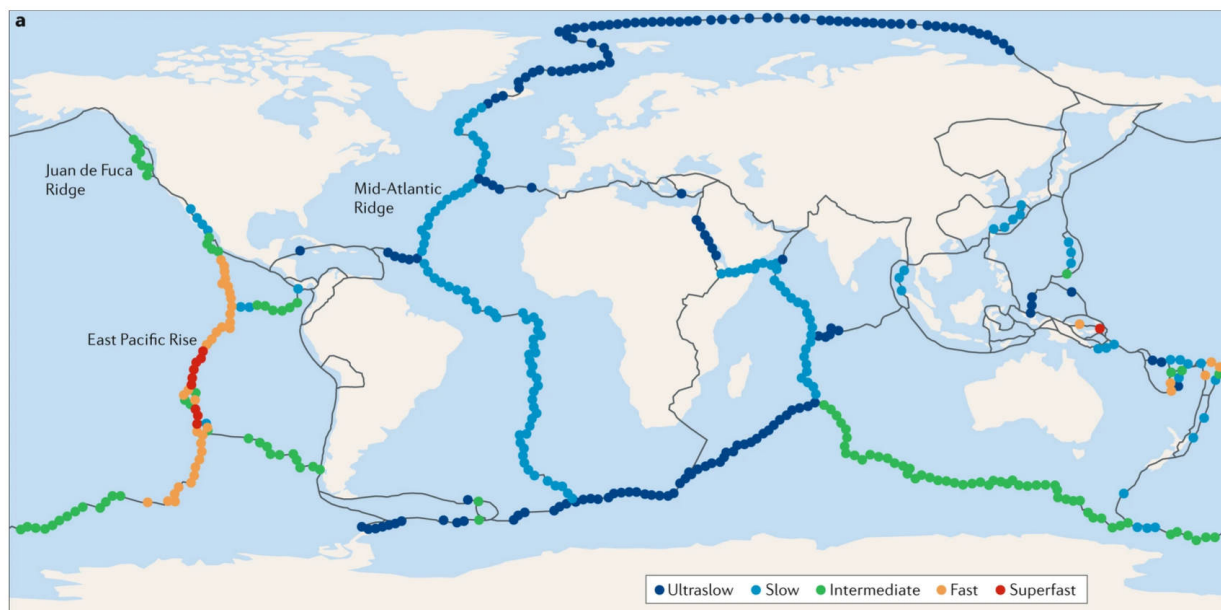


FIGURE 5 – Carte présentant les différentes vitesses d’expansion des dorsales classées en cinq catégories : Dorsales très lentes (bleu foncé;  $< 20 \text{ mm.an}^{-1}$ ), lentes (bleu;  $20\text{-}50 \text{ mm.an}^{-1}$ ), intermédiaires (vert;  $50\text{-}80 \text{ mm.an}^{-1}$ ), rapides (orange;  $80\text{-}140 \text{ mm.an}^{-1}$ ) et très rapides (rouge;  $> 140 \text{ mm.an}^{-1}$ ). Tiré de Dick (2019).

transformations chimiques au contact des roches mantelliques qu’elle traverse sous l’effet de la pression et de la température. En s’infiltrant en profondeur, l’eau se réchauffe progressivement à proximité du magma et s’appauvrit en sulfates, qui captent les protons  $\text{H}^+$  et les électrons arrachés aux métaux des roches pour former des sulfures. L’eau s’enrichit également en éléments réduits comme le méthane et l’hydrogène, et en différents métaux (e.g. fer, manganèse, zinc, silicium ou encore en plomb, cadmium, lithium) qui se dissolvent en proportions variables suivant l’acidité du fluide (Lalou, 1991). Ce fluide, moins dense, anoxique et très acide (pH autour de 2), dont la composition varie en fonction du type de roches traversées, remonte vers la surface sous l’effet de la densité. Au contact de l’eau de mer froide, les sulfures polymétalliques précipitent pour former des cheminées hydrothermales.

Il existe différents types d’émissions en milieu hydrothermal selon la profondeur d’enfouissement du fluide et du degré de mélange avec l’eau de mer (Figure 6). Un panache noir est émis lors de la remontée de fluide pur. Très chaud (i.e. pouvant atteindre  $400^\circ\text{C}$ ), avec une vitesse d’écoulement rapide (Mittelstaedt *et al.*, 2012), sa couleur noire est due aux sulfures

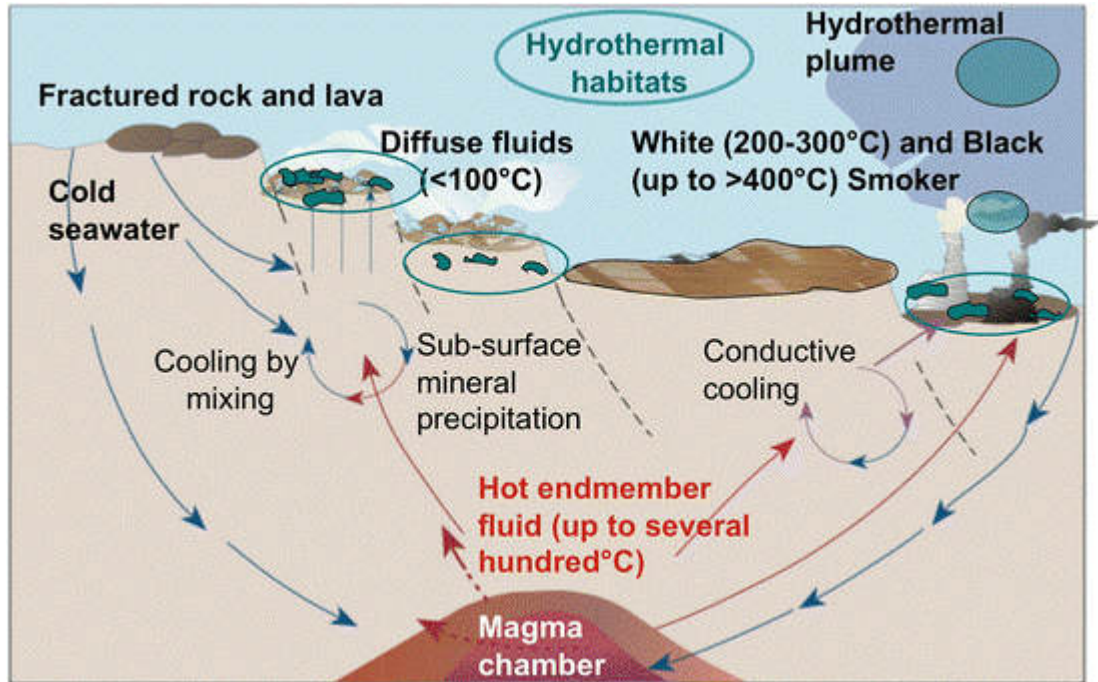


FIGURE 6 – Schéma simplifié de la circulation hydrothermale et des différents fluides qu'il en résulte. Tiré de Koschinsky (2014).

polymétalliques qui précipitent, créant des édifices appelés fumeurs noirs (Hannington *et al.*, 1995). Lorsque le fluide entre en contact avec de l'eau avant son expulsion, une bonne partie des sulfures polymétalliques précipitent en amont et un panache blanc est émis en surface. Moins chaud (i.e. allant de 100°C à 200°C environ) et avec une vitesse d'émission moins rapide, sa couleur est issue de la précipitation de silicate, d'anhydrite et de baryte qui conduit à la formation des fumeurs blancs (Hannington *et al.*, 1995). Enfin, des émissions plus diffuses apparaissent dans les fissures, crevasses ou interstices des édifices, lorsque le fluide est dilué en sub-surface ou que l'eau de mer s'est infiltrée peu profondément dans la croûte océanique, subissant ainsi une modification partielle de sa composition chimique. Ce fluide, beaucoup moins chaud (i.e. généralement inférieur à 100°C) et transparent, peut diffuser lentement sur de grandes surfaces.



## Les bassins arrière-arc

Les bassins arrière-arc sont formés en parallèle de zones de subduction. Lorsque deux plaques convergent, la lithosphère océanique entre en subduction et plonge dans le manteau (Figure 7). Cette subduction va provoquer la fusion partielle du manteau et produire du magma qui va ensuite remonter en surface et former un arc volcanique. Ce mécanisme de subduction va entraîner la mise en place d'une cellule de convection en arrière de l'arc volcanique qui va être à l'origine d'une remontée de magma et de la formation d'une zone d'accrétion en surface où de la croûte océanique va être créée et former par la suite un bassin arrière-arc. Dans le Pacifique ouest, l'activité hydrothermale est principalement localisée au niveau des bassins arrière-arc, le long des dorsales à l'origine de leur ouverture, ou au niveau des volcans en arrière des zones de subduction (Figure 4). Ainsi, alors que les rides médio-océaniques, telles que les dorsales est-Pacifique et médio-Atlantique, forment des systèmes continus de dorsales qui s'étendent sur plusieurs milliers de kilomètres, les dorsales et arcs volcaniques du Pacifique ouest forment des systèmes fragmentés et isolés (Desbruyères *et al.*, 2006a), avec des contextes géologiques et géodynamiques variés (Figure 5) (Hall, 2002; Schellart *et al.*, 2006; Bézou *et al.*, 2009). Au nord du Pacifique se trouve la fosse d'Okinawa, l'arc Izu-Ogasawara (ou Izu-Bonin) et la fosse des Mariannes (Figure 8). Au sud, se situent les bassins de Manus, Woodlark, Nord-Fidji, et Lau et les arcs volcaniques de Futuna, du Tonga et de Kermadec (Figure 8 et 9). La création de ces derniers résulte des interactions complexes entre la plaque Pacifique, qui plonge à l'est dans la fosse de Tonga et de Kermadec, et la plaque australienne qui plonge au nord-est dans la fosse des Iles Salomon et du Vanuatu (ou Nouvelles Hébrides) (Ruellan et Lagabrielle, 2005).

Relativement récent comparés aux dorsales médio-océaniques (i.e. < 10 millions d'années), les bassins du sud-ouest Pacifique ont des géodynamiques très variées (Figure 5). Le bassin de Manus présente une vitesse d'expansion rapide (> 100 mm.an<sup>-1</sup>) (Both *et al.*, 1986). Situé dans la mer de Bismarck en arrière de l'arc de Nouvelle Bretagne, ce bassin s'est formé il y a environ 5 millions d'années (Ma). De l'autre côté de la fosse de Nouvelle Bretagne se trouve

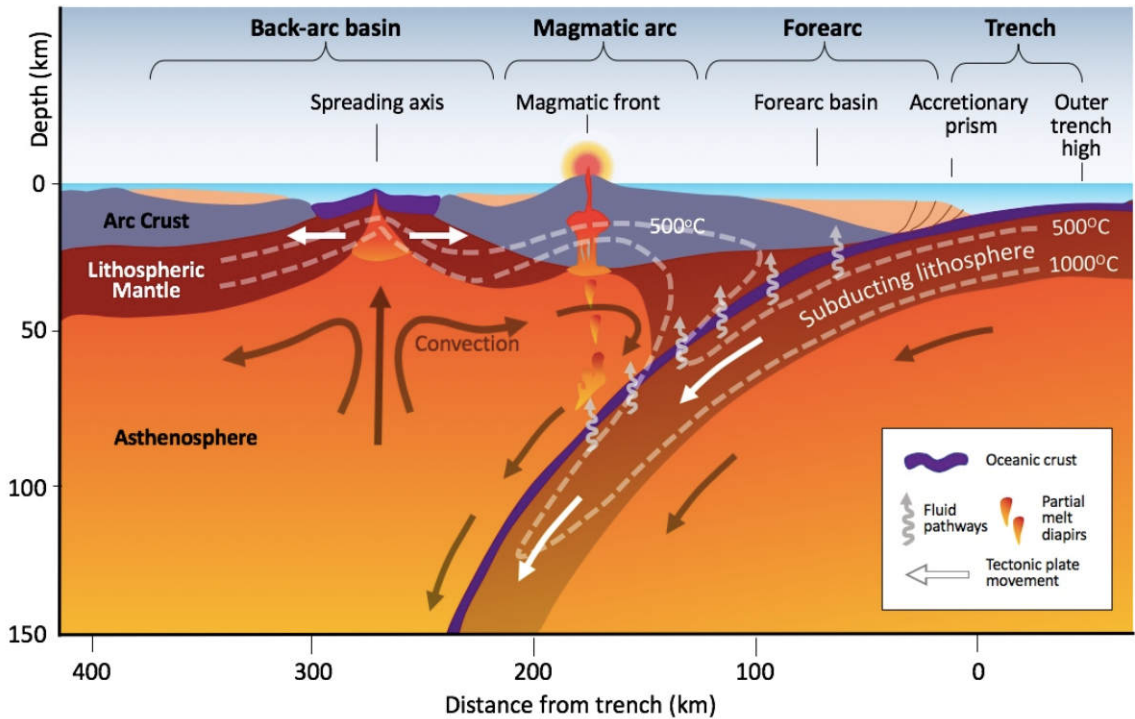


FIGURE 7 – Schéma de la formation d'un bassin arrière-arc. Extrait du site web <https://www.geologynorth.uk/ballantrae-ophiolite-complex/>

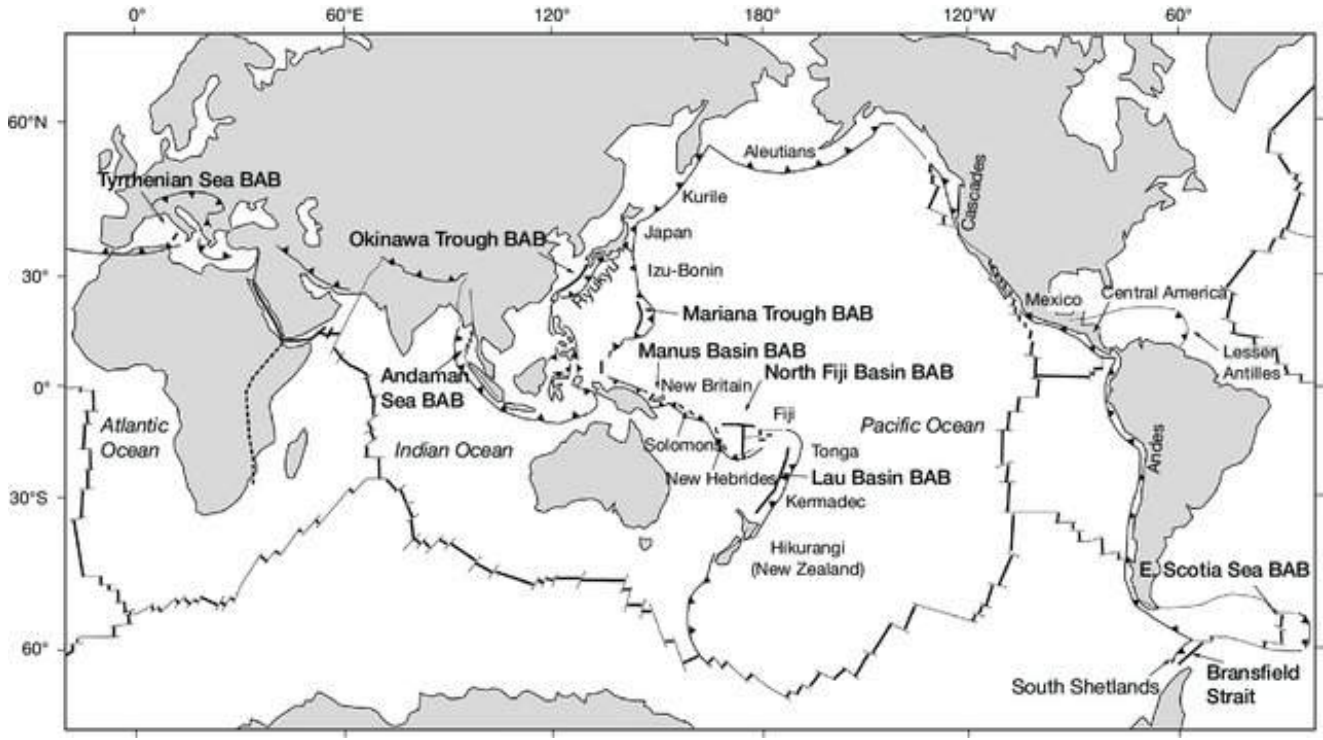


FIGURE 8 – Carte mondiale des bassins arrière-arc (BAB). Tirée de Guinot et Segonzac (2018).



le bassin de Woodlark. Avec des vitesses d'expansion plus lentes, variant de 38 à 67 mm.an<sup>-1</sup> (Taylor *et al.*, 1995), il s'agit du plus ancien bassin du sud-ouest Pacifique. Ouvert il y a 5-7 Ma, il s'étend de la pointe sud-est de la Papouasie Nouvelle Guinée à la fosse des Iles Salomon avec une zone de subduction à l'est. Au nord, il s'enfonce dans la fosse de Nouvelle Bretagne. Le bassin Nord Fidjien est très particulier avec plusieurs dorsales dont certaines se rejoignent, et présente des vitesses d'expansion variables selon les zones (i.e. de 10 à 80 mm.an<sup>-1</sup>). Formé il y a 3-4 Ma, sa forme triangulaire est le résultat de trois grandes étapes d'ouverture initiées il y a 10-12 Ma (Ruellan et Lagabrielle, 2005). Les rides de Woodlark et du Nord-Fidji ont pu être davantage connectées au début de la création du bassin Nord Fidjien (Boulart *et al.*, 2022). Avant la collision entre l'arc Mélanésien et le Plateau d'Ontong-Java il y a 18 Ma, la partie nord du bassin Nord-Fidjien (aujourd'hui disparu par subduction) est aussi supposée avoir fait le lien entre la dorsale des Iles Salomon et celle du bassin Sud-Fidjien maintenant fossiles (Boulart *et al.*, 2022). Le bassin de Lau, à l'est, est le plus jeune. Formé il y a environ 1-2 Ma, il présente des sources mantelliques variables entre le nord et le sud du bassin et une vitesse d'expansion moyenne de 74 mm.an<sup>-1</sup> (Desbruyères *et al.*, 1994). La vitesse d'expansion de ce bassin augmente en allant vers le nord, pour atteindre jusqu'à 160 mm.an<sup>-1</sup> (Bevis *et al.*, 1995). Enfin, l'arc volcanique de Futuna est situé à l'ouest de l'extrémité nord de la fosse des Tonga, zone où les vitesses de subduction les plus rapides ont été enregistrées (180 à 240 mm.an<sup>-1</sup>; Konn *et al.*, 2018). Localisé à l'intersection des bassins Nord-Fidjien et de Lau, il présente une diversité géochimique importante (Konn *et al.*, 2018).

L'environnement hydrothermal des bassins arrière-arc est structuré à différentes échelles spatiales allant de la zone d'émission (i.e. fumeur ou zone de diffusion; du cm au m), à des bassins distincts (plusieurs centaines de kilomètres). Pour la dorsale Est-Pacifique, Chevaldonné *et al.* (1997) ont proposé une définition des structures hydrothermales qu'il est possible d'observer à différentes échelles spatiales. Selon ces auteurs, une zone d'émission correspond à une seule sortie de fluide hydrothermal localisée. Un site est composé de plusieurs zones d'émissions spatialement continues sur quelques mètres et appartenant au même réseau

de fissures. Un champ englobe un ensemble de sites distants de quelques centaines de mètres à quelques kilomètres, sous l'influence de mêmes variations spatio-temporelles des propriétés du fluide, et reliés en profondeur par un réseau hydrothermal unique. Un secteur (ici un bassin) est constitué de plusieurs champs espacés de dizaines ou centaines de kilomètres. Si la distinction entre ces entités est relativement évidente le long des dorsales du Pacifique est et médio-Atlantique, elle l'est beaucoup moins dans le système des bassins arrière-arc, en particulier en raison d'un déficit de connaissances. Dans le cadre de cette étude, pour établir les différentes échelles spatiales, nous avons choisi de nous appuyer sur la nomenclature des champs et sites déjà répertoriés dans la base de donnée InterRidge (Beaulieu et Szafranski, 2020), ou référencés lors d'études antérieures (Konn *et al.*, 2018; Boulart *et al.*, 2022), mais également sur nos propres observations des fonds lors de l'échantillonnage.

## **Ecosystèmes hydrothermaux**

Bien que toxique par sa teneur en sulfure d'hydrogène et l'absence d'oxygène entre autres, le fluide hydrothermal fournit une source d'énergie alternative à celle du soleil qui soutient le développement de communautés biologiques spécialisées. Des microorganismes (i.e. archées et bactéries) sont capables d'oxyder différents composés réduits (e.g.  $H_2S$ ,  $H_2$ ,  $CH_4$ ) présents dans le fluide afin de fixer le carbone inorganique via un processus appelé chimiosynthèse (Jannasch et Mottl, 1985). Les sulfures étant dominants dans l'environnement hydrothermal, leur oxydation est très répandue mais le méthane, le dihydrogène, l'ammonium ou le fer ferreux sont aussi des éléments utilisés (e.g. Nakagawa et Takai, 2008; Petersen *et al.*, 2011). D'autre part, les voies métaboliques de la fixation du carbone sont variées et incluent le cycle de Calvin-Benson-Bassham, le cycle de Krebs inverse, et la voie de Wood-Ljungdahl, parfois appelée voie réductrice de l'acétyl-CoA (Nakagawa et Takai, 2008). Ces micro-organismes chimioautotrophes colonisent l'environnement hydrothermal sous forme libre ou en symbiose avec différentes espèces d'invertébrés benthiques (e.g. annélides, gastéropodes, bivalves et crustacés) (Childress et Fisher, 1992; Dubilier *et al.*, 2008). Ils constituent ainsi la base de la

chaîne trophique associée aux écosystèmes hydrothermaux.

La faune hydrothermale associée est ainsi composée d'espèces hautement spécialisées et est caractérisée par une faible diversité mais un fort taux d'endémisme et une forte biomasse, principalement due aux espèces symbiotiques de grandes tailles (Tunnicliffe, 1991). Cette mégafaune symbiotique forme des habitats tridimensionnels, fournissant nourriture et microhabitats, augmentant ainsi le nombre de niches écologiques disponibles pour un nombre plus important d'espèces mobiles plus petites (Govenar *et al.*, 2005). Les organismes qui composent cette petite faune, majoritairement non symbiotique, appartiennent à différents guildes trophiques (e.g. brouteurs, suspensivores, déposivores, détritivores ou carnivores, etc...) (Van Dover, 2000; Levesque *et al.*, 2003; Desbruyères *et al.*, 2006b).

## **Organisation spatiale de la biodiversité hydrothermale**

En raison de la nature fragmentée de ces écosystèmes, l'étude de la distribution des espèces et des communautés peut être abordée dans le cadre de la théorie des métapopulations selon laquelle le taux de perturbation des habitats joue un rôle primordial (Mullineaux *et al.*, 2018). La structure de la biodiversité en milieu hydrothermal dépend ainsi de la combinaison de multiples processus agissant à différentes échelles spatio-temporelles. A grande échelle géographique, les patrons de distribution actuels des espèces sont le reflet d'évènements de vicariance liés à l'histoire tectonique des dorsales et bassins (Tunnicliffe et Fowler, 1996; Moalic *et al.*, 2012) auxquels s'ajoutent les mécanismes de dispersion qui isolent plus ou moins les différentes provinces biogéographiques (Van Dover, 2002). Ainsi, les espèces de la mégafaune symbiotique de grande taille ainsi que celles de la petite faune associée divergent d'une province biogéographique à l'autre (Figure 10). Les communautés de la dorsale Est-Pacifique sont dominées par les polychètes siboglinidés (e.g. *Riftia pachyptila*), les polychètes alvinellidés (e.g. *Alvinella pompejana*), les bivalves mytilidés (*Bathymodiolus sp.*) et vesicomidés (*Calyptogena magnifica*) et des gastéropodes (e.g. *Lepetodrilus elevatus*)

(Tunncliffe, 1991). Le long des dorsales du nord-est Pacifique, la faune présente des similarités avec celle de l'Est-Pacifique même si les moules en sont absentes. On y retrouve ainsi des polychètes siboglinidés (e.g. *Ridgeia piscesae*), des polychètes alvinellidés (i.e. *Paralvinella sulfincola* et *P. palmiformis*) et de nombreux gastéropodes (e.g. *Depressigyra globulus*, *Provanna variabilis*, *Lepetodrilus fucensis*) (Sarrazin et Juniper, 1998). Les polychètes siboglinidés et alvinellidés sont absents des communautés de la dorsale médio-atlantique dont les biomasses sont dominées par des mytilidés du genre *Bathymodiolus* (i.e. *Bathymodiolus azoricus* et *B. puteoserpentis*) et des crevettes alvinocarididés (i.e. *Chorocaris chacei*, *Alvinocaris markensis* et *Rimicaris exoculata*) (Cuvelier *et al.*, 2011). Dans les bassins arrière-arc du Pacifique, les espèces symbiotiques dominantes sont des gastéropodes emblématiques de la famille des Provannidae *Alviniconcha* spp. et *Ifremeria nautilei* auxquels s'ajoutent des moules du genre *Bathymodiolus* (Desbruyères *et al.*, 1994) (Figure 11). La dorsale centrale indienne abrite des communautés dominées par des crevettes alvinocarididés du genre *Rimicaris*, des moules du genre *Bathymodiolus*, des gastéropodes du genre *Alviniconcha* et des pouce-pieds du genre *Neolepas* (Van Dover *et al.*, 2001). D'autres systèmes découverts plus récemment sont dominés par des cirripèdes du genre *Vulcanolepas*, des crabes du genre *Kiwa*, des anémones de mer et des gastéropodes comme la dorsale est de Scotia (Antarctique) (Rogers *et al.*, 2012), ou des crevettes du genre *Rimicaris* comme la dorsale Cayman (Connelly *et al.*, 2012).

À l'échelle mondiale, le nombre de provinces biogéographiques défini pour ces environnements a varié d'une étude à l'autre, en fonction de l'avancée de l'état des connaissances et des méthodes d'analyses mises en œuvre (Van Dover, 2002; Bachraty *et al.*, 2009; Rogers *et al.*, 2012; Moalic *et al.*, 2012). Thaler et Amon (2019) ont distingué 11 provinces différentes qui se séparent entre les bassins océaniques, et au sein de chaque bassin (Figure 12). Ces provinces sont ainsi : la dorsale médio-Atlantique, le nord-ouest Pacifique, le sud-ouest Pacifique, la dorsale de Juan de Fuca, le nord de la dorsale Est-Pacifique, le sud de la dorsale Est-Pacifique, la dorsale Cayman, la dorsale centrale indienne, l'Océan Austral, l'Arctique et la Mer Méditerranée. Les bassins arrière-arc du Pacifique sud-ouest forment ainsi

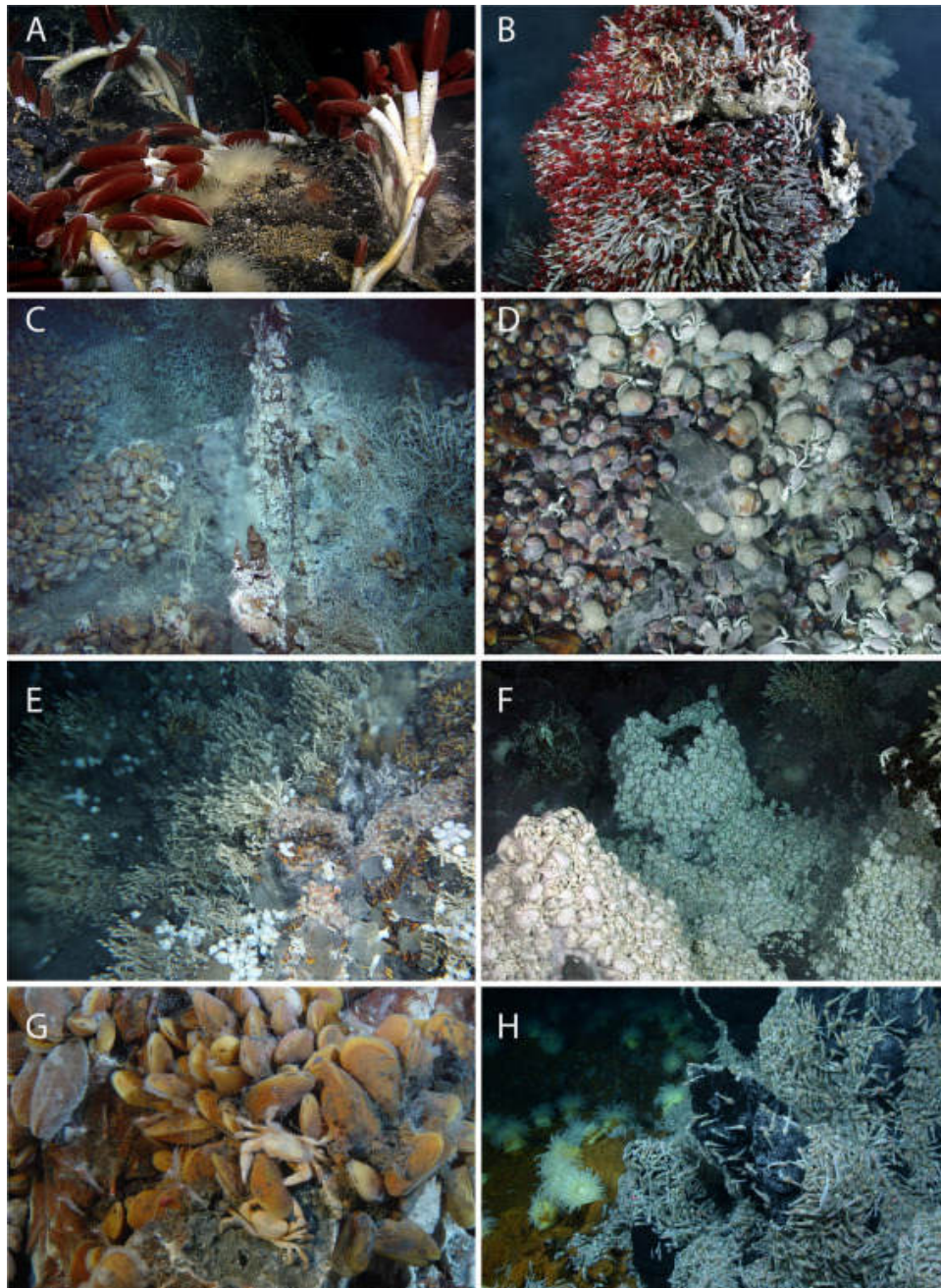


FIGURE 10 – Exemples de la mégafaune symbiotique dominant les sources hydrothermales selon la province biogéographique. Les verres tubicoles du genre *Riftia* de la dorsale du Pacifique est (A) et du genre *Ridgeia* de la dorsale de Juan de Fuca (B). Les moulières à *Bathymodiolus* (C) et les gastéropodes *Alviniconcha* et *Ifremeria* (D) des bassins arrière-arc du Pacifique sud-ouest. Les cirripèdes pédonculés, moulières et gastéropodes de la dorsale Indienne (E). Les crabes yéti de la dorsale est de Scotia (F). Les moulières à *Bathymodiolus* de la dorsale Atlantique (G), et les crevettes *Rimicaris hybisae* de la dorsale des Caymans (H). Tiré de Van Dover *et al.* (2018).



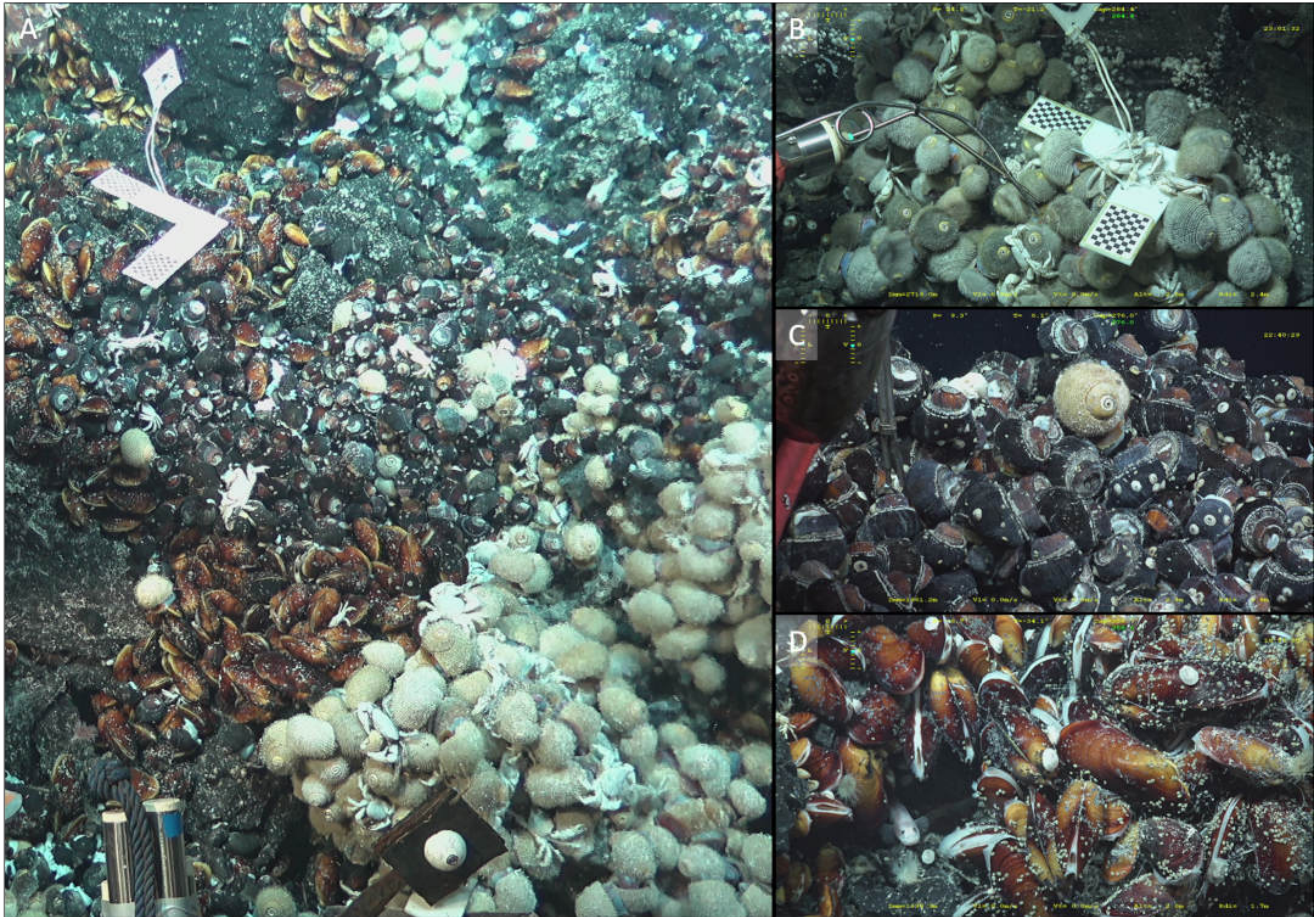


FIGURE 11 – Illustrations de la mégafaune des bassins arrière-arc (A) : les agrégations de gatéropodes *Alviniconcha* (B) et *Ifremeria* (C), et moulières à *Bathymodiolus* (D).

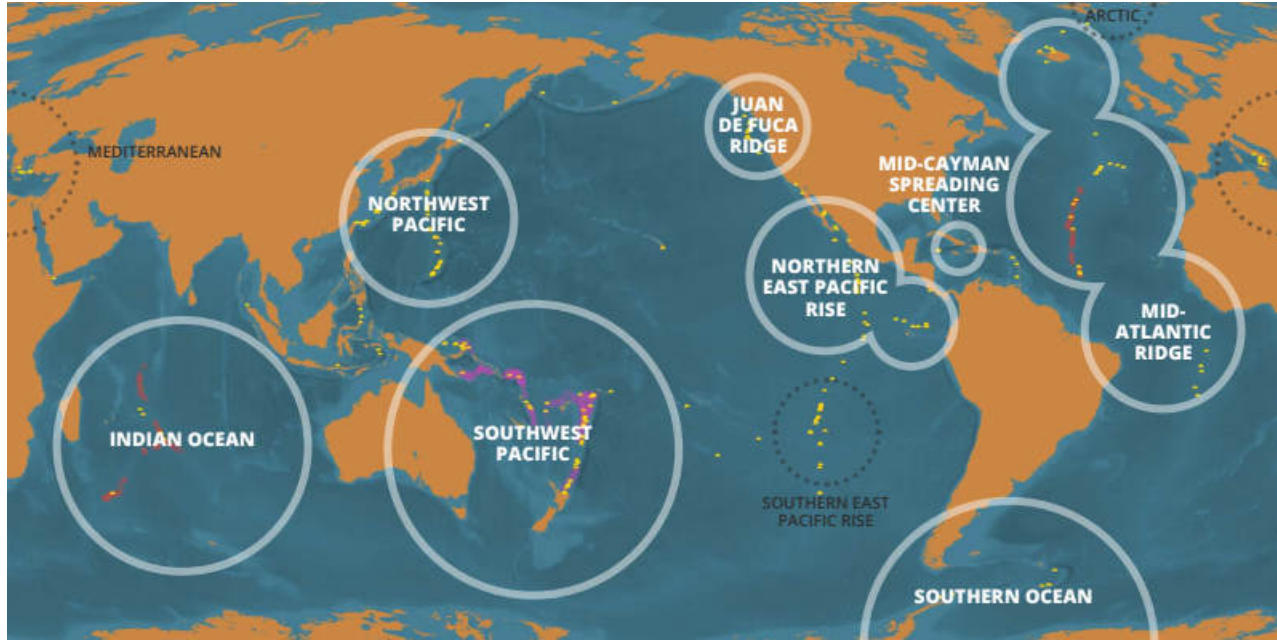


FIGURE 12 – Distribution globale des 11 provinces biogéographiques identifiées à ce jour. Tiré de Thaler et Amon (2019).

une province distincte. La variabilité des taux d'accrétion influence la distribution spatiale et la durée de vie des champs hydrothermaux et par conséquent la diversité spécifique des communautés associées (Tunnicliffe, 1991; Juniper et Tunnicliffe, 1997). Les dorsales médio-océaniques rapides présentent une diversité spécifique plus importante que les dorsales lentes où les distances plus grandes entre les différentes zones actives rendent les échanges entre populations plus rares, augmentant ainsi le risque d'extinction (Van Dover, 2002). D'autre part, la proximité avec d'autres écosystèmes chimiosynthétiques (e.g. zones de suintements froids, carcasses de baleine ou amas de bois coulés) pourraient avoir influencé la biodiversité en tant que zone relais (Gebruk *et al.*, 1997; Samadi *et al.*, 2007).

À l'échelle d'une dorsale ou d'un bassin arrière-arc, la distance entre les populations ou les communautés va être un facteur structurant dans ces écosystèmes distribués de manière très éparse (de quelques mètres à plusieurs centaines de kilomètres), puisqu'elle conditionne la capacité des espèces à maintenir des populations locales et à coloniser de nouveaux sites. Les caractéristiques topographiques, telles que les failles transformantes ou la circulation océanique profonde sont à même de limiter la dispersion pouvant entraîner des événements de

vicariance de part et d'autre de ces barrières géographiques (Vrijenhoek *et al.*, 1997; Van Dover, 2002; Plouviez *et al.*, 2009). La répartition spatiale de la faune hydrothermale le long d'un système de dorsales va également dépendre de facteurs démographiques et des traits d'histoire de vie propres aux espèces, incluant la capacité de dispersion, la fécondité, le taux de survie des larves et le succès de recrutement lui-même fonction, entre autres, de la disponibilité en habitat. Jusqu'au début des années 2000 il existait peu de données sur les échanges de la faune hydrothermale entre champs ou segments de dorsales, et plus particulièrement sur la capacité de cette faune à recoloniser de nouveaux sites distants. Face à la difficulté d'observer et d'échantillonner les larves *in situ*, les capacités de dispersion des espèces ont pu être estimées à travers l'étude de la structure génétique des populations pour inférer les flux géniques (Won *et al.*, 2002; Jollivet *et al.*, 2004; Matabos *et al.*, 2008b; Teixeira *et al.*, 2011; Thaler *et al.*, 2011; Van Der Heijden *et al.*, 2012; Breusing *et al.*, 2016; Lee *et al.*, 2019; Plouviez *et al.*, 2009) ou à partir de modèles biophysiques qui intègrent la circulation des courants et des données biologiques des espèces (e.g. fécondité, durée de vie larvaire) (Mitarai *et al.*, 2016; Breusing *et al.*, 2016, 2021). En complément, l'étude *in situ* de la recolonisation de sites hydrothermaux détruits à la suite d'une éruption volcanique a permis d'obtenir des estimations du potentiel de dispersion des espèces de plusieurs centaines de km (Mullineaux *et al.*, 2010).

Également à l'échelle d'une dorsale ou d'un fragment de dorsale, la variabilité de la composition chimique du fluide hydrothermal influence la distribution de la biodiversité en supplément de la distance entre les sites hydrothermaux ou de la fréquence de la perturbation des sites. En fonction de la profondeur mais aussi de la chimie du fluide, les communautés hydrothermales varient fortement en termes de composition d'espèces le long de la dorsale médio-atlantique entre 11°N et 38°N (Desbruyères *et al.*, 2000). Dans le bassin de Lau, des différences de composition des communautés ont été recensées sur une distance de 400 km en relation avec la nature des laves (i.e. basaltique vs. andésitique) et la composition chimique du fluide (Podowski *et al.*, 2010).

À l'échelle locale, le mélange du fluide émis avec l'eau de mer conduit à un gradient

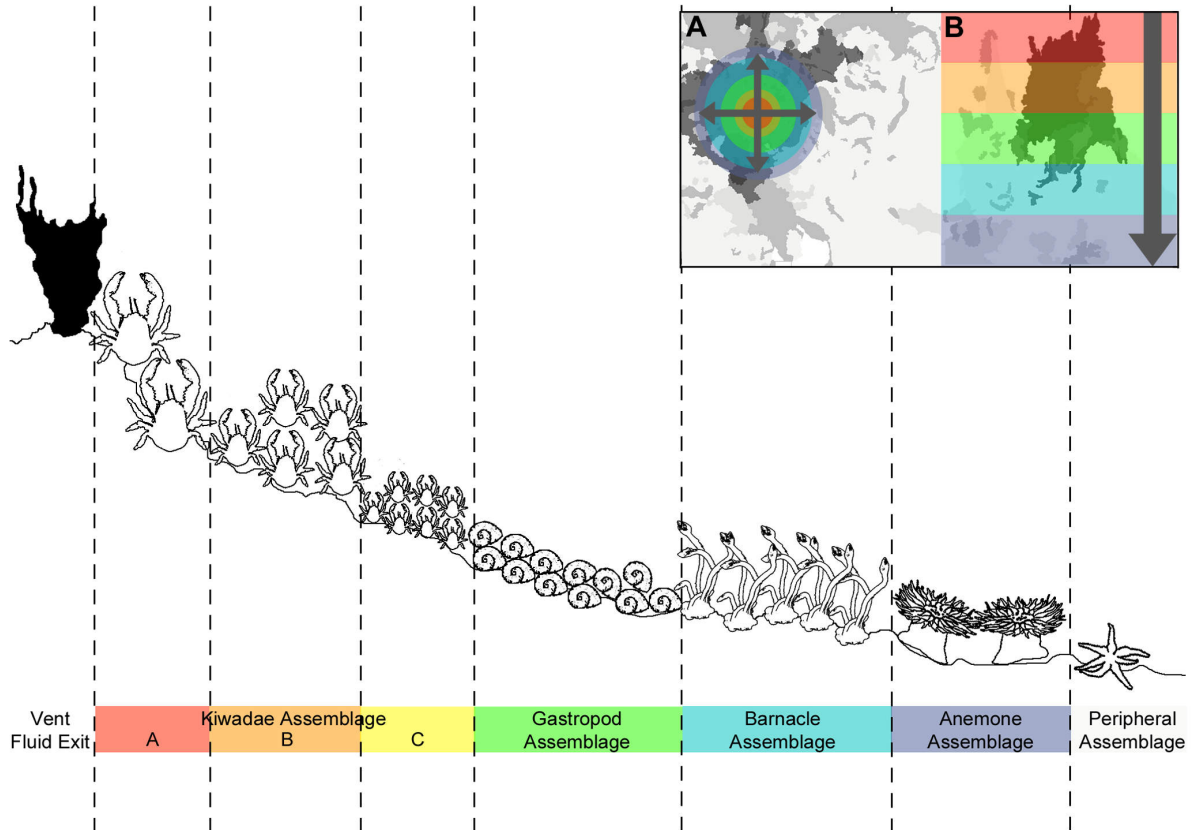


FIGURE 13 – Schéma simplifié de la structuration spatiale de différents habitats le long du gradient de dilution du fluide hydrothermal sur l'horizontal (A) et la verticale (B). Tiré de Marsh *et al.* (2012).

de dilution qui structure la distribution des espèces selon leur degré de tolérance aux conditions physico-chimiques (e.g. hypoxie, pH acide, forte température et forte concentration en sulfures) (Vismann, 1991; Levesque *et al.*, 2003; Bates *et al.*, 2005) et leur capacité à utiliser les ressources disponibles (Levesque *et al.*, 2003; Lelièvre *et al.*, 2018) (Figure 13). Les interactions biotiques comme la prédation (Micheli *et al.*, 2002; Sancho *et al.*, 2005), la compétition pour l'espace et les ressources (Matabos *et al.*, 2008a), ou même les relations de facilitation ou d'inhibition (Mullineaux *et al.*, 2000, 2003; Henry *et al.*, 2008) peuvent également structurer la composition faunistique de ces écosystèmes à l'échelle d'un site ou d'un assemblage.

C'est donc un ensemble de facteurs interagissant aux différentes échelles spatio-temporelles, qui structurent la biodiversité associée aux écosystèmes hydrothermaux. Alors que nous commençons à avoir une bonne compréhension des facteurs structurant les commu-

nautés le long des dorsales continues telles que la dorsale médio-Atlantique (Cuvelier *et al.*, 2009; Girard *et al.*, 2020; Sarrazin *et al.*, 2020; Van Audenhaege *et al.*, 2022), la dorsale Est-Pacifique (Mullineaux *et al.*, 1998; Govenar *et al.*, 2005; Sancho *et al.*, 2005; Micheli *et al.*, 2002) ou la dorsale Juan de Fuca (Sarrazin *et al.*, 1999; Sarrazin et Juniper, 1999), l'organisation de la biodiversité et les facteurs structurant restent encore peu connus au niveau des systèmes hydrothermaux des bassins arrière-arc du Pacifique ouest.

## Mesure de la biodiversité en milieu hydrothermal

L'étude de la biodiversité en milieu hydrothermal se heurte à différents problèmes d'ordre méthodologique. Tout d'abord, l'effort d'échantillonnage de la faune est très hétérogène en fonction des zones géographiques (Beaulieu *et al.*, 2015). À titre d'exemple, les listes faunistiques des bassins arrière-arc de l'ouest Pacifique sont ainsi incomplètes en comparaison de celles de la dorsale du Pacifique est ou de la dorsale médio-Atlantique. Elles ne concernent que quelques bassins, principalement ceux de Lau et Manus au sud (Desbruyères *et al.*, 1994; Collins *et al.*, 2012), même si un effort récent est à souligner pour les bassins nord (Kojima et Watanabe, 2015; Watanabe et Kojima, 2015; Giguère et Tunnicliffe, 2021). D'autre part, ces listes sont souvent établies par des écologistes, en se basant sur les descriptions taxonomiques existantes et en regroupant les individus en morpho-espèces. Cela peut tendre à sous-estimer la biodiversité étant donné le nombre important d'espèces cryptiques – espèces qui ne présentent pas de différences morphologiques permettant de les délimiter mais une différenciation génétique importante – comme cela a été révélé par de nombreuses études moléculaires en milieu hydrothermal (Johnson *et al.*, 2008; Matabos *et al.*, 2008b, 2011; Plouviez *et al.*, 2009, 2019). Par ailleurs, certains groupes comme les gastéropodes présentent une forte plasticité morphologique des coquilles, pas toujours mentionnée dans les descriptions taxonomiques, pouvant conduire à des erreurs d'identification. C'est aussi le cas des changements morphologiques liés au développement ontogénique des organismes, également peu mentionnés.

Dans ce contexte, certaines régions géographiques, comme les bassins arrière-arc comportent un nombre important d'espèces non décrites ou en cours de description. Identifier les individus en couplant des approches s'appuyant sur une identification à partir de critères morphologiques et du barcode moléculaire peut être un moyen efficace pour obtenir une meilleure résolution taxonomique et ainsi mieux quantifier et analyser la biodiversité aux différentes échelles spatiales (Vrijenhoek, 2009).

## **Exploitation minière et impact potentiel**

Dans le Pacifique Sud-Ouest, les dépôts de sulfures polymétalliques issus de l'activité hydrothermale, riches en métaux d'intérêt commercial (e.g. zinc, argent et or) et en terres rares, en font une zone à fort intérêt minier (Hoagland *et al.*, 2010). La demande de permis et de concessions en vue de leur exploitation est croissante, que ce soit hors ou dans les ZEE (e.g. le projet de Nautilus Minerals dans le bassin de Manus). Bien qu'elle n'ait pas encore commencé, l'activité minière pourrait fortement impacter les communautés hydrothermales de manière directe et indirecte. Ainsi, l'exploitation provoquerait la destruction ou la fragmentation de l'habitat et une perte potentielle importante de biodiversité. Les panaches de sédiment créés par cette activité pourraient également affecter différents processus chimiques et biologiques pour la faune située à proximité, mais aussi pour les organismes vivant dans la colonne d'eau ou en surface lors de la remontée des sédiments ou lors de la séparation des minerais en surface (Boschen *et al.*, 2013; Gollner *et al.*, 2017; Boschen-Rose *et al.*, 2021) (Figure 14). En 2019, le gouvernement Fidjien a demandé un moratoire de 10 ans pour apporter des connaissances sur les environnements hydrothermaux de la région et mieux évaluer l'impact de l'exploitation minière sur ces écosystèmes (Kakee, 2020).

La connectivité des populations et le degré de variabilité de la biodiversité, de l'échelle locale à l'échelle régionale, sont des paramètres essentiels pour définir des mesures de gestion dans un écosystème faisant face à de telles pressions anthropiques. Au-delà d'un inventaire de la biodiversité hydrothermale, connaître les facteurs qui en contrôlent et

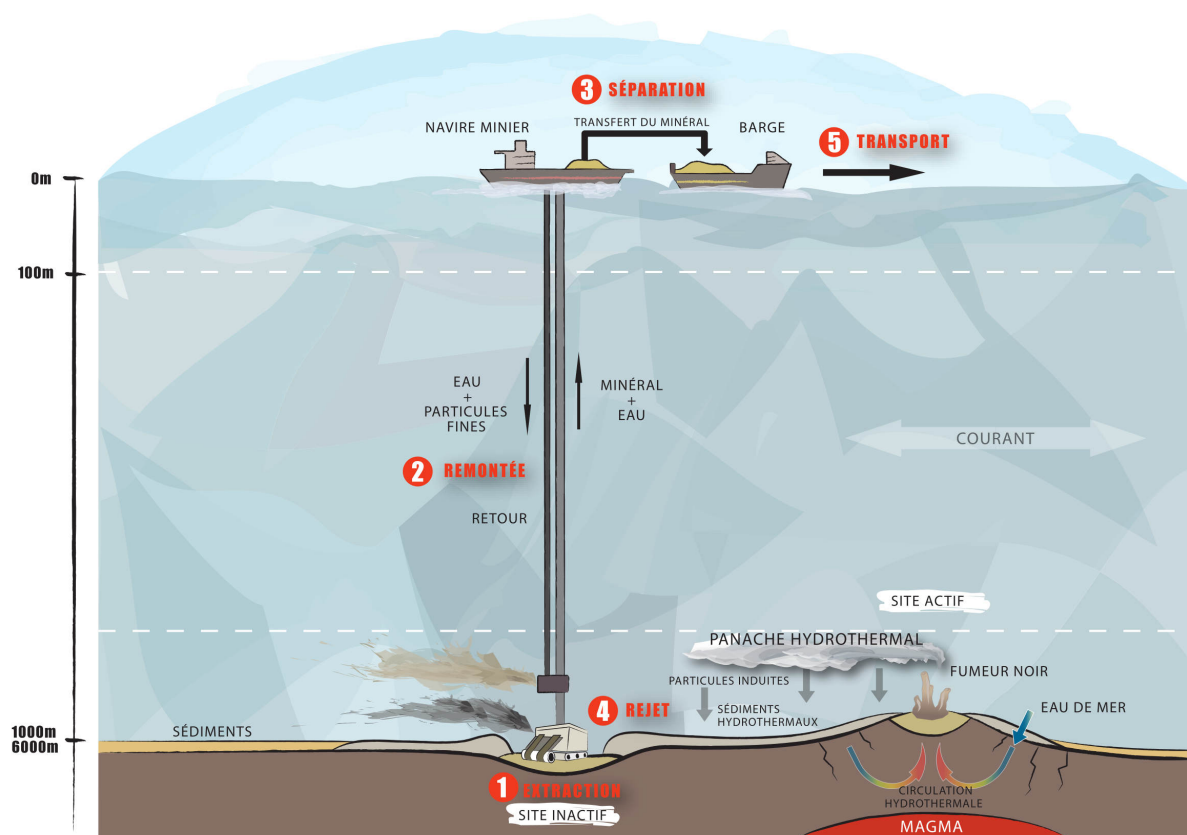


FIGURE 14 – Illustration de l’exploitation de sulfures polymétalliques issus de l’activité hydrothermale d’un site inactif. ©Capsule graphik

déterminent les patrons de distribution constitue un prérequis indispensable pour évaluer le degré de résilience des communautés face aux perturbations naturelles (e.g. éruptions, activité tectonique) ou anthropiques (e.g. exploitation minière).

Dans ce contexte, le projet ANR CERBERUS et la campagne Chubacarc qui lui était associée, ont pour but de mieux comprendre les causes de l'organisation de la biodiversité hydrothermale des bassins arrière-arc du Pacifique sud-ouest à l'échelle régionale. Pour ce faire, les principaux objectifs de l'ANR étaient : (1) la description de la diversité biologique, géochimique et géologique ; (2) la détermination des facteurs qui contrôlent la distribution des espèces et la partition de la biodiversité (facteurs biotiques et abiotiques) ; (3) la compréhension de l'histoire évolutive de la faune hydrothermale en lien avec la connectivité potentielle ; et (4) la modélisation des échanges larvaires et la prédiction de l'impact de l'exploitation minière.

## **Les objectifs de la thèse**

La forte structuration spatiale des bassins arrière-arc est la manifestation d'un contexte géodynamique complexe associé à des structures tectoniques et des produits magmatiques variables (Mahlke *et al.*, 2011). Il en résulte différents types de minéralisation correspondant à des fluides ayant des signatures chimiques différentes, ainsi que différents substrats. Nous émettons donc l'hypothèse que l'hétérogénéité existant aux différentes échelles va conduire à une mosaïque de niches écologiques et donc une forte hétérogénéité dans la distribution des espèces et des assemblages faunistiques, et qu'à petite échelle cette hétérogénéité impacte la croissance et la reproduction des espèces, elles-mêmes susceptibles d'influencer la résilience des populations et des communautés. L'objectif principal de cette thèse est donc de tester cette hypothèse à travers la description de la distribution de la biodiversité et des liens avec les caractérisations chimiques de l'habitat, et les traits d'histoire de vie des espèces aux échelles les plus pertinentes. Pour ce faire, cette étude se focalise sur trois habitats caractéristiques des sites actifs associés aux bassins arrière-arc (Desbruyères *et al.*,



2006b) : les moulières à *Bathymodiolus* et les agrégations de gastéropodes des genres *Ifremeria* et *Alviniconcha*. Plus spécifiquement, ce travail s'articule autour de trois objectifs :

1. Caractériser la diversité et la structure des assemblages faunistiques associés à ces trois habitats au sein et entre les bassins et déterminer les facteurs structurants ;
2. Réaliser un inventaire de la biodiversité associée aux sites actifs des bassins arrière-arc du Pacifique ouest ;
3. Caractériser la gamétogénèse et la dynamique des populations de deux espèces de gastéropodes caractéristiques des assemblages dominants, au sein et entre bassins, en fonction des différentes caractéristiques environnementales des habitats.

Pour répondre à ces différents objectifs, ce manuscrit est composé de trois chapitres. Le premier vise à confirmer les identifications des gastéropodes selon les critères morphologiques et à rechercher des espèces cryptiques potentielles (Poitrimol *et al.*, 2022). Il permet de comparer les patrons de distribution observés des espèces au sein de différentes familles à l'échelle de la zone d'étude, pour *in fine*, mieux comprendre la distribution des espèces au regard de la connectivité entre les bassins du sud-ouest Pacifique et de leur histoire géologique. Le deuxième chapitre a pour objectif de décrire la variabilité spatiale de la structure démographique et de la gamétogénèse des populations de deux espèces de gastéropodes largement répandues au sein des bassins arrière-arc du sud-ouest Pacifique, *Lepetodrilus schrolli* et *Shinkailepas tollmanni*, en relation avec la variabilité environnementale et l'habitat. Il vise ainsi à apporter des connaissances sur la biologie de la reproduction et la stratégie de recrutement de ces deux espèces, éléments clefs dans la compréhension de la résilience des populations face aux perturbations. Le dernier chapitre décrit la diversité de la macrofaune associée aux habitats à *Alviniconcha*, *Ifremeria* et *Bathymodiolus* et les changements de la composition faunistique des communautés à différentes échelles spatiales. A partir d'une partition de la diversité  $\beta$  et d'une analyse des relations entre les caractéristiques physico-chimiques des habitats et la composition en présence-absence des communautés, il met en lumière le rôle des principaux facteurs structurant aux différentes échelles.

# CHAPITRE 1

---

## Contrasted phylogeographic patterns of hydrothermal vent gastropods along South West Pacific : Woodlark Basin, a possible contact zone and/or stepping-stone

---

Cette partie fait l'objet d'un article accepté dans la revue PLoS ONE. Elle a été rédigée en collaboration avec : Éric Thiébaud, Claire Daguin-Thiébaud, Anne-Sophie Le Port, Marion Ballenghien, Adrien Tran Lu Y, Didier Jollivet, Stéphane Hourdez et Marjolaine Matabos.

## 1.1 Introduction

Among deep-sea environments, hydrothermal vents are found in different geological contexts including mid-oceanic ridges, back-arc basins, volcanic arcs, and active seamounts (Beaulieu *et al.*, 2013). Mineral deposits described in these environments contain high concentrations of metals that are of increasing interest to mining companies (Van Dover, 2011). Although not yet started, mining activities are expected to strongly impact vent communities which harbour highly specialized endemic fauna that relies on local microbial chemosynthesis (Tunnicliffe, 1991). The potential impacts are either direct or indirect, and include habitat destruction and complete removal of organisms living there, but also the creation of a sediment plume that will affect several chemical and biological processes for the underlying fauna (Boschen *et al.*, 2013; Gollner *et al.*, 2017; Boschen-Rose *et al.*, 2021). In the South West Pacific, the mineral richness of vent sites and their close proximity to the coastline led to a large number of exploration and exploitation mining leases in the region (Petersen *et al.*, 2016; Thaler et Amon, 2019). Because ecosystem resilience strongly depends on the vent fauna capacity to recolonize sites, informing future exploitation of massive sulphide mounds requires a good understanding of species distribution and how they are connected among sites (Van Dover *et al.*, 2020). Examining biogeographic patterns of the vent fauna at the scale of the western Pacific is thus essential to describe current species ranges.

Current biogeographical patterns reflect the constant reorganisation of ridges, changes in ocean floor geomorphology and opening/closing of basins, some of which erased by subduction processes, making their identification difficult (Plouviez *et al.*, 2013; Matabos et Jollivet, 2019). To date, eleven biogeographic provinces have been reported for the hydrothermal vent fauna based on taxon composition (Thaler et Amon, 2019), but their delineation faces several issues. First, these provinces are based on an incomplete inventory of the diversity of the hydrothermal vent fauna and species spatial distribution. Secondly, in addition to the decreasing number of taxonomists, it can be difficult for ecologists to identify with confidence vent species based on taxonomic descriptions that do not always report

## 1.1 Introduction

on morphological ontogenic changes and, in the case of mollusks, are often based on shell morphology of only a few specimens. In mollusks, the strong morphological plasticity of the shell (e.g. as reported by Chen *et al.* (2019a)) and the morphological stasis of species can lead to species misidentification (Vrijenhoek, 2009; Matabos *et al.*, 2011; Johnson *et al.*, 2015) and consequently the overestimation of the geographic range of species (Desbruyères *et al.*, 2006a). In addition, an increasing number of DNA-barcoding studies have highlighted the presence of well-separated cryptic vent species among ridge segments due to geographical barriers (Johnson *et al.*, 2008; Matabos *et al.*, 2008b, 2011; Plouviez *et al.*, 2009, 2019). Finally, heterogeneity in sampling efforts also leads to a lack of information on key zones to properly assess species range (Beaulieu *et al.*, 2015).

The South West Pacific region which forms an independent biogeographic province comprises relatively recent back-arc basins and volcanic arcs (i.e. < 10 million years old) that present various geological and geodynamic contexts (Hall, 2002; Schellart *et al.*, 2006; Bézos *et al.*, 2009). Although data on larval distribution and indirect estimates of larval dispersal provided by biophysical models of water masses circulation and phylogeographic analyses have contributed to a better understanding of population connectivity along mid-oceanic ridges (Breusing *et al.*, 2016, 2021; Mullineaux *et al.*, 2018), less is known for the back-arc basin discontinuous system. The complex geological history of these basins and present-day hydrodynamic regimes may limit larval dispersal within and between basins (Mitarai *et al.*, 2016). A modelling study reported various patterns of connectivity depending on the planktonic larval duration and the dispersal depth with: (1) a lack of connectivity between the Manus Basin and those of North Fiji and Lau with the Woodlark Basin acting possibly as a stepping-stone, and (2) a strong connection of nearby basins (Mitarai *et al.*, 2016). At intermediate spatial scales, this study suggested unidirectional larval transport from the Woodlark Basin to the Manus Basin and from the Lau Basin to North Fiji Basin. The Solomon and New Hebrides Basins, two newly-opened back-arc basins located between the Woodlark Basin and the North Fiji Basin, may also represent possible stepping-stones to connect eastern and western basins. Conversely, vent

fields are often well connected within a basin with no directionality.

Genetic studies on several gastropods and crustaceans based on cytochrome oxidase I gene (*CoxI*) and/or microsatellite loci confirmed the occurrence of variable phylogeographic patterns from large scale connectivity with only one panmictic population (Yahagi *et al.*, 2020) to strong regional genetic differences that separates the Manus Basin populations from those of the North Fiji and Lau Basins (Thaler *et al.*, 2011, 2014; Lee *et al.*, 2019). Contrasted geographic ranges have also been observed for closely related species. For example, amongst the three different species of the snail *Alviniconcha* found in the South West Pacific, *A. kojimai* and *A. boucheti* are largely distributed over the Manus, North Fiji, and Lau Basins, and the Futuna Volcanic Arc, while *A. strummeri* distribution is limited to the Futuna Arc and the Lau Basin (Johnson *et al.*, 2015; Laming *et al.*, 2020; Castel *et al.*, 2022). The *Lepetodrilus schrolli* species complex is another example of taxa composed of cryptic species in the region (Johnson *et al.*, 2008), with *Lepetodrilus schrolli* only found in the Manus Basin while *Lepetodrilus* aff. *schrolli* is present in both the North Fiji/Lau and Manus Basins, but with a strong genetic differentiation between its eastern (North Fiji/Lau Basins) and western (Manus Basin) populations (Plouviez *et al.*, 2019). These results question the link between the Manus Basin and the more eastern basins including the potential barriers to dispersal or the presence of intermediate stepping-stone sites.

In the South West Pacific, most studies on the diversity of vent ecosystems have focused on a few basins, i.e. the Manus, Lau and North Fiji Basins, while some other active areas are insufficiently known, in particular the Woodlark Basin, or the Solomon and Vanuatu (ex New Hebrides) Trench (Mitarai *et al.*, 2016). Very recently, hydrothermal vent communities have been discovered and described for the first time in the Woodlark Basin (Boulart *et al.*, 2022). These communities are not profoundly different from communities reported in other western Pacific back-arc basins. Preliminary barcoding analyses of the main engineer species suggested that the Woodlark Basin may act as a biodiversity dispersion centre for the hydrothermal vent fauna and a crossroad between the East/West basins in this Pacific

## 1.2 Materials and Methods

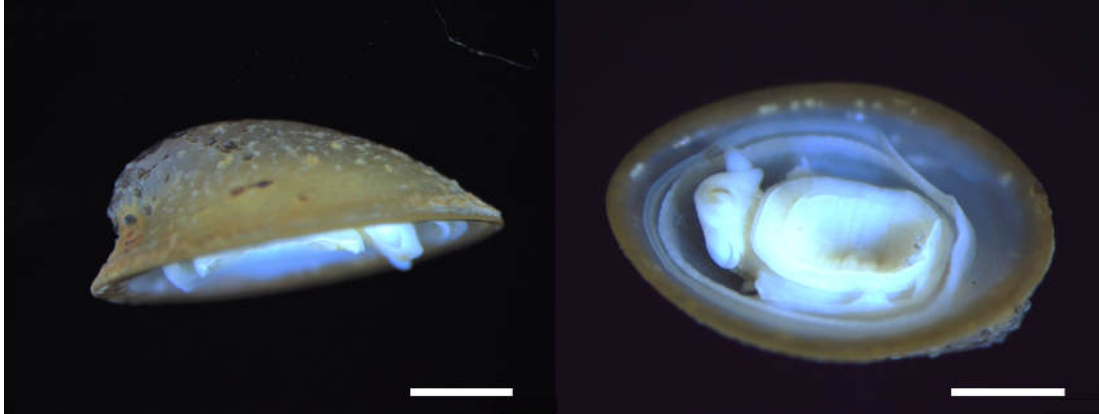


Figure 1.1 – Illustrations of a *Lepetodrilus shcrolli* individual conserved in ethanol. White scalebar : 1 mm.

region. In this context, the aims of our study were to: (1) perform a barcoding analysis to confirm morphological descriptions of gastropod species and identify potential cryptic species; (2) compare the phylogeographic patterns of a range of families at the regional scale of the South West Pacific. The final aim of the study was therefore to contribute to a better understanding of species distribution and connectivity across the Manus, Woodlark, North Fiji, and Lau back-arc basins, and the Futuna Volcanic Arc. We focused on six genera from four families of vent gastropods widely distributed in the region: the Lepetodrilidae *Lepetodrilus* (Figure 1.1), the Neomphaloidae *Symmetromphalus* and *Lamellomphalus* (Figures 1.2 and 1.3), the Phenacolepadidae *Shinkailepas* (Figures 1.4 and 1.5), and the Provannidae *Desbruyeresia* and *Provanna* (Figures 1.6 and 1.7).

## 1.2 Materials and Methods

### 1.2.1 Ethics statement

Gastropods used in this study were collected with necessary authority permissions of the foreign countries. Permission for sampling in Exclusive Economic Zones (EEZ) was issued by the Papua New Guinea, The Republic of Fiji and Kingdom of Tonga. We obtained the agreement to sample in Wallis et Futuna waters by the Haut Commissariat à la République

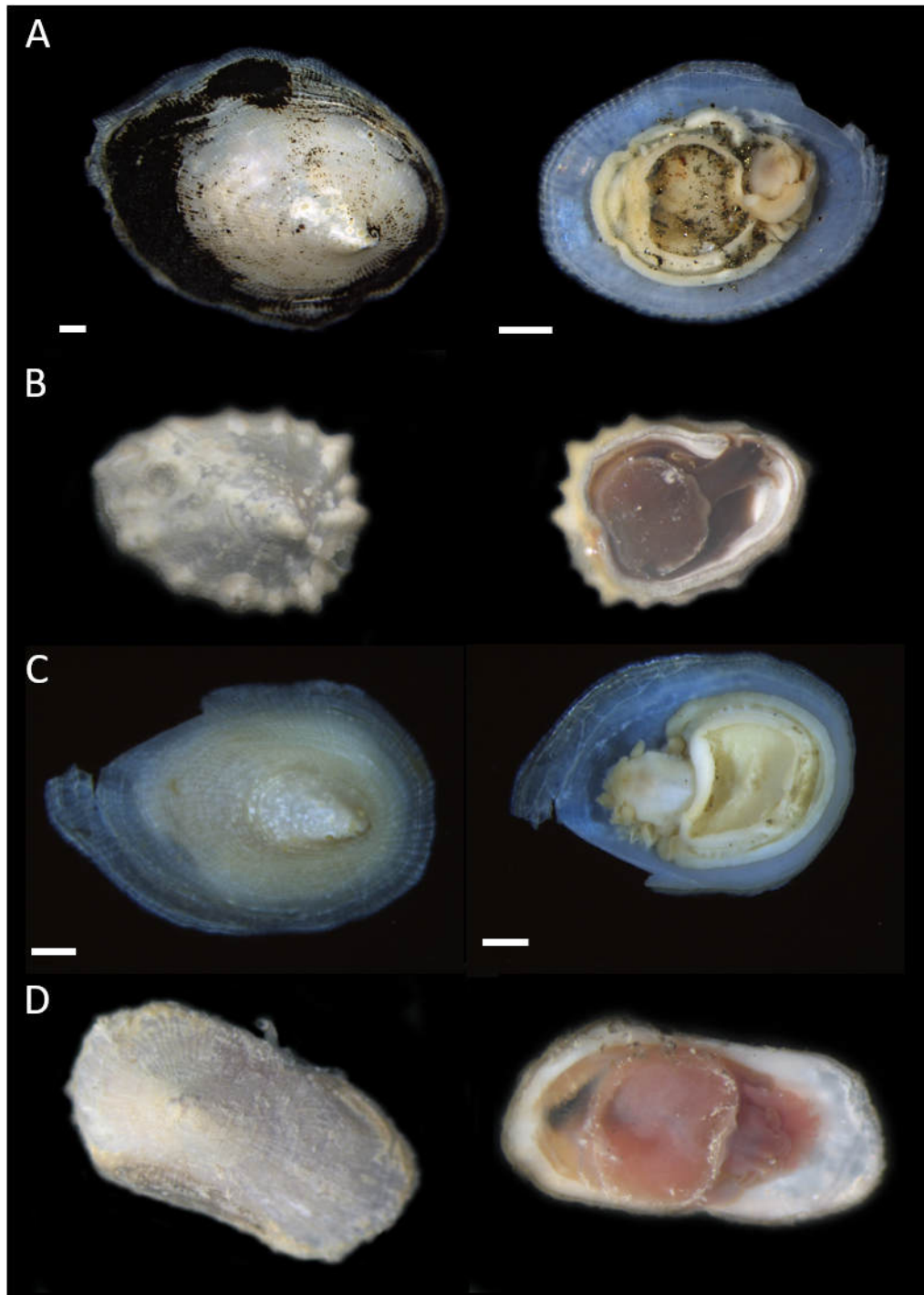


Figure 1.2 – Illustrations of *Symmetromphalus* individuals from Woodlark (A), Manus (B-C) and Lau Basins (D). A and C are conserved in ethanol, B and D were pictured alive. White scalebar : 1 mm.

1.2 Materials and Methods

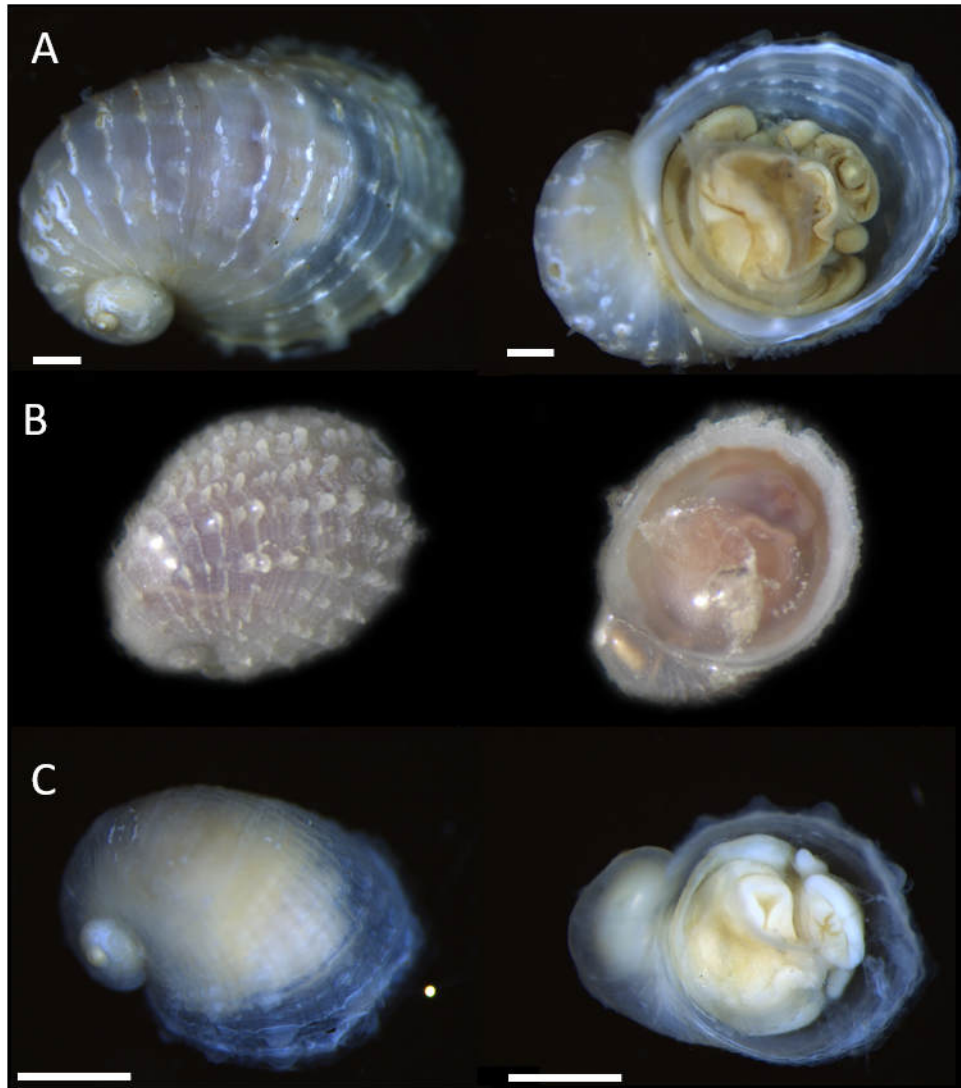


Figure 1.3 – Illustrations of *Lamellomphalus* individuals from Manus Basin (A) and Futuna Volcanic Arc (B). A and C are conserved in ethanol, B was pictured alive. White scalebar : 1 mm.



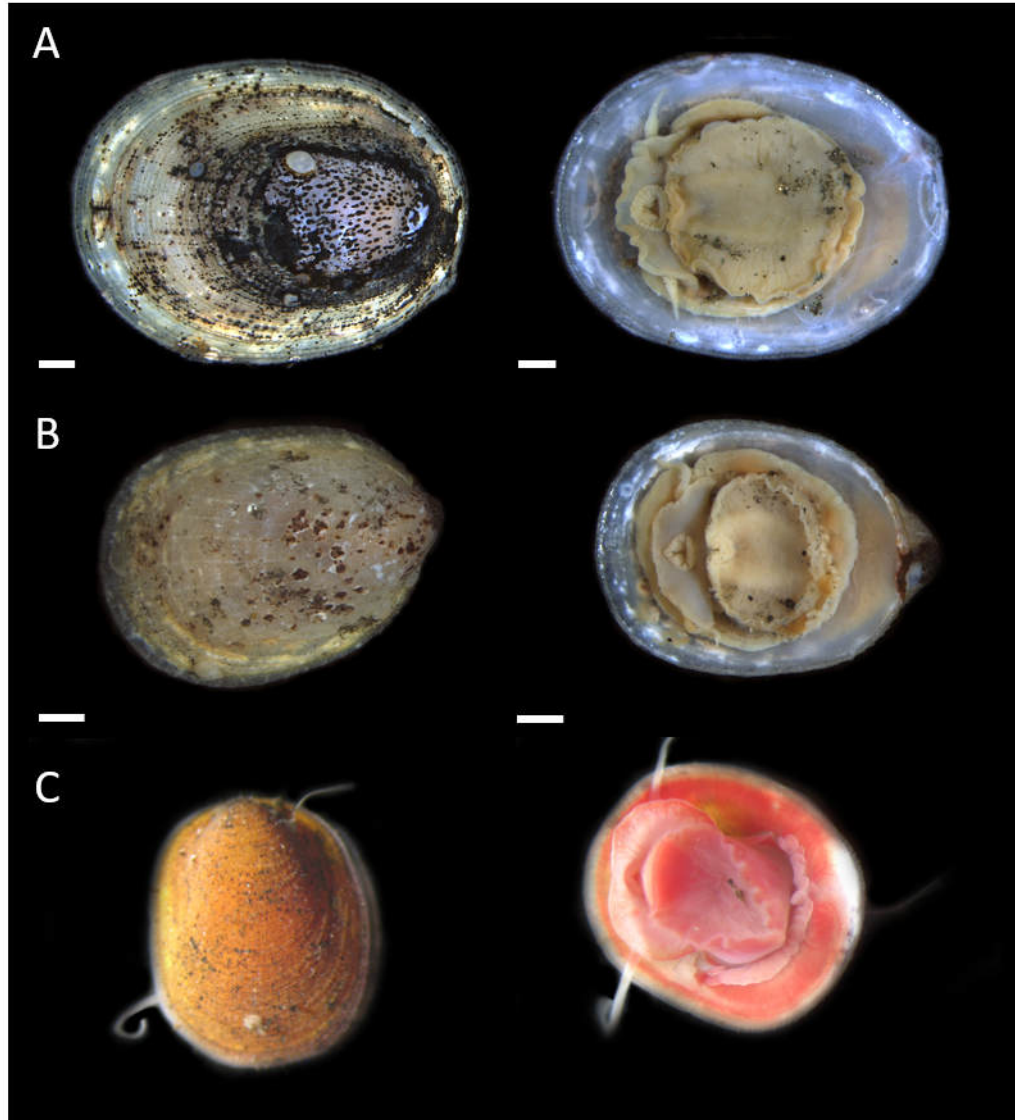


Figure 1.4 – Illustrations of *Shinkailepas 'tufari'* individuals from Woodlark (A), Manus (B) and Lau Basins (C). A and B are conserved in ethanol, C was pictured alive. White scalebar : 1 mm.

1.2 Materials and Methods

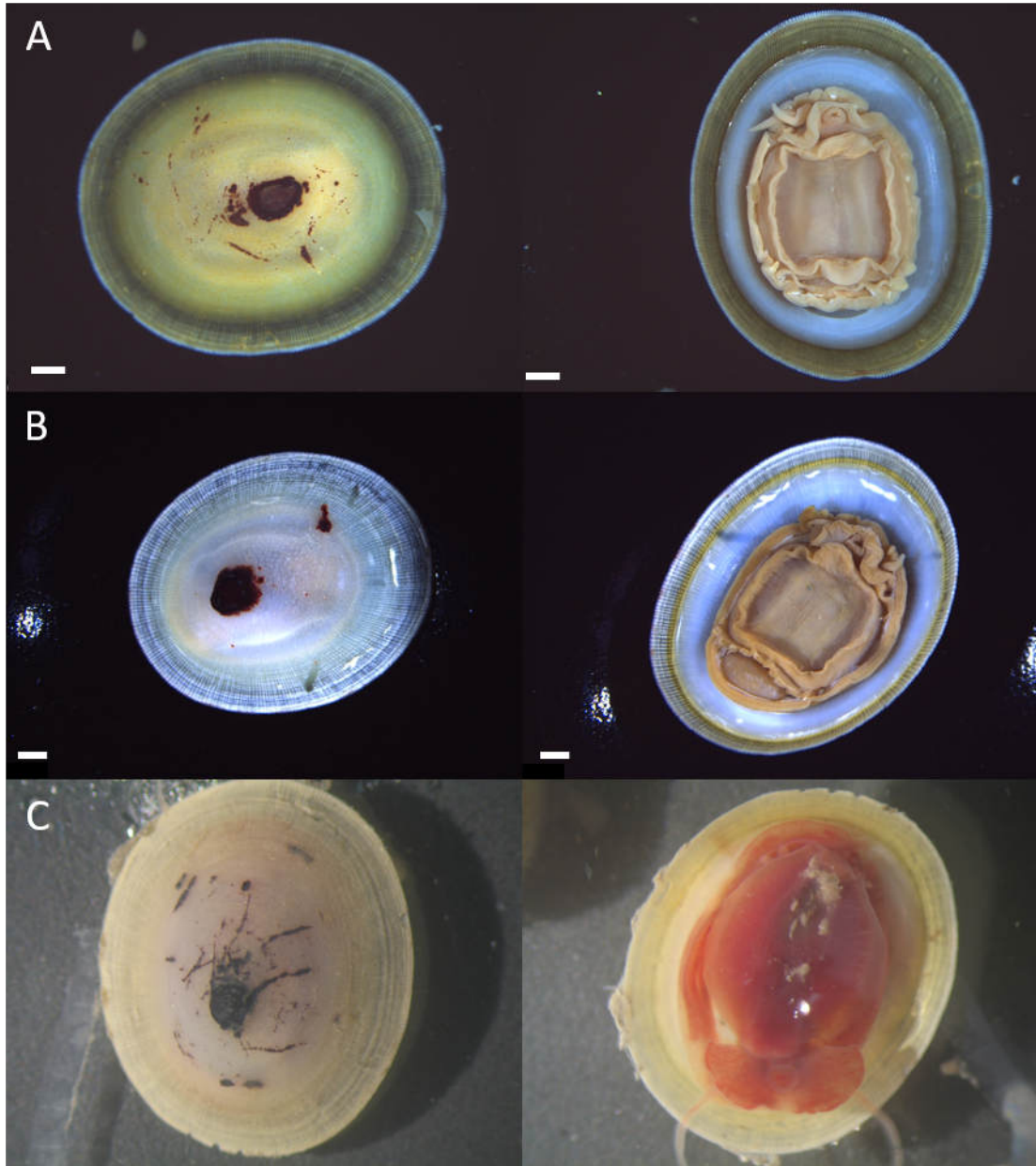


Figure 1.5 – Illustrations of *Shinkailepas tollmanni* individuals from the Futuna Volcanic Arc (A), the Manus (B) and Lau Basins (C). A and B are conserved in ethanol, C was pictured alive. White scalebar : 1 mm.

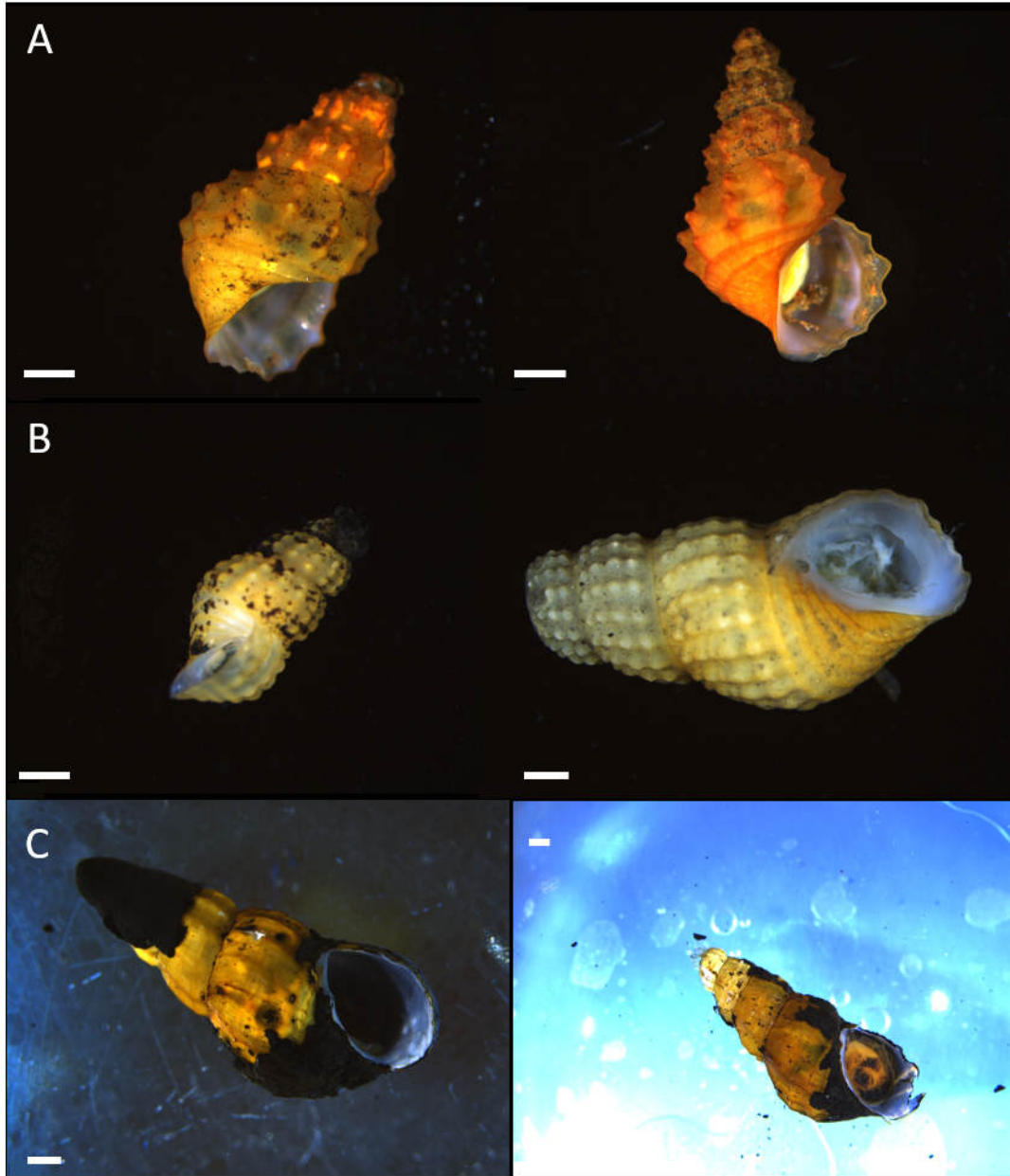


Figure 1.6 – Illustrations of *Desbruyeresia* individuals conserved in ethanol: *D. cancellata* (A), *D. melanioides* (B) and *D. costata* (C). White scalebar : 1 mm.

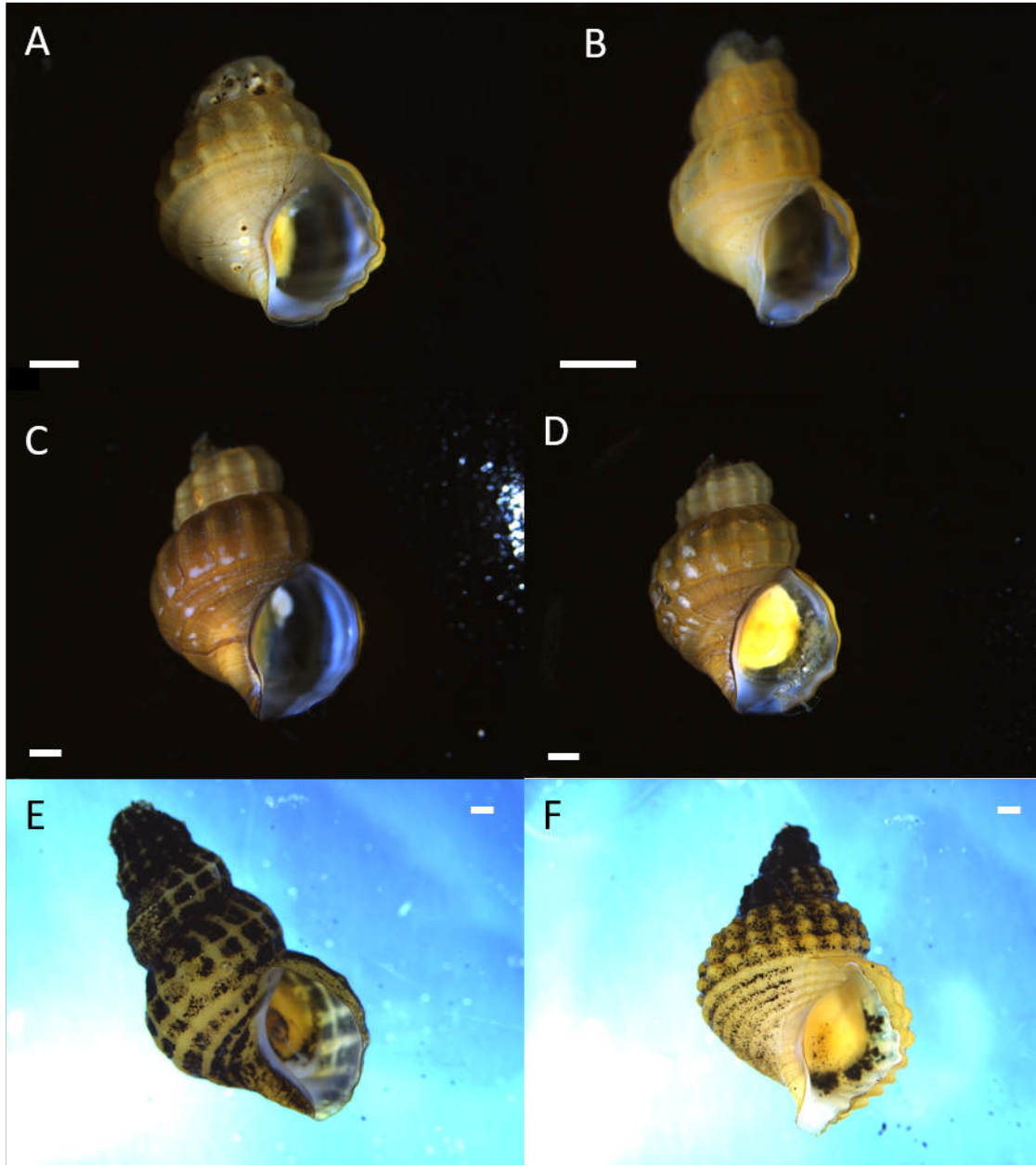


Figure 1.7 – Illustrations of *Provanna* individuals conserved in ethanol from the Lau (A), Manus (B-E) and Woodlark Basins (F). White scalebar : 1 mm.

in New Caledonia and the Préfecture in Wallis and Futuna. We also made an official request under the Nagoya agreements for the use of samples for genetic academic researches.

### 1.2.2 Sampling

A wide-range sampling of vent species was conducted during the CHUBACARC cruise held between March and June 2019 in the southwestern Pacific back-arc basins aboard the French research vessel L'Atalante (Hourdez et Jollivet, 2019). Vent fauna was collected in four distinct habitats defined based on engineer species along a gradient of venting (i.e. *Bathymodiolus* beds, *Ifremeria* aggregations, *Alviniconcha* aggregations, *Arcovestia* clumps), and representative of the sampled sites. Collections were made using the hydraulic arm and the suction sampler of the ROV *Victor6000* and transferred in either insulated bioboxes or the suction sampler device containers. One to five vent fields were sampled within each basin, representing a total of twelve vent fields in the Lau, North Fiji, Manus and Woodlark Basins, and the Futuna Volcanic Arc (Figure 1.8A-B, Table 1.1). Samples were washed through a 250 µm sieve and gastropods from six genera (i.e. *Lepetodrilus*, *Symmetromphalus*, *Lamellomphalus*, *Shinkailepas*, *Desbruyeresia* and *Provanna*) sorted on board and stored in 96% ethanol until DNA extraction. Individuals were then morphologically identified to the lowest possible taxonomic level using species taxonomic morphological descriptions (Beck, 1992b,a, 1993; Warén et Bouchet, 1993; Desbruyères *et al.*, 2006b; Chen *et al.*, 2019b; Zhang et Zhang, 2017). Additional specimens from the Kermadec Volcanic Arc were included for some groups. These specimens were collected during the Hydrothermadec cruise (R/V Sonne, chief scientist Andre Kochinsky).

### 1.2.3 Molecular methods

For each species, a subset of specimens was selected from each location where they were present (Figure 1.8B Table 1.1). Except for *Shinkailepas tollmanni* and *Lepetodrilus schrolli* and *L. aff. schrolli* individuals for which DNA extraction was performed on board

## 1.2 Materials and Methods

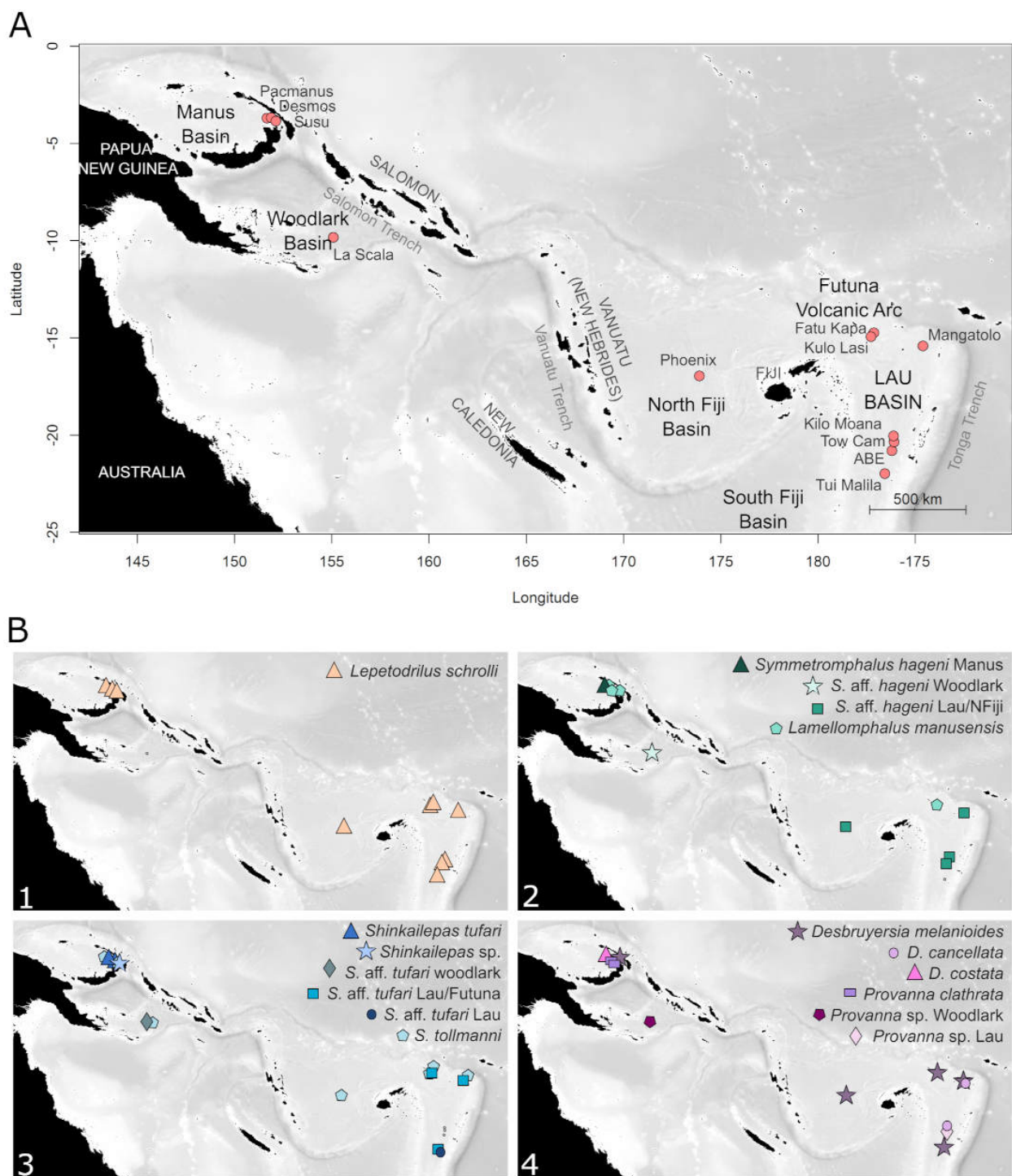


Figure 1.8 – Back-arc-basins sampling area in the South West Pacific (A) and sampling location of the various gastropod species from the Lepetodrilidae (B1), Neomphaloidae (B2), Phenacolepadidae (B3) and Provannidae (B4) families. Red dots represent sampled fields.

Table 1.1 – Location of gastropods sampled along the South West Pacific back-arc basins and number of individuals used for DNA barcoding.

Basin	Vent field	Coordinates	Number of individuals						
			<i>Lepetodrilus schrolli</i> complex	<i>Symmetromphalus hageni</i> complex	<i>Lamellomphalus manusensis</i>	<i>Shinkailepas tufari</i> complex	<i>Shinkailepas tollmanni</i>	<i>Desbruyeresia spp.</i>	<i>Provanna spp.</i>
Manus	Pacmanus	03°43'S 151°40'E	6	9	5	4	15	5	-
	Desmos	03°41'S 151°51'E	16	-	3	-	-	-	5
	Susu	03°48'S 152°06'E	10	-	16	17	11	1	5
Woodlark	La Scala	09°48'S 155°03'E	22	8	-	9	8	-	8
North Fiji	Phoenix	16°57'S 173°55'E	4	8	-	-	8	5	-
Futuna	Fatu kapa	14°45'S 177°10'W	4	-	-	1	10	1	-
	Kulo Lasi	14°56'S 177°15'W	26	-	5	-	9	-	-
Lau	Mangatolo	15°24'S 174°39'W	3	1	-	1	14	5	-
	Kilo Moana	20°03'S 176°08'W	-	-	-	-	-	3	-
	Tow Cam	20°19'S 176°08'W	8	4	-	-	-	4	7
	ABE	20°45'S 176°11'W	3	3	-	-	-	-	-
	Tui Malila	21°59'S 176°24'W	5	-	-	8	-	-	-
Kermadec*	Brothers Caldera	34°51'S 179°03'E	4	-	3	-	-	-	-

\*Samples collected from Hydrothermadec cruise

## 1.2 Materials and Methods

just after sampling (and for which the shell was further stored in ethanol after tissue lysis for further identification and possible shell biometry), a picture of the full specimen (shell and soft tissues) was taken for each individual using a DMC 4500 camera mounted on a LEICA M165 C stereoscopic microscope. DNA was extracted from the foot or the whole body depending on the individual size. If possible, the head and radula were saved to refine species identification based on morphology. For *S. tufari*, *Provanna* spp., *Desbruyeresia* spp., *Symmetromphalus* sp., and *Lamellomphalus*, DNA was extracted using NucleoSpin®96 Tissue kit according to the manufacturer's instructions, and eluted in 100 µl of elution buffer. A CTAB/PVP extraction procedure (derived from Doyle et Doyle (1987): see Jolly *et al.* (2003)) was used for *S. tollmanni* and *Lepetodrilus* sp., and DNA pellets were resuspended in 100 µl of Tris-HCl 5 mM pH 8 buffer. For each taxon, a fragment of the *Cox1* mitochondrial gene was amplified using the universally-applicable primers LCO1490 and HCO2198 (Folmer *et al.*, 1994). In case these primers did not yield a clear amplification signal, degenerate versions of these primers, which accounted for the high level of polymorphism often found in marine mollusks (C. Daguin-Thiébaud, unpublished) were also used (Table 1.2). DNA amplification was performed with a T100 thermocycler (Biorad) by using a 25 µl reaction volume containing DNA, 1X GoTaq®Flexi Buffer (Promega), 0.05 mg/µl of Bovine Serum Albumin, 2 mM MgCl<sub>2</sub>, 0.12 mM of each dNTP, 600 nM of each primer, 0.5 U of GoTaq®G2 Flexi DNA polymerase (Promega) and ultrapure water. Polymerase Chain Reactions were performed as follows: (1) a 3 min initial denaturation at 94°C; followed by (2) 36 cycles including a 30 s denaturation at 94°C, a 30 s primer annealing at 46°C and a 1 min elongation at 72°C; and (3) a final 10 min elongation at 72°C. The PCR products were then sent to Eurofins Genomics (Ebersberg, Germany) for bidirectional Sanger sequencing. Raw sequence electrophoregrams were carefully checked with Codon Code Aligner v5.1.5 before forward and reverse sequences were assembled, aligned, edited and trimmed using BioEdit v7.2.5 (Hall, 1999). All sequences with geographic details are available in the GenBank database with accession numbers OK635351-374, OK635388-416, OK635475-499, OK635506-573, OK576792-867, OM264371-375, OM791835-837, OM865896-6006 (see also Table 1.3).



Table 1.2 – Primers used in the present study for each taxon.

Taxon	Primers	Primer sequences (5' - 3')	References
<i>S. tufari</i> complex <i>S. tollmanni</i>	LCO1490	GGTCAACAAATCATAAAGATATTGG	(Folmer <i>et al.</i> , 1994)
<i>Symmetromphalus</i> <i>Lamellomphalus</i>	HCO2198	TAAACTTCAGGGTGACCAAAAAATCA	
<i>Desbruyeresia</i>	LCO1490bathy*	GTTCTACAAAYCATAAAGAYATTGG	
<i>Provanna</i>	HCO2198bathy*	TAAACYTCTGGATGMCCRAARAAYCA	This study
<i>Lepetodrilus</i>	LCO1490lepetofam	TTTCMACTAAYCATAAAGACATYGG	This study
	LCO2198schrolnux	TANACTTCTGGRTGRCCRAARAATCA	This study

\* in addition to the Folmer original primers, for some samples. See information within Genbank submitted sequences.

#### 1.2.4 Phylogenetic analysis

For each genus, a phylogenetic tree was constructed using the Neighbor-joining method and Kimura 2-parameters (K2P) genetic distances with 1000 bootstraps to assess the node robustness with MEGA X software v10.2.4 (Kumar *et al.*, 2018). A Maximum-Likelihood (ML) tree was also constructed using the same parameters. These tree reconstructions were done with the aim of comparing our sequences to previously published sequences from the vent gastropods of the West Pacific to infer phylogenetic relationships between lineages (Table 1.3). To do so, the sequences sometimes required to be cut to match the published sequences. Our sequences were submitted to the GenBank Basic Local Alignment Search Tool (BLAST, <https://blast.ncbi.nlm.nih.gov>) to confirm the morphological identification of each individual. Due to the lack of *Cox1* reference sequences in Genbank for *Provanna*, the taxonomic identification of some of our specimens was limited to the genus level. To infer the most parsimonious links between mitochondrial haplotypes of different geographic locations within each species or genus, haplotype networks were constructed from our sequences using the Minimum Spanning Network method with the PopART software (Bandelt *et al.*, 1999) (<http://popart.otago.ac.nz>, v4.8.4). Mean genetic distances were calculated between lineages previously identified with NJ and ML trees and haplotype networks using the K2P model of substitutions with 1000 bootstraps using MEGA X software. The Automatic Barcode Gap Discovery method (ABGD),

### 1.3 Results

a method used for species delimitation (Puillandre *et al.*, 2012), was used with the same model of substitutions and default settings to assess the occurrence of potential cryptic species within each taxa. Haplotype ( $Hd$ ) and nucleotide ( $\pi$ ) diversities of each lineage were inferred using DNAsp v5 (Librado et Rozas, 2009). To test the hypothesis of demographic changes, the null hypothesis of the mutation-drift equilibrium was tested using Tajima's  $D$  and the Fu and Li's  $F$  statistics (Fu et Li, 1993). Distributions of pairwise differences between sequences were established for lineages containing more than 10 sequences, and the observed size-frequency histograms were compared using a Chi-square goodness of fit test on counts to the distributions of differences expected under either a constant population size model or an expansion model (Rogers et Harpending, 1992). Populations satisfying both neutrality tests and a significant fit to the expansion model were considered as presently expanding and the expansion rate was estimated by the statistic  $\tau$ . This statistic can be linked to the time since population expansion using the formula:  $\tau = 2 \mu T$  (Harpending, 1994). In addition, global and/or pairwise  $Fst$  values were computed from haplotype frequencies estimated within mitochondrial clades (i.e. cryptic species) or geographic groups (i.e. metapopulations) when possible and tested against zero (no differentiation) with 1000 permutations of haplotypes between groups using DNAsp v5 (Librado et Rozas, 2009).  $Dxy$  distances and  $Da$  net nucleotide divergences between phylogenetic clades were also estimated with the same software.

## 1.3 Results

A total of 340 *Cox1* sequences were obtained from individuals belonging to the four gastropods families and six genera with fragment lengths varying from 469 to 636 base-pair (bp) (Table 1.11). Species with dense populations such as *Lepetodrilus schrolli* or *Shinkailepas tollmani* were sub-sampled from the whole collection of sampled individuals. Lineages highlighted by the trees produced by the NJ and ML methods being the same, only NJ trees are shown in the results. ML trees are available in supplementary material (see Appendix A.1).

Table 1.3 – List of accession numbers from gastropod individuals used for phylogenetic trees.

Genus	GenBank Accession numbers	References
<i>Lepetodrilus</i>	OM865896-6006	This study
	EU306431-444, EU306451-456	Johnson <i>et al.</i> , 2008
	MZ509428-430, MW497312-314, MW807763-765	Giguère et Tunnicliffe, 2021
<i>Symmetromphalus</i>	OK635541-573	This study
	MW497416	Giguère et Tunnicliffe, 2021
<i>Lamellomphalus</i>	OK635388-416	This study
	OM791835-837	This study
	KY399885	Zhang et Zhang, 2017
	AB330999	Heß <i>et al.</i> , 2008
<i>Shinkailepas</i>	OK635506-540, OM264371-375	This study
	OK576792-867	This study
	LC549687-LC549719	Yahagi <i>et al.</i> , 2020
	LC215328-331, LC387564	Fukumori <i>et al.</i> , 2019
	LC215293-295	Yahagi <i>et al.</i> , 2019
	LC178463-464	Yahagi <i>et al.</i> , 2017
MW807774-777, MW497415	Giguère et Tunnicliffe, 2021	
<i>Desbruyeresia</i>	OK635351-374	This study
	GQ290596	Johnson <i>et al.</i> , 2010
	MW497309-311	Giguère et Tunnicliffe, 2021
	MK560876	Chen <i>et al.</i> , 2019
LC090201-203	Chen <i>et al.</i> , 2016	
<i>Provanna</i>	OK635475-499	This study
	LC095875	Chen <i>et al.</i> , 2018
	GQ290594-595	Johnson <i>et al.</i> , 2010
	MK790057-059	Linse <i>et al.</i> , 2019
	MK560877	Chen <i>et al.</i> , 2019
AB810200-216	Ogura <i>et al.</i> , 2018	

### 1.3 Results

Table 1.4 – Variation among *CoxI* nucleotides sequences for each taxon and lineages.

Lineages	Ind.	Seq. (bp)	<i>H</i>	<i>h</i>	<i>S</i>	<i>s</i>	<i>Hd</i> ( $\pm$ sd)	$\pi$ ( $\pm$ sd)
<i>Lepetodrilus schrolli</i> complex	107	620	65	52	66	29	0.955 $\pm$ 0.014	0.0162 $\pm$ 0.0005
<i>L. schrolli</i>	45		31	22	38	24	0.977 $\pm$ 0.011	0.0071 $\pm$ 0.0004
<i>L. aff. schrolli</i>	62		34	30	42	27	0.877 $\pm$ 0.038	0.0052 $\pm$ 0.0007
<i>Symmetromphalus</i>	33	629	20	15	58	5	0.947 $\pm$ 0.023	0.0353 $\pm$ 0.0027
<i>S. hageni</i> Manus	9		7	6	7	7		
<i>S. aff. hageni</i> Woodlark	8		3	2	2	2		
<i>S. aff. hageni</i> Lau/NFiji	16		10	7	9	6	0.917 $\pm$ 0.049	0.0030 $\pm$ 0.0004
<i>Lamellomphalus manusensis</i>	29	629	5	3	8	4	0.416 $\pm$ 0.107	0.0023 $\pm$ 0.0007
<i>L. manusensis</i> Manus	24		3	2	2	2		
<i>L. manusensis</i> Futuna	5		2	1	2	2		
<i>Shinkailepas tufari</i> complex	40	636	25	19	119	11	0.942 $\pm$ 0.027	0.0581 $\pm$ 0.0048
<i>S. tufari</i>	19		9	6	11	7	0.778 $\pm$ 0.096	0.0024 $\pm$ 0.0006
<i>Shinkailepas</i> sp.	2		2	2	4	4		
<i>S. aff. tufari</i> Woodlark	9		6	4	5	4		
<i>S. aff. tufari</i> Lau/Futuna	3		1	0	0	0		
<i>S. aff. tufari</i> Lau	7		7	7	16	11		
<i>Shinkailepas tollmanni</i>	75	636	49	42	57	42	0.961 $\pm$ 0.014	0.0052 $\pm$ 0.0004
<i>Desbruyeresia</i>	24	469	20	17	85	7	0.982 $\pm$ 0.018	0.0757 $\pm$ 0.0072
<i>Desbruyeresia melanioides</i>	14		12	11	22	14	0.967 $\pm$ 0.044	0.0098 $\pm$ 0.0015
<i>Desbruyeresia cancellata</i>	5		4	3	7	6		
<i>Desbruyeresia costata</i>	5		4	3	5	4		
<i>Provanna</i>	25	530	19	15	55	3	0.973 $\pm$ 0.019	0.0484 $\pm$ 0.0032
<i>Provanna clathrata</i>	10		9	8	11	7	0.978 $\pm$ 0.054	0.0057 $\pm$ 0.0011
<i>Provanna</i> sp. Woodlark	8		5	3	5	4		
<i>Provanna</i> sp. Lau	7		5	4	4	4		

Ind: number of individuals; *H*: number of haplotypes; *h*: number of unique haplotypes; *S*: number of segregating sites; *s*: number of singleton sites; *Hd*: haplotype diversity;  $\pi$ : nucleotide diversity.

### 1.3.1 *Lepetodrilidae*

The phylogenetic tree based on *Lepetodrilus Cox1* sequences (Figure 1.9A) confirmed the occurrence of two strongly supported distinct lineages in the South West Pacific: one with all our samples from the Lau Basin, Futuna Arc and the North Fiji Basin clustering with *L. aff. schrolli* sequences previously obtained by Johnson *et al.* (2008) from the same basins, and another one with all our samples from the Manus Basin, along with *L. schrolli* sequences obtained by the same authors from the Manus Basin. Interestingly, sequences of individuals from the Woodlark Basin were sub-divided into these two distinct lineages, indicating that both lineages are sympatric at this site. As observed in Johnson *et al.* (2008), sequences identified as *L. aff. schrolli* from the Mariana Trough formed a third lineage which was much more divergent than the two others. These different lineages are clearly different from the other species of *Lepetodrilus* reported in the northwestern Pacific, *L. nux*.

Sequences analysis of the 107 specimens from the *Lepetodrilus schrolli* complex of cryptic species revealed 66 segregating sites, which included 37 parsimony-informative sites and 29 singletons across the 620 bp fragment. All mutations were synonymous. The haplotype network clearly separated lineages between the Manus Basin and the eastern basins (i.e. Lau Basin, Futuna Arc and North Fiji Basin), with the Woodlark Basin individuals belonging to both lineages (Figure 1.10). The two lineages corresponding to two geographic metapopulations were strongly and highly significantly differentiated with *Fst* and *Dxy* equal to 0.772 and 0.027, respectively. At least 4 haplotypes sampled at the Futuna Arc and the Lau Basin displaying a central position in the haplotype network provided an intermediate but specific signature (i.e. a few diagnostic mutations) between the two lineages. Due to these four later individuals, the ABGD analysis did refute that these two lineages correspond to two distinct species (Prior maximal distance  $P = 7.7410^{-3}$ ; Barcode gap distance = 0.024) but the distribution of pairwise differences clearly showed two distinct Gaussian distributions with a small overlap between the intra- and interlineage divergence levels (Figure 1.11A).

The lineage *L. aff. schrolli* haplotype network exhibited a star-like shape with two

### 1.3 Results

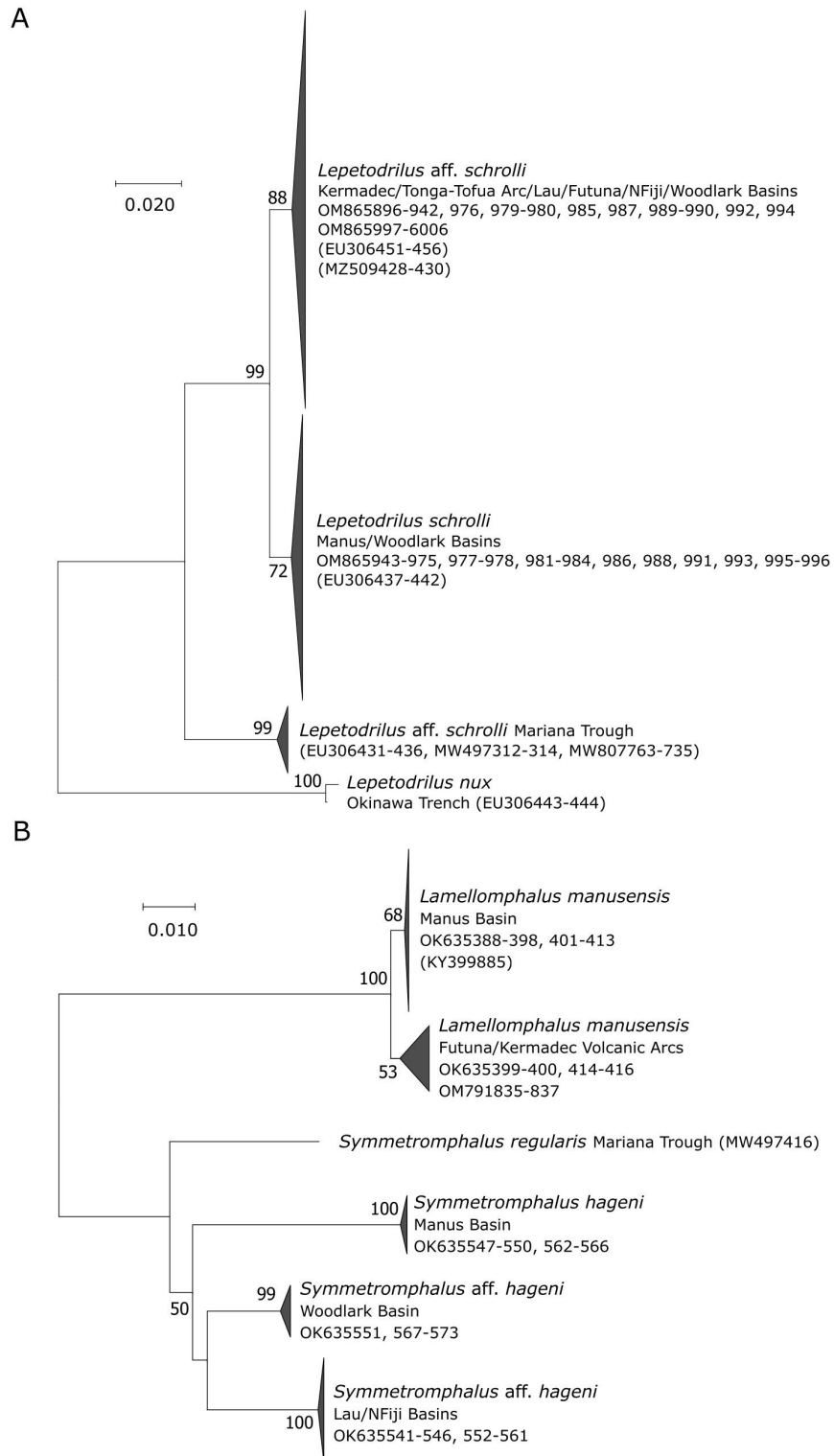


Figure 1.9 – *Cox1* Neighbor-Joining trees inferred from *Cox1* sequences from *Lepetodrilus* (A) and *Symmetromphalus* and *Lamellomphalus* (B) within their family. Number at nodes indicates the proportion of occurrences in 1000 bootstraps; percentages below 50% are not shown. Genbank accession numbers of the present study and published sequences are indicated. Published sequences are in brackets. Sequence lengths: (A) = 496 bp, (B) = 541 bp.

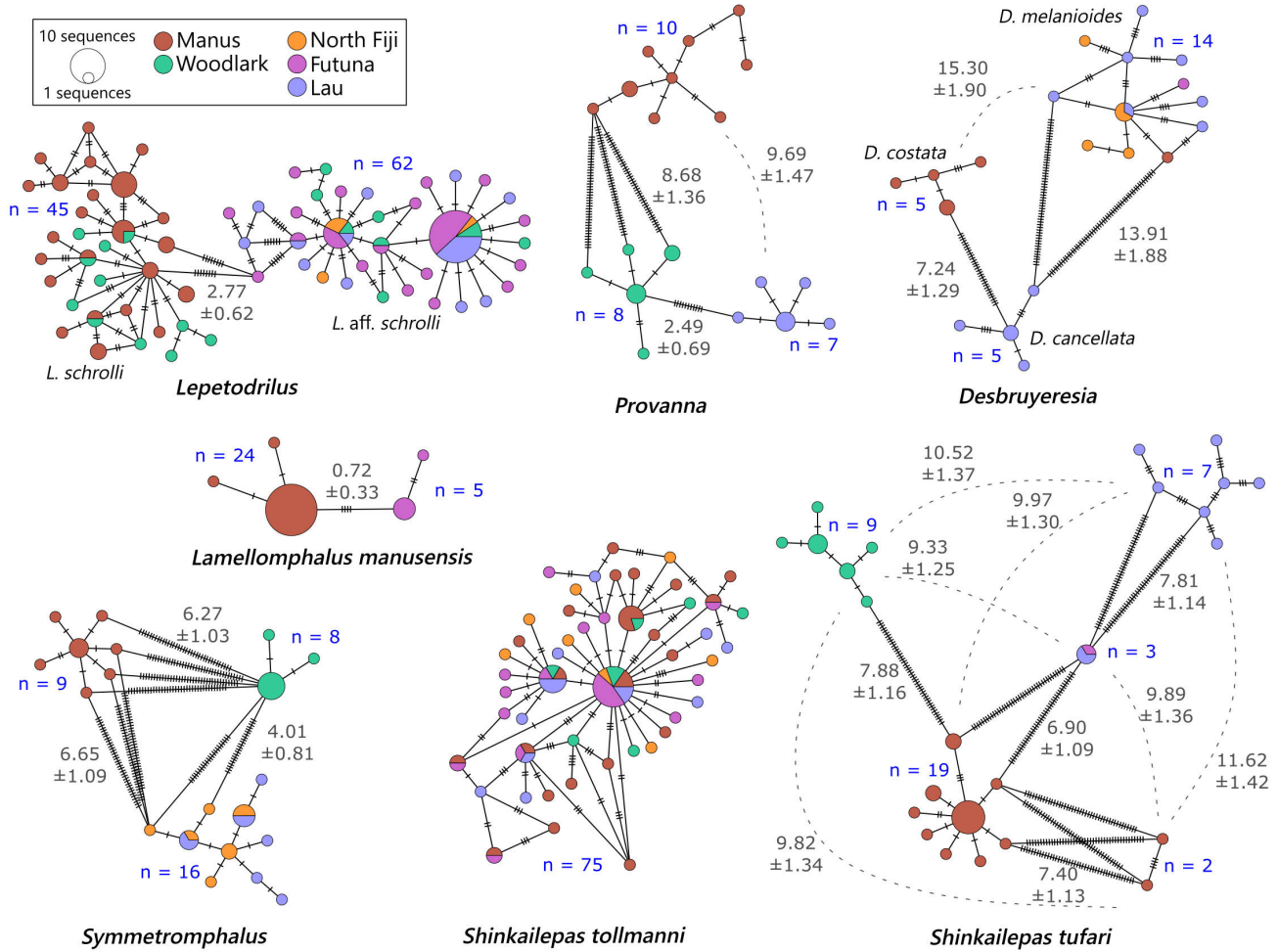


Figure 1.10 – Minimum Spanning Networks based of *CoxI* haplotypes from each taxon. Circles represent the different haplotypes; their diameter indicates the number of individuals with the same haplotype and colour their location. Mutational steps are symbolised by dashes. n = number of sequences within each lineage. Grey numbers represent the divergence between the different lineages (mean K2P% ± Sd).

### 1.3 Results

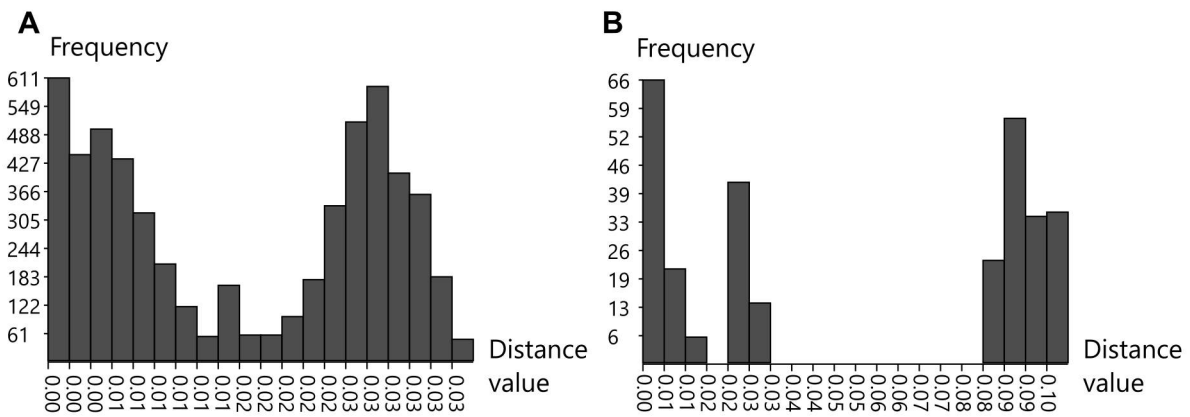


Figure 1.11 – Distribution of pairwise differences obtained from ABGD analyses of *L. schrolli* complex (A) and *Provanna* (B) *Cox1* sequences.

main haplotypes and numerous derived haplotypes that were shared between the eastern basins populations, but also included some individuals of the Woodlark Basin site. Within this group, one of the two dominant haplotypes was more frequent in the North Fiji Basin and can possibly indicate a slight differentiation between this basin and the Lau Basin/Futuna Arc populations ( $F_{st} = 0.06$ ,  $p > 0.05$ ). The mismatch distribution of *L. aff. schrolli* displayed a unimodal shape with an excess of rare variants that fitted well with the model of population expansion if the four intermediate haplotypes are removed (Figure 1.12). The best fit was obtained with  $\tau$  values ranged between 1.8 and 2, suggesting that the population is expanding since 725 kyr with a mutation rate of 0.2% per site and million years (using a mean rate inferred from Johnson *et al.* (2006, 2015) and Breusing *et al.* (2020) with the formula  $r = D/2T$ , where D is the species divergence and T the time elapsed since their splitting) if we assume a one-year duration per generation. In the *L. schrolli* lineage, the haplotype network was more diversified with much more equally frequent haplotypes shared between the Manus and Woodlark Basins. However, the two basins were significantly differentiated one to each other with a significant  $F_{st}$  value equal to 0.07 ( $p < 0.05$ ). The mismatch distribution of *L. schrolli* displayed a unimodal shape with an excess of rare variants that did not fit either the expected curve under the population expansion model or that of the constant size model (Figure 1.12).



Although significant, Tajima's  $D$  and Fu & Li's  $F$  statistics were not negative enough to support a recent population expansion with a peak of sequence differences rather centered around 5 mutations (lack of rare/recent mutations in the population but excess of 3-5 bp divergent haplotypes), which could instead indicate that if bottlenecked, this event was too much recent to detect any expansion.

### 1.3.2 Neomphalidae

The NJ tree based on *Symmetromphalus* and *Lamellomphalus Cox1* sequences is presented in Figure 1.9B. This tree includes the only previously published *Cox1* sequence for *Symmetromphalus regularis* from the Mariana Trough and, clearly distinguished this latter species from three strongly supported and divergent lineages in the South West Pacific which were specific to the Manus Basin, the Woodlark Basin and the eastern basins (i.e. North Fiji and Lau Basins), respectively. The lack of *Cox1* sequences in the Genbank database for the other *Symmetromphalus* species described so far did not allow the identification of the three lineages to the species level. However, given that *Symmetromphalus hageni* was originally described from specimens from the Manus Basin (Beck, 1992a), we hereafter use the species name *S. hageni* for our Manus Basin samples, and *S. aff. hageni* for the two other lineages from the North Fiji-Lau and Woodlark Basins.

The 33 sequences (629 bp long) displayed 58 segregating sites including 53 parsimony-informative sites mostly involved in the divergence of lineages and 5 singletons. Among the 20 haplotypes identified, 15 were unique. Haplotype networks highlighted the co-occurrence of the three lineages identified in the phylogenetic tree, with one or two dominant haplotypes per lineage and a crown of derived haplotypes (Figure 1.10). The average divergence between lineages within the genus ranged from 4.01 to 6.65%. The net divergence,  $Da$ , was greater between lineages from the two geographically closer basins of Manus and Woodlark (i.e. 0.52) than between lineages from the Woodlark Basin and the more distant eastern basins (Woodlark Basin vs Lau Basin;  $Da = 0.37$ ). These results were corroborated by the ABGD

### 1.3 Results

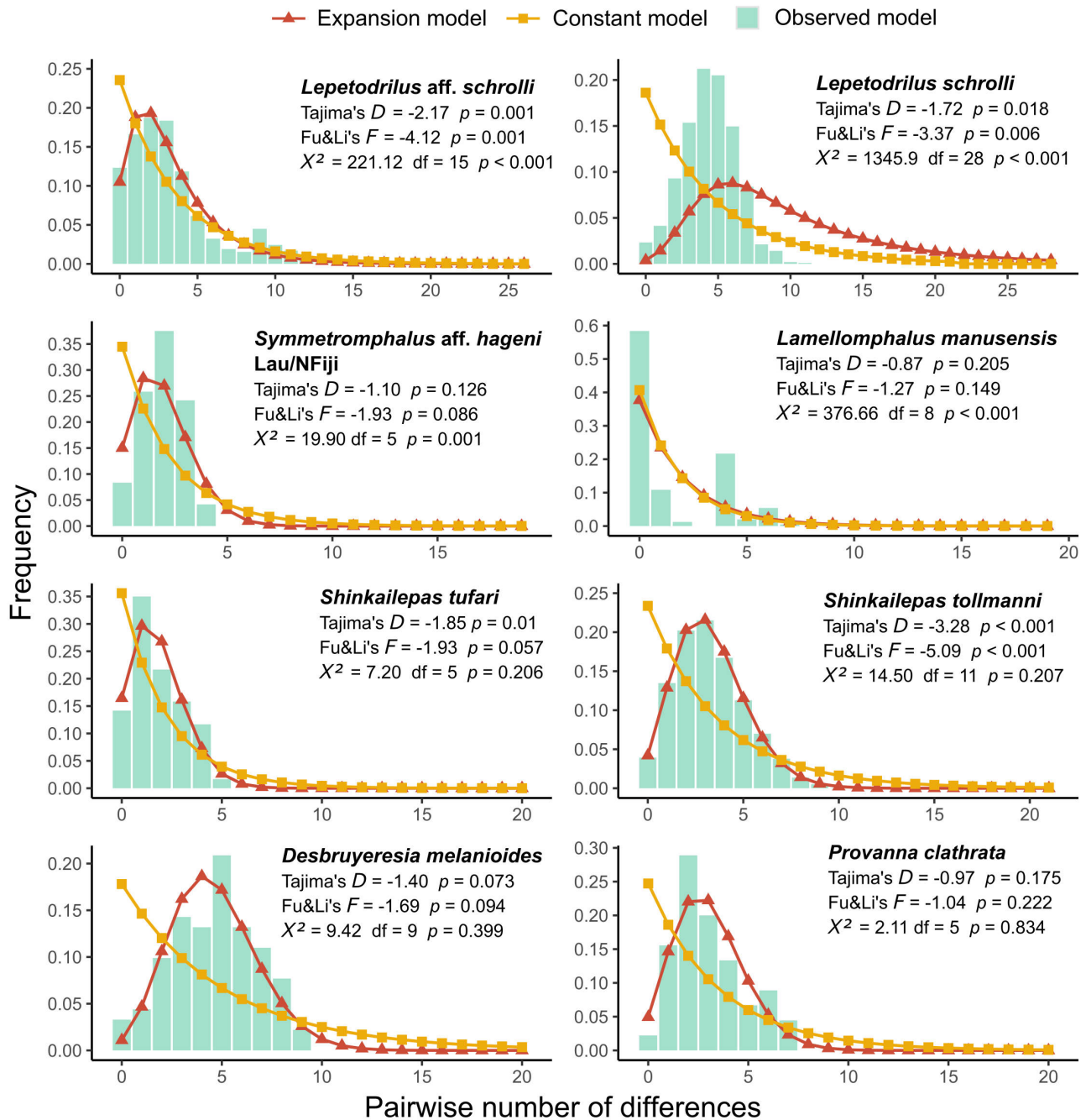


Figure 1.12 – Observed and simulated match-mismatch curves. The chi-square goodness of fit test results presented compare the observed distribution to the expected under an expanding population one. Results of Chi-squared test comparing the observed distribution to the expected under a constant population one (not shown in the figure) always indicated that observed distribution did not fit the expected one ( $p < 0.001$ ).

analysis that showed evidence for three potential cryptic species within our *Symmetromphalus* sequences ( $P = 2.1510^{-2}$ ; Barcode gap distance = 0.021). The overall differentiation between lineages was high with a nearly fixed *Fst* value of 0.88. The mismatch distribution was only drawn for *S. aff. hageni* from the eastern basins (North Fiji-Lau Basins), for which we had enough individuals. This distribution exhibited a unimodal shape that better fitted the expected curve under the population expansion model (Figure 1.12). Tajima's *D* and Fu & Li's *F* statistics were not significantly different from zero expected from the drift/mutation equilibrium but this might be due to the small sample size we had.

*Lamellomphalus manusensis* also displayed two geographic lineages, one with individuals from the Manus Basin and one with those collected at the Futuna and Kermadec Volcanic Arcs, but these two lineages are much less divergent (i.e.  $Da = 0.0064$ ) than those reported for *Symmetromphalus*. The 29 sequences (629 bp long) displayed as a whole 8 segregating sites including 4 parsimony-informative sites and 4 singletons combined in 5 distinct haplotypes. Because this genus was rather rare, it was not possible to estimate accurately the level of population differentiation associated with the different basins but the divergence between the Manus Basin and the Futuna Volcanic Arc was weak and absent between individuals from the Futuna and Kermadec Volcanic Arcs.

### 1.3.3 Phenacolepadidae

Within the genus *Shinkailepas*, the NJ tree clearly distinguished nine lineages involving four valid and well-known species in the West Pacific: *S. tollmanni*, *S. myojinensis*, *S. kaikatensis* and *S. tufari* and two undescribed species from both the Mariana Trough and Mariana Volcanic Arc (Figure 1.13). Among individuals morphologically identified as *S. tufari* from the CHUBACARC cruise, four lineages clearly discriminated from the North West Pacific species. The species name *S. tufari* is hereafter used for the Manus Basin specimens as this basin corresponds to the type locality of the species (Beck, 1992b). Other putative lineages of *S. tufari* found in the other basins have been then referenced as *S. aff. tufari*. One distinct

### 1.3 Results

lineage, with only two individuals, was however also found in the Manus Basin. This rare lineage first identified as *S. tufari* based on morphological characteristics merged with *Shinkailepas* sp. individuals from the Mariana Volcanic Arc and should represent another geographic species. This lineage is related to *S. kaikatensis* reported in the Izu-Bonin-Mariana Volcanic Arc. Among the 40 specimens identified as *S. tufari sensu lato*, 119 segregating sites were reported including 108 parsimony-informative sites mostly involved in the lineage divergence. All but one mutation were synonymous, and the non-synonymous one is unique to the two individuals from *Shinkailepas* sp. lineage (Table 1.4). Out of these *tufari*-like sequences, the lineages were sub-divided into 25 haplotypes among which 19 were unique. The haplotype network highlighted the distinct geographical distribution of the five lineages with average divergences ranging from 6.9% to 11.62% (Figure 1.10). These lineages were also supported by the ABGD analysis ( $P = 5.9910^{-2}$ ; Barcode gap distance = 0.041) confirming the existence of 5 putative cryptic species. Three lineages were only reported from one basin (Manus (defined as *S. tufari*), Woodlark and Lau Basins: see Table 1.4) but the lineage typical of the Futuna Volcanic Arc was also collected in the Lau Basin. In contrast to *Symmetromphalus*, divergence was greater between the Lau and Woodlark Basins (net divergence  $Da = 0.090$ ) than between Manus and Woodlark ( $Da = 0.071$ ) with the near fixation of haplotypes between basins ( $Fst = 0.95$ ;  $p < 0.001$ ). The mismatch distribution of *S. tufari* best fitted the expected curve of population expansion, despite non-significant Tajima's  $D$  and Fu & Li's  $F$  statistics. The non-deviation of the two tests from neutral expectations may therefore be attributable to the small number of sequences available (Figure 1.12).

In contrast to *S. tufari* complex, both the NJ tree and the haplotype network clearly indicated that *S. tollmanni* specimens from all basins and the Futuna Volcanic Arc belong to a single phylogenetic lineage which also comprises the *S. tollmanni* sequences from Yahagi *et al.* (2020) and Fukumori *et al.* (2019) (Figures 1.10 and 1.13). The analysis of the 75 *S. tollmanni* sequences led to 57 segregating sites including 15 parsimony-informative sites and 42 singletons forming 49 distinct haplotypes. All but one mutation were synonymous, and

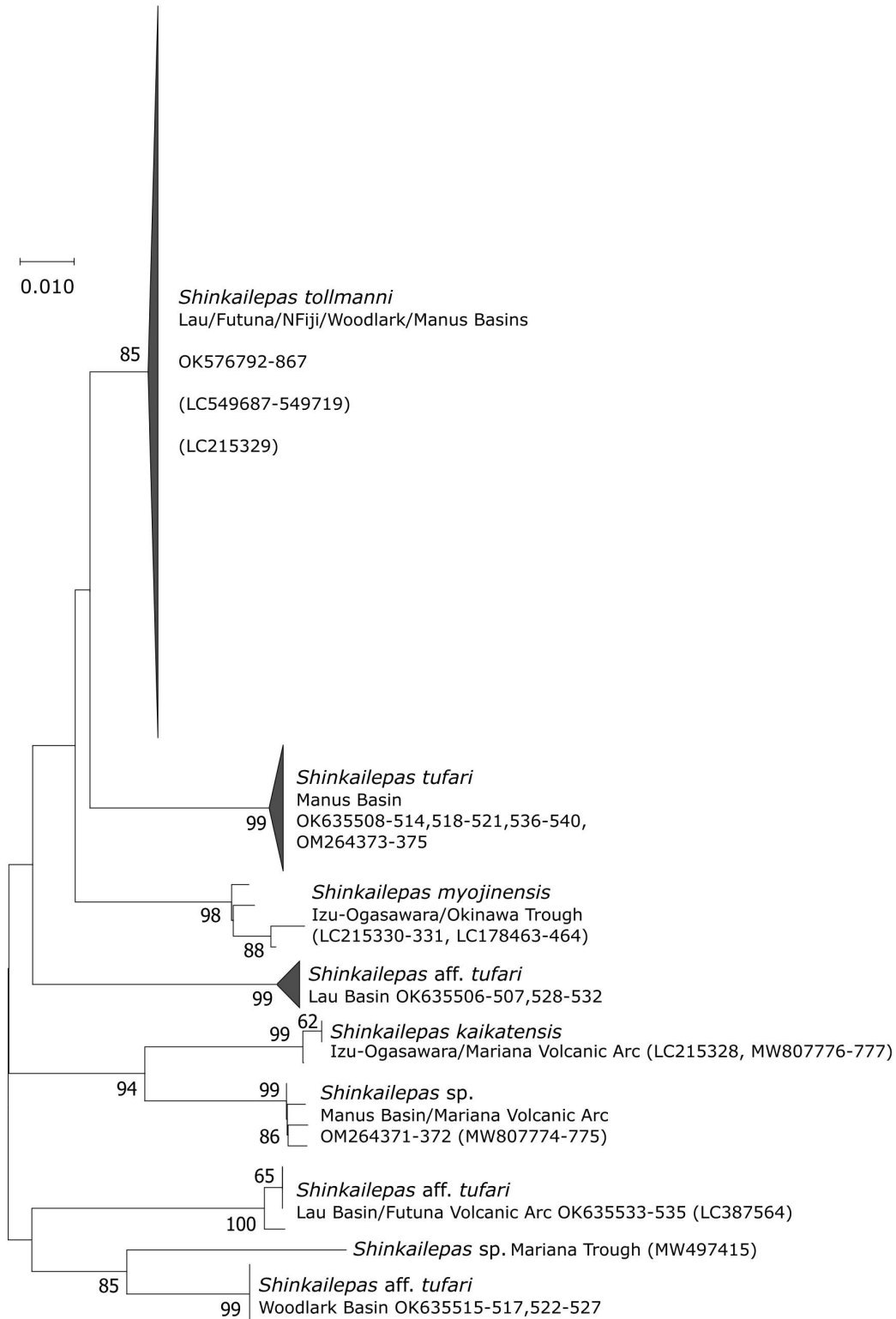


Figure 1.13 – *Cox1* Neighbor-Joining trees showing the position of individuals from *Shinkailepas* within their genus. Numbers at nodes indicate the proportion of occurrences in 1000 bootstraps; percentages below 50% are not shown. Genbank accession numbers of the present study and published sequences are indicated. Published sequences are in brackets. Sequence lengths: 281 bp.

### 1.3 Results

the non-synonymous one was a singleton. No genetic differentiation was found between the four basins and the Futuna Volcanic Arc ( $F_{st} = -0.0037$ ;  $p > 0.05$ ). The haplotype network had a star-like shape with the most dominant haplotype being shared between all sampled localities. The occurrence of a single lineage was also supported by the small genetic divergence between individuals (i.e. 0.52%, Table 1.4). The mismatch distribution was unimodal with an excess of rare variants that fitted the expected curve of population expansion (Figure 1.12). This was also supported by significant negatives Tajima's  $D$  and Fu & Li's  $F$  statistics. The best fit was obtained with a  $\tau$  value of 2.8, suggesting that the population is expanding since 1.1 My with a mutation rate of 0.2% per site and million years if we assume a one-year duration per generation.

#### 1.3.4 Provannidae

The NJ tree based on *Desbruyeresia* and *Provanna Cox1* sequences is presented in Figure 1.14. Within the genus *Desbruyeresia*, the phylogenetic tree exhibited 6 main lineages corresponding to 6 morphologically described species. Three are exclusive to the North Pacific (i.e. *D. marianaensis*, *D. armata*, and *D. chamorroensis*) and two are from the South Pacific (i.e. *D. melanioides* and *D. cancellata*) (Figure 1.14). The last species (i.e. *D. costata*) was reported in both the North and the South Pacific. Our western Pacific samples fell within 3 of these morphological species (i.e. *D. melanioides*, *D. cancellata* and *D. costata*).

The analysis of the 24 *Desbruyeresia* sequences collected during the CHUBACARC cruise displayed 85 segregating sites including 78 parsimony-informative sites, which were nearly all involved in species divergence. All mutations were synonymous. Seventeen of the 20 haplotypes were unique. The haplotype network was performed on the three main lineages, which corresponded to *D. melanioides*, *D. cancellata* and *D. costata* (Figures 1.10 and 1.14). The average divergence between these 3 species ranged from 7.2 to 15.3% with nearly fixed haplotypes ( $F_{st} = 0.94$ ;  $p < 0.001$ ). *Desbruyeresia costata*, a species originally described from the Okinawa Trough (Chen *et al.*, 2019b), exclusively occurred in the Manus Basin, while *D. cancellata* was sampled in the Lau Basin. Only one individual of *D. cancellata*

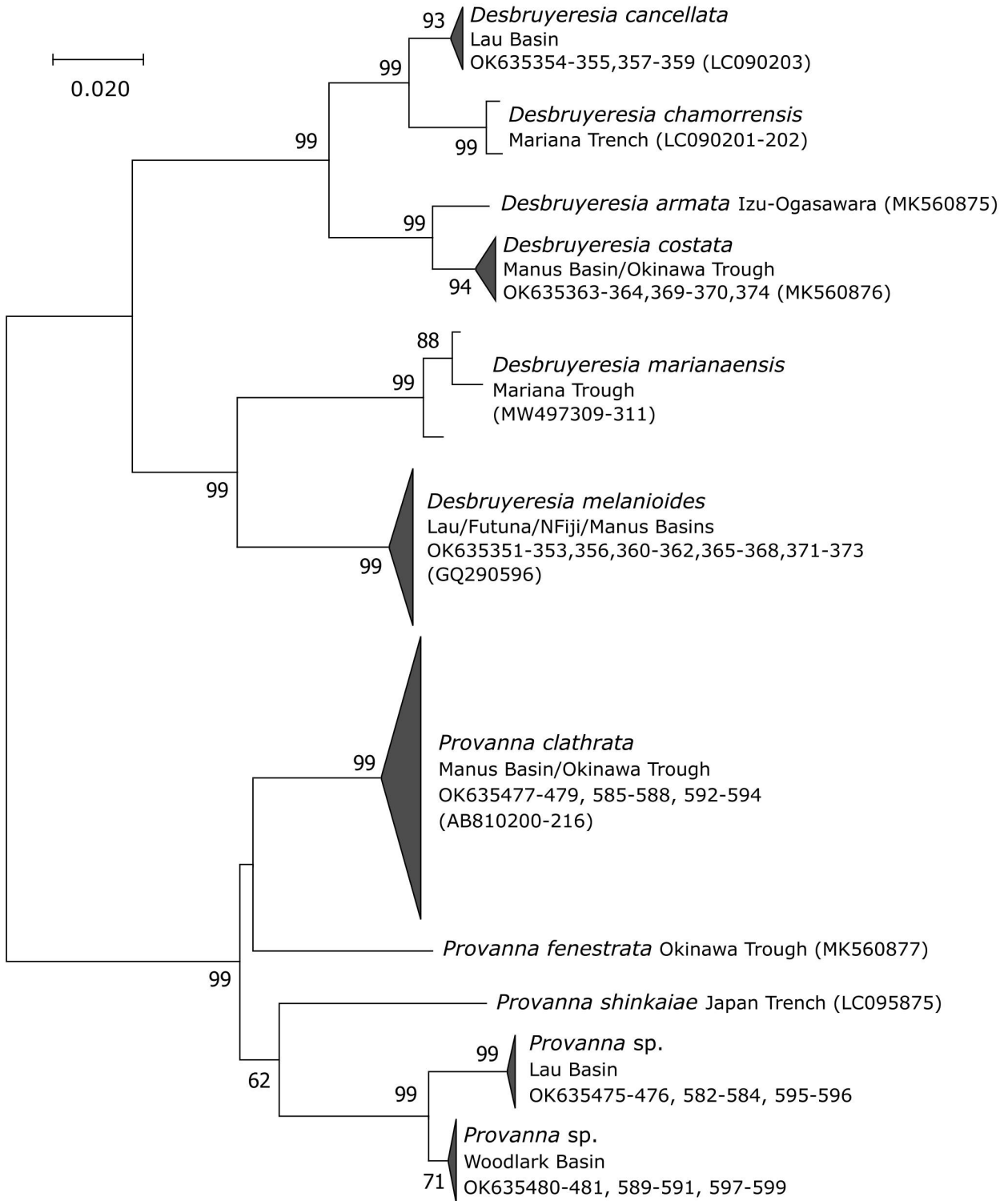


Figure 1.14 – *CoxI* Neighbor-Joining trees showing the position of individuals from *Desbruyeresia* and *Provanna* within their family. Number at nodes indicates the proportion of occurrences in 1000 bootstraps; percentages below 50% are not shown. Genbank accession numbers of the present study and published sequences are indicated. Published sequences are in brackets. Sequence lengths: 469 bp.

### 1.3 Results

was morphologically identified from the North Fiji Basin but was not barcoded. Conversely, the third species *D. melanioides* was widely distributed across the eastern localities (i.e. Lau Basin, Futuna Volcanic Arc and North Fiji Basin) and displayed no spatial genetic structure in the sampled area. The number of haplotypes was however too small to produce accurate *Fst* estimates between basins for this later species. Based on morphology, we also identified one individual from *D. melanioides* at the Woodlark Basin site, but it was not barcoded. The mismatch distribution was unimodal with an excess of rare variants and fitted the expected curve of population expansion (Figure 1.12). Tajima's *D* and Fu & Li's *F* statistics, although negative, were not significant probably because of the small number of sequences available.

Genetic analyses of specimens from the genus *Provanna* also indicated species diversification at the scale of the West Pacific. Three distinct lineages can be depicted from the NJ tree, one being closer to the previously described species in the Okinawa Trough, i.e. *P. fenestrata*. This lineage corresponds to the species *Provanna clathrata* described from the Okinawa Trough. The two others unnamed lineages were closer to *P. shinkaiiae* also found in the northwestern Pacific. The lack of *Cox1* sequences in the Genbank database for the western Pacific species did not allow to identify our specimens to the species level within this genus. As already reported for *Desbruyeresia*, this genus comprises one lineage composed of individuals from the Manus Basin and the Okinawa Trough. The 25 *Provanna* individuals sampled during the CHUBACARC cruise exhibited 55 segregating sites, which included 52 parsimony-informative sites mostly involved in the lineage divergence. Only one mutation was nonsynonymous and shared by all specimens coming from the Manus Basin. Over the 19 haplotypes identified, 13 were unique. The haplotype network identified three geographic lineages endemic to the Manus, Woodlark and Lau Basins respectively (Figure 1.10). The average divergence between these lineages ranged from 2.49 to 9.69% with more divergence accumulated between the Manus and Woodlark Basins ( $Da = 0.077$ ) than between the Lau and Woodlark Basins ( $Da = 0.022$ ). This geographic pattern of divergence was quite similar to *Symmetromphalus* (see: Table 1.4) with again nearly fixed haplotypes between basins (*Fst*



= 0.95;  $p < 0.001$ ). The ABGD analysis suggested the co-occurrence of two potential cryptic species, with individuals segregating between the Manus Basin and the Woodlark/Lau Basins ( $P = 2.1510^{-2}$ ; Barcode gap distance = 0.054) by a clear barcode gap in genetic distances of 0.04 and 0.08 (Figure 1.11B). The mismatch distribution obtained from the most sampled species (i.e. *Provanna clathrata* collected at the Manus Basin) exhibited an excess of rare variants and better fitted the expected curve of population expansion (Figure 1.12). Tajima's  $D$  and Fu & Li's  $F$  statistics were however not significant, likely due to the small sample size.

## 1.4 Discussion

Assessing the geographical range of species is essential in understanding how communities are structured and how they should eventually be protected. Cryptic species, highlighted through barcoding approaches, are common at deep-sea hydrothermal vents (Johnson *et al.*, 2008; Matabos *et al.*, 2008b, 2011; Plouviez *et al.*, 2009, 2019). When left undetected, their occurrence can lead to an underestimation of biodiversity or incorrect species distribution boundaries. In this study, *Cox1* barcoding analyses provided new insights into the distribution range of several gastropod species across the South West Pacific. While the concept of species has been strongly debated for decades (De Queiroz, 2007; Roux *et al.*, 2016), following the ABGD approach/definition for species delimitation, cryptic species were found within two taxa, *Shinkailepas tufari* and *Symmetromphalus hageni*. These two complexes included species restricted to the Manus Basin, the Woodlark Basin, and one or several of the eastern basins including the Lau Basins and the North Fiji Basin, and the Futuna Volcanic Arc. These findings are in agreement with the notion of geographic species and the concept of the stepwise colonisation of deep-sea vents, at least in the discontinuous systems of the western Pacific. *Symmetromphalus regularis*, described from the Mariana Trough, has been reported at the Lau and North Fiji Basins (Desbruyères *et al.*, 2006a). However, individuals from this study are clearly distinct from this species, suggesting that *S. regularis* is absent from the South West

#### 1.4 Discussion

Pacific. Further morphological observation might help to identify the different species, although shell plasticity seems to occur, especially in *Symmetromphalus* where shell shape and thickness were highly variable among Manus Basins individuals (C. Poitrimol, pers. obs.).

The genus *Provanna* depicted a similar pattern with three distinct lineages although the ABGD method only detected two potential species, individuals from the Lau and Woodlark Basins belonging to the same species, yet with a complete geographic isolation of these populations. Indeed, the intraspecific divergence represented in the pairwise distance histograms, ranging from 0 to 3% of divergence, was composed of two modes separating individuals from the two basins. The average divergence between these two lineages (i.e. 2.5%) is in the same order of magnitude as the one segregating *Symmetromphalus* species between the same basins (i.e. 4%), suggesting that they could share the same evolutionary history of populations. The lack of significance of the barcode gap method between these two geographic populations of *Provanna* may be due to the very small number of individuals analysed, leading to an underestimation of the haplotype diversity. A higher sampling effort will increase the statistical power of the ABGD with a more accurate information on the status of the two lineages. The two unnamed *Provanna* species/subspecies are probably attributable to the *Provanna* species already described from the western Pacific region: *P. segonzaci* in the Lau Basin and *P. buccinoides* in the Lau and North Fiji Basins but also *Provanna nassariaeformis*, originally described from the Mariana Trough and further reported in the Manus Basin (Desbruyères *et al.*, 2006a). The lack of sequences in Genbank for these latter species prevented us from identifying our specimens with the original descriptions. Although we did observe morphological (shell) differences between our samples, original descriptions were based on small individuals and do not describe morphological ontogenic changes. Diagnostic characteristics in *Provanna* species (Warén et Ponder, 1991; Warén et Bouchet, 1993) notably involve the number of spires and ornaments on the shell, but our barcoding results clearly showed that this number changes as the animal grows and might thus not represent a reliable trait for morphological identification (C. Poitrimol, pers. obs.). Other genes need to be investigated to confirm species delimitations.

Also, further morphological observation of the shell microstructures, soft body parts or radula could reveal some variations between the putative species and refine their initial descriptions. For example, while *Alviniconcha* species have long been considered cryptic, closer examination revealed that they are morphologically distinguishable (Laming *et al.*, 2020; Castel *et al.*, 2022).

In contrast to the geographic species complexes depicted in morphological species such as *S. tufari* or *S. hageni*, other gastropod species indicated a higher level of connectivity between some basins. *Lepetodrilus schrolli* has previously been identified as cryptic, with *L. schrolli* occurring at the Manus Basin and *L. aff. schrolli* in the Lau and North Fiji Basins (Johnson *et al.*, 2008), but *L. aff. schrolli* was then also identified at the Manus Basin (Plouviez *et al.*, 2019). Our results confirmed the existence of two lineages separating the Manus Basin from the North Fiji and Lau Basins and the Futuna and Kermadec Volcanic Arcs (Figure 1.9A). The two lineages and/or subspecies are however mixed at the newly discovered site at the Woodlark Basin (present study). This can reinforce previous barcoding analyses of Plouviez *et al.* (2019) who did find *L. aff. schrolli* at the opening of the Manus Basin on the flanks of the Susu volcanoes. According to our ABGD analysis, the two lineages may still belong to a single species that experienced spatial isolation of its populations with possible secondary contacts, at least in the Woodlark Basin. Secondary contacts with admixtures might be probable with the superimposition of lineages at some locations, and could explain why we have found putative intermediate haplotypes between *L. schrolli* and *L. aff. schrolli* at the Futuna Volcanic Arc sites. This has been previously shown between overlapping lineages of *Lepetodrilus elevatus* at 9°50N on the East Pacific Rise (Matabos *et al.*, 2008b). Further genetic studies involving a greater number of nuclear markers are however needed to clarify the status of this species. Interestingly, the level of divergence between the two lineages is similar or close to those observed between the *Provanna* eastern species and the Woodlark and Lau/Fiji Basins species of *Symmetromphalus*. This observation could reflect similar evolutionary histories of vicariance between different taxa associated with an ongoing speciation of these taxa in allopatry and the central role of the Woodlark Basin in allowing both the dissemination and the faunal connection

## 1.4 Discussion

of different basins.

While various distribution patterns emerged among gastropod taxa, phylogeographic breaks consistently occur between the Manus Basin and/or the Woodlark Basin and the others eastern populations from South West Pacific (i.e. *Symmetromphalus*, *Provanna*, *Lepetodrilus* and *Shinkailepas* species complexes). In addition, levels of divergence were not correlated with geographic distances. A geographic split between populations of the Manus Basin and the North Fiji/Lau Basins was already reported for a number of taxa, including *Ifremeria nautilei* (a large symbiotic gastropod), the shrimp *Rimicaris variabilis*, the crab *Austinograea alayseae* and the limpet *Lepetodrilus schrolli* (Thaler *et al.*, 2011, 2014; Lee *et al.*, 2019; Plouviez *et al.*, 2019; Tran Lu Y *et al.*, 2022) . This study is however the first to publish genetic data associated with the Woodlark Basin and its stepping-stone role on the vent fauna dissemination. Geological events or hydrographic barriers can contribute to explain the vicariant events that caused these geographic isolations. Physical barriers created by the New Guinea archipelago have already been proposed to explain the Manus Basin vent fauna isolation (Thaler *et al.*, 2011). In addition, a major reorganisation of the plates was initiated in the western Pacific about 25 million years ago (Mya) (Hall, 2002). The opening of actual southwestern basins is relatively recent (<10 My): the Woodlark Basin, the oldest, opened 5-7 Mya, followed by the Manus Basin (5 Mya), the North Fiji Basin (3-4 Mya) and the Lau Basin (1-2 Mya). These geological rearrangements, although progressive, could have led to a step-by-step ridge colonization and further species isolation by vicariance. The range of divergences observed between cryptic lineages of the different gastropod taxa is probably indicative of a shared evolutionary history at different times of the geological formation of these basins (i.e. 2.5-4%; 6-10 %; 14-15%, Table 1.4). Assuming a mean substitution rate of 0.2% per million years across gastropod species (Johnson *et al.*, 2015; Breusing *et al.*, 2020) the geographic lineages would have diverged respectively between 6-10, 15-26 and 35-38 Mya. Although divergence times must be considered with caution, as substitution rates can vary depending on taxa. The opening of the South Fiji Ridge and the associated Solomon Basin 25 Mya ago and its further subduction

leading to the present-day basins about 10 Mya ago could have played a major role for the two most recent series of divergences found in the vent fauna, which could be more obviously retrieved in the poor-dispersive species. These divergence times between geographic lineages were also concordant with reported diversification events of deep-sea organisms during the Oligocene and Miocene (Williams *et al.*, 2013; Lin *et al.*, 2020).

The pattern and level of population divergence however differed among species, and could be explained by biotic factors inherent to species ecology and life-history traits such as reproduction and larval biology which affect larval dispersal. Contrasted phylogeographic patterns also occurred between closely related species. This pattern was already reported in the genus *Alviniconcha* in this region, with *A. kojimai* and *A. boucheti* largely distributed along the Manus, North Fiji, and Lau Basins, and the Futuna Volcanic Arc, while *A. strummeri* has a more limited distribution to the eastern basins (Johnson *et al.*, 2015; Laming *et al.*, 2020; Castel *et al.*, 2022). This pattern is partly surprising as closely related species are expected to share reproductive traits that are often phylogenetically constrained (Eckelbarger et Watling, 1995; McHugh et Rouse, 1998; Collin, 2004). Surprisingly, patterns of differentiation repeatedly differ between congeneric species in several gastropod genera with two alternative and opposed dispersal strategies. While *Shinkailepas tollmanni*, *Lamellomphalus manusensis* or *Desbruyeresia melanioides* are widely distributed across the South West Pacific basins with very weak divergence between geographic populations, other species from the same genera or family were limited to nearly each basin (i.e. *Shinkailepas tufari* and *Symmetromphalus hageni* complexes of species, *Desbruyeresia cancellata*). Such variability in the distribution patterns of closely related species were also reported in other groups of benthic organisms such as the deep-sea stalked barnacles in the West Pacific. For instance, the genera vent neolepadid barnacles *Vulcanolepas/Leucolepas* display high species diversity with one species per basin: *V. buckeridgei* in the Lau Basin, *V. fijensis* in the North Fiji Basin, a new undescribed *Vulcanolepas* species in the Woodlark Basin, *Leucolepas longa* in the Manus Basin, *V. oshaeai* in the Kermadec Volcanic Arc, and *V. verенаe* in the Mariana Trough (Chan et Chang, 2018; Chan *et al.*, 2019;

## 1.4 Discussion

Watanabe *et al.*, 2021; Boulart *et al.*, 2022). On the contrary, the non-hydrothermal deep-water stalked barnacle *Scalpellum stearnsii* forms a complex of 4 cryptic species with one species present throughout the South West Pacific, from Papua New Guinea to Fiji (Lin *et al.*, 2020). Finally, intermediate patterns were also highlighted on non-hydrothermal bathyal barnacles in the genus *Waikalesma* with two species, i.e. *W. boucheti* and *W. dianagonoesae*, present in sympatry in Papua New Guinea but with different geographic distribution (Chan *et al.*, 2016).

Currents will differentially affect larval dispersal potential, and hence species range, depending on closed interactions with the planktonic larval duration, larval behaviour and the depth at which they disperse (Hilário *et al.*, 2015). While species with lecithotrophic larvae, potentially associated with short Pelagic Larval Duration (PLD), would have a limited distribution range, species with planktotrophic larvae, associated with a longer PLD, are expected to be widely distributed if not lost from active areas. However, such strategies may lead to opposite larval duration depending on the depth at which larvae are able to move as the low temperature near the seafloor may allow lecithotrophic larvae to have longer PLDs than planktotrophic larvae because of their reduced metabolism (Young *et al.*, 1997; Mullineaux *et al.*, 1998). In addition, some larvae like those of the vent polychaete *Alvinella pompejana* may arrest their development in cold water until suitable conditions are encountered (Pradillon *et al.*, 2001, 2005), resulting in long-lasting propagules. *Shinkailepas* and *Desbruyeresia* larvae have been shown to be planktotrophic (Warén et Bouchet, 1993; Chen *et al.*, 2019b; Yahagi *et al.*, 2017, 2020) but most of their congeneric species exhibit highly fragmented genetic structure and species diversification. Variable larval lifespan and/or ontogenic behaviour could explain the contrasted distributions within these genera, as connectivity between basins would vary according to PLD and depth of dispersal (Mitarai *et al.*, 2016). The South Equatorial Current may connect all South West basins once every hundred of thousands of years via stepping-stones for species with long larval lifespan (170 days at 1 000 m) (Mitarai *et al.*, 2016). Connection is predicted to be successful westward from the Woodlark Basin to Manus Basin, and from the Lau to the North Fiji Basins, once every  $\approx 5$

000 to  $\approx$  12 000 years considering a pelagic larval duration of 82 days between 100 to 1 500 m (Mitarai *et al.*, 2016). However, eastward gene flow from the Manus Basin to the North Fiji and Lau Basins has been suggested for several taxa (Thaler *et al.*, 2011, 2014; Plouviez *et al.*, 2019; Breusing *et al.*, 2021) but not *Ifremeria nautilei* when looking at more contemporary gene flow (Tran Lu Y *et al.*, 2022). Different larval behaviours have already been observed between North West Pacific *Shinkailepas* species (Metaxas, 2011; Yahagi *et al.*, 2017). While for some species larvae are believed to migrate to the surface, thus taking advantage of food resources and stronger currents, others remain close to the seabed, inducing different dispersal capacities. Vertical migration to shallow water has been suggested for *Shinkailepas tollmanni* for which larvae, although encapsulated until they reach their trochophore stage, are thought to stay pelagic for over a year (Yahagi *et al.*, 2020), potentially allowing long-distance dispersal through the Manus, Woodlark, North Fiji, and Lau Basins, and the Futuna Volcanic Arc. Conversely, in the specific case of *Shinkailepas tufari*, larvae might be more likely to stay near the seabed which could account for their more limited distribution ranges. *Symmetromphalus*, *Provanna* and *Lepetodrilus* have lecithotrophic larvae (Beck, 1992a; Warén et Bouchet, 1993; Tyler *et al.*, 2008; Chen *et al.*, 2018; Plouviez *et al.*, 2019) . *Lepetodrilus schrolli* is widely distributed from the Manus Basin to the Kermadec Volcanic Arc, a rather wide distribution for a non-feeding larva. The low temperature of deep waters or delayed larval development behaviour could play a central role in the species distribution with some basins acting as stepping-stones (Mitarai *et al.*, 2016). Finally, differences in dispersal might be related to offspring availability, a species with high occupancy and high fecundity being able to produce more larvae over time and space (Vrijenhoek, 2010). Species occupancy indeed results from their success in colonising habitat but also on the availability and frequency of their habitat. Finally, our results raise questions about the faunal links between the two distinct biogeographic provinces of the North West and the South West Pacific (Bachraty *et al.*, 2009; Thaler et Amon, 2019). While separation of species was generally greater between the North West and the South West Pacific than within the South West Pacific, the provannid gastropods, *Desbruyeresia costata* and *Provanna*

## 1.4 Discussion

*clathrata* from the Manus Basin have a limited distribution range across the South West back-arc basins but display connections with the Okinawa Trough. In the same way, *Shinkailepas* sp. found in the Manus Basin was previously described from the northwestern Pacific. Even with larvae dispersing almost one year at a depth of 100 m, populations from the Manus Basin are not connected to those of the Marianna Trough, where the nearest northern vent sites are found to date (Mitarai *et al.*, 2016). Considering the large geographic gap between the South West and North West regions of the Pacific, the link between the Okinawa Trough and Mariana Trough with Manus Basin implies the occurrence of yet undiscovered sites that could act as stepping-stones, throughout the Philippine Arc for instance. In comparison, analysis of the distribution of hydrothermal and non-hydrothermal deep-sea barnacles showed distinct distributions of closely related species between the northern and southern West Pacific (Lin *et al.*, 2020; Watanabe *et al.*, 2021). Our results also support the hypothesis introduced by Boulart *et al.* (2022) establishing that the Woodlark Basin could act as a biological stepping-stone. Depending on taxa, populations from the Woodlark Basin are either closer to the ones in the eastern basins (e.g. *Symmetromphalus* aff. *hageni* and *Provanna* sp.), or closer to those of the Manus Basin (*S. tufari*). For other species (e.g. *S. tollmanni*, *D. melanioides*) the Woodlark Basin appears to be widely connected with all other basins, consisting of a metapopulation in the region as also observed for *Ifremeria nautilei* (Boulart *et al.*, 2022), or exhibit lineages from both the North Fiji/Lau Basins and the Manus Basin (e.g. *Lepetodrilus schrolli* complex). the Woodlark Basin hence seems to act as an intermediate between the Manus Basin and the eastern regions including the North Fiji and Lau Basins or the Futuna Volcanic Arc but also constitutes a contact zone for some taxa.

To conclude, new cryptic species are likely to co-occur over the complex system of disconnected basins typical of the West Pacific. Most of them are geographic and strengthen the hypothesis of speciation in allopatry as a by-product of the plate tectonism. Very contrasted phylogeographic patterns are however observed within hydrothermal vent gastropods from southwestern Pacific back-arc basins and suggest that species may have



evolved under contrasted if not opposite dispersal strategies: a situation that could be favoured by fragmentation and habitat instability. Connectivity between basins is therefore highly variable according to species and their early life history traits. So far, larval lifespan and behaviour are poorly known for many vents species and seem to greatly differ even between congeneric species. Understanding the colonisation potential of vent species from their life history traits could help to improve larval dispersal modelling studies and thus better understand connectivity between basins (Hilário *et al.*, 2015). Our results have an important impact in terms of biological conservation: as species colonisation potential is highly variable, susceptibility to deep-sea mining will be different between taxa, with a great proportion of vulnerable species which seem to poorly disperse. Anticipation of the effect of mining will therefore require the study of all the species of the ecosystem and should integrate species with the lowest dispersal ability. In addition, due to the intermediate position of the Woodlark Basin in connecting the western Pacific basins, mining vent sites in this basin could potentially influence the 'rescue' effect of any of the other basins on the Manus Basin vent communities.

## CHAPITRE 2

---

Reproductive biology and population structure of two hydrothermal gastropods (*Lepetodrilus schrolli* and *Shinkailepas tollmanni*) from the South West Pacific back-arc basins

---

Ce chapitre correspond à une première version d'un article à soumettre dans Marine Biology avec : Marjolaine Matabos, Alicia Veuillot, Annah Ramière, Cécile Cathalot, Cédric Boulart, Olivier Rouxel et Éric Thiébaud.

## 2.1 Introduction

Understanding processes involved in replenishment of local population, recolonization and connectivity is paramount to assess the resilience of benthic faunal communities to natural and anthropogenic disturbances and their long-term persistence. In the deep sea, hydrothermal vents, reported along mid-ocean ridges, back-arc basins and volcanic arcs (Beaulieu *et al.*, 2015; Beaulieu et Szafranski, 2020), form original fragmented and ephemeral systems whose spatio-temporal dynamics (e.g. vent distribution, disturbance rate) can greatly impact the dynamics of populations and communities (Mullineaux *et al.*, 2018). Natural disturbances which result from volcanic eruptions and tectonic events may eradicate local benthic communities partially or totally, or create new suitable habitats. Depending on vent systems, disturbance rate due to volcanic eruptions ranges from very high (e.g. several eruptions per year on submarine arc volcanoes) to very low (e.g. one every 10 000 years at slow spreading mid-oceanic ridges; Mullineaux *et al.*, 2018). Finally, physico-chemical conditions can be highly variable in space and time. While vent fluid chemical composition can be similar at 1000 km-scale (e.g. East Pacific Ridge; Mullineaux *et al.*, 2018), it can vary at 10 km-scale in some back-arc basins (e.g. eastern Lau Spreading Center and Manus Spreading Center; German et Seyfried, 2014) with significant impact on vent community composition (Mullineaux *et al.*, 2018). At the vent scale, the mixing of vent fluids with seawater generate spatial gradients in environmental conditions (e.g. temperature, reduced compounds concentrations) resulting in a zonation in the distribution of benthic fauna (e.g. Podowski *et al.*, 2010; Shank *et al.*, 1998). In the South West Pacific back-arc basins, hydrothermal vent fauna is characterised by macrofaunal assemblages distributed along an environmental gradient, from the large gastropod *Alviniconcha* spp. clumps in high fluid areas to clumps of a second large gastropod *Ifremeria nautilei* in moderate flux areas and mussel beds of *Bathymodiolus* sp. in low flux areas (Podowski *et al.*, 2010).

Over the last decades, connectivity between vent fauna populations have been mainly assessed through population-genetics or modelling studies that rely on ocean circulation and selected species life history traits, such as planktonic larval duration and larval

## 2.1 Introduction

vertical distribution (Mitarai *et al.*, 2016; Breusing *et al.*, 2021). However, these methods provide very different measure of connectivity. While most population genetics studies inform on connectivity over several generations, biophysical model measure connectivity only from spawning to larval settlement following one or several spawning events. Data on patterns of larval dispersal and connectivity are essential but insufficient to assess persistence of spatially structured populations (Burgess *et al.*, 2014). Knowledge of life history traits related to the reproductive effort such as age at first reproduction, fecundity, reproductive pattern, and sex ratio is essential to improve our understanding of the recolonization potential of communities. In vent systems, fast growth, early reproduction and wide dispersal of larvae have been expected life history strategies adapted to the hydrothermal environment properties (Ramirez-Llodra, 2002). However, life history traits can be variable, even for closely related species (Metaxas, 2011; Yahagi *et al.*, 2017), and this biological information is still unknown for numerous deep-sea vent organisms.

Recruitment patterns have been established for several hydrothermal vent taxa. Discontinuous recruitment has been described within polychaetes (Zal *et al.*, 1995; Thiébaud *et al.*, 2002), bivalves (Comtet et Desbruyères, 1998) and gastropods (Sadosky *et al.*, 2002), whereas continuous recruitment has been reported for some gastropods and bivalves (Berg, 1985; Hessler *et al.*, 1988; Kelly et Metaxas, 2008; Marticorena *et al.*, 2020). Whatever the recruitment pattern, a majority of hydrothermal species exhibit a continuous or quasi-continuous reproduction (Tyler et Young, 1999; Matabos et Thiébaud, 2010). This is the case for several gastropod species from the Lepetodrilidae, Sutilizonidae, Skeneidae, and Peltospiridae families (Gustafson et Lutz, 1994; Kelly et Metaxas, 2007; Tyler *et al.*, 2008; Matabos et Thiébaud, 2010; Bayer *et al.*, 2011; Marticorena *et al.*, 2020). In addition, hydrothermal vent fluid properties could play an important role on reproduction and populations structure of vent fauna by influencing temperature, food availability (e.g. sulphides resources for autotrophic bacteria) and quality, and by providing a potential toxic environment. As an example, gametogenic maturity and fecundity of *L. fucensis* differed between actively venting and senescent habitats

(Kelly et Metaxas, 2007). The vent condition, i.e. high flux or waning vents, also influenced its sex ratio with a dominance of females in very active vents and a dominance of males in peripheral and senescent vents (Bates, 2008). Finally, biotic interactions (i.e. predation and competition) can influence recruitment and population structure through grazing or competition of space and/or resources (Micheli *et al.*, 2002; Sancho *et al.*, 2005; Lenihan *et al.*, 2008).

To date, most studies on reproductive biology and recruitment of vent fauna species have focused on specimens that colonize mid-oceanic ridges, mainly the East Pacific Rise, the North East Pacific Ridges and the Mid-Atlantic Ridge. Apart from Nakamura *et al.* (2014) study on *Lepetodrilus nux* limpet from the North West Pacific, reproductive studies in the West Pacific back-arc basins are still very sparse and are generally limited to anatomical studies (i.e. Beck, 1992b, 1993). Yet there are at least two reasons to consider the biology of the species in these basins. First, in comparison with continuous mid-oceanic ridges where connectivity is only interrupted by transform faults and/or microplates (Plouviez *et al.*, 2019), the back-arc basins of the West Pacific form a system of discontinuous newly-formed ridges. In the South West Pacific, the few studies that have analysed the effective dispersal of the associated vent fauna highlighted a relatively complex and contrasting evolutionary history linked to the complex tectonic history of the region and contrasting species life-history traits (Thaler *et al.*, 2011; Plouviez *et al.*, 2019; Poitrimol *et al.*, 2022). Second, emerging mining activities targeting hydrothermal vent sulphide mounds focus mainly on the region suggesting that these areas will be facing new anthropogenic disturbances in the future.

The present study provides new insights into the reproductive biology and recruitment patterns of two vent gastropod species, the Lepetodrilidae *Lepetodrilus schrolli* L. Beck, 1993, and the Phenacolepadidae *Shinkailepas tollmanni* (L. Beck, 1992). This should lead to a better understanding of the recolonization potential of the species and thus provides information that may be useful for connectivity models between populations in the South West Pacific back-arc basins. Both species are dominant, widely distributed and representative of

## 2.2 Materials and Methods

the small vent fauna inhabiting the complex three-dimensional habitat (shells and/or crevices) formed by *Ifremeria nautiliei* clumps and *Bathymodiolus* beds (Appendix B.1). *Lepetodrilus schrolli*, previously considered as a species complex comprising three genetically well distinct lineages: *L. schrolli* from the Manus Basin, *L. aff. schrolli* from the North Fiji, Lau and Manus Basins and *L. aff. schrolli* from the Mariana Trough (Johnson *et al.*, 2008; Plouviez *et al.*, 2019), would now appear to be a single species with a strong geographic structure that extends from the Manus Basin to the Kermadec Volcanic Arc throughout the Woodlark, North Fiji, Lau Basins and Futuna Volcanic Arc (Poitrimol *et al.*, 2022). It is a gonochoric species but, unlike the other *Lepetodrilus* species described, most individuals lack a penis. Just a few specimens with a well-developed penis were reported from the North Fiji Basin (Warén et Bouchet, 2001). Ova fertilization is thought to take place in the mantle cavity but this has not been proven (Beck, 1993). *Shinkailepas tollmanni* formerly known as *Olgasolaris tollmanni* L. Beck, 1992 is also a gonochoric gastropod. The right cephalic lappet is transformed to a penis with dorsal seminal groove in males. Fertilization is internal (Sasaki *et al.*, 2010) and this species produce egg capsules that can be found attached to *Ifremeria* shells.

From a spatially nested sampling design, the objectives of this study are to: (1) identify patterns of spatial variability of populations structure within and between back-arc basins according to the environmental variability and habitat (*Bathymodilus* beds vs. *Ifremeria* clumps), and infer their recruitment strategy (continuous vs. discontinuous); (2) determine the sex ratio of the populations; (3) study the gametogenesis through histological observations to describe variability of female's reproduction status; and (4) estimate the fecundity of *L. schrolli*.

## 2.2 Materials and Methods

### 2.2.1 Sampling

All specimens of the gastropods *Lepetodrilus schrolli* and *Shinkailepas tollmanni* were sampled using the hydraulic arm of the Remotely Operate Vehicle (ROV) *Victor6000* during

the CHUBACARC cruise (Hourdez et Jollivet, 2019) held onboard the French research vessel *L'Atalante* between March and June 2019. Samples were collected in *Ifremeria nautili* and *Bathymodiolus* spp. habitats from low to moderate diffused flow areas, in several hydrothermal vent fields from 3 back-arc basins of the South West Pacific, i.e. the Manus, North Fiji and Lau Basins, and one volcanic arc, i.e. Futuna (Figure 2.1, Table 2.1). To investigate variation in reproductive and population structure features in relation to environmental conditions, a physico-chemical characterisation of each sampling area was conducted prior to sampling. *In situ* temperature was measured with the high-temperature probe of the ROV and free inorganic sulphides [ $\Sigma S = H_2S + HS^- + S^{2-}$ ] with the *in situ* chemical miniaturized analyser CHEMINI on three replicate points (Vuillemin *et al.*, 2009). As the sample was pumped without any filtration, the chemical species analysed with CHEMINI correspond to an operationally defined fraction of sulphides called free inorganic sulphides which includes dissolved and particulate sulphides that are enough labile to be measured by the colorimetric method (Cotte *et al.*, 2020). Water samples were collected with the PIF water sampler on one point. Fluids were then analysed on board for pH and methane concentration was measured back in the laboratory by GC-FID and HID (Donval *et al.*, 2008).

On board, samples were washed through a 250  $\mu$ m sieve and individuals of *L. schrolli* and *S. tollmanni* were sorted. Fifty individuals were stored in 4% buffered seawater formalin and transferred to 80% ethanol after 4-5 month for histological observations while all other individuals were preserved in 96% ethanol for population structure studies.

## 2.2.2 Population structure

To infer population structure, size-frequency distributions of the species were analysed by measuring the curvilinear shell length (i.e. the longest distance from the apex to the anterior edge of the shell along the dorsal side) for *L. schrolli* and the maximal antero-posterior shell length for *S. tollmanni* (Appendix B.1). Only samples with at least 100 individuals were selected, and a random sub-sample of 500 individuals was used for larger samples.

2.2 Materials and Methods

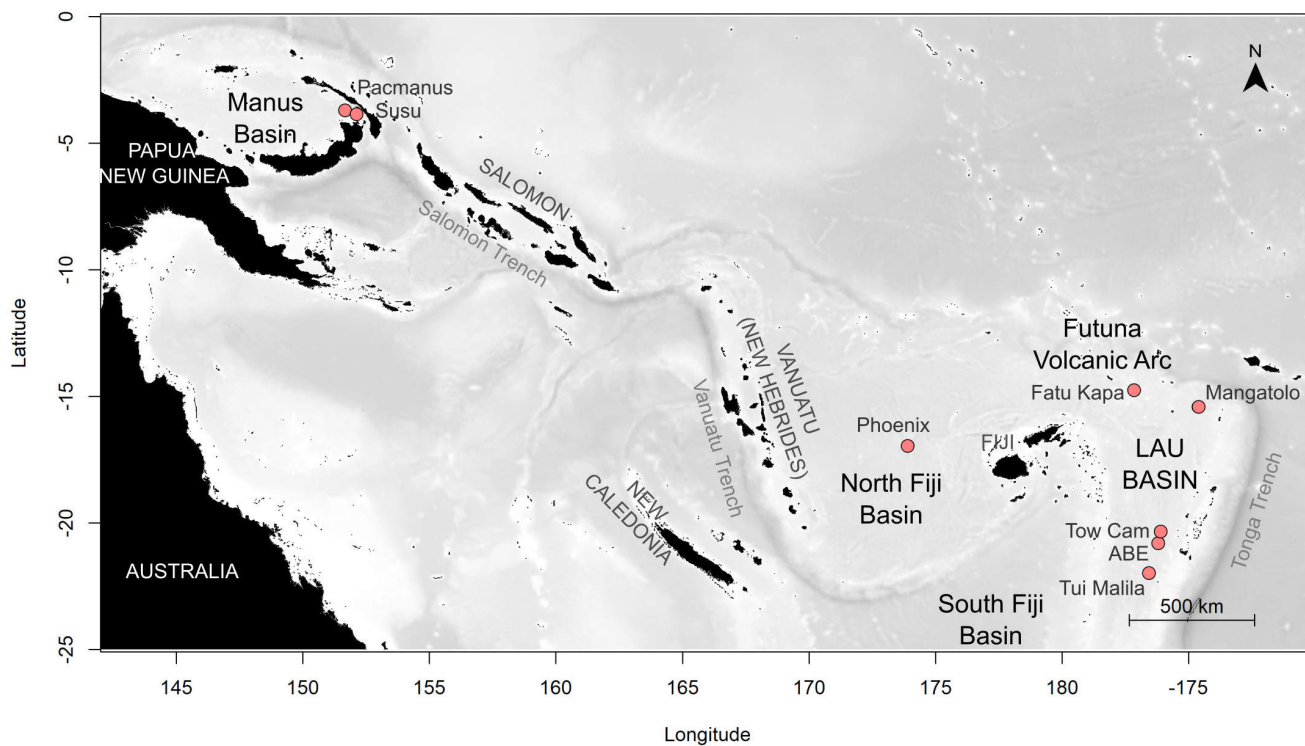


Figure 2.1 – Back-arc-basins sampling area in the South West Pacific. Red dots represent sampled vent field.



Table 2.1 – *Lepetodrilus schrolli* and *Shinkailepas tollmanni* sampling locations at the southwestern Pacific back-arc basins. For each sample, environmental data are provided: the habitat type (Hab.; I: *Ifremeria*, B: *Bathymodiolus*, depth, *in situ* maximal temperature (T°C) and pH, mean free inorganic sulphides ( $\Sigma S$ ) and methane ( $CH_4$ ) concentrations.

Species	Basin	Field	Site	Sample	Hab.	Longitude	Latitude	Depth (m)	T°C (max)	$\Sigma S$ ( $\mu M$ ) Mean	pH	$CH_4$ ( $\mu M$ )
<i>L. schrolli</i>	Manus	Pacamanus	Big Papi	PM1	I	151° 40.342'E	03° 43.707'S	1703	12.07	24.89	-	0.29
			Fenway	PM2	B	151° 40.370'E	03° 43.681'S	1698	19.28	-	-	-
				PM3	I	151° 40.367'E	03° 43.665'S	1699	19.16	-	-	-
			Solwara 8	PM4	I	151° 40.441'E	03° 43.825'S	1739	10.36	-	-	-
			Solwara 6	PM5	B	151° 40.861'E	03° 43.649'S	1725	5.44	1.99	7.4	0.12
			Solwara 7	PM6	I	151° 40.374'E	03° 43.040'S	1769	6.43	9.88	7.28	0.2
		Susu	North Su	SU1	B	152° 06.060'E	03° 47.942'S	1210	9.96	2.71	7.47	0.18
				SU2	I	152° 06.046'E	03° 47.935'S	1216	7.73	24.06	6.93	0.44
				SU3	B	152° 06.089'E	03° 47.957'S	1195	10.4	6.68	7.31	0.11
			South Su North	SU4	I	152° 06.291'E	03° 48.499'S	1341	5.8	94.03	7.14	0.18
	South Su South	SU5	I	152° 06.310'E	03° 48.583'S	1352	9.35	57.08	6.62	0.58		
		SU6	B	152° 06.310'E	03° 48.583'S	1352	7.35	13.93	6.43	0.56		
	Lau	Mangatolo		MG1	I	174° 39.208'W	15° 24.874'S	2031	17.45	61.77	6.36	1.03
			Tow Cam	North	TC1	I	176° 08.203'W	20° 19.047'S	2698	4.26	3.36	7.35
		TC4			B	176° 08.211'W	20° 19.051'S	2696	4.24	4.09	7.43	0.07
		South		TC2	B	176° 08.250'W	20° 19.074'S	2711	11.98	21.13	6.92	-
				TC3	I	176° 08.263'W	20° 19.084'S	2711	7.09	13.27	7.3	0.13
ABE		ABE	AB1	I	176° 11.479'W	20° 45.784'S	2153	7.64	16.02	6.02	-	
			AB2	B	176° 11.480'W	20° 45.784'S	2154	3.25	3	7.57	-	
Tui Malila		Tui Malila	TM1	B	176° 34.096'W	21° 59.352'S	1886	5.57	5.92	7.31	0.61	
			TM2	B	176° 34.088'W	21° 59.351'S	1874	8.85	5.17	7.2	0.12	
<i>S. tollmanni</i>		Manus	Pacamanus	Solwara 6	PM7	I	151° 40.852'E	03° 43.653'S	1729	12.7	25.98	7.38
	Susu			Suzette	SU8	I	152° 05.783'E	03° 47.368'S	1506	9.19	3.42	7.49
			South Su North	SU4	I	152° 06.291'E	03° 48.499'S	1341	5.8	94.03	7.14	0.18
	North Fiji	Phoenix	Phoenix North	PH1	I	173° 55.111'E	16° 56.936'S	1974	9.15	12.44	7.35	0.15
	Futuna	Fatu Kapa	AsterX	FK1	I	177° 09.134'W	14° 45.110'S	1562	12.89	0.5	5.88	0.23
	Lau	Mangaloto	Mangatolo South	MG2	I	174° 39.330'W	15° 24.958'S	2040	21.33	7.11	6.72	0.51
			Tow Cam	South	TC3	I	176° 08.263'W	20° 19.084'S	2711	7.09	13.27	7.3
		Tui Malila	Tui Malila	TM1	B	176° 34.096'W	21° 59.352'S	1886	5.57	5.92	7.31	0.61
				TM2	B	176° 34.088'W	21° 59.351'S	1874	8.85	5.17	7.2	0.12
			TM3	I	176° 34.098'W	21° 59.355'S	1886	18.83	8.93	6.53	0.34	

## 2.2 Materials and Methods

Measurements were conducted with the Leica Application Suite software linked to a Leica MC 170 HD camera mounted on a Leica M125 stereoscopic microscope for *L. schrolli*, and through the ZEN pro 3.2 software connected to a ZEISS AxioCam 208 Color camera mounted on a ZEISS SteREO Discovery.V20 stereoscopic microscope for *S. tollmanni*. Post-larval and juveniles shell of *S. tollmanni* were photographed under an Olympus SX16 microscope linked by an Infinity 1 Camera to the Infinity capture software and measured using ImageJ (Schneider *et al.*, 2012). Measurement error was determined using the maximum difference among ten repeated measures of the same individual on 10 specimens covering the whole size range of both species. It was fixed at 0.213 mm for *L. schrolli* and 0.125 mm for *S. tollmanni*. Length-class interval was set at 0.5 and 0.4 mm for *L. schrolli* and *S. tollmanni* respectively according to three criteria proposed by Jollivet *et al.* (2000): (1) most size-classes must have at least five individuals; (2) the number of adjacent empty classes must be minimized; and (3) the interval has to be much greater than the error of measurement.

Size-frequency distributions were compared to a normal distribution using a Kolmogorov-Smirnov one-sample test adapted by Lilliefors (Lilliefors, 1967) which is less sensitive to *ex æquo*. When distribution differed significantly from a normal distribution, modal decomposition, assuming that gastropods sizes followed a Gaussian distribution within cohorts, was performed using the Mixdist Package in R. Gaussian components number, associate mean and standard deviation were first estimated through Bhattacharya's (1967) method adapted by Pauly et Caddy (1985). Non-parametric Kruskal-Wallis tests were used to test for differences in shell lengths among samples within a basin, followed by a Nemenyi and Dunn multiple comparison test to identify differences. As the number of samples did not make it possible to perform numerous Kruskal-Wallis tests to detect significant habitat or field effects, only one Kruskal Wallis test was performed per species and per basin. Variations among habitats within a vent field and among fields within a basin were highlighted from the analysis of the results of the Nemenyi and Dunn multiple comparison test.

To determine the relationships between the size-frequency distribution and

the environmental conditions, a Redundancy Analysis (RDA) was performed on Hellinger-transformed size-frequency data (Legendre et Gallagher, 2001). This transformation corresponds to the square root of relative abundances of size classes and has the advantage of fulfilling the metric and Euclidean properties. Environmental variables considered included depth, maximal temperature (°C), mean concentration of  $\Sigma S$  ( $\mu M$ ) and  $CH_4$  ( $\mu M$ ), mean pH, basin and vent field; these two later were coded as dummy variables. Samples with missing data were not considered for this analysis. A forward selection was applied to select significant variable using the *forward.sel* function of the R package *adespatial* (Dray *et al.*, 2021). Before the RDA, a Wilcoxon-Mann-Whitney test was computed to test differences in the physico-chemical variables between habitats. All statistical analyses were performed with R statistical software 4.0.3 (R Core Team, 2020).

### 2.2.3 Sex ratio and reproductive biology

Due to the lack of penis in *L. schrolli*, about 100 individuals randomly selected among ten samples from various fields and habitats were measured and sexed by examination of gonad aspect after shell removal. Male gonad could be identified by series of white strips while “grain-like” structures could be distinguished in female ones (figure 2.2A-B). All specimens of *S. tollmanni* were sexed when possible. Male and females could be easily distinguished by the presence of a penis (figure 2.3A-B) beside the right cephalic tentacles (Beck, 1992b). To assess if mean length of females was greater than that of the males, a unilateral Wilcoxon-Mann-Whitney test was computed. Finally, to test for the deviation from a balanced 1:1 sex ratio, a Chi-squared goodness of fit test was applied.

Reproductive characteristics of both species were assessed through gonad histological observations and classical microscopy. Individuals were removed with forceps from their shells after being measured as described above. The whole soft-body part was then dehydrated with a series of increasing concentration of ethanol, cleaned in xylene, infiltrated of liquid paraffin and embedded into paraffin blocks. Serial 9  $\mu m$  and 7  $\mu m$  thick-sections of gonads were

## 2.2 Materials and Methods

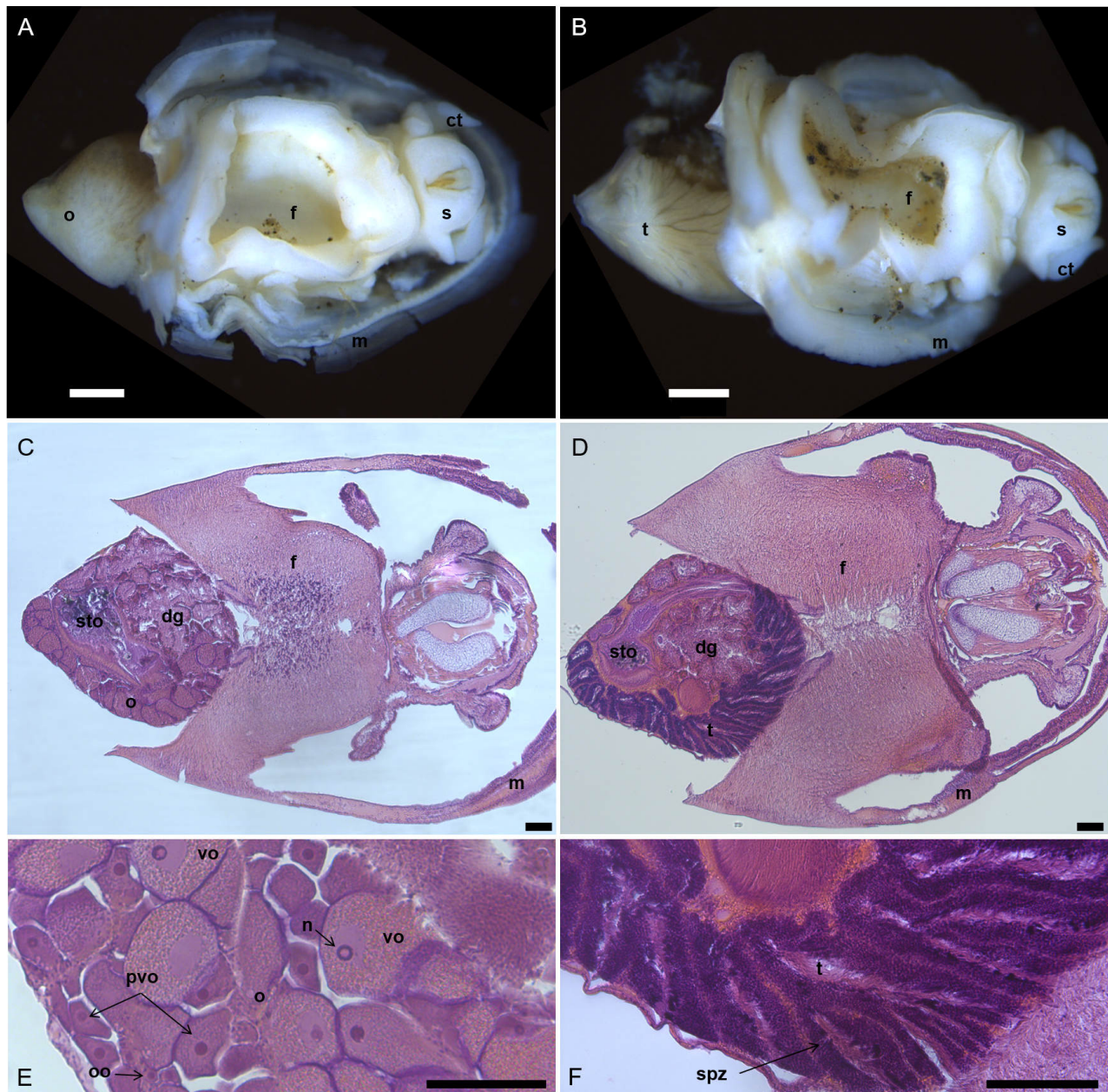


Figure 2.2 – *Lepetodrilus schrolli* female and male reproductive structures. Female soft-body, ventral view (A). B. Male soft-body, ventral view. C. General view of female transversal section, ventral view. D. General view of male transversal section, ventral view. E. Detailed view of ovary. F. Detailed view of testis. Abbreviations: (ct) cephalic tentacle; (dg) digestive gland; (f) foot; (m) mantle; (n) nucleus; (o) ovary; (oo) oogonia; (pvo) previtellogenic oocyte; (s) snout; (spz) spermatozoa; (sto) stomach; (vo) vitellogenic oocyte. White scalebar: 500  $\mu\text{m}$ . Black scalebar: 100  $\mu\text{m}$ .

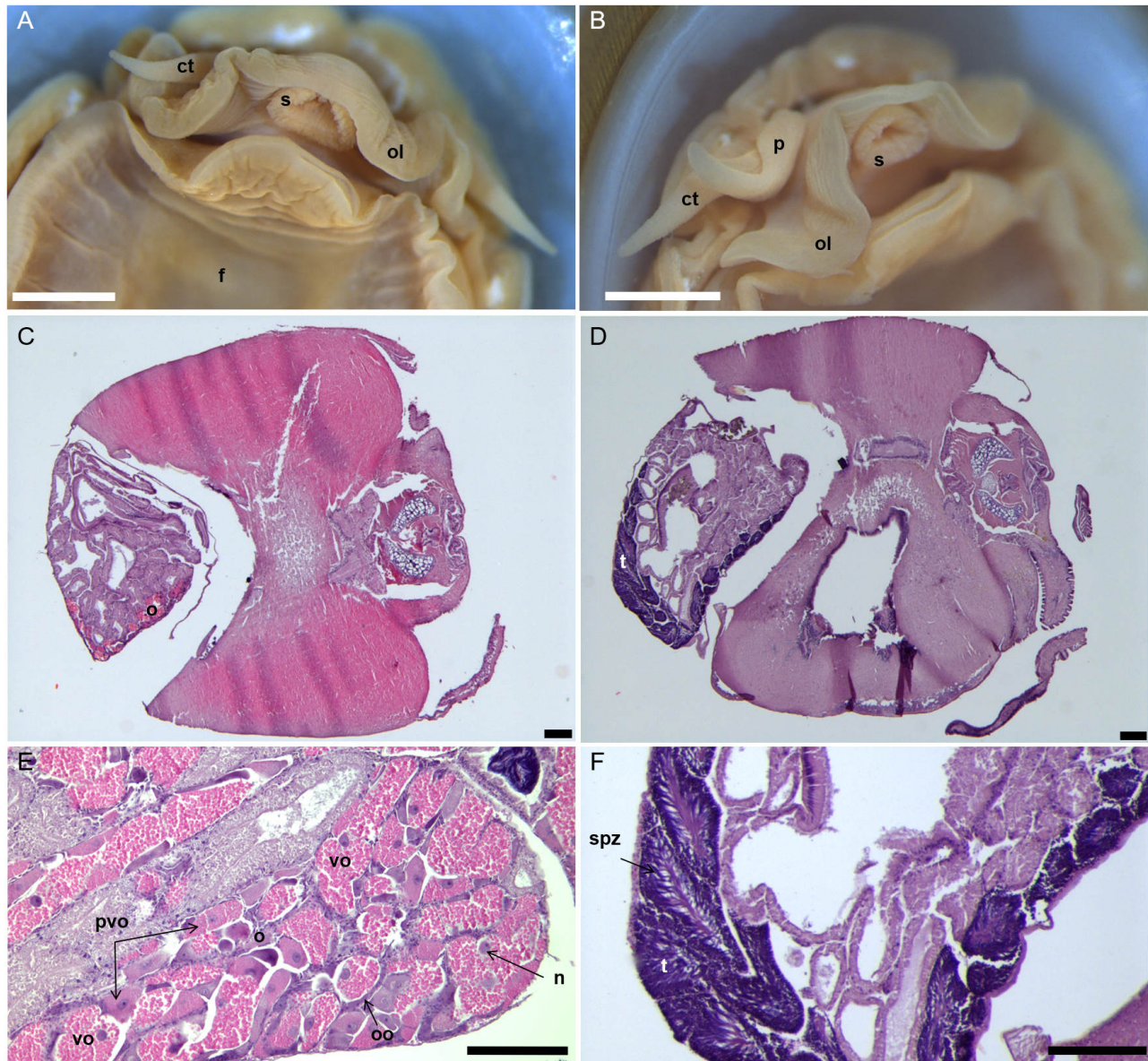


Figure 2.3 – *Shinkailepas tollmanni* female and male reproductive structures. Detailed view of female anterior part, ventral view (A). Detailed view of male anterior part, ventral view (B). General view of female transversal section, ventral view (C). General view of male transversal section, ventral view (D). Detailed view of ovary (E). Detailed view of testis (F). Abbreviations: (ct) cephalic tentacle; (f) foot; (n) nucleus; (o) ovary; (oo) oogonia; (ol) oral lobe; (p) penis; (pvo) previtellogenic oocyte; (s) snout; (spz) spermatozoa; (vo) vitellogenic oocyte. White scalebar: 1 mm. Black scalebar: 200  $\mu$ m.

## 2.2 Materials and Methods

produced with a microtome for *Lepetodrilus schrolli* and for *Shinkailepas tollmanni* individuals respectively. Sections were mounted onto microscope slides and stained with haematoxylin and eosin following the protocol proposed by Gabe (1968). Photographs of histological sections were taken using the Leica Application Suite AF software connected to a Leica DFC 450C camera on a Leica DMI6000 B inverted videomicroscope. Oocytes were then measured and counted using the ImageJ software.

For gametogenesis studies, two oocytes development stages were targeted: vitellogenic stage which represent mature oocytes, and previtellogenic stage considered as non-mature. Oogonia were not considered. Maximum and minimum Feret's diameter of at least 100 previtellogenic and vitellogenic oocytes per individual were measured from two to five sections selected in the beginning, middle and end part of the gonad. Only oocytes that have been sectioned through the nucleus were considered. As oocyte shape is variable, maximum and minimum Feret's diameter were used to calculate the area of an ellipse to infer the area-equivalent diameter which is  $\sqrt{\frac{4 \times \text{area}}{\pi}}$ . This is the estimated diameter of a circle with the same area as the object. Measurement error, fixed at 5  $\mu\text{m}$ , was determined using the maximum difference between ten repeated measurements of the same ten oocytes of various size and shape. According to the three criteria mentioned earlier (Jollivet *et al.*, 2000), oocytes sizes were grouped into 11  $\mu\text{m}$  size class and the relative frequencies of oocyte size class were computed for each female. To test for synchrony in reproductive development, size-frequency distributions of oocyte size among females within a vent site and among vent sites within a basin were compared using a Kruskal-Wallis multisample test. When significant differences occurred, a Nemenyi and Dunn post hoc test was performed. The percentage of vitellogenic oocytes per female was used to infer gametogenic maturity and difference among samples was analysed through a Kruskal-Wallis multisample test followed by a Nemenyi and Dunn post hoc test. The relationship between the proportion of vitellogenic oocyte and the female size was analysed using the Spearman rank correlation coefficient.

Actual fecundity was estimated by counting and measuring the total number of

vitellogenic oocytes within the gonad of eleven females of *L. schrolli* from the Manus and Lau Basins. Spearman's correlation test was used to test whether or not fecundity depended on size.

## 2.3 Results

### 2.3.1 Environmental conditions

Environmental conditions are presented in Table 2.1. Maximal temperature recorded within the *Ifremeria* habitat ranged from 4.26 (i.e. TC1 at Tow Cam) to 21.33°C (i.e. MG2 at Mangatolo). Mean  $\Sigma S$  concentrations ranged from 0.50 (i.e. FK1 at Fatu Kapa) to 94.03  $\mu M$  (SU4 at Susu), while  $CH_4$  concentrations ranged from 0.07 (i.e. TC1) to 1.03  $\mu M$  (i.e. MG1). The pH varied from 5.88 (i.e. FK1) to 7.49 (i.e. SU8). Within the *Bathymodiolus* habitat, maximal temperature ranged from 4.24°C (i.e. TC4) to 19.28°C (i.e. PM2 at Pacmanus). Mean  $\Sigma S$  concentrations ranged from 1.99 (i.e. PM5) to 21.13  $\mu M$  (i.e. TC2 at Tow Cam);  $CH_4$  concentrations varied from 0.07 (i.e. TC4) to 0.61  $\mu M$  (i.e. TM1); pH had a range from 6.43 (i.e. SU6) to 7.57 (i.e. AB2). Significant difference between habitat were detected for mean  $\Sigma S$  concentrations only (Wilcoxon-Mann-Whitney test:  $w = 32$ ,  $p$  value  $< 0.05$ ).

### 2.3.2 *Lepetodrilus schrolli*

**Population structure** Length frequency distributions were established from 9,484 individuals of *L. schrolli* from the Manus and Lau Basins, sampled in *Ifremeria* and *Bathymodiolus* habitats (Table 2.2). Shell length of *L. schrolli* specimens ranged from 0.51 to 9.86 mm, with mean lengths varying from 2.89 to 5.93 mm and median lengths from 2.95 to 5.65 mm. Except for *L. schrolli* in PM2, PM4 and PM6 samples collected at Pacmanus vent field in both *Ifremeria* and *Bathymodiolus* habitats, all size-frequency distribution significantly differed from a normal distribution (Lilliefors test,  $p$  value  $< 0.05$ , Table 2.2). However, most size-frequency distributions were unimodal and were characterised by a large number of medium size individuals coupled with a few small and/or large individuals, which led to a

### 2.3 Results

strong asymmetry for some samples (Figure 2.4, see supplementary Appendix B.2 for all size-frequency histograms). Between one to three Gaussian components of varying proportion were identified through modal decomposition with Mixdist. However, analyses did not allow to infer biologically meaningful cohorts and were hence not shown in the present manuscript. The Kruskal-Wallis test highlighted significant differences in shell length among samples within basins (Manus Basin:  $H = 1884.5$ ,  $df = 11$ ,  $p$  value  $< 0.001$ ; Lau Basin:  $H = 948.2$ ,  $df = 8$ ,  $p$  value  $< 0.001$ ). The Dunn's multiple pairwise comparisons test among samples from the Manus Basin showed variability at the vent field scale. Within Pacmanus, all but three pairs of samples out of fifteen significantly differed (i.e. PM3 vs. PM4 both from *Ifremeria* habitats, PM2 vs. PM3 and PM1 vs. PM5 pairs from *Ifremeria* and *Bathymodiolus* habitats respectively). Among Susu samples, all but four pairs out of fifteen significantly differed (i.e. SU1 vs. SU4 and SU5 from *Ifremeria* and *Bathymodiolus* habitat, SU4 vs. SU2 and SU5 from *Ifremeria* habitat). Variability within a field also occurred among the Lau Basin samples. Samples AB1 and AB2 from ABE vent field were significantly different ( $p$  value  $< 0.001$ ); only TC1 and TC2 differed significantly ( $p$  value  $< 0.01$ ) within Tow Cam, while the Tui Malila samples TM1 and TM2 were not significantly different.

The habitat type did not seem to impact shell length. Twenty-six out of thirty-five (i.e. 74%) and fifteen out of twenty pairs of samples (i.e. 75%) from different habitats (*Ifremeria* vs. *Bathymodiolus*) differed significantly in the Manus and Lau Basins respectively. By comparison, twenty four out of thirty-one pairs of Manus Basin samples (i.e. 77%) and eleven out of sixteen pairs of Lau Basin samples (i.e. 69%) from a same habitat (i.e. *Ifremeria* vs. *Ifremeria* or *Bathymodiolus* vs. *Bathymodiolus*) differed significantly. Variables subset by forward selection for RDA analysis selected only one explanatory variable for *L. schrolli* (i.e. the Tow Cam vent field). However, the adjusted  $R^2$  was low (adjusted  $R^2 = 0.28$ ).

**Sex ratio and reproductive biology** Sexing was possible for individuals with a curvilinear shell length greater than 2 mm. None of the sexed individuals had a penis. Female shell length ranged from 2.29 to 9.63 mm with a mean and median length of 5.35 and 5.24 mm respectively. Male



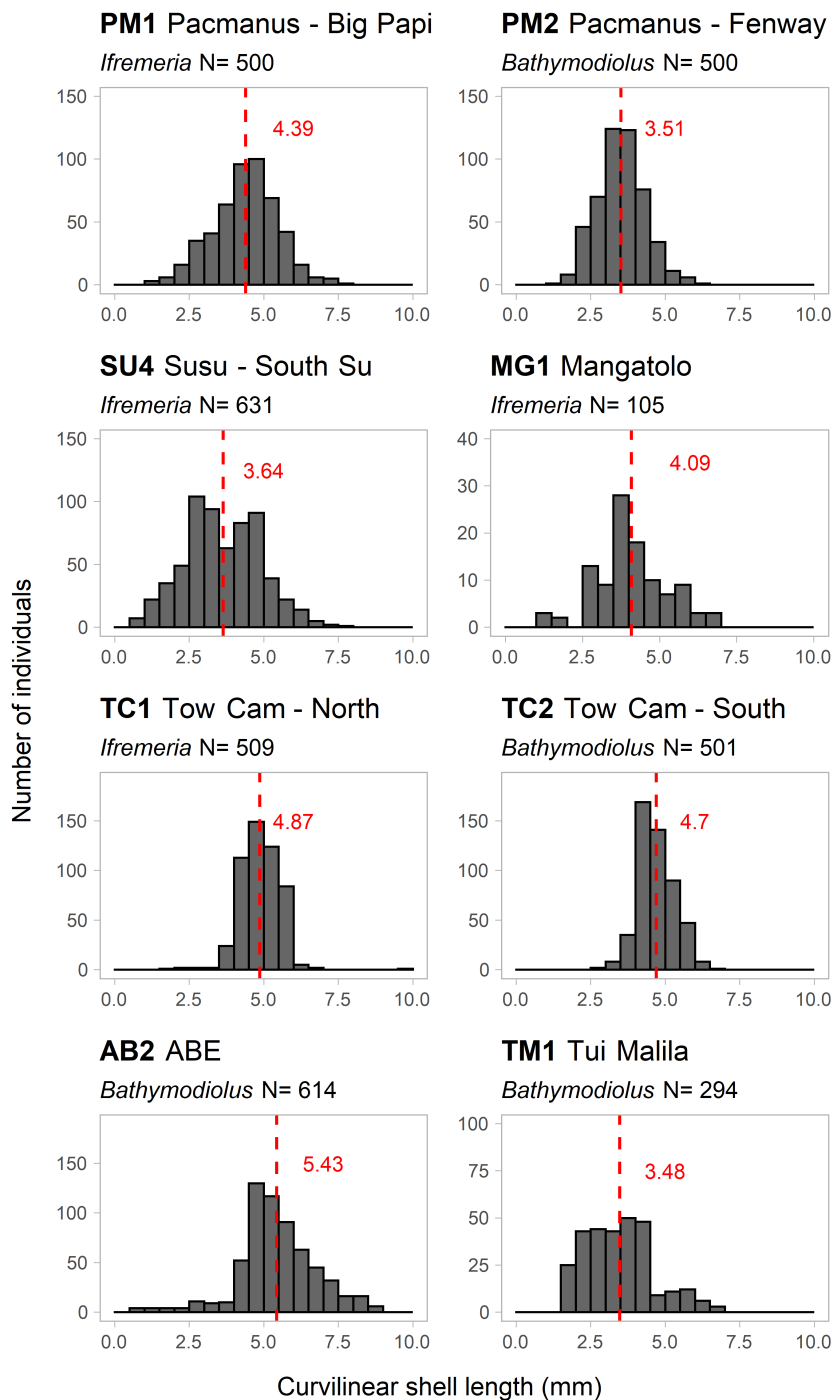


Figure 2.4 – Example of size-frequency histograms of *Lepetodrilus schrolli* collected in *Ifremeria* and *Bathymodiolus* habitats. N = number of measured individuals. Mean size is indicated in red.

## 2.3 Results

Table 2.2 – Number, shell length range, mean and median (mm) of individuals of *L. schrolli* and *S. tollmanni* used for demographic analysis within each sample collected in the South West Pacific back-arc basins.

Species	Field	Hab.	Sample	Number of individuals	Shell length range	Mean	Median	p values
<i>L. schrolli</i>	Pacmanus	I	PM1	500	1.13 - 7.80	4.39	4.46	*
		B	PM2	500	1.42 - 6.20	3.51	3.51	0.77
		I	PM3	500	1.79 - 6.96	3.7	3.63	**
		I	PM4	440	1.54 - 5.77	3.88	3.9	0.12
		B	PM5	500	1.33 - 8.27	4.71	4.62	**
		I	PM6	500	0.75 - 5.25	2.89	2.95	0.056
	Susu	B	SU1	500	1.52 - 8.16	3.87	3.82	***
		I	SU2	500	1.72 - 5.45	3.58	3.54	**
		B	SU3	500	1.99 - 9.51	5.93	5.65	***
		I	SU4	631	0.51 - 7.84	3.64	3.55	**
		I	SU5	500	1.00 - 7.13	3.78	3.84	***
		B	SU6	500	1.13 - 6.81	4.05	4.1	***
	Mangatolo	I	MG1	105	1.31 - 6.98	4.09	3.96	**
	Tow Cam	I	TC1	509	1.85 - 9.86	4.87	4.83	*
		B	TC2	501	2.52 - 6.52	4.7	4.61	***
		I	TC3	500	2.72 - 6.17	4.76	4.67	***
		B	TC4	501	2.40 - 6.94	4.79	4.78	*
	ABE	I	AB1	182	1.57 - 7.95	4.8	4.84	**
		B	AB2	614	0.74 - 8.94	5.43	5.29	***
	Tui Malila	B	TM1	294	1.71 - 6.90	3.48	3.41	**
B		TM2	199	2.16 - 5.50	3.61	3.55	*	
<i>S. tollmanni</i>	Pacmanus	I	PM7	477	0.55 - 10.24	7.2	7.21	***
	Susu	I	SU8	355	0.68 - 12.20	9.09	9.31	***
		I	SU4	319	3.22 - 11.66	8.4	8.4	**
	Phoenix	I	PH1	143	3.21 - 10.46	8.69	8.76	*
	Futuna	I	FK1	118	8.15 - 11.56	9.61	9.66	0.84
	Mangatolo	I	MG2	161	0.74 - 11.74	8.57	9.13	***
	Tow Cam	I	TC3	384	1.17 - 11.16	9.7	9.72	***
	Tui Malila	B	TM1	202	0.76 - 9.22	6.98	7.28	***
		B	TM2	350	3.43 - 8.43	6.88	6.87	*
		I	TM3	1090	0.70 - 8.90	6.52	6.9	***

B: Bathymodiolus; Hab.: Habitat; I: Ifremeria. Levels of significance of the Kolmogorov-Smirnov one-sample test adapted by Lilliefors: \* p value <0.05; \*\* p value <0.01; \*\*\* p value <0.001.

shell length ranged from 2.22 to 6.92 mm with a mean and median length of 4.47 and 4.42 mm respectively. For each sample, females were significantly larger than males (unilateral Wilcoxon-Mann-Whitney tests:  $p$  values  $< 0.01$ , Table 2.3). The sex ratio was not significantly different from 1:1 (Chi-squared goodness of fit analysis:  $p$  values  $> 0.05$ , Table 2.3), except for one sample from the Pacmanus vent field that displayed a female-biased sex ratio (i.e PM5).

Ovary and testis were posteriorly located, underlying the digestive gland and rising on its left (Figure 2.2A-D). Gametogenesis was described through the analyses of 182 females with a curvilinear shell length ranging from 3.48 to 9.13 mm, collected in *Ifremeria* and *Bathymodiolus* habitats from the two very distant Manus and Lau Basins (Table 2.3). Three stages of oocyte development were observed and present in all gonads: oogonia and previtellogenic and vitellogenic oocytes. Oogonia seemed to develop from the germinal epithelium along the entire gonad. Although they have been observed in each female, oogonia were not considered for oocyte size-frequency distribution analyses, their proportion would have been underestimated due to photographs. Previtellogenic oocytes, considered as non-mature, presented a smooth and dark cytoplasm while the vitellogenic mature oocytes were distinguishable by their pink coloured granular yolk in their voluminous cytoplasm (Figure 2.2E). Previtellogenic oocytes diameter ranged from 8.0 to 95.6  $\mu\text{m}$  with a mean and median diameter of 26.48 and 23.57  $\mu\text{m}$  respectively. Vitellogenic oocytes diameter ranged from 19.6 to 126.2  $\mu\text{m}$  with a mean and median diameter of 75.08 and 75.73  $\mu\text{m}$  (Table 2.3). All females presented the same pattern of oocytes size-frequency distribution with a large proportion of previtellogenic oocytes and a smaller proportion of vitellogenic oocytes (Figure 2.5A, see supplementary Appendix B.3 for all *L. schrolli* oocytes size-frequency histograms). The proportion of vitellogenic oocytes ranged from 1.00 to 33.52% (Table 2.3) and was dependent of the female size (Spearman correlation test  $S = 1181767$ ,  $\rho = -0.18$ ,  $p$  value = 0.02): the larger was the female, the smaller was the proportion of vitellogenic oocytes (Figure 2.6A). The proportion of vitellogenic oocytes differed significantly between samples within a basin (Kruskal-Wallis test, Manus Basin:  $H = 39.032$ ,  $df = 10$ ,  $p$  value  $< 0.001$ ; Lau Basin:  $H = 16.833$ ,  $df = 8$ ,  $p$  value  $<$

## 2.3 Results

Table 2.3 – Number and characteristics of individuals of *Lepetodrilus schrolli* and *Shinkailepas tollmanni* used for the sex ratio, gametogenesis and fecundity analysis within each sample from the South West Pacific.

Species	Field	Hab.	S.	Sex ratio					Gametogenesis			Fecundity		
				N	Mean length (mm)		M/F	$\chi^2$	N	oocyte size range ( $\mu\text{m}$ )	Prop. vo range (%)	N	Nb of vo	
					F	M								
<i>L. schrolli</i>	Pacmanus	I	PM1	103	5.77	5.24**	1.06	0.09						
		B	PM2						7	11.17 - 110.43***	7 - 19			
		I	PM3	100	4.32	3.66***	1.27	1.44	8	11.71 - 112.75*	14 - 28			
		I	PM4						9	8.99 - 117.19***	10 - 34			
		B	PM5	103	5.32	4.66***	0.66*	4.28	10	7.96 - 121.70***	7 - 20	1	205	
		I	PM6						9	12.65 - 124.13***	4 - 15			
	Susu	B	SU1						5	11.29 - 118.23	2 - 11			
		I	SU2						10	8.59 - 110.00**	9 - 22			
		B	SU3	102	6.68	5.33***	0.96	0.04	10	9.35 - 106.84***	2 - 15	2	156; 63	
		I	SU4						10	9.34 - 104.45**	7 - 18			
		I	SU5	101	4.3	3.84**	0.94	0.09	8	11.23 - 98.63***	2 - 14	1	52	
		B	SU6						7	9.91 - 105.18**	7 - 13			
	Mangatolo	I	MG1	91	4.56	3.76**	0.9	0.27	10	10.31 - 106.86	6 - 14	2	538; 338	
	Tow Cam	I	TC1	101	5.26	4.52***	1.24	1.2	10	10.53 - 113.35***	9 - 16			
		B	TC2	100	5.01	4.18***	0.96	0.04	10	10.27 - 126.23***	9 - 29			
		I	TC3						10	10.16 - 109.15**	7 - 23			
		B	TC4						10	9.22 - 116.65***	7 - 24	1	142	
	ABE	I	AB1						10	10.46 - 99.25	1 - 16	1	607	
		B	AB2	100	6.99	5.38***	0.89	0.36	9	11.57 - 106.23***	1 - 22	1	411	
	Tui Malila	B	TM1	101	4.96	4.19***	1.46	3.57	10	10.44 - 98.04**	7 - 22	1	393	
B		TM2						10	9.84 - 111.00**	8 - 20	1	80		
<i>S. tollmanni</i>	Pacmanus	I	PM7	440	7.4	7.14***	1.22*	4.4	9	13.28 - 130.61***	16 - 32			
	Susu	I	SU8	326	9.16	9.13	1.26*	4.43						
		I	SU4	287	8.59	8.20**	1.04	0.09						
	Phoenix	I	PH1	118	8.61	8.51	1.11	0.31						
	Futuna	I	FK1	94	9.8	9.35***	1.35	2.09						
	Mangatolo	I	MG2	148	9.31	9.1	1.21	1.32						
	Tow Cam	I	TC3	358	9.85	9.65***	1.34**	7.55	7	14.47 - 152.92***	19 - 44			
	Tui Malila	B	TM1	348	7.38	7.29	1.1	0.74						
		B	TM2	988	6.9	6.86	1.12	2.95						
		I	TM3	190	6.88	6.92	1.07	0.19						

B: Bathymodiolus; F: Female; **Hab.:** Habitat; I: Ifremeria; M: Male; N: Number of individual; S.: Sample; vo: Vitellogenic oocyte. Wilcoxon-Mann-Whitney (testing if F lengths > M lengths), Chi-squared goodness of fit (testing the deviation from a balanced sex ratio) and Kruskal-Wallis (testing differences among females oocyte sizes) test levels of significance: \* p value <0.05; \*\* p value <0.01; \*\*\* p value <0.001.

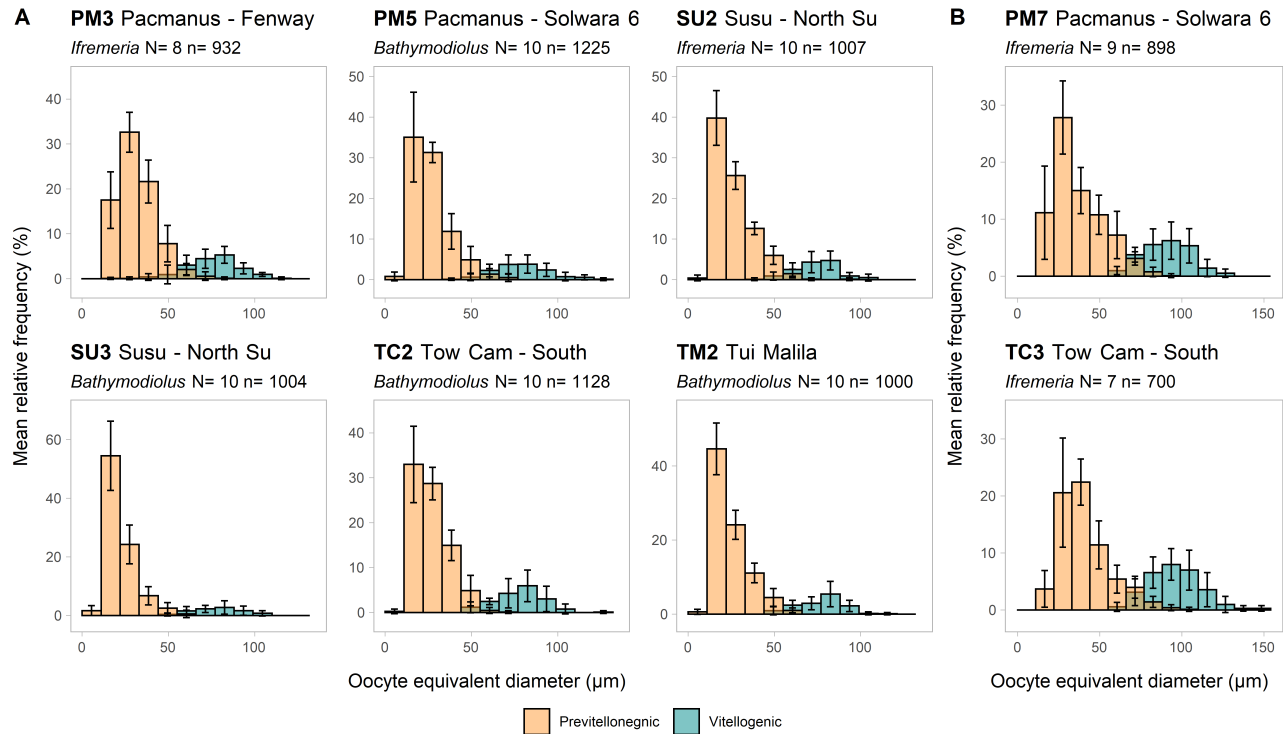


Figure 2.5 – Examples of mean oocyte size-frequency distribution histograms for females of *Lepetodrilus shcrolli* (A) and *Shinkailepas tollmanni* (B). N = number of measured individuals n= number of measured oocytes.

0.05 ). Pairwise comparison tests showed that only two samples from Pacmanus, for which the highest proportions of oocytes were observed (i.e. PM3 and PM4 from *Ifremeria* Habitat), differed significantly from some Susu samples (i.e. SU1, SU3, SU5 for both samples and SU6 for PM4 only from *Ifremeria* and *Bathymodiolus* habitats) in the Manus Basin, while no differences were detected between samples from the Lau Basin.

Significant variation in oocyte size distribution occurred among females within a sample, except for females from the SU1, MG1 and AB1 sample from Susu, Mangatolo and ABE vent fields respectively (Table 2.3). The Dunn's multiple pairwise comparisons test among females of a sample showed that between one to four females were responsible of these differences. No significant differences among females from TC3 and TM2 samples from Tow Cam and Tui Malila vent fields were identified from the multiple comparisons test, although the Kruskal-Wallis detected significant a difference among females. Kruskal-Wallis tests also

## 2.3 Results

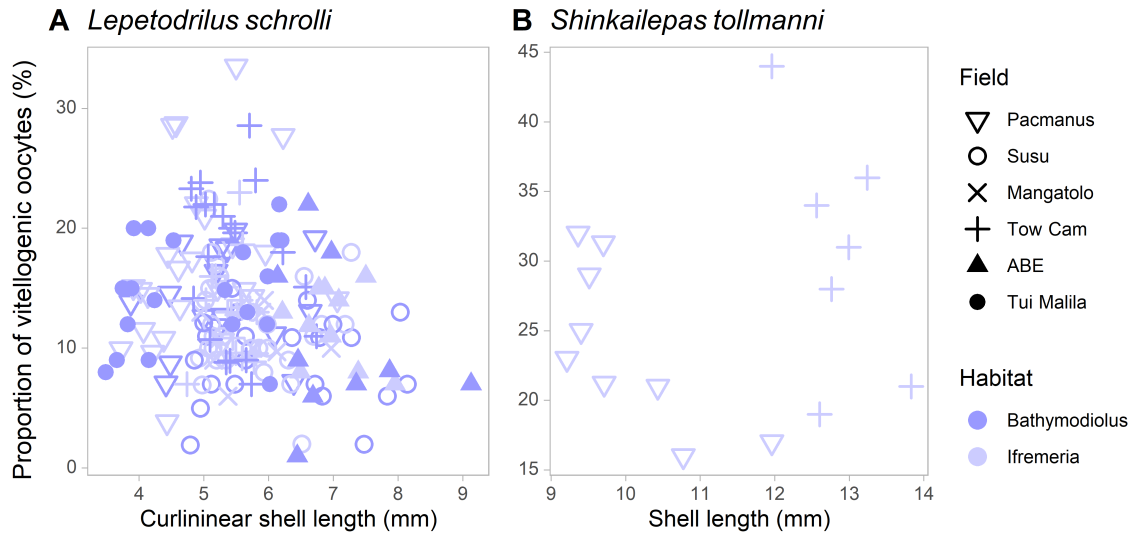


Figure 2.6 – Proportion of vitellogenic oocyte according to females' size for *Lepetodrilus schrolli* (A) and *Shinkailepas tollmanni* (B).

showed significant variations in oocytes size distribution among samples at the basin scale (Manus Basin:  $H = 815.11$ ,  $df = 10$ ,  $p$  value  $< 0.001$ ; Lau Basin :  $H = 109.43$ ,  $df = 8$ ,  $p$  value  $< 0.001$ ). The variability in oocyte size distribution in the Lau Basin was due to three samples (i.e AB1, AB2 and TC2 from ABE and Tow Cam) that differed from all other samples ( $p$  value  $< 0.001$ ) but not from each other. In the Manus Basin, Pacmanus samples PM2, PM3 and PM4 did not differ from each other, nor did PM5 and PM6 from *Ifremeria* and *Bathymodiolus* habitat. In Susu, *Ifremeria* habitat samples SU2 and SU4 differed from SU1, SU3 and SU6 collected in *Bathymodiolus* habitat, however, SU5 also from an *Ifremeria* habitat differed only from SU3. All Pacmanus samples differed from Susu's, except PM5 and SU2 from various habitats. The habitat type did not seem to have an impact on gametogenesis.

Actual fecundity was estimated from 11 females from *L. schrolli* with a shell length ranging from 3.75 to 7.89 mm and randomly selected among different samples (Table 2.3). The number of mature oocytes varied between 52 and 605 vitellogenic oocytes per female, with a mean of 276 vitellogenic oocytes. Fecundity was independent of size (Spearman correlation test:  $S = 178$ ,  $\rho = 0.19$ ,  $p$  value = 0.58).

### 2.3.3 *Shinkailepas tollmanni*

**Population structure** Size-frequency distributions were established from 3,599 individuals of *S. tollmanni* from the Manus, North Fiji Basins, the Futuna Volcanic Arc and the Lau Basin sampled in *Ifremeria* and *Bathymodiolus* habitats (Table 2.2). Shell length ranged from 0.55 to 12.20 mm with mean lengths among samples varying from 6.52 to 9.70 mm and median lengths from 6.90 to 9.72 mm. All size-frequency distributions, except the one from the FK1 sample (i.e. Fatu Kapa vent field at the Futuna Volcanic Arc), differed from a normal distribution (Lilliefors test,  $p$  value  $< 0.05$ ). Similarly to *L. schrolli*, size-frequency distributions were characterised by a large number of medium size individuals and a few small and/or large size individuals (Figure 2.7, see supplementary Appendix B.4 for all size-frequency histograms). Between two to four Gaussian components of varying proportions were identified by modal decomposition with Mixdist on non-normal size-frequency distributions, yet, as for *L. schrolli*, analyses did not allow to infer biological meaningful cohorts and were not shown in the present manuscript. Kruskal-Wallis test highlighted significant differences in shell length among samples at the scale of the southwestern Pacific ( $H = 2099.6$ ,  $df = 9$ ,  $p$  value  $< 0.001$ ). The Dunn's multiple pairwise comparisons test among samples showed significant variations among samples within a basin. The three pairs of samples from the Manus Basin and all six pairs but one from the Lau Basin samples differed significantly; only the samples TM2 and TM3 were not significantly different from each other. Due to the low number of samples from the *Bathymodiolus* habitat (i.e. two samples over ten), we focused only on samples from the Lau Basin to observe differences according to the habitat. All of the four pairs of samples from the two distinct habitats but one differed significantly ( $p$  value  $< 0.001$ ), as did the two pairs from a same habitat (i.e. *Ifremeria* vs. *Ifremeria* and *Bathymodiolus* vs. *Bathymodiolus*) ( $p$  value  $< 0.001$ ). Variables subset by forward selection for RDA analysis, select two explanatory variables (i.e. Tui Malila and Pacmanus vent fields). Only the first axis of the RDA was significant and was correlated to Tui Malila vent field (adjusted  $R^2 = 0.64$ ).

## 2.3 Results

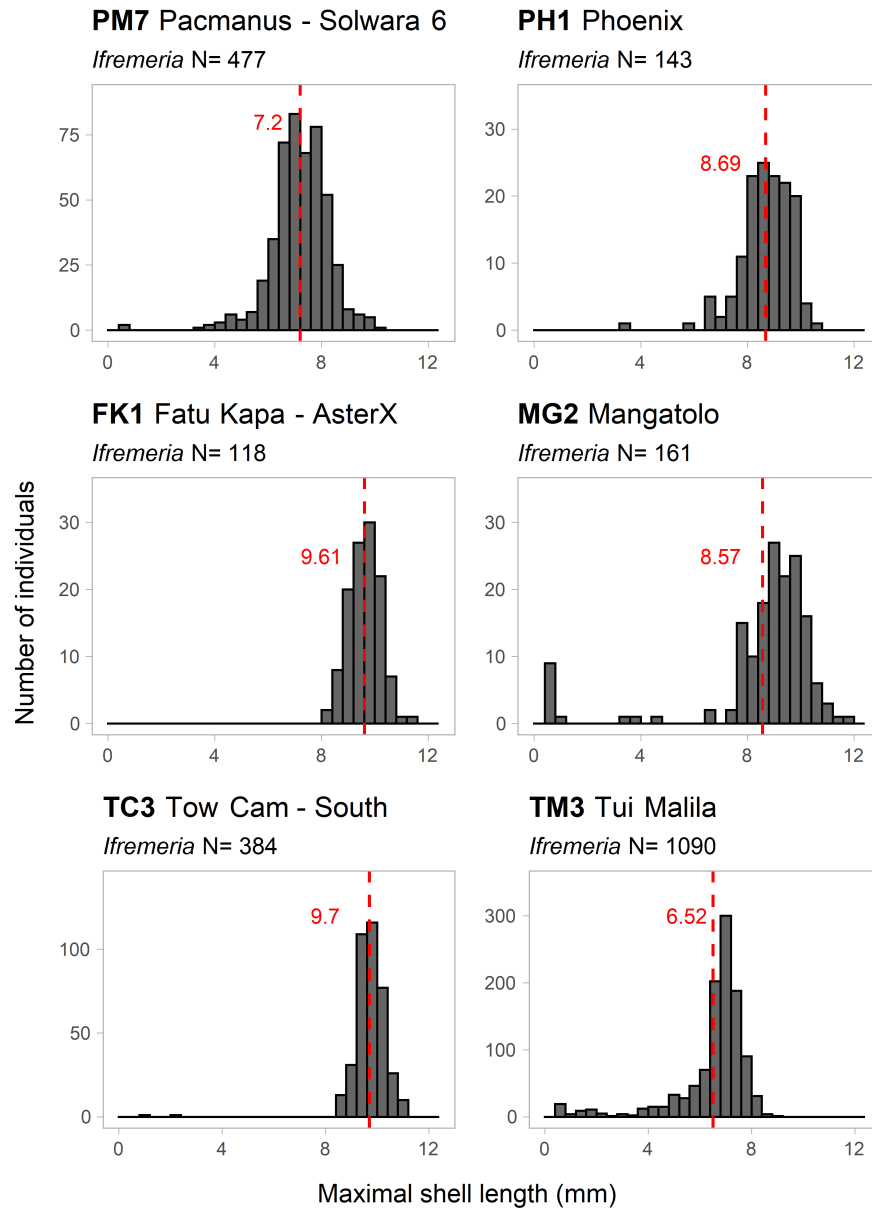


Figure 2.7 – Example of size-frequency histograms of *Shinkailepas tollmanni* collected in *Ifremeria* and *Bathymodiolus* habitats. N = number of measured individuals. Each mean is indicated in red.



**Sex ratio and reproductive biology** Sexing was possible for individuals with a shell length greater than 4.4 mm. Female shell length ranged from 4.93 to 12.20 mm with a mean and median lengths of 7.90 and 7.55 mm respectively. Male shell length ranged from 4.42 to 11.80 mm with a mean and median lengths of 7.84 and 7.53 mm respectively. Female mean size was significantly higher than male size in four samples from the Pacmanus, Susu, Fatu Kapa and Tow Cam vent field (i.e. PM7, SU4, FK1 and TC3, unilateral Wilcoxon-Mann-Whitney tests:  $p$  values  $< 0.01$ , Table 2.3). Three samples out of ten from the Pacmanus, Susu and Tow Cam vent field were significantly different from a balanced sex-ratio and were all in favour of males (i.e. PM7, SU8 and TC3, Table 2.3).

Ovary and testis were dorsally located and extends downward on the left and backward of the digestive gland (Figure 2.3C-D). Gametogenesis was described from 16 females ranging from 9.21 to 13.83 mm, collected in two samples from the two very distant Manus and Lau Basins in the *Ifremeria* habitat (Table 2.2). As for *L. schrolli*, three stages of development were observed (Figure 2.3E). Oogonia developed from the germinal epithelium along the entire gonad. Oogonia have been observed in each female, but for the same reasons as for *L. schrolli* they were not considered for oocyte size-frequency distribution analyses. Previtellogenic oocyte diameter ranged from 13.28 to 109.37  $\mu\text{m}$  with a mean and median of 38.47 and 34.70  $\mu\text{m}$  respectively and vitellogenic oocyte ranged from 55.92 to 152.92  $\mu\text{m}$  with a mean and median of 92.95 and 82.31  $\mu\text{m}$ . All females presented the same pattern of oocytes size-frequency distribution with a large proportion of previtellogenic oocytes and a smaller proportion of vitellogenic oocytes (Figure 2.5B). Vitellogenic oocytes proportion ranged from 16 to 44% (Table 2.3) and was independent of the female size (Spearman correlation test:  $S = 668.98$ ,  $\rho = 0.02$ ,  $p$  value = 0.95) (Figure 2.6B). The Kruskal-Wallis test highlighted significant differences in oocyte size-frequency distribution among females from the two samples observed (Table 2.3). According to the Dunn's multiple pairwise comparisons two females were responsible of these differences in both cases.

## 2.4 Discussion

The Chubacarc cruise, held in 2019, visited a large number of vent fields over 5 back-arc basins and volcanic arc in the South West Pacific. The associated large-scale sampling allowed the study of population structure and reproductive traits of two dominant widespread gastropod species, *Lepetodrilus schrolli* and *Shinkailepas tollmani* providing the first population and reproductive study of vent species in the southwestern Pacific. To date, only *L. nux* at the Okinawa Trough in the northwestern Pacific was investigated for population and reproductive biology (Nakamura *et al.*, 2014). Individuals of *Lepetodrilus schrolli* and *Shinkailepas tollmanni* colonised both the shells of *Bathymodiolus* and *Ifremeria* which inhabit areas of low and intermediate diffuse areas respectively (Podowski *et al.*, 2010). In the Lau Basin, Podowski *et al.* (2010) argued that (1) temperatures of about 20°C correspond to the upper limit of *Bathymodiolus* while its lower limits is defined by its minimum sulphide requirements; (2) the ecological niche of *Ifremeria nautili* is more constrained by biotic interactions with *Bathymodiolus* and *Alviniconcha* although this species was present at greater temperature and sulphide concentrations. The ranges of physico-chemical parameters observed in our study are in agreement with previous observations by Podowski *et al.* (2010) and confirm that *Ifremeria* is present in more intense diffusion zones with higher sulphide concentrations. No significant differences between both habitats were observed for the other physico-chemical variables, underlining the difficulty of discriminating between the two habitats sampled on the basis of these variables alone.

### 2.4.1 Recruitment patterns

*Lepetodrilus schrolli* and *Shinkailepas tollmanni* demographic structures were variable among samples along the southwestern Pacific back-arc basins but did not followed any particular pattern. While some populations presented a polymodal distribution, it is unlikely that the identified Gaussian component corresponded to a cohort as defined in ecology,

which is a group of individuals from the same population and born at the same time. The distributions were quite variable in all samples in terms of number of components and mean size but had some common characteristics. Each sample was dominated by a large number of sexually mature medium-size individuals with a few large and/or small individuals. The absence of a visible massive cohort of small individuals suggested the absence of a major episode of recruitment before sampling. Two main mechanisms can be proposed to explain these results. First, a discontinuous recruitment with a massive arrival of juveniles that was responsible of the group of medium-size individuals and other minor recruitment events. On the other hand, this pattern could result from a continuous recruitment with the regular arrival of a small number of young individuals that grow fast and accumulate in one or two Gaussian components of medium-size individuals. Among the gastropod family Lepetodrilidae discontinuous larval supply was suggested for *Lepetodrilus elevatus* (Sadosky *et al.*, 2002) while *Lepetodrilus fucensis* appeared to show continuous recruitment (Kelly et Metaxas, 2008), which seems a more likeable interpretation for *L. schrolli* and *S. tollmanni* limpets. The assumption of continuous recruitment is supported by the histological observations of *L. schrolli* and *S. tollmanni* gonads showing all development stages of gametes simultaneously in the tissues. On the other hand, the hypothesis of a massive recruitment event on the scale of the different basins of the South West Pacific was unlikely. The observed heterogeneity of size structures would be the result of specific local processes. Indeed, probability of successful settlement and mortality rates can be influenced by biotic or abiotic factor such as competition, predation or physical-chemical variations which in turn may also affect demographic structures and induce heterogeneous patterns (Kelly et Metaxas, 2008). Zoarcid fish along the East Pacific Rise showed a selective predation on *L. elevatus*, and especially large individuals (Sancho *et al.*, 2005), while accidental grazing by adults in areas of high faunal density may also increase juveniles mortality (Micheli *et al.*, 2002; Mullineaux *et al.*, 2003; Lenihan *et al.*, 2008). In areas of vigorous diffuse venting, competition for space and/or resources can affect community composition (Mullineaux *et al.*, 2003). Physical and chemical conditions structure

## 2.4 Discussion

organisms spatial distribution, and hydrothermal communities organize themselves according to temperature, pH,  $O_2$  concentration and chemical composition and concentration of different compounds (Kelly et Metaxas, 2008; Matabos *et al.*, 2008a; Podowski *et al.*, 2010; Sen *et al.*, 2013; Mullineaux *et al.*, 2018). However, none of the environmental conditions measured in this study nor the habitat type (*Ifremeria* or *Bathymodiolus*) could explained the variability we observed among populations size distributions of *L. schrolli* and *S. tollmanni*. In addition, unlike previous finding in *L. fucensis* (Bates, 2008) and *L. nux* (Nakamura *et al.*, 2014) the larger individuals of *L. schrolli* and *S. tollmanni* were not found at vents with the highest temperature. On the other hand, changes in local hydrodynamics such as currents and turbulence could result in episodic larval supply which may vary among fields or among vents within a field, and influence size-frequency distributions.

### 2.4.2 Reproductive biology

Our results brought new insights into the reproductive biology and anatomy of two abundant and widespread gastropod vent species. Both species were gonochoric and sexes were for the most part equally represented in local populations, except for some local bias in sex ratio towards females for *L. schrolli* and towards male for *S. tollmanni* in three samples. A balanced sex ratio combined with high population density will increase the chances of mating, enhance copulation and even allow multi-male fertilisation potentially favouring genetic diversity. Unlike others *Lepetodrilus* species, *L. schrolli* lacks a penis (Beck, 1993). The presence of a penis was reported for few individuals at North Fiji (Warén et Bouchet, 2001), but none of the males analysed in the present study had one, yet their gonads were full of spermatozoa (Figure 2.2D,F). This is not consistent with Beck's hypothesis of seasonal reproduction with the penis appearing at the time of breeding (Beck, 1993). The absence of penis could suggest an external fertilisation but pseudo-copulation with physical contact between males and females can be facilitated by high densities of individuals with equal number of males and females. Pseudo-copulation allow semi-internal (or entaquatic) fertilization in the mantle

cavity like others *Lepetodrilus* species (Fretter, 1988). This has already been considered for Lepetodrilidae limpets from *Pseudorimula* genus that also lack secondary reproductive organ (Haszprunar, 1989; Marticorena *et al.*, 2020). Internal fertilization is favoured by hydrothermal gastropods to protect gametes from possible harmful conditions of their environment (Fretter, 1988; Matabos et Thiébaud, 2010). Alternatively, some species such as *Shinkailepas tollmanni* produce capsules to protect their embryos (Beck, 1992b).

A sexual size dimorphism was observed for *L. schrolli* with females larger than males. According to histological observations, a sequential hermaphroditism does not seem likely. Such a dimorphism in size has been already observed in *L. nux* from the North West Pacific vent sites (Nakamura *et al.*, 2014). It was also reported in different coastal gastropods such as littorinids in which males are usually smaller and grow more slowly than females (Chow, 1987; Riascos et Guzman, 2010). The dimorphism is commonly explained by sexual selection although in *L. schrolli* there was no positive and significant relationship between fecundity and size. Females might grow to a larger size to physically accommodate the development of a large gonad for eggs provisioning. Size at first maturity varies among *Lepetodrilus* species, the presence of mature oocytes starts at around 2 mm for *L. nux* (Nakamura *et al.*, 2014), 2.4 mm for *L. tevnianus* (Bayer *et al.*, 2011) and 3.9 mm for *L. fucensis* (Kelly et Metaxas, 2007). The smallest female we observed in histology measured 3.48 mm long and had mature oocytes while the smallest female sexed on the basis of gonad morphology was 2.29 mm. Unfortunately, the absence of histological analyses on females smaller than 3.9 mm prevents us from defining the first size at sexual maturity for this species. The same is true for *S. tollmanni*, where the smallest female observed on histology was 9.21 mm, while the smallest female sexed was 4.93 mm. Early maturity is expected at vents where resources are not limited and environmental conditions are highly dynamic, and contribute to maximise the number of offsprings produced.

For both species female gonads analysis showed similar pattern with all stages of oocyte development present in the gonads (oogonia, previtellogenic oocytes and vitellogenic oocytes), suggesting potential continuous or quasi-continuous reproduction (Berg, 1985), with

## 2.4 Discussion

a much higher proportion of previtellogenic oocytes than vitellogenic (on average 86.6% for *L. schrolli* and 73.2% for *S. tollmanni*). The large overlap in size between vitellogenic and previtellogenic oocytes could be due to the irregular shape of the oocytes. The measurement of the equivalent diameter could overestimate or underestimate the size of the oocytes, especially for the larger ones, and thus enlarge the size range of the different oocyte stages (Copley et Young, 2006; Kelly et Metaxas, 2007). The strong variability of oocytes size distributions among females within a site, among sites and fields, supported the hypothesis of a continuous or quasi-continuous and an asynchronous gametogenesis between individuals. Among the Lepetodrilidae family as well as others gastropod families such as Peltospiridae, Sutilizonidae and Skeneidae, continuous reproduction is a widespread strategy (Tyler *et al.*, 2008; Matabos et Thiébaud, 2010; Bayer *et al.*, 2011; Nakamura *et al.*, 2014; Marticorena *et al.*, 2020). Continuous or quasi-continuous gametogenesis is also common in other vent taxa including polychaetes (Zal *et al.*, 1995; Faure *et al.*, 2007) and shrimps (Ramirez-Llodra, 2002). This type of gametogenesis can be explained by the regular energy flows provided by chemosynthesis (Tyler *et al.*, 1994; Marticorena *et al.*, 2020). Individuals can therefore allocate part of the consumed food resources to produce eggs continuously. This reproductive trait would allow hydrothermal species to maintain viable populations and quickly adapt to changes in environmental conditions and venting activity (Tyler *et al.*, 2008; Matabos et Thiébaud, 2010).

Vitellogenic oocytes of *L. schrolli* have a maximum size of 126  $\mu\text{m}$  while those of *S. tollmanni* reached 153  $\mu\text{m}$ . These maximal sizes are in the same order of magnitude as those observed in other hydrothermal limpets from the Juan de Fuca Ridge, East Pacific Rise and Mid-Atlantic ridge (Matabos et Thiébaud, 2010; Bayer *et al.*, 2011; Marticorena *et al.*, 2020). Although egg size often correlates with the development mode of marine invertebrates, large oocytes being associated with lecithotrophic development and small ones with planktotrophic development, this is not true for some gastropods, such as lepetodrilids, which have small eggs (<200  $\mu\text{m}$ ) but larval shell morphology suggesting lecithotrophic development (Lutz *et al.*, 1986; Tyler *et al.*, 2008). Conversely, *S. tollmanni* carried bigger vitellogenic oocytes but a recent study

reported a planktotrophic development for this species (Yahagi *et al.*, 2020). Recent studies suggest larval long-distance dispersal capacities, up to a year, in *S. tollmanni* and another Phaecolepadidae (i.e. *S. myojinensis*) (Yahagi *et al.*, 2017, 2020). Although *Lepetodrilus* larvae are thought to be lecithotrophic (Tyler *et al.*, 2008; Plouviez *et al.*, 2019), the cold temperature at the seafloor may imply metabolism reduction and thus allow longer distance dispersal (Young *et al.*, 1997; Mullineaux *et al.*, 1998).

In *L. schrolli*, the number of vitellogenic oocyte ranged between 52 and 607 mature oocytes per female with a mean value of 276, and was variable even among females within the same sample. This mean fecundity was relatively high in comparison with mean values already reported for different Lepetodrilidae species: 27.9 for *L. ovalis*, 37.2 for *L. atlanticus*, 53.9 for *L. pustulosus*, 125.7 for *L. fucensis* and 187 for *Pseudorimula atlantica* (Kelly et Metaxas, 2007; Tyler *et al.*, 2008; Marticorena *et al.*, 2020). However, it is lower than the maximum observed values of 850 for *L. pustulosus* (Tyler *et al.*, 2008) and 5,149 for *L. fucensis* (Kelly et Metaxas, 2007). Unlike other *Lepetodrilus* species (Kelly et Metaxas, 2007; Tyler *et al.*, 2008; Bayer *et al.*, 2011), the size of the *L. schrolli* individual did not seem to influence the reproductive effort, at least for the observed size range. Furthermore, the proportion of vitellogenic oocytes decreased with female size suggesting that the reproductive effort could decreased for the largest individuals.

Finally, our study showed no influence of the habitat on either the reproductive biology or population structure. Kelly et Metaxas (2007) showed that in *L. fucensis*, fecundity and oocytes development rate fluctuate according to the habitat, with low oocyte development and low fecundity in individuals living in senescent habitats. In addition, Marticorena *et al.* (2020) suggested that warmer habitat could provide a greater food resource and allow individuals to allocate more energy to vitellogenesis. Despite this, we did not identified relationships between the gametogenesis variability among samples, or the actual fecundity of *L. schrolli* and environmental conditions measured nor the habitat. This may simply be due to the fact that we did not sample senescent habitats and that both species are rather well adapted to the range of physico-chemical variations we could observed in the *Bathymodiolus* and *Ifremeria*

## 2.4 Discussion

habitats. Indeed, Kelly et Metaxas (2007) only observed differences between actively venting and senescent sources in *L. fucensis* gametogenesis and fecundity but not between active sources. The variability observed in gametogenesis between samples would probably be due to inter-individual variability.





## CHAPITRE 3

---

# Biodiversity partitioning of hydrothermal vent fauna associated with mussels and gastropods assemblages along South West Pacifique back-arc basins

---

Ce chapitre correspond à une première version d'un article à soumettre dans *Frontiers in Marine Science* avec : Éric Thiébaud, Cécile Cathalot, Cédric Boulart, Olivier Rouxel, Didier Jollivet, Stéphane Hourdez et Marjolaine Matabos.

### 3.1 Introduction

Hydrothermal vents are found in areas of high volcanic and tectonic activity along fast and slow mid-oceanic ridges, volcanic arcs, active seamounts and back-arc basins (Beaulieu *et al.*, 2013) and result from seawater percolating through the oceanic crust. Seawater infiltrating the crust heats up and accumulates minerals through reactions with the mantle rocks. The resulting hot hydrothermal fluid - less dense, acid, anoxic and enriched with sulfide, methane and metals - rises to the surface where it precipitates in contact with the cold seawater to form hydrothermal structures (Lalou, 1991). Although highly toxic, this fluid contains reduced compounds used by microorganisms to fix inorganic carbon through chemosynthesis (Childress et Fisher, 1992). These chemoautotrophic organisms, free or living in symbiosis with large invertebrate organisms, represent the trophic base of these systems and sustain large animal communities of highly specialised fauna (Tunnicliffe, 1991). Benthic communities inhabiting vent systems are then composed of a few large symbiont-bearing invertebrate species and a large variety of small and numerous consumers including grazers, suspension-feeders, deposit-feeders, scavengers, predators, commensals and parasites (Van Dover, 2000; Desbruyères *et al.*, 2006b). Symbiotic megafauna species form three-dimensional habitats, providing food and microhabitats, thus increasing the number of ecological niches available for smaller mobile organisms (Govenar *et al.*, 2005). These large megafaunal species are commonly used to identify various habitats or assemblages which can be easily described from submersible observations and are distributed along the vent fluid dilution gradient (Sarrazin *et al.*, 1997; Shank *et al.*, 1998; Podowski *et al.*, 2010). Along this environmental gradient, the distribution of organisms varies according to their physico-chemical tolerance (e.g. hypoxia, pH acidity, high temperature and sulfide concentration) (Vismann, 1991; Bates *et al.*, 2005), their ability to use the resources it provides (Levesque *et al.*, 2003), and biotic interactions including predation and competition for space and resource (Mullineaux *et al.*, 2000, 2003; Henry *et al.*, 2008). For instance, in the western back-arc basins three main assemblages dominated by symbiotic megafauna, i.e. the Provannids snails *Alviniconcha* spp. and *Ifremeria nautilei* and the mussel

### 3.1 Introduction

beds *Bathymodiolus* (Desbruyères *et al.*, 1994; Collins *et al.*, 2012) colonise the diffused flow gradient from high to lower temperature (Podowski *et al.*, 2009, 2010). The *Alviniconcha* habitat exhibits the highest temperatures (i.e. up to 42.4°C) and  $H_2S$  concentrations, followed by the *Ifremeria* (i.e. up to 32.5°C), and the *Bathymodiolus* (i.e. up to 32°C) habitats respectively (Podowski *et al.*, 2010). On the other hand, little is known about the small macrofauna associated with each assemblage. Beyond local variations of vent communities composition, different patterns of species diversity between vents within a region or between regions have been reported and attributed to various processes including variations in the physico-chemical properties of the habitat among vents, disturbance frequencies and dispersal barriers (Mullineaux *et al.*, 2018). In addition to these processes acting on ecological time scales, processes acting on evolutionary time scale and related to the complex tectonic history of mid-ocean ridges and back-arc basins may also influence the diversity distribution, yielding to geographic isolations, secondary contacts or recolonization events (Matabos *et al.*, 2008b; Plouviez *et al.*, 2009; Matabos et Jollivet, 2019).

In the western Pacific, hydrothermal vents are located mainly along back-arc spreading centres and volcanic arcs, geologically recent relative to mid-oceanic ridges (i.e. < 10 million years; Hall, 2002). While mid-oceanic ridges such as the Mid-Atlantic Ridge or the East Pacific Rise are continuous ridges systems that extend over thousands of kilometres, back-arc basins and volcanic arcs constitute fragmented and isolated systems (Desbruyères *et al.*, 2006a) with different geological and geodynamic contexts (Hall, 2002; Schellart *et al.*, 2006; Bézos *et al.*, 2009). The West Pacific is divided into two biogeographic provinces based on taxa compositions (Bachraty *et al.*, 2009; Thaler et Amon, 2019) with the North West province including the Okinawa and Mariana Trough back-arc basins and the Izu-Bonin Volcanic Arc, and the South West province including the Manus, Woodlark, North Fiji and Lau back-arc basins and the Futuna and Kermadec Volcanic Arcs. Southwestern back-arc basins show contrasting geodynamic contexts associated with diverse tectonic structures and magma products. This geological diversity induces different type of mineralization and therefore a wide variability of fluid chemistry

among hydrothermal vents (Mahlke *et al.*, 2011). This variation in mineralisation and fluid chemistry seems to influence species association and distribution within basins. For example, in the Lau Basin, differences in the chemical composition of vent fluids between fields related to a latitudinal gradient in lava type, from basalt to andesite, influence species distribution and biotic interactions between *Bathymodiolus brevior* and *Ifremeria nautilei* (Podowski *et al.*, 2010). In this basin, the distribution of host/symbiont associations in the genus *Alviniconcha* also vary along the latitudinal gradient in relation to the differences in the vent geochemistry (Beinart *et al.*, 2012). Hence the complex geological context of the region is expected to drive biodiversity partitioning over multiple scales, but to date the relative influence of the geological context, habitat heterogeneity and fluid chemistry on biodiversity structure has not been investigated at this scale. Since the study of Desbruyères *et al.* (2006a) on the distribution and composition of vent communities along the western Pacific basins and volcanic arcs (i.e. the Okinawa and Mariana Through and the Manus, North Fiji and Lau Basins), no studies have focused on communities' diversity structure along the southwestern Pacific basins. Most of these studies focused on megafauna discarding the associated macrofauna and were conducted at smaller spatial scales including only one or two basins, more particularly the Manus (Galkin, 1997; Collins *et al.*, 2012), Lau (Podowski *et al.*, 2009, 2010; Kim et Hammerstrom, 2012; Sen *et al.*, 2013; Diaz-Recio Lorenzo *et al.*, 2021) and North Fiji Basins (Desbruyères *et al.*, 1994) and only more recently the Woodlark Basin (Boulart *et al.*, 2022).

Changes in species composition along a spatial, temporal or environmental gradient ( $\beta$  diversity) can be estimated using the dissimilarity between samples (Whittaker, 1972; Anderson *et al.*, 2011). This dissimilarity is the consequence of two distinct processes: species replacement or turnover between two samples (i.e. species are replaced by others), and the difference in species richness between two samples (i.e. species are lost or gained) (Legendre, 2014). These two processes are related to different phenomena. Species are replaced by others along a geographic, biological or environmental gradient in response to environmental filtering, historical events, or biotic interactions such as competition (Leprieur *et al.*, 2011). Species

### 3.1 Introduction

replacement implies the simultaneous gain and loss of species. On the other hand, a difference of species richness between assemblages or sites can be due to physical barriers, a smaller number of niches available locally or to the absence of species with low dispersal abilities. In this case, nestedness is a particular case of richness difference when species at a given site is a strict subset of the species at a richer site. On the other hand, processes structuring biodiversity vary according to the scale considered. While the physico-chemical conditions of the local environment will structure biodiversity at small spatial scales, historical processes will influence biodiversity on larger scales. Understanding processes occurring across scales is paramount to better understand biodiversity distribution patterns. This knowledge is essential to establish optimal ecosystem management measures, which is even more important in the South West Pacific back-arc basins highly targeted for its mineral resources and that could be strongly impacted by mining exploitation activities (Boschen *et al.*, 2013; Gollner *et al.*, 2017; Boschen-Rose *et al.*, 2021).

In this study, we hypothesized that the heterogeneity existing at different scales among the southwestern Pacific back-arc basins will lead to a great number of ecological niches and thus a high degree of heterogeneity in the distribution of species and faunal assemblages. While the physico-chemical conditions of the local environment should structure biodiversity at small spatial scales, historical processes should influence biodiversity at larger scales. The objective of this study is to test for this hypothesis through the description of the distribution of biodiversity at the regional and local scales and investigate the associated spatial and environmental drivers through the chemical characterisation of three distinct habitats, the *Alviniconcha*, *Ifremeria* and *Bathymodiolus* assemblages.

## 3.2 Materials and Methods

### 3.2.1 Study area and data collection

Vent community samples were collected at four back-arc basins (i.e. the Manus, Woodlark, North Fiji and Lau Basins) and one volcanic arc (i.e. Futuna) in the South West Pacific during the CHUBACARC oceanographic cruise held in March/May 2019 on the French Research vessel *L'Atalante* (Hourdez et Jollivet, 2019). A hierarchical sampling was conducted including three nested spatial scales: (1) the sites at scales ranging from few meters to tens of metres, (2) the fields at scales between few hundred metres to kilometres, and (3) the basins distant from hundreds to thousands of kilometres. Between one to four fields per basin, and one to six sites per field were sampled (Figure 3.1, Table 3.1). While a clear definition of spatial scales is essential to describe diversity in patchy habitats such as hydrothermal vents, there is currently no consensus on a standard and clear definition of the different terms to describe a vent 'site' or 'field' (Tunnicliffe, 1991; Chevaldonné *et al.*, 1997). In the present study, vent fields were defined according to the InterRidge Global Database of Active Submarine Hydrothermal Vent Fields version 3.4 (Beaulieu *et al.*, 2013) and sites were defined based on *in situ* observations.

We sampled three vent habitats located from low to moderate diffuse flow areas and identified according to their dominant engineer species, including the *Bathymodiolus*, the *Ifremeria* and the *Alviniconcha* habitats (Table 3.1, Appendix D.2 and D.3). Sampling was carried out in several steps using the Remotely Operated Vehicle (ROV) *Victor6000* (Figure 3.2). Individuals of the engineer species which defined the habitat were first collected using the hydraulic arm of the ROV and placed in a biobox (roughly four-five grabs). Sampling was then completed using the suction device of the ROV when possible to collect the associated small organisms and mobile epifauna. A total of 60 samples<sup>1</sup> was collected, including 42 completed with the suction sampler (Table 3.1). The box and suction numbers of each sample are provided in the Appendix D.4.

---

1. A sample is defined as a collection in a box, with or without suction

### 3.2 Materials and Methods

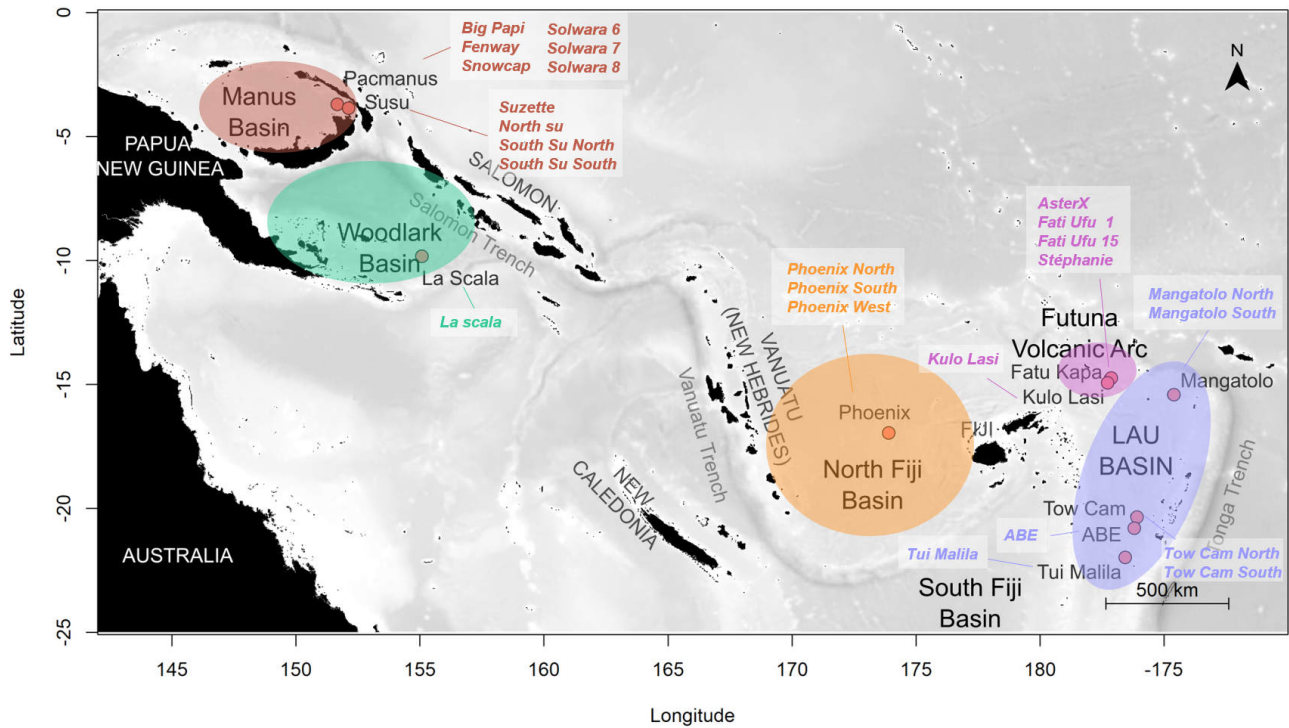


Figure 3.1 – Back-arc-basins sampling area in the South West Pacific. Red dots represent sampled vent field. The sites sampled are listed in italics.



Table 3.1 – Sampling locations at the southwestern Pacific back-arc basins. For each sample, sampling informations and environmental data are provided: the sampled habitat (Hab., A: *Alviniconcha*, B: *Bathymodiolus*, I: *Ifremeria*), if there was a sample from the faunal suction device in addition to the biobox (aspi, Y: Yes, N: No), the proportion (%) of *Alviniconcha*, *Bathymodiolus* and *Ifremeria* among engineer species individuals, geographical coordinates (Longitude and Latitude), depth (m), *in situ* mean and maximal temperature (°C), pH, mean total dissolved sulphide ( $\Sigma S$   $\mu M$ ), methane ( $CH_4$   $\mu M$ ), sulfur (S  $\mu M/Kg$ ) and phosphorus (P  $\mu M/Kg$ ).

Basin	Field	Site	Hab.	Sample	Suction	A	B	I	Longitude	Latitude	Depth	T°C mean	T°C max	$\Sigma S$ mean	pH	CH <sub>4</sub>	S	P
Manus	Pacmanus	Big Papi	I	PM1	N	2	17	81	151° 40.342'E	03° 43.707'S	1703	5.8	12.07	24.89	-	0.29	27.96	3.39
			A	PM11	Y	100	.	.	151° 40.335'E	03° 43.731'S	1708	11.79	17.38	24.58	6.81	0.35	27.01	3.08
	Fenway	A	PM10	N	94	.	6	151° 40.373'E	03° 43.684'S	1698	6.6	10.59	21.47	6.24	0.85	26.49	3.24	
		B	PM2	N	.	100	.	151° 40.370'E	03° 43.681'S	1698	9.79	19.28	-	-	-	-	-	
		I	PM3	N	.	.	100	151° 40.367'E	03° 43.665'S	1699	12.33	19.16	-	-	-	-	-	
		B	PM8	Y	.	100	.	151° 40.360'E	03° 43.675'S	1696	3.14	3.57	3.04	7.28	0.27	27.12	3.22	
	Snow Cap	B	PM9	Y	.	83	17	151° 40.213'E	03° 43.691'S	1640	3.59	4.98	1.82	7.22	0.52	27.56	3.07	
	Solwara 6	B	PM5	Y	.	99	1	151° 40.861'E	03° 43.649'S	1725	3.95	5.44	1.99	7.4	0.12	27.07	3.29	
		I	PM7	Y	.	9	91	151° 40.852'E	03° 43.653'S	1729	9.01	12.7	25.98	7.38	0.2	26.28	3.96	
	Solwara 7	I	PM6	Y	.	.	100	151° 40.374'E	03° 43.040'S	1769	4.75	6.43	9.88	7.28	0.2	26.88	3.25	
	Solwara 8	A	PM12	Y	71	.	29	151° 40.458'E	03° 43.821'S	1737	12.97	17.62	-	-	-	-	-	
		I	PM4	Y	18	.	82	151° 40.441'E	03° 43.825'S	1739	7.97	10.36	-	-	-	-	-	
	Susu	North Su	B	SU1	Y	.	95	5	152° 06.060'E	03° 47.942'S	1210	6.08	9.96	2.71	7.47	0.18	27.18	4.44
			A	SU11	N	78	.	22	152° 06.046'E	03° 47.933'S	1218	6.68	18.22	9.11	7.32	0.21	27.06	3.3
I			SU2	Y	.	.	100	152° 06.046'E	03° 47.935'S	1216	5.87	7.73	24.06	6.93	0.44	25.69	3.74	
B			SU3	Y	.	100	.	152° 06.089'E	03° 47.957'S	1195	8.27	10.4	6.68	7.31	0.11	26.93	3.44	
South Su North		A	SU10	N	96	.	4	152° 06.292'E	03° 48.497'S	1343	7.95	16	69.4	6.39	0.5	26.59	3.09	
		I	SU4	Y	.	2	98	152° 06.291'E	03° 48.499'S	1341	4.47	5.8	94.03	7.14	0.18	27.27	2.88	
		B	SU7	Y	.	100	.	152° 06.299'E	03° 48.483'S	1360	3.64	3.82	7.04	7.27	0.2	27.27	3	
South Su South		I	SU5	Y	5	2	93	152° 06.310'E	03° 48.583'S	1352	5.63	9.35	57.08	6.62	0.58	25.99	2.81	
		B	SU6	Y	.	100	.	152° 06.310'E	03° 48.583'S	1353	5.58	7.35	13.93	6.43	0.56	26.48	2.92	
		A	SU9	N	100	.	.	152° 06.309'E	03° 48.583'S	1354	7.51	27.25	55.63	6.54	0.28	25.75	2.83	
Suzette	A	SU12	N	99	.	1	152° 05.783'E	03° 47.368'S	1505	6.58	9.46	1.44	7.32	0.15	26.66	2.73		
	I	SU8	Y	6	.	94	152° 05.783'E	03° 47.368'S	1506	5.42	9.19	3.42	7.49	0.1	26.26	2.68		
Woodlark	La Scala	La Scala	I	LS1	Y	10	.	90	155° 03.161'E	09° 47.944'S	3388	4.88	7.29	9.08	7.66	-	26.05	2.29
			A	LS2	N	100	.	.	155° 03.160'E	09° 47.945'S	3388	10.63	18.95	31.4	7.25	-	26.06	2.6
			A	LS3	N	100	.	.	155° 03.117'E	09° 47.939'S	3344	3.26	4.18	7.31	7.73	-	-	-

Basin	Field	Site	Hab.	Sample	Suction	A	B	I	Longitude	Latitude	Depth	T°C mean	T°C max	ΣS mean	pH	CH <sub>4</sub>	S	P
North Fiji	Phoenix	Phoenix North	I	PH1	Y	2	.	98	173° 55.111'E	16° 56.936'S	1974	5.06	9.15	12.44	7.35	0.15	30.06	3.69
		Phoenix South	I	PH2	Y	1	.	99	173° 55.133'E	16° 57.005'S	1961	6.49	13.21	21.11	6.21	0.15	30	3.33
			B	PH3	Y	.	100	.	173° 55.127'E	16° 57.002'S	1961	6.18	8.9	17.22	7.41	0.15	29.78	3.05
			A	PH4	Y	80	.	20	173° 55.127'E	16° 57.000'S	1961	14.55	30.25	56.85	6.68	0.45	28.66	3.02
		Phoenix West	A	PH5	Y	98	.	2	173° 55.078'E	16° 56.963'S	1973	4.54	9.58	10.52	7.39	0.13	30.42	3.52
Futuna	Fatu Kapa	AsterX	I	FK1	Y	11	.	89	177° 09.134'W	14° 45.110'S	1562	7.82	12.89	0.5	5.88	0.23	33.47	3.84
			A	FK2	Y	76	.	24	177° 09.132'W	14° 45.110'S	1562	12.98	24.35	14.94	6.47	0.35	32.63	4.79
		Fati Ufu 1	A	FK6	N	84	.	16	177° 11.116'W	14° 45.597'S	1519	13.9	19.97	18.78	5.95	0.32	24.55	2.79
			I	FK8	Y	1	.	99	177° 11.113'W	14° 45.599'S	1519	12.48	23.14	1.49	6.36	0.12	27.42	2.94
		Fati Ufu 15	I	FK5	Y	2	.	98	177° 10.970'W	14° 45.326'S	1516	9.23	15.92	2.78	7.01	0.21	26.84	2.87
		Stephanie	I	FK3	N	2	.	98	177° 09.960'W	14° 44.243'S	1548	6.4	9.8	4.65	6.87	0.11	33.33	4.46
	A		FK4	N	62	.	38	177° 09.960'W	14° 44.245'S	1547	8.5	11.67	27.21	6.52	0.37	33.26	4.86	
		Kulo Lasi	Kulo Lasi	I	KL1	Y	0	1	99	177° 15.551'W	14° 56.468'S	1371	4.89	10.79	141.25	7.2	-	28.16
Lau	ABE	ABE	I	AB1	Y	2	.	98	176° 11.479'W	20° 45.784'S	2153	4.84	7.64	16.02	6.02	-	26.98	4.58
			B	AB2	Y	.	94	6	176° 11.480'W	20° 45.784'S	2154	2.62	3.25	3	7.57	-	26.69	5.07
			A	AB3	Y	83	.	17	176° 11.478'W	20° 45.783'S	2153	10.92	19.19	63.74	6.98	-	27.52	3.44
	Mangatolo	Mangatolo North	I	MG1	Y	.	.	100	174° 39.208'W	15° 24.874'S	2031	7.52	17.45	61.77	6.36	1.03	30.47	4.57
			A	MG3	Y	74	.	26	174° 39.208'W	15° 24.876'S	2031	16.64	20.57	79.96	5.9	0.83	30.18	4.1
		Mangatolo South	I	MG2	Y	7	.	93	174° 39.330'W	15° 24.958'S	2040	11.04	21.33	7.11	6.72	0.51	30.43	4.9
			A	MG4	Y	64	.	36	174° 39.331'W	15° 24.961'S	2039	15.49	29.09	33.13	7.2	0.21	31.67	4.52
	Tow Cam	Tow Cam North	I	TC1	Y	.	.	100	176° 08.203'W	20° 19.047'S	2698	3.03	4.26	3.36	7.35	0.07	29.61	3.19
			B	TC4	Y	.	100	.	176° 08.211'W	20° 19.051'S	2696	3.4	4.24	4.09	7.43	0.07	28.98	3.04
		Tow Cam South	B	TC2	Y	.	81	19	176° 08.250'W	20° 19.074'S	2711	8.65	11.98	21.13	6.92	-	29.28	2.8
			I	TC3	N	20	.	80	176° 08.263'W	20° 19.084'S	2711	5.13	7.09	13.27	7.3	0.13	29.44	3.42
			A	TC5	Y	87	.	13	176° 08.263'W	20° 19.085'S	2711	12.28	21.24	55.83	6.75	0.4	27.44	2.76
			A	TC6	Y	100	.	.	176° 08.258'W	20° 19.074'S	2716	12.27	22.38	10.96	7.28	0.1	30.14	3.14
			B	TC7	N	.	100	.	176° 08.261'W	20° 19.080'S	2710	5.99	10.13	5.61	5.8	-	26.87	28.11
	Tui Malila	Tui Malila	B	TM1	Y	8	89	3	176° 34.096'W	21° 59.352'S	1886	4.08	5.57	5.92	7.31	0.61	28.84	3.62
B			TM2	Y	.	77	23	176° 34.088'W	21° 59.351'S	1874	6.24	8.84	5.17	7.2	0.12	28.69	3.13	
I			TM3	N	23	.	77	176° 34.098'W	21° 59.355'S	1886	10.55	18.83	8.93	6.53	0.34	28.83	3.32	
I			TM4	N	.	.	100	176° 34.094'W	21° 59.354'S	1877	15.13	22.07	25.24	6.7	0.18	28.11	2.6	
A			TM5	N	100	.	.	176° 34.091'W	21° 59.356'S	1884	25.75	40.04	85.58	6.32	0.11	26.43	18.36	
A			TM6	Y	100	.	.	176° 34.099'W	21° 59.348'S	1886	9.75	19.73	9.35	6.82	0.23	29.07	3.16	

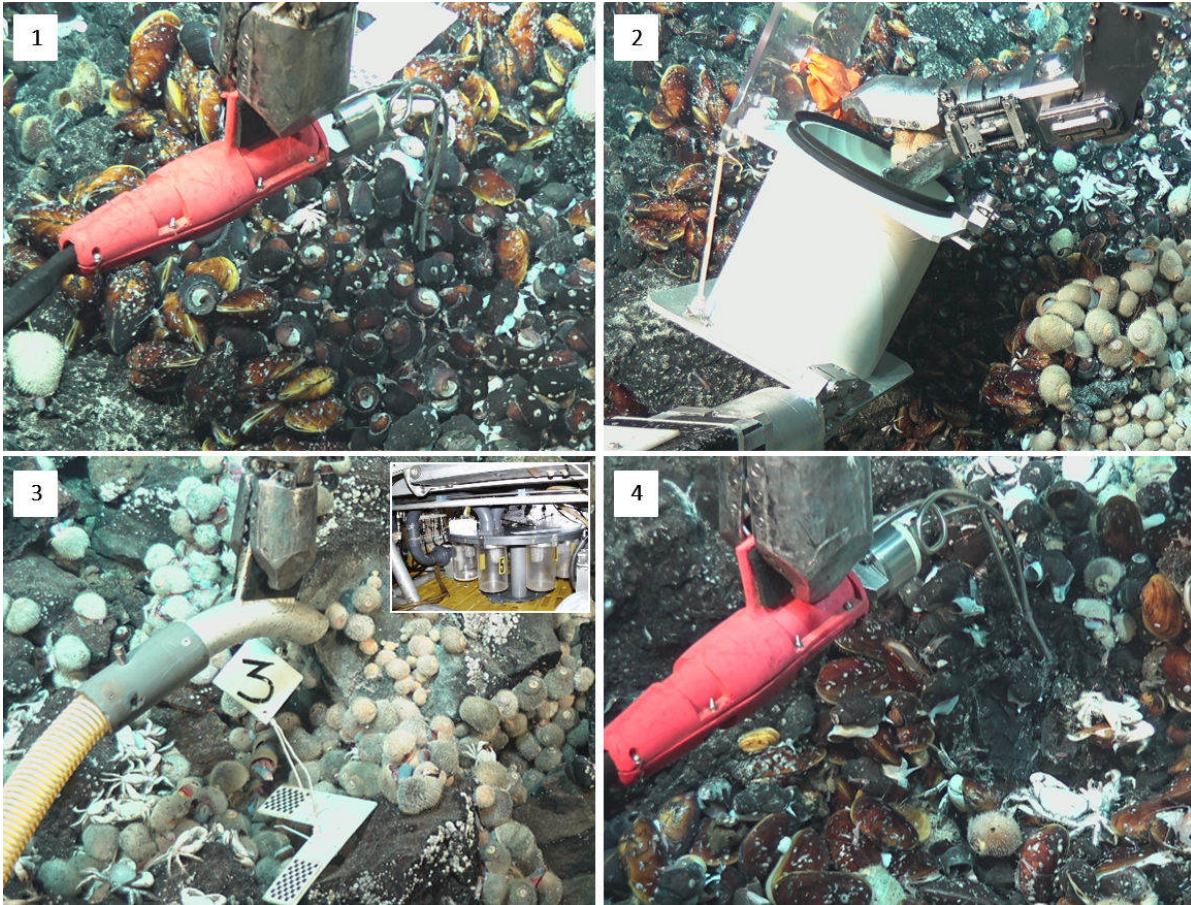


Figure 3.2 – Sampling procedure: (1) Series of physico-chemical measurements and samples (PIF, CHEMINI, electrodes, optode), (2) fauna sampling in a biobox, (3) suction on the sampled area, (4) series of physico-chemical measurements on substrate (CHEMINI, electrodes, optode).

### 3.2 Materials and Methods

On board, organisms belonging to the biomass-dominant species (e.g. *Alviniconcha*, *Ifremeria* and *Bathymodiolus*) were washed through a 250 µm sieve with filtered seawater to collect all associated fauna found on the shells or between individuals. All the macrofauna was sorted and the retained organisms were fixed in 96% ethanol. In the laboratory, individuals were identified to the lowest taxonomic level possible, in general the morphospecies. Taxon assignment was based on the use of morphological descriptions, combined with molecular barcode data of the Cytochrome Oxidase I mitochondrial gene, produced as part of the Cerberus project (Chabert, 2021; Poitrimol *et al.*, 2022). Barcode data were used to confirm morphological identification and identify cryptic species, which greatly improved the taxonomic resolution and quality of our data. However, it was not possible to barcode all species at the scale of all sampled sites. When identification of morphospecies was not possible (e.g. due to insufficient barcode effort, the need to use more specific techniques for morphological identification, or time and expertise constraints), the taxonomic resolution was downgraded to the highest taxonomic level. If the occurrence of several species within a genus was known, the term "spp." was assigned.

To investigate the links between environmental conditions and the associated fauna, the physico-chemical characteristics of the habitat were measured prior and after the fauna sampling when possible. *In situ* temperature was measured using the high-temperature probe of the ROV and free inorganic sulphides [ $\Sigma S = H_2S + HS^- + S^{2-}$ ] were assessed with the *in situ* chemical miniaturized analyser CHEMINI (Vuillemin *et al.*, 2009). Time-series measurements were performed at 3 locations within the biological area with the probes positioned at a distance of about 2 cm above the surface of mussels or large gastropods to represent at best the micro-habitats surrounding the organisms. In addition, water samples were collected with the PIF water sampler at one point prior to fauna sampling. Fluids were then analysed on board for pH using a pH probe. Methane, sulfur and phosphorus concentration were measured back in the laboratory by Gas Chromatography coupled to Flame Ionization Detector (GC-FID) and Gas Chromatography coupled to Helium Ionization Detector (GC-HID) (Donval *et al.*, 2008).

### 3.2.2 Diversity analysis

All analysis were conducted using the R statistical software (R Core Team, 2020) with RStudio environment (RStudio Team, 2020).

**$\alpha$  diversity**  $\alpha$  diversity, i.e. the local diversity (Whittaker, 1960), was measured using different indices. First, species richness, which is the number of species<sup>2</sup> in each sample, was calculated. As it was not possible to properly standardize the sampling effort in our study, measures of the observed species richness could be biased. Hence, to compare species richness among all samples, rarefaction curves were computed based on the total number of sampled individuals with the function *rarecurve* of the *vegan* package (Oksanen *et al.*, 2020). From these data, the expected number of species was calculated for a theoretical sample of 50 individuals (ES50), as the smallest sample size was 54 individuals, using the *rarefy* function. Although this method is largely used to compare species richness by reducing samples to a common size, it is based on two assumptions that can be misleading: (1) samples are homogenous with similar distributions of individuals among species, (2) species are distributed randomly (Gray, 2000). Shannon entropy ( $H'$ ) and Pielou's evenness ( $J'$ ) indices were calculated for each sample. A Kruskal-Wallis rank sum test was used to test differences of species richness, ES50, Shannon and Pielou indices among the three habitat types. Nemenyi and Dunn multiple comparison test was then applied to identify significantly different pairs.

**$\gamma$  diversity** To compare  $\gamma$  diversity, i.e. the regional species richness (Whittaker, 1960), among habitats at the South West Pacific, species accumulation curves were produced for each habitat with the function *specaccum* (Oksanen *et al.*, 2020). A Venn diagram was used to show the share and unique species among the three habitats.

**$\beta$  diversity** To analyse the variations in community composition among samples at the regional scale, a Principal Coordinate Analysis (PCoA) was performed on the presence-absence

---

2. The term "species" is used here by convention; in our case they are actually taxa.

### 3.2 Materials and Methods

samples-by-species matrix using the square root of the Jaccard dissimilarity coefficient to obtain a distance matrix which is Euclidean. This analysis was computed with the *cmdscale* function of stats. Differences in community composition was tested at different spatial scales, between basins, between fields within a basin, between sites within field and between habitats with a PERMANOVA test (9999 permutations). The habitat and basin were crossed fixed factors and field and site nested random factors within a basin or basin/field. The function *adonis2* of vegan was used for the PERMANOVA test. This test was followed by pairwise post-hoc PERMANOVAs to identify the scales of differences using the *pairwise.adonis2* function of pairwiseAdonis package.

Dissimilarity indices (e.g. Jaccard dissimilarity indice) are composed of three components for computing dissimilarity between two samples 1 and 2: *a* the number of species common to the two samples, *b* the number of species unique to the sample 1, and *c* the number of species unique to the samples 2. Of these, similarity equals to *a* and dissimilarity to *b* and *c*. Dissimilarity can be partitioned into species replacement  $2 \times \min(b, c)$  and richness difference  $|b - c|$ . Several methods have been proposed to compute the components of dissimilarity (i.e. species replacement and richness difference). Legendre (2014) summarises these methods into two families of indices, the Podani and Baselga family indices, which differ in the denominator they used for the calculation of these two components, while they both applied  $2 \times \min(b, c)$  and  $|b - c|$  as numerator. Because of their logic of construction Podani family indices are ecologically easier to interpret and were thus selected for the present analyses (Legendre, 2014). The denominator used by Podani family is the one used in dissimilarity coefficient calculation (i.e.  $a + b + c$ , for Jaccard dissimilarity) and the "nestedness" measurement is a special case of richness difference. In our dataset, two major sources of  $\beta$  diversity are expected: 1) the geographical gradient between fields and basins within a habitat and, 2) the environmental gradient between habitats within a basin, from areas of low diffusion (i.e. *Bathymodiolus* beds), to areas of high diffusion (i.e. *Alviniconcha* clumps). For these two main sources,  $\beta$  diversity was partitioned for each pair of samples into species replacement and species richness difference

components using the Podani family indices with the function *beta.div.comp* of the *adespatial* package (Dray *et al.*, 2021) as detailed in Legendre (2014). This partition was first produced at the regional scale for each habitat to see how  $\beta$  diversity patterns evolve along the geographical gradient and then at the basin scale to observe the evolution of  $\beta$  diversity among habitats along the environmental gradient within a basin. For this later analysis, we focused on two basins for which enough samples were available: the Manus and Lau Basins. Species replacement and species richness difference indices were interpreted in terms of ecological processes.

Because the dissimilarity ( $D$ ) is composed of species replacement and species richness difference and the similarity ( $S$ ) equals  $1 - D$ , Podani et Schmera (2011) and Podani *et al.* (2013) suggested to illustrate these values ( $S$ , replacement and richness difference) which total equals to 1, in a triangular plot (SDR-simplex). This representation allows the visualisation of the relative importance of the similarity and the two components of the dissimilarity among all pair of samples. Those plots were computed at the regional scale for each habitat and at the basin scale for the Manus and Lau Basins.

### 3.2.3 Link with the environment

**Physico-chemical conditions.** Temperature and  $\Sigma S$  were averaged per sampling period (i.e. before/after macrofauna sampling) for each sample to detect potential differences in the physico-chemical conditions once the engineer species removed. To ensure consistency and because the measurement after sampling was not always completed, only measurements conducted before sampling were used to characterise each sample in the present study. The following physico-chemical measurements were considered: two variables related to temperature, i.e. the maximal temperature (T.max) and the mean temperature (T.mean), the mean  $\Sigma S$  ( $\Sigma S$ .mean), the pH, the methane concentration ( $CH_4$ ), the sulfur concentration ( $S$ ) and the phosphorus concentration ( $P$ ). A principal component analysis (PCA) on centered and scaled data was applied to detect spatial variations in physico-chemical conditions among the three habitats between sites, fields and basins, and to identify the variables that most explained

### 3.2 Materials and Methods

the differences. This analysis was computed with *prcomp* function and a biplot was produced with the *fviz\_pca\_biplot* function of the *factoextra* package (Kassambara et Mundt, 2020). A first analysis was performed by removing samples with missing data, resulting in 46 out of 60 samples. As most of the samples were removed because of missing methane concentration data (Table 3.1), a second analysis was carried out without methane concentration data to include a higher number of samples, including those from the ABE, La Scala and Kulo Lasi vent fields. The second analysis included 54 samples out of 60.

**Environmental and Spatial drivers of faunal composition** To explore the correlations between the environmental and spatial variables, and the composition of vent community of each sample, a distance-based redundancy analysis (dbRDA) was used on the square root of the Jaccard dissimilarity coefficient. The dbRDA is an extension of the RDA proposed by Legendre et Anderson (1999) to apply a constrained ordination on data using non-Euclidean measures. This method allows to explore the relationships between a response matrix (i.e. samples-species data) and an explanatory matrix (i.e. environmental and spatial data). The variables included the physico-chemical variables mentioned previously and three additional spatial variables, i.e. latitude, longitude and depth. To select the most parsimonious model, the optimal combination of variables which explains community composition was determined by a forward selection using the *forward.sel* function of package *adespatial* (Dray *et al.*, 2021). Permutation tests involving 9999 random permutations were run to test the significance of the canonical relationships and of the individual canonical axes using the *anova* function of *vegan* (Oksanen *et al.*, 2020). Similarly, dbRDA and variables forward selection were performed by considering samples for which methane data were present or not. The dbRDA was conducted using the *dbrda* function of the *vegan* package.

The relative influence of the spatial and environmental variables on community composition was quantified through variance partitioning (Peres-Neto *et al.*, 2006). The proportions of variance explained by the physico-chemical conditions alone, the spatial variables alone and the interactions between environment and space were estimated from



three dbRDAs with the *varpart* function of *vegan*. Three different matrices were used: the dissimilarity matrix of the square root of the Jaccard dissimilarity coefficient, the environmental and the spatial data selected by the forward selection respectively. All testable fractions were tested with ANOVA permutation tests (999 permutations) on dbRDAs using the *anova* function of *vegan* (Oksanen *et al.*, 2020).

### 3.3 Results

A total of 60 fauna samples were collected with the hydraulic arm of the ROV from ten vent fields along the southwestern Pacific back-arc basins. Of these, 21 were collected from the *Alviniconcha* habitat, 15 from the *Bathymodiolus* habitat and 24 from the *Ifremeria* habitat. *Alviniconcha* and *Ifremeria* habitats were sampled in all vent fields, but this was not the case for *Bathymodiolus*. There were no mussels at all in the Woodlark Basin, and only a few in the Futuna volcanic area and in the Magatolo vent field (North of the Lau Basin), but more as isolated mussels than in mussel beds. There were very few mussel beds in Phoenix vent field (North Fiji Basin), the only *Bathymodiolus* sample there was a very small mussel bed (see Appendix D.3:PH3). While habitats are defined in terms of the three biomass-dominant engineer species, mixtures between these 3 species were possible due to their highly patchy distribution. In the samples from the *Alviniconcha* habitat, the target engineer species formed between 62 and 100% of the abundances of the sampled engineer species. In samples from the *Bathymodiolus* and *Ifremeria* habitats, these species formed between 77 and 100% of the abundances of engineer species. No *Bathymodiolus* was collected in the *Alviniconcha* samples and only one mussel sample included some *Alviniconcha* individuals (i.e. TM1, Table 3.1). In most cases, mixing occurred between *Alviniconcha* and *Ifremeria* although one of the two species was dominant depending on the habitat considered (see Appendix D.3: MG3-4, TM3, PM12).

### 3.3 Results

#### 3.3.1 Diversity analysis

A total of 132 364 individuals belonging to 114 taxa were sorted and identified based on their morphology and molecular COI barcoding data (Table 3.2). The total diversity was clearly underestimated as some taxa were identified at the family level such as the capitellidae among polychaetes or at higher taxonomic level such as copepods among arthropods. Only 57% of taxa have species-level assignment. Polychaetes and gastropods were dominant and accounted for 44.7 and 31.6% of the taxa assigned respectively: 51 taxa belonged to polychaetes (23 genera and 19 families) and 36 to gastropods (17 genera and 13 families). The remaining 23.7% were mainly arthropods (15 taxa), bivalves (3 taxa), and echinoderms (3 taxa). Nematodes, nemerteans, plathelminthes, cnidarians, solenogastres and sipuncula were all represented by one taxon. Considering each habitat separately, a very similar pattern was reported and the proportion of each phylum was very close among habitats, with a dominance of mollusc and annelid species (Figure 3.3A-B). In terms of abundance of the different phyla, the proportions of each phylum were very different among habitats. In the *Alviniconcha* habitat, Arthropoda (mainly copepods) was the most numerically dominant phylum with more than 90% of sampled individuals. Without considering the engineer species, the second most abundant taxa were the polychaetes *Branchinotogluma trifurcus* and *Paralvinella hessleri*. Mollusca (mainly gastropods) were dominant in abundance in the two other habitats accounting for 74% and 86% of the total abundance in *Ifremeria*, and *Bathymodiolus* habitats respectively (Figure 3.3C-D). The gastropods *Lepetodrilus schrolli* and *Shinkailepas tollmanni* and the copepods were the most abundant taxa in the *Ifremeria* habitat while the gastropod *L. schrolli*, the nematods and the copepods were the most abundant taxa in the *Bathymodiolus* habitat.

**$\alpha$  diversity** For each sample,  $\alpha$  diversity was estimated by combining the collections sampled with the hydraulic arm of the ROV and the suction device although this later sampler was not used consistently. For most samples, considering the collection with the suction device had

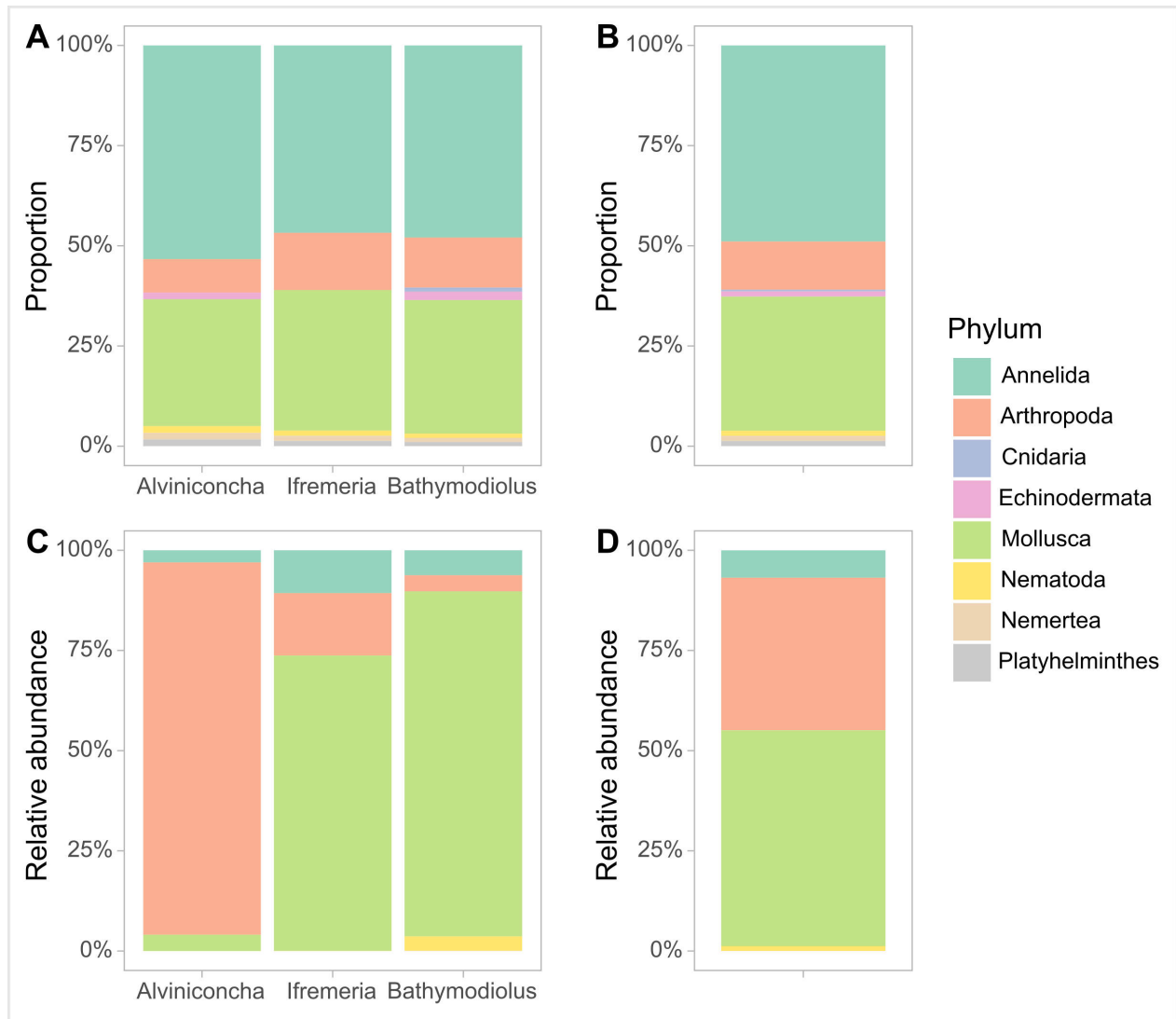


Figure 3.3 – Phylum proportion by habitat (A) and at the South West Pacific scale (B) and phylum abundance by habitat (C) and at the South West Pacific scale (D).

Table 3.2 – Inventory of taxa collected from the *Alviniconcha*, *Bathymodiolus* and *Ifremeria* habitats in southwestern Pacific back-arc basins.

Phylum	Class	Family	Taxa	Habitat			Basin				
				<i>Alviniconcha</i>	<i>Bathymodiolus</i>	<i>Ifremeria</i>	Manus	Woodlark	North Fiji	Futuna	Lau
Annelida	Polychaeta	Alvinellidae	<i>Paralvinella fijiensis</i>	+	+	+			+	+	+
			<i>Paralvinella hessleri</i>	+		+	+	+			
			<i>Paralvinella</i> sp. nov.	+		+	+				
			<i>Paralvinella unidentata</i>	+	+	+	+			+	+
		Ampharetidae	<i>Amphisamytha</i> spp.	+	+	+	+	+	+	+	+
		Amphinomidae	<i>Archinome</i> spp.		+	+	+		+		+
		Bonelliidae			+		+				
		Capitellidae	Capitellidae spp.	+	+	+	+			+	+
		Chrysopetalidae	<i>Iheyomytilidicola</i> sp.		+			+			
			<i>Thrausmatos</i> sp.	+	+	+	+			+	+
		Cirratulidae	Cirratulidae spp.		+						+
		Dorvilleidae	<i>Ophryotrocha</i> sp.		+			+			
			<i>Parougia</i> sp.		+	+	+	+		+	+
		Hesionidae	<i>Amphiduroopsis</i> sp. A	+	+	+	+	+			+
			<i>Amphiduroopsis</i> sp. B	+	+	+	+	+		+	+
			<i>Hesiolyra</i> sp.	+	+	+	+	+			+
			<i>Hesiospina</i> sp.		+					+	+
		Iphionidae	<i>Thermiphione fijiensis</i>		+	+					+
		Maldanidae	<i>Nicomache</i> sp.		+						+
		Nereididae	<i>Nereis</i> sp. A		+			+			
			<i>Nereis</i> sp. B		+					+	+
			<i>Nereis</i> sp. C				+				+
		Phyllodocidae	<i>Galapagomystides</i> spp.	+	+	+	+	+		+	+
			<i>Protomystides</i> spp.	+	+	+	+	+		+	+
		Polynoidae	<i>Branchinotogluma</i> aff. <i>marianus</i> A	+	+	+	+			+	+
			<i>Branchinotogluma</i> aff. <i>marianus</i> B	+	+	+	+	+	+		
			<i>Branchinotogluma</i> aff. <i>ovata</i>		+	+					+
			<i>Branchinotogluma</i> aff. <i>trifurcus</i>	+	+	+	+	+			
			<i>Branchinotogluma ovata</i>	+	+	+	+				
			<i>Branchinotogluma pettiboneae</i>	+	+	+	+				
			<i>Branchinotogluma segonzaci</i>	+	+	+	+			+	+
			<i>Branchinotogluma</i> sp. A	+	+	+	+			+	+
			<i>Branchinotogluma</i> sp. B		+					+	
			<i>Branchinotogluma</i> sp. C	+	+			+			+
			<i>Branchinotogluma</i> sp. D	+		+	+			+	+
			<i>Branchinotogluma</i> sp. E	+		+				+	+
			<i>Branchinotogluma trifurcus</i>	+	+	+				+	+
			<i>Branchipolynoe</i> spp.	+	+	+	+			+	+
			Eulagiscinae		+			+			
			<i>Harmothoe</i> spp.		+	+	+	+			
		<i>Lepidonotopodium</i> spp.	+	+	+	+	+	+	+	+	
		<i>Levensteiniella</i> spp.	+	+	+	+	+		+	+	

Phylum	Class	Family	Taxa	Habitat			Basin							
				<i>Alviniconcha</i>	<i>Bathymodiolus</i>	<i>Ifremeria</i>	Manus	Woodlark	North Fiji	Futuna	Lau			
Annelida	Polychaeta	Polynoidae	<i>Macellicephalinae</i>		+	+	+					+		
			<i>Thermopolynoe branchiata</i>	+	+	+	+	+	+	+	+	+		
		Siboglinidae	<i>Siboglinidae</i> spp.		+	+	+						+	
		Sigalionidae	<i>Sigalionidae</i> sp.		+			+						
		Spionidae	<i>Malacoceros</i> sp.	+										+
			<i>Prionospio</i> sp. A	+	+	+	+							
			<i>Prionospio</i> sp. B	+	+	+								+
			<i>Prionospio</i> sp. D	+	+	+					+	+		+
		Terebellidae	Terebellidae		+			+						
		Sipunculidae	Sipunculidae	+	+			+						+
Arthropoda	Arachnida	Halacaridae	Halacaridae		+	+	+	+					+	
	Copepoda		Copepoda spp.	+	+	+	+	+	+	+	+		+	
	Malacostraca	Alvinocarididae	<i>Alvinocaris longirostrice</i>		+			+						
			<i>Manuscaris liui</i>		+			+						
			<i>Nautilocaris saintlaurentae</i>				+							+
			<i>Rimicaris variabilis</i>	+	+	+	+	+	+	+	+	+		+
		Amphipoda	Amphipoda		+	+	+	+						+
		Bythograeidae	<i>Austinograea</i> spp.	+	+	+	+	+	+	+	+	+		+
		Cumacea	Cumacea				+				+			
	Isopoda	Isopoda				+	+							
	Munidopsidae	<i>Munidopsis</i> sp.			+			+					+	
	Ostracoda	Ostracoda	+	+	+	+	+						+	
	Thecostraca	Chionelasmidae	<i>Eochionelasmus ohtai</i>	+	+	+	+			+	+		+	
Neolepadidae		<i>Vulcanolepas</i> sp.		+			+							
Neoverrucidae		Neoverrucidae sp.		+	+			+					+	
Cnidaria	Anthozoa	Actiniaria		+			+					+		
Echinodermata	Holothuroidea	Chiridotidae	Chiridota		+								+	
		Holothuroidea	Holothuroidea	+									+	
	Ophiuroidea	Ophiuridae	Ophiuridae		+			+						
Mollusca	Bivalvia	Mytilidae	<i>Bathymodiolus brevior</i>		+	+				+	+		+	
			<i>Bathymodiolus manusensis</i>		+	+	+							
			Nuculanida sp.		+	+	+							
	Gastropoda	Eosiphonidae	<i>Enigmaticolus desbruyeresi</i>		+	+						+	+	
		Lepetodrilidae	<i>Lepetodrilus schrolli</i>	+	+	+	+	+	+	+	+	+	+	
			<i>Pseudorimula</i> sp.	+	+	+	+			+			+	
		Neolepetopsidae	Neolepetopsidae		+			+						
		Neomphalidae	<i>Lamellomphalus manusensis</i>	+	+	+	+							
			<i>Planorbidella depressa</i>		+	+							+	+
			<i>Symmetromphalus</i> aff. <i>hageni</i> LNF	+	+	+					+			+
			<i>Symmetromphalus</i> aff. <i>hageni</i> W			+				+				
			<i>Symmetromphalus hageni</i>		+	+	+							
		Pectinodontidae	<i>Bathyacmaea becki</i>		+			+						
		Peltospiridae	<i>Pachydermia sculpta</i>	+	+						+			+
<i>Pachydermia</i> sp. A	+											+		

Phylum	Class	Family	Taxa	Habitat			Basin						
				<i>Alviniconcha</i>	<i>Bathymodiolus</i>	<i>Ifremeria</i>	Manus	Woodlark	North Fiji	Futuna	Lau		
Mollusca	Gastropoda	Peltospiridae	<i>Peltospiridae</i> n. sp. A			+		+					
			<i>Peltospiridae</i> n. spp.	+	+	+			+	+	+		
		Phenacolepadidae	<i>Shinkailepas</i> aff. <i>tufari</i> L		+	+						+	
			<i>Shinkailepas</i> aff. <i>tufari</i> LF	+								+	
			<i>Shinkailepas</i> aff. <i>tufari</i> Manus			+		+					
			<i>Shinkailepas</i> aff. <i>tufari</i> W						+				
			<i>Shinkailepas tollmanni</i>	+	+	+	+	+	+	+	+	+	
			<i>Shinkailepas tufari</i>	+	+	+	+						
			Provannidae	<i>Alviniconcha boucheti</i>	+		+	+					+
				<i>Alviniconcha kojimai</i>	+	+	+	+	+	+	+	+	+
		<i>Alviniconcha strummeri</i>		+	+	+				+	+	+	
		<i>Desbruyeresia cancellata</i>		+						+			
		<i>Desbruyeresia costata</i>			+			+					
		<i>Desbruyeresia melanioides</i>		+	+	+	+			+	+	+	
		<i>Ifremeria nautilei</i>		+	+	+	+	+	+	+	+	+	
		<i>Provanna</i> sp. M			+	+	+						
		<i>Provanna</i> sp. L		+	+							+	
		<i>Provannidae</i> sp. A				+	+						
		Raphitomidae	<i>Phymorhynchus hyfifluxi</i>		+							+	
			<i>Phymorhynchus</i> sp. C		+			+					
		Seguenzioidea	<i>Ventsia tricarinata</i>		+	+					+	+	
		Skeneidae	<i>Bruceiella globulus</i>	+	+	+				+	+	+	
		Trochidae	Trochidae		+			+					
Xylodisculidae	<i>Xylodiscula</i> sp.		+							+			
	Solenogastres	<i>Solenogastres</i> spp.	+	+	+			+	+	+			
Nematoda		Nematoda spp.	+	+	+	+		+	+	+			
Nemertea		Nemertea	+	+	+	+			+				
Platyhelminthes		Platyhelminthes	+	+	+	+			+	+			

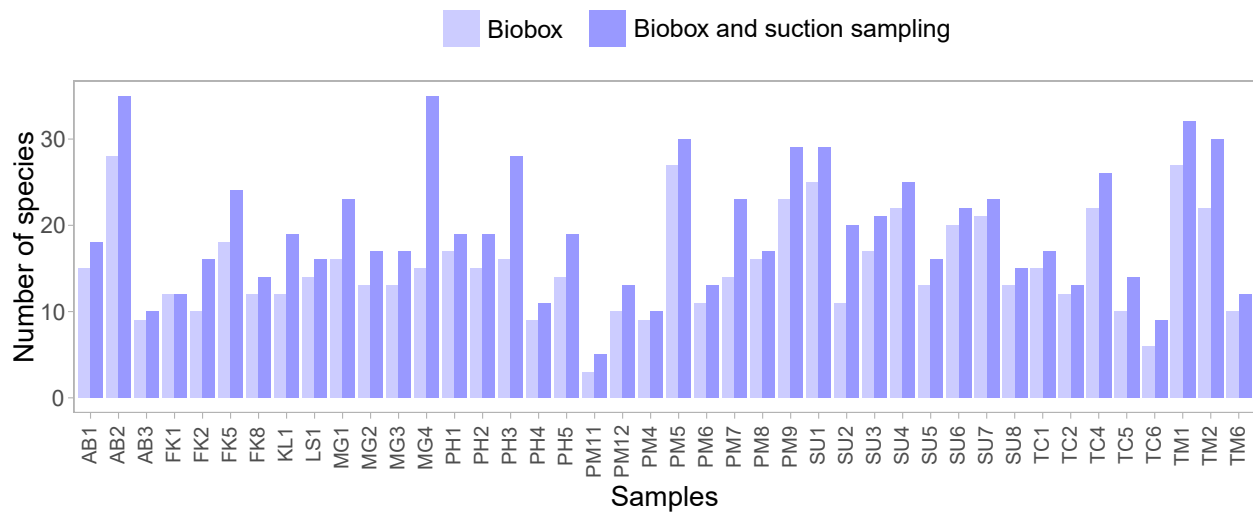


Figure 3.4 – Number of species from biobox only and biobox plus suction collector.

minor effect on local species richness estimates by adding only a few species (Figure 3.4). On the contrary, for a few samples such as the samples MG4 at the Mangatolo vent field (Lau Basin) or PH3 at the Phoenix vent field (North Fiji Basin), more than 10 species were added by adding individuals collected by the suction sampler. While species richness and the number of individuals were highly variable among samples, the rarefaction curves suggested that the *Alviniconcha* habitat tended to be less rich than samples from the other habitats (Figure 3.5A). Species-richer samples were reported from the *Bathymodiolus* habitat in the Lau Basin.

Species richness (SR) in the *Alviniconcha* habitat ranged from 3 for the sample SU9 to 35 for the sample MG4 while the expected number of species for 50 individuals (ES50) varied from 1.37 to 18.01 for samples PH4 and MG4 respectively; the means of these two parameters were 12.2 and 5.28 respectively (Table 3.3 and Figure 3.6A-B). In this habitat, the total number of individuals fluctuated between 54 to 12 884 for the sample SU9 and PH4 respectively (Figure 3.6C). Note that in this habitat the sample MG4 contrasted with the others by its particularly high richness and diversity, the second highest SR and ES50 being 19 and 3.23 respectively for the sample PH5. This sample was characterised by a high proportion of *Ifremeria* (i.e. 64%). In the *Ifremeria* habitat, SR varied from 10 (PM4) to 25 (SU4) with a mean value of 17.2 whereas ES50 ranged from 2.28 (PM3) to 11.05 (FK3) with a mean value of 7.05. The total number of individuals

### 3.3 Results

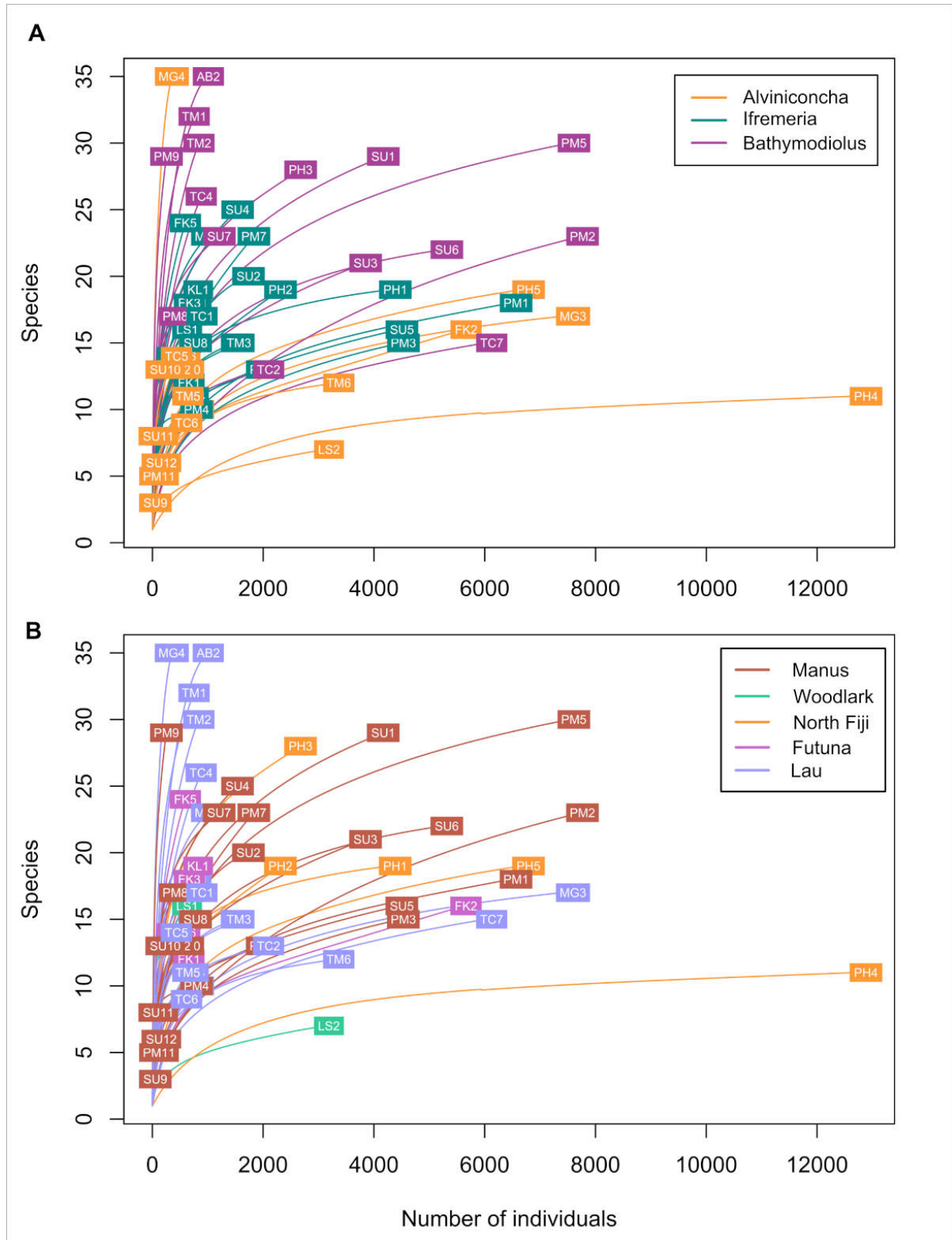


Figure 3.5 – Samples rarefaction curves computed based on the total number of individuals: colored per habitat (A) and per basins (B).



ranged from 355 (FK8) to 6 566 (PM1). In the *Bathymodiolus* habitat, SR and ES50 varied from 13 (TC2) to 35 (AB2), and from 2.34 (PM2 and TC7) to 17.05 (PM9) with mean values of 24.9 and 7.55 respectively. The total number of individuals ranged from 254 (PM9) to 7 765 (PM2). SR, ES50 and the number of individuals per sample were significantly different between habitats (Kruskal-Wallis test,  $p < 0.001$  and  $p < 0.05$ ) (Figure 3.6A-C). Post-hoc comparisons showed that SR and ES50 measures were significantly lower in the *Alviniconcha* habitat compared to *Ifremeria* ( $p < 0.05$ ). Only SR was significantly lower in the *Alviniconcha* habitat compared to *Bathymodiolus* ( $p < 0.05$ ). SR was significantly different between the *Bathymodiolus* and *Ifremeria* habitats ( $p < 0.001$ ) with a lower value in the later one but not the ES50. The number of individuals were significantly different between *Alviniconcha* and *Bathymodiolus* habitats ( $p < 0.05$ ).

The Shannon and Pielou indices were also highly variable among samples whatever the habitat considered (Table 3.3 and Figure 3.6D-E). The Shannon index was rather low, and varied from 0.06 (PH4) to 2.82 (MG4) in the *Alviniconcha* habitat, from 0.19 (PM3) to 2.21 (MG1) in the *Ifremeria* habitat and from 0.2 (TC7) to 2.76 (PM9) in the *Bathymodiolus* habitat. In parallel, Pielou's evenness varied from 0.02 (PH4) to 0.89 (SU9) in the *Alviniconcha* habitat, from 0.07 (PM3) to 0.77 (LS1) for the *Ifremeria* habitat and from 0.06 (PM2) to 0.82 (PM9) for the *Bathymodiolus* habitat. The very low values of Shannon index and Pielou's evenness for some samples whatever the habitat can be explained by the dominance of a few species. The Shannon index was significantly different among habitats (Kruskal-Wallis test,  $p < 0.05$ ) and post-hoc Nemenyi and Dunn test showed that only the difference between the *Alviniconcha* and *Ifremeria* habitats was significant ( $p < 0.05$ ) with a less diverse community in the *Alviniconcha* habitat (Figure 3.6D). No significant differences in the Pielou's evenness were reported between habitats (Kruskal-Wallis test,  $p > 0.05$ ).

**$\gamma$  diversity** The species accumulation curves plotted at the regional scale confirmed the results on  $\alpha$  diversity. The *Bathymodiolus* habitat was the richest in terms of species number with a total of 96 taxa collected in the different back-arc basins, followed by the *Ifremeria* habitat with

### 3.3 Results

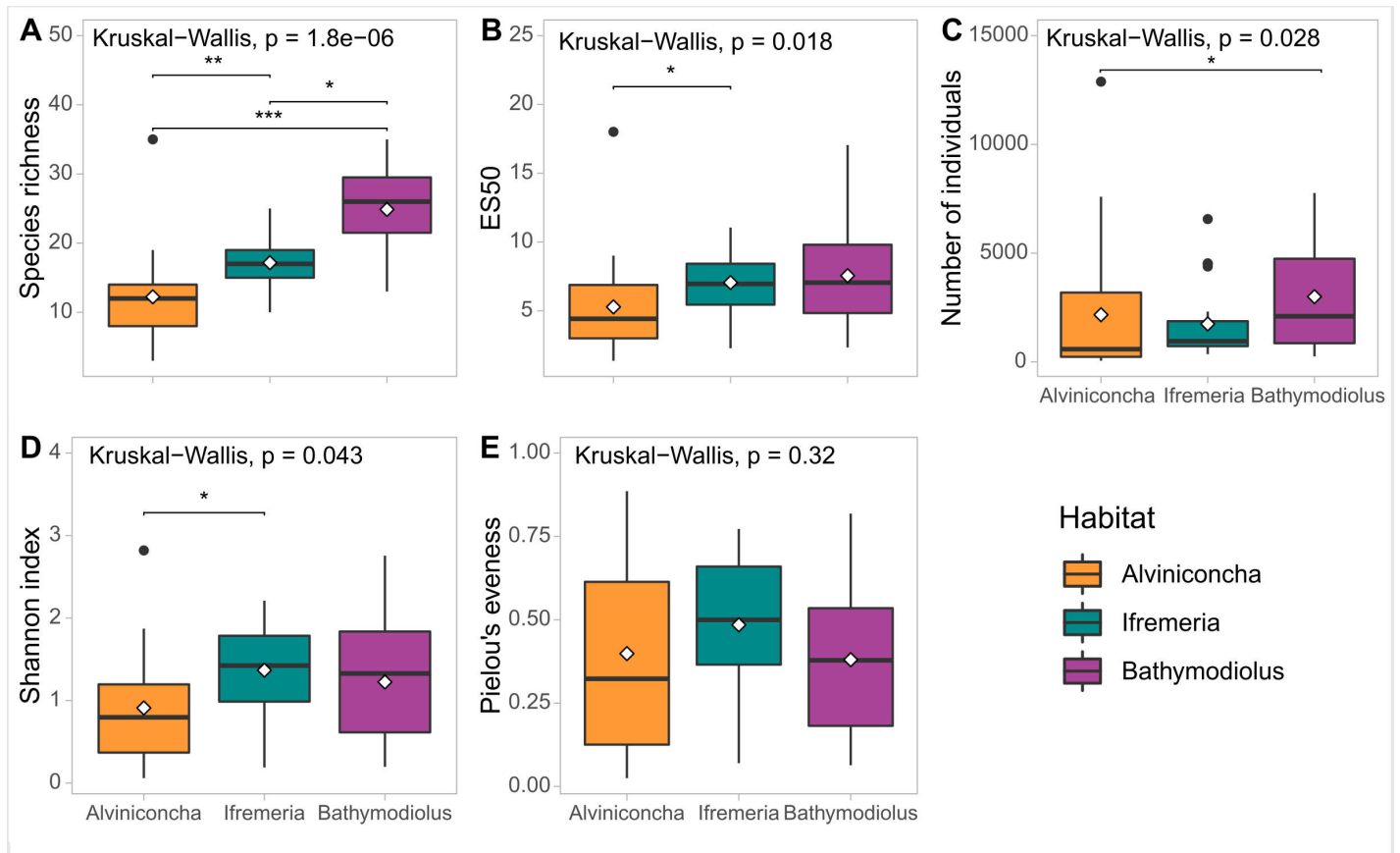


Figure 3.6 – Diversity indices: Species richness (A), the expected number of species ES50 (B), the total number of individuals (C), Shannon index(D) and Pielou's evenness (E) of macrofaunal communities by habitat. White rhombus indicates the average. Kruskal-Wallis test results and level of significance of the post-hoc Nemenyi and Dunn test: \*  $p$  value <0.05; \*\*  $p$  value <0.01; \*\*\*  $p$  value <0.001.

CHAPITRE 3 : *Structure des communautés hydrothermales et biogéographie*

Table 3.3 – Species richness (SR), Expected number of Species (ES50), total number of individuals (Nb. ind.), Shannon index (H') and Pielou's evenness (J') measures among the different samples from the southwestern Pacific back-arc basins.

Basin	Field	Site	Hab.	sample	Hab.	SR	ES50	Nb. Ind.	H'	J'		
Manus	Pacmanus	Big Papi	I	PM1	I	18	3.33	6566	0.41	0.14		
			A	PM11	A	5	4.06	120	0.99	0.61		
		Fenway	A	PM10	A	13	6.88	577	1.20	0.47		
			B	PM2	B	23	2.34	7765	0.20	0.06		
			I	PM3	I	15	2.28	4532	0.19	0.07		
			B	PM8	B	17	10.85	413	2.12	0.75		
		Snow Cap	B	PM9	B	29	17.05	254	2.76	0.82		
		Solwara 6	B	PM5	B	30	4.36	7609	0.49	0.15		
			I	PM7	I	23	5.85	1833	1.27	0.41		
		Solwara 7	I	PM6	I	13	4.71	1984	0.88	0.34		
		Solwara 8	A	PM12	A	13	7.74	399	1.77	0.69		
			I	PM4	I	10	6.77	797	1.17	0.51		
		Susu	North Su	North Su	B	SU1	B	29	5.76	4168	0.74	0.22
					A	SU11	A	8	7.14	108	1.69	0.81
I	SU2				I	20	4.74	1735	0.60	0.20		
B	SU3				B	21	6.76	3848	1.33	0.44		
South Su North	A			SU10	A	13	9.01	233	1.87	0.73		
	I			SU4	I	25	8.28	1537	1.58	0.49		
	B			SU7	B	23	10.09	1207	1.98	0.63		
South Su South	I			SU5	I	16	4.01	4505	0.52	0.19		
	B			SU6	B	22	5.31	5316	0.74	0.24		
	A			SU9	A	3	3.00	54	0.97	0.89		
Suzette	A			SU12	A	6	4.42	163	0.98	0.55		
	I			SU8	I	15	7.25	780	1.57	0.58		
Woodlark	La Scala	La Scala	I	LS1	I	16	10.69	628	2.14	0.77		
			A	LS2	A	7	2.13	3188	0.19	0.10		
			A	LS3	A	6	4.53	152	0.80	0.44		
North Fiji	Phoenix	Phoenix North	I	PH1	I	19	6.57	4385	0.90	0.31		
		Phoenix South	I	PH2	I	19	8.21	2313	1.68	0.57		
			B	PH3	B	28	7.25	2676	1.53	0.46		
			A	PH4	A	11	1.37	12884	0.06	0.02		
		Phoenix West	A	PH5	A	19	3.23	6791	0.37	0.13		

### 3.3 Results

Basin	Field	Site	Hab.	sample	Hab.	SR	ES50	Nb. Ind.	H	J
Futuna	Fatu Kapa	AsterX	I	FK1	I	12	7.15	661	1.67	0.67
			A	FK2	A	16	2.24	5663	0.18	0.07
		Fati Ufu 1	A	FK6	A	14	4.91	586	0.69	0.26
			I	FK8	I	14	7.61	355	1.63	0.62
		Fati Ufu 15	I	FK5	I	24	10.66	596	2.08	0.66
		Stephanie	I	FK3	I	18	11.05	668	2.20	0.76
A	FK4		A	15	6.37	757	0.84	0.31		
	Kulo Lasi	Kulo Lasi	I	KL1	I	19	8.14	661	1.72	0.58
Lau	ABE	ABE	I	AB1	I	18	8.86	785	1.98	0.69
			B	AB2	B	35	9.51	1010	1.34	0.38
			A	AB3	A	10	4.22	832	0.49	0.21
	Mangatolo	Mangatolo North	I	MG1	I	23	11.03	1006	2.21	0.71
			A	MG3	A	17	2.10	7594	0.17	0.06
		Mangatolo South	I	MG2	I	17	8.99	682	1.99	0.70
			A	MG4	A	35	18.01	351	2.82	0.79
	Tow Cam	Tow Cam North	I	TC1	I	17	5.54	895	1.06	0.37
			B	TC4	B	26	7.05	881	0.93	0.28
		Tow Cam South	B	TC2	B	13	3.47	2098	0.36	0.14
			I	TC3	I	15	5.16	1519	1.02	0.37
			A	TC5	A	14	8.13	436	1.51	0.57
			A	TC6	A	9	3.42	618	0.48	0.22
			B	TC7	B	15	2.34	6126	0.20	0.07
	Tui Malila	Tui Malila	B	TM1	B	32	11.80	754	1.96	0.57
			B	TM2	B	30	9.37	840	1.71	0.50
			I	TM3	I	15	6.61	1562	1.22	0.45
			I	TM4	I	11	5.73	736	1.14	0.47
A			TM5	A	11	5.02	641	0.77	0.32	
A			TM6	A	12	2.99	3365	0.29	0.12	

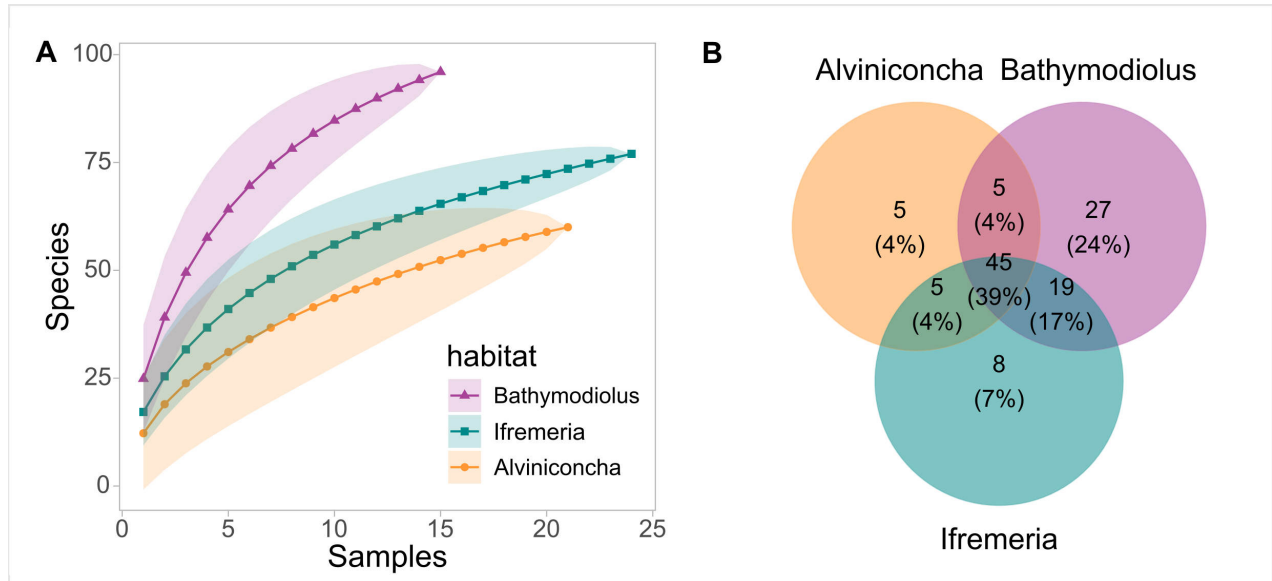


Figure 3.7 – Accumulation curves (A) and venn diagramm showing the number of shared and specific to one habitat species (B).

77 taxa and then the *Alviniconcha* habitat with 60 taxa (Figure 3.7A).

In terms of species composition, 45 species (39.5%) were shared between the three habitats. A greater number of species (i.e. 27), mainly polychaetes (44 %) was found exclusively in the *Bathymodiolus* habitat while only 8 and 5 species were endemic to the *Ifremeria* and *Alviniconcha* habitats respectively (Figure 3.7B). The *Bathymodiolus* and *Ifremeria* habitats shared more species than they did with the *Alviniconcha* habitats.

**$\beta$  diversity** The first two axes of the PCoA analysis explained 18.1% of the variance in the composition of the vent communities (Figure 3.8). In the factorial plan I-II, the first two axis discriminated the samples according to their habitats, from the *Alviniconcha* habitat to the *Bathymodiolus* habitat and according to the longitude, separating the eastern basins from the western ones (i.e. North Fiji/Lau/Futuna vs Woodlark/Manus). While the samples from the *Bathymodiolus* habitat were well separated from the other samples, the distribution of the samples from the *Alviniconcha* and *Ifremeria* habitats clearly overlapped in the factorial plan I-II, suggesting that the communities from these two habitats were less different in terms of species composition, especially in the eastern basins. Species which had a correlation greater

### 3.3 Results

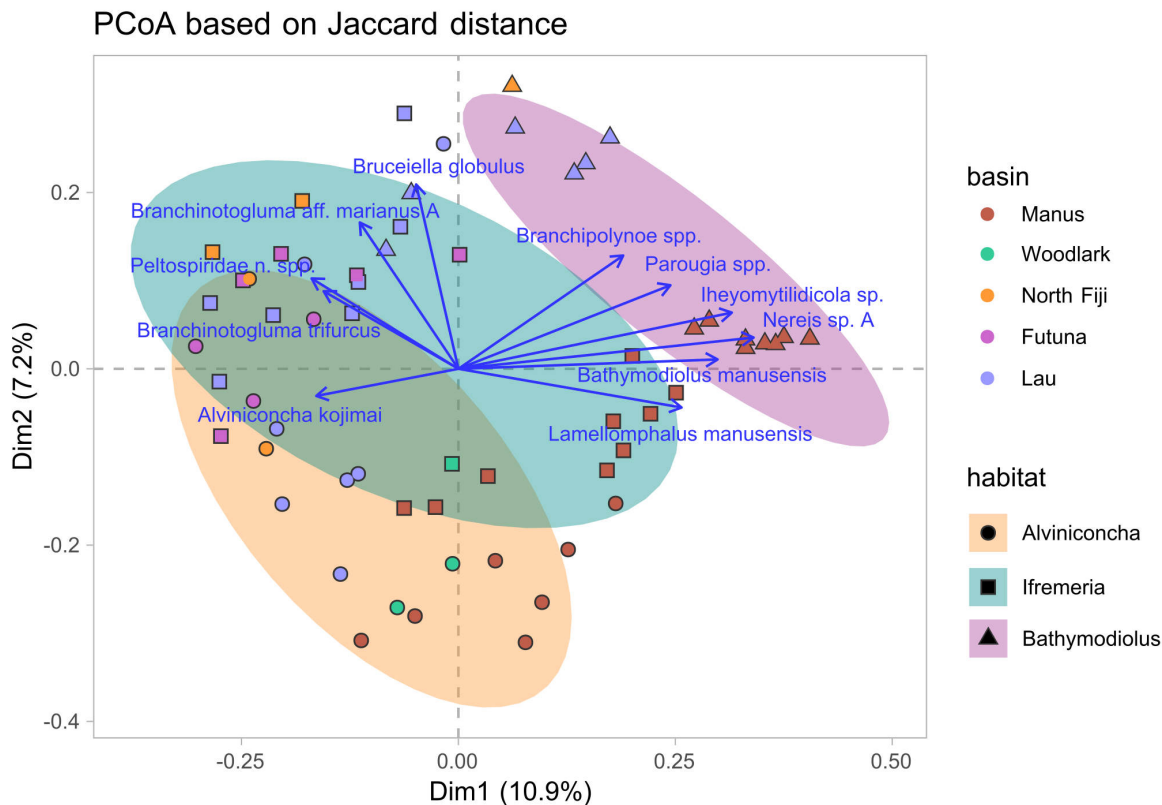


Figure 3.8 – Principal Coordinate Analysis (PCoA) based on the square root of the Jaccard dissimilarities representing the samples community composition variability at the regional scale and among the different habitats. Species which had a correlation greater than 0.6 with the first two axes were displayed in blue.

than 0.6 with the first two axes (displayed in blue on the PCoA, Figure 3.8) and contributed the most to discriminate the different samples included species only present in the eastern basins (i.e. the coiled gastropod *Bruceiella globulus*, the limpets *Peltospiridae n. spp.*, and the polynoids *Branchinotogluma aff. marianus A* and *B. trifurcus*, Table 3.2) or only collected in the Manus Basin, mainly from *Bathymodiolus* and *Ifremeria* habitats (i.e. *Bathymodiolus manusensis* and *Lamellomphalus manusensis*). Other discriminant species were exclusively found in mussel beds (i.e. the polychaetes *Nereis sp. A* and *Iheyomytilidicola sp.*), or most often within the mussels (i.e. the deep-sea mussels commensal scale-worms *Branchipolynoe spp.* and the Dorvilleids *Parougia spp.*), or in the *Alviniconcha* habitat (i.e. *Alviniconcha kojimai*).

The PERMANOVA analysis identified significant variations in species composition

Table 3.4 – Results of the PERMANOVA analysis based on the square root of Jaccard dissimilarities to test for differences in vent macrofaunal assemblages between basins and habitats (fixed factors), and fields within a basin and sites within a field (nested random factors)(A) and results of the post-hoc pairwise basins comparison (B). Df: degrees of freedom, SS: sum of squares, *F*: pseudo-F value by permutation, *P*: *p* values based on 9999 permutations. PERMANOVA and post-hoc test level of significance: \* *p* value <0.05; \*\* *p* value <0.01; \*\*\* *p* value <0.001.

A		Df	SS	$R^2$	<i>F</i>	<i>P</i>
	basin	4	3.1429	0.14539	2.7754	0.0001 ***
	habitat	2	2.1205	0.0981	3.7452	0.0001 ***
	basin*habitat	6	2.2335	0.10332	1.3149	0.001 ***
	basin/field	5	2.0414	0.09444	1.4422	0.0004 ***
	basin/field/site	15	4.4345	0.20515	1.0443	0.2249
	Residuals	27	7.6437	0.3536		
	Total	59	21.6165	1		

B		Lau	Futuna	North Fiji	Woodlark
	Futuna	0.11			
	North Fiji	0.46	0.61		
	Woodlark	***	**	*	
	Manus	***	***	***	**

between basins, between habitats and the interaction of these two factors was also significant. It also highlighted significant variability among fields within a basin, but not among sites within a field (Table 3.4A). Post-hoc pairwise comparison showed that macrofaunal compositions from all three habitats differed from each other ( $p < 0.001$ ) and that assemblages from the Woodlark and Manus Basins were distinct from all other basins, while the three eastern basins were not distinct from each other (Table 3.4B). No differences were detected between fields within a basin by pairwise comparison test, probably related to a lack of power of statistical tests.

$\beta$  diversity was partitioned according to the Podani family indices into species replacement and species richness difference for each habitat type along the South West Pacific back-arc basins. The *Alviniconcha* habitat had a total  $\beta$  diversity of 0.35 composed for

### 3.3 Results

51% of species replacement and for 49% of richness difference. The total  $\beta$  diversity of the *Bathymodiolus* and *Ifremeria* habitats was 0.36 and 0.32 respectively and both composed for 72% of species replacement and for 28% of species richness difference. Consistent with these results, the SDR-simplex approach showed that among-samples variation was dominated by species replacement for the *Ifremeria* and *Bathymodiolus* habitats with mean relative values around 50%, whereas it was lower for the *Alviniconcha* habitat which contained many more pairs of samples with high richness differences (Figure 3.9). There were several pairs of samples with no species replacement among samples from the *Alviniconcha* habitat. The resulting perfect nestedness (i.e. replacement values of 0 along the similarity axis) indicate that the species in a sample is a strict subset of the species in the richer sample; this did not occur for the *Ifremeria* and *Bathymodiolus* samples. *Alviniconcha* pairs of samples showed a transition from strong nestedness with high richness differences to high species replacement. The variations among pairs of samples were more similar for the *Ifremeria* and *Bathymodiolus* habitats, and were less influenced by differences in species richness.

$\beta$  diversity was also partitioned among samples from the Manus and Lau Basins to assess  $\beta$  diversity between habitats in a basin. Total  $\beta$  diversity in the Manus Basin was 0.36 composed for 51% of species replacement and for 49% of richness difference. Total  $\beta$  diversity in the Lau Basin was 0.34 composed for 57% of species replacement and for 43% of richness difference. The SDR-simplex approach showed that among samples variation was dominated here again by species replacement (Manus Basin: mean relative Similarity = 27.8, Repl = 37.2, RichDiff = 35.0; Lau Basin: mean relative Similarity = 31.4, Repl = 39.2, RichDiff = 29.4) (Figure 3.10). Pairs of samples in the Manus Basin showed a transition from a perfect nestedness with high richness difference to a high species replacement and a relatively low number of shared species. The relative importance of species richness difference and species replacement depended on the habitats considered. Regarding the type of habitat of samples pairs, variation was dominated by species richness difference when comparing (i) samples from the *Alviniconcha* habitat with samples from one of the other two habitats or (ii) samples from



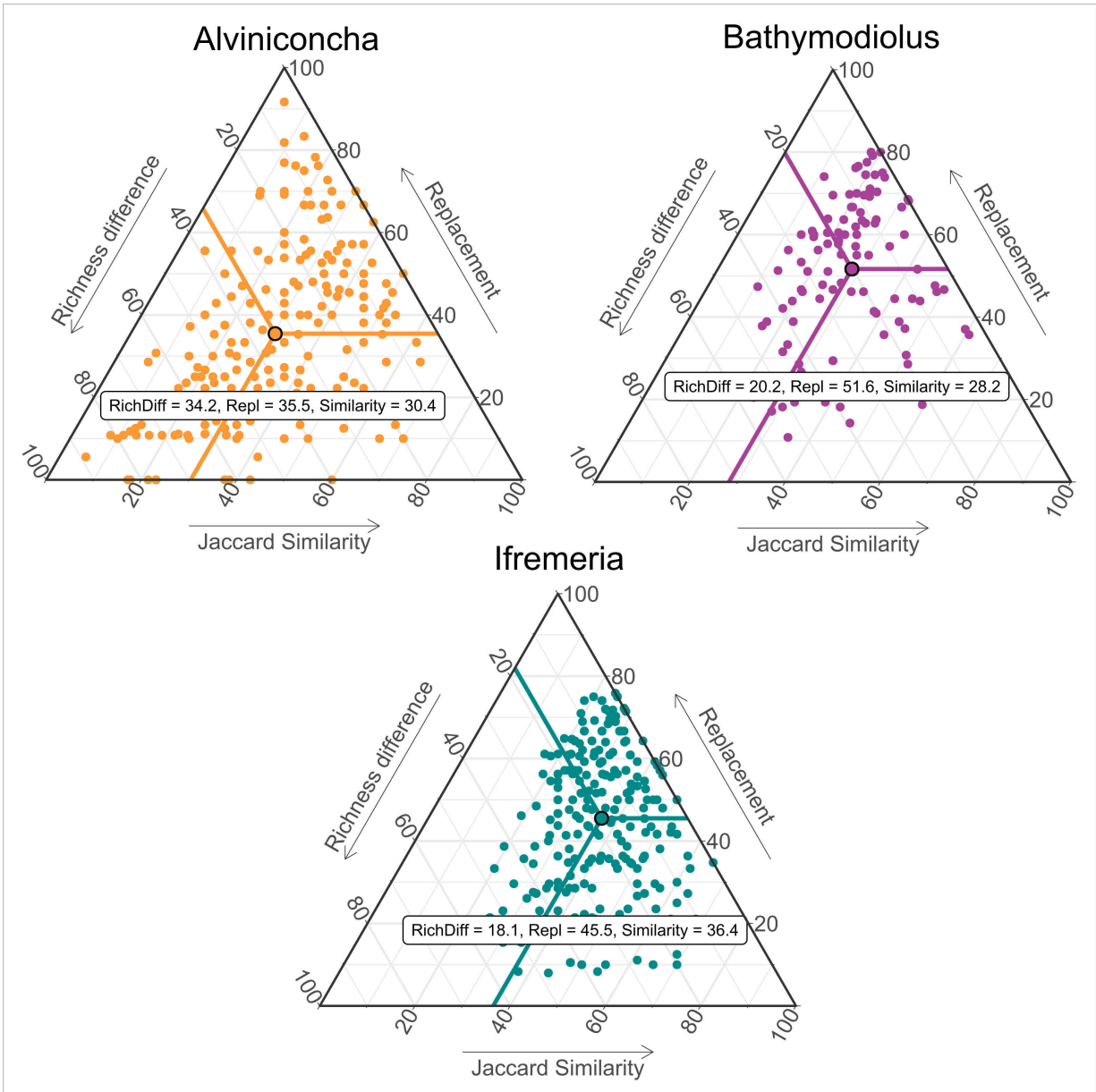


Figure 3.9 – SDR-simplex by habitat. Each point refers to a pair of samples represented by three values: the Jaccard similarity and Podani family indices, species replacement (Repl) and species richness difference (RichDiff). Their mean values are shown in the box. The point circled in black represents the mean position of the sample pairs.

### 3.3 Results

the *Alviniconcha* habitat (i.e. yellow, orange and light green dots on Figure 3.10). Conversely, species richness difference was more balanced and species replacement was dominant between pairs of samples from the *Bathymodiolus* and *Ifremeria* habitats or between samples from the *Bathymodiolus* habitat (i.e. blue and violet dots on Figure 3.10).

Patterns were different between samples from the Lau Basin (Figure 3.10).  $\beta$  diversity was less influenced by species richness differences for pairs of samples (i) between the *Alviniconcha* habitat and one of the other two habitats or (ii) from the *Alviniconcha* habitat, and by the species replacement for samples from the *Bathymodiolus* and *Ifremeria* habitats. In the Lau Basin, the mechanisms involved in the  $\beta$  diversity were quite similar whatever the type of habitat.

#### 3.3.2 Environmental and spatial drivers of faunal composition

**Physico-chemical conditions** Pre- and post-sampling measurements were conducted for 48 samples for the temperature and only 28 for  $\Sigma S$ . No trend was observed between measurements carried out before or after sampling for either the mean temperature or  $\Sigma S$  (Figure 3.11 and 3.12). Contrary to expectations, mean temperatures and mean  $\Sigma S$  concentrations were not constantly higher for measurements made after sampling (see for instance samples FK2 and FK8 for mean temperature on Figure 3.11). At very local scale, a high variability was observed for mean temperature and  $\Sigma S$  between the different points of measurement (Figure 3.11 and 3.12). For instance, a difference of 30°C was reported for the mean temperature between the three measurements performed at the sample TM5 before sampling (Figure 3.11) and a difference of almost 320  $\mu M$  was observed for the mean  $\Sigma S$  between the measurements carried out at sample KL1 and SU4 before sampling (Figure 3.12).

Mean temperature ranged from 3.3°C (LS3) to 25.8°C (TM5) in the *Alviniconcha* habitat, from 3.0°C (TC1) to 15.1°C (TM4) in the *Ifremeria* habitat and from 2.6°C (AB2) to 9.8°C (PM2) in the *Bathymodiolus* habitat (Table 3.1). Maximal temperature recorded in the *Alviniconcha* habitat reached 40.0°C (TM5) while it was about twice as low in the *Ifremeria*

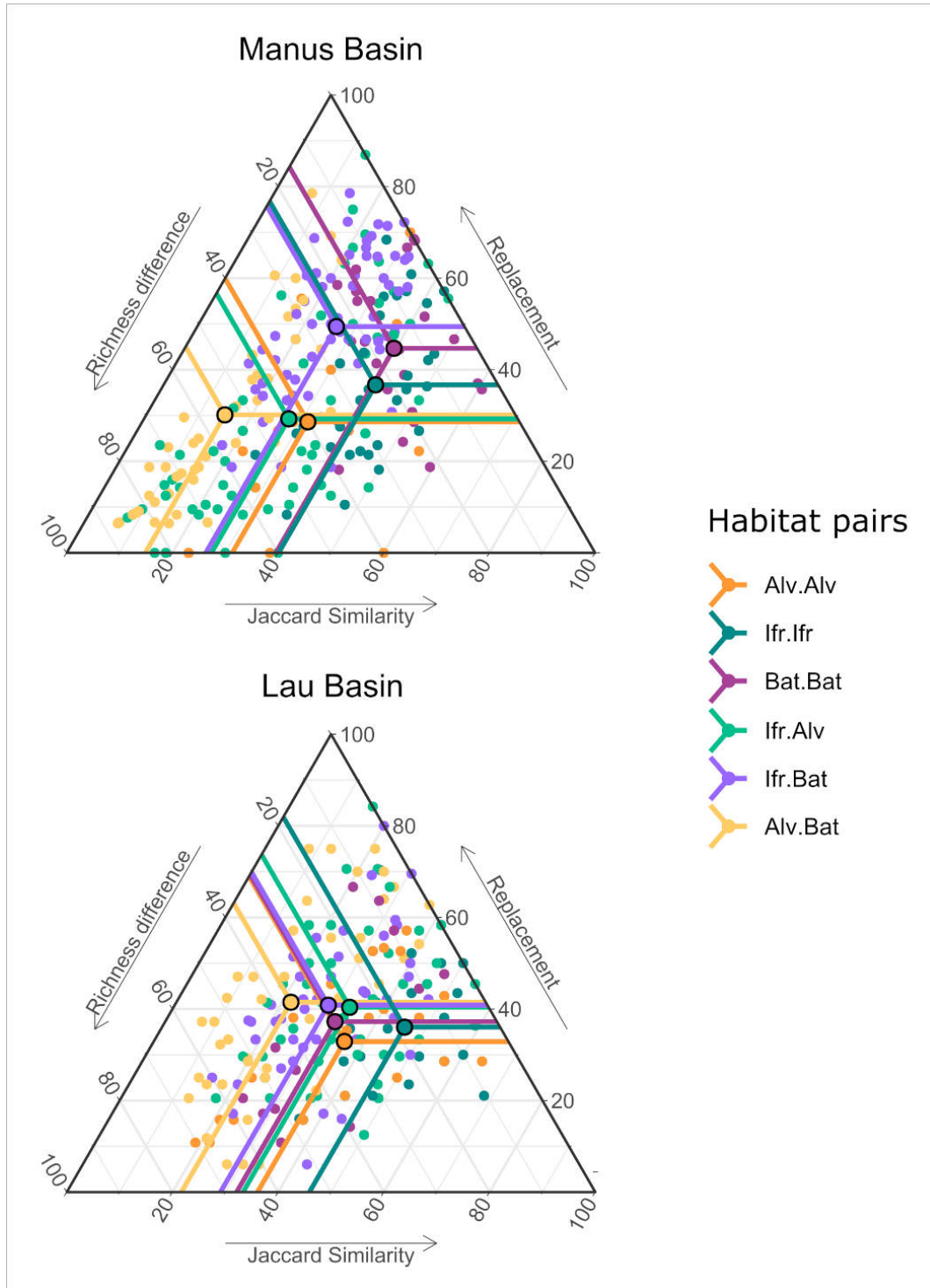


Figure 3.10 – SDR-simplex for the Manus and Lau Basins. Each point refers to a pair of samples represented by three values: the Jaccard similarity and Podani family indices, species replacement (Repl) and species richness difference (RichDiff). The different colors indicates the compared in the sample pair: Alv.Alv, *Alviniconcha* vs *Alviniconcha*; Ifr.Ifr, *Ifremeria* vs *Ifremeria*; Bat.Bat, *Bathymodiolus* vs *Bathymodiolus*; Ifr.Alv, *Ifremeria* vs *Alviniconcha*; Ifr.Bat, *Ifremeria* vs *Bathymodiolus*; Alv.Bat, *Alviniconcha* vs *Bathymodiolus*. Points circled in black represents the mean position of each type of sample pairs.

### 3.3 Results

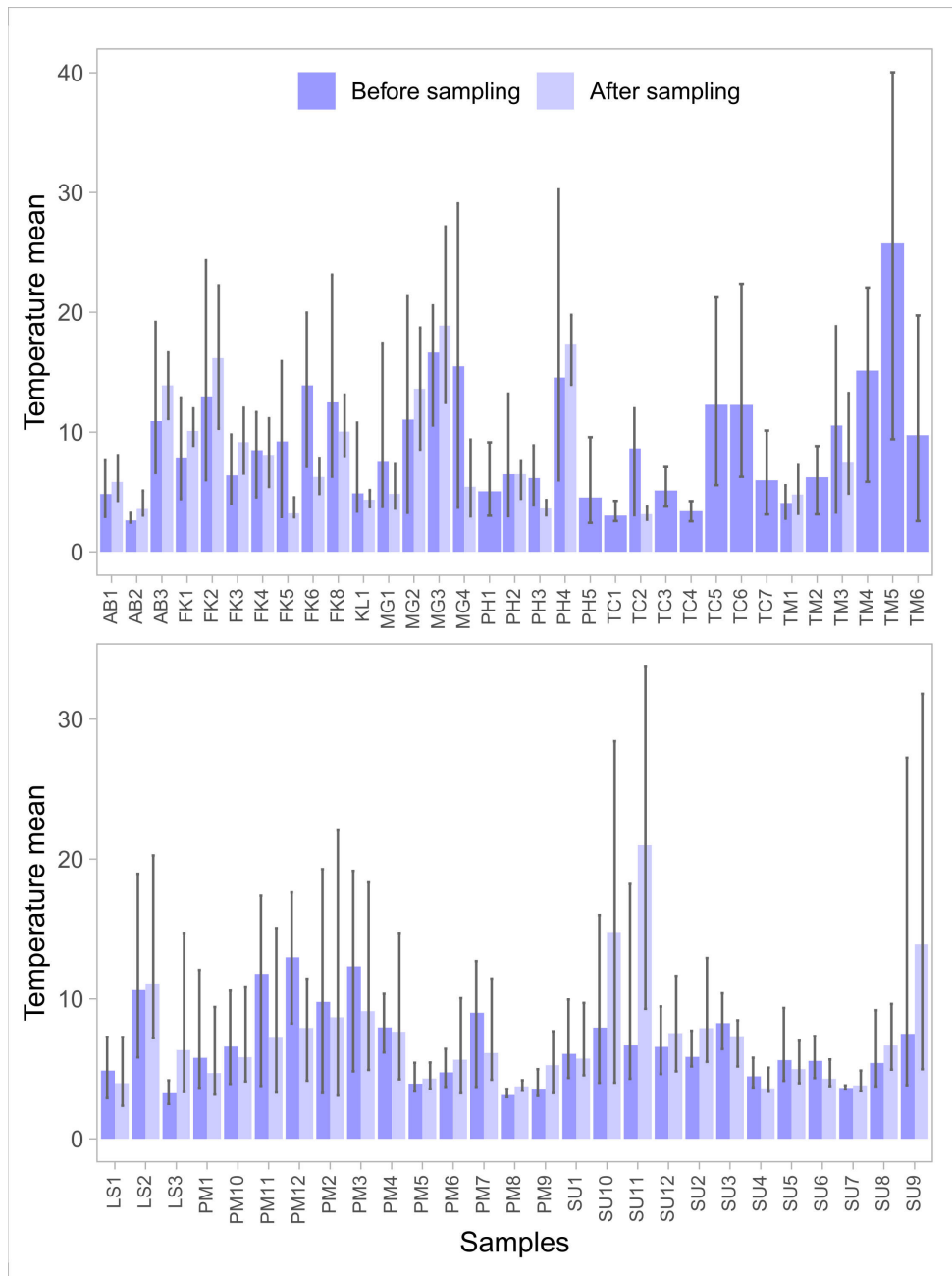


Figure 3.11 – Before and after sampling average temperature (°C) for each sample. Bars indicate the minimal and maximal values.

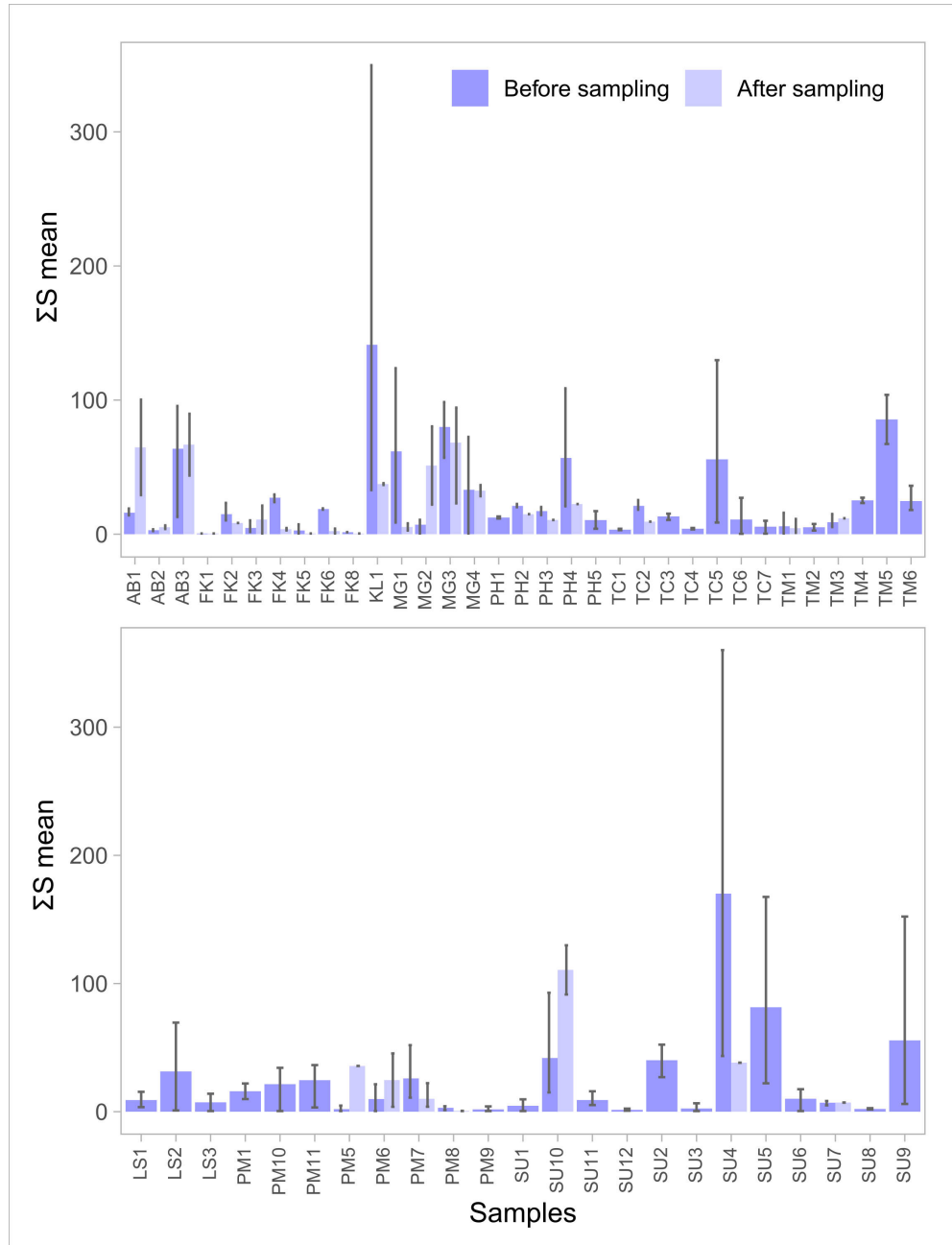


Figure 3.12 – Before and after sampling average  $\Sigma S$  (μM) for each sample. Bars indicate the minimal and maximal values.

### 3.3 Results

(i.e. 23.1°C, FK8) and *Bathymodiolus* (i.e. 19.3°C, PM2) habitats. Mean  $\Sigma S$  among samples ranged from 1.44  $\mu M$  (SU12) to 85.58  $\mu M$  (TM5) in the *Alviniconcha* habitat, from 0.5  $\mu M$  (FK1) to 141.25  $\mu M$  (KL1) in the *Ifremeria* habitat and from 1.82  $\mu M$  (PM9) to 21.13  $\mu M$  (TC2) in the *Bathymodiolus* habitat (Table 3.1). pH values ranged from 5.9 (MG3) to 7.73 (LS3) in the *Alviniconcha* habitat, from 5.88 (FK1) to 7.66 (LS1) in the *Ifremeria* habitat and from 5.8 (TC7) to 7.57 (AB2) in the *Bathymodiolus* habitat (Table 3.1). Methane ranged from 0.1  $\mu M$  (TC6) to 0.85  $\mu M$  (PM10) in the *Alviniconcha* habitat, from 0.07  $\mu M$  (TC1) to 1.03  $\mu M$  (MG1) in the *Ifremeria* habitat and from 0.07  $\mu M$  (TC4) to 0.61  $\mu M$  (TM1) in the *Bathymodiolus* habitat (Table 3.1); sulfur from 24.55  $\mu M$  (FK6) to 33.26  $\mu M$  (FK4) in the *Alviniconcha* habitat, from 25.69  $\mu M$  (SU2) to 33.47  $\mu M$  (FK1) in the *Ifremeria* habitat and from 26.48  $\mu M$  (SU6) to 29.78  $\mu M$  (PH3) in the *Bathymodiolus* habitat (Table 3.1); and phosphorus values from 2.6  $\mu M$  (LS2) to 18.36  $\mu M$  (sample TM5) in the *Alviniconcha* habitat, from 2.29  $\mu M$  (sample LS1) to 4.9  $\mu M$  (sample MG2) in the *Ifremeria* habitat and from 2.8  $\mu M$  (TC2) to 28.11  $\mu M$  (TC7) in the *Bathymodiolus* habitat (Table 3.1).

Mean and maximal temperature were both significantly different between habitats (Kruskal Wallis test,  $p < 0.001$ ). They were significantly different only between the *Alviniconcha* and the two other habitats. *Alviniconcha* habitat was warmest than *Ifremeria* and *Bathymodiolus* habitat (Figure 3.13A-B). For the mean  $\Sigma S$ , significant differences were detected among habitats (Kruskal Wallis test,  $p < 0.001$ ) (Figure 3.13C). Mean  $\Sigma S$  was significantly lower in the *Bathymodiolus* habitat than in the *Alviniconcha*. No significant difference was observed between the *Ifremeria* habitat and the two others. Finally, no significant differences among habitats were noted for pH, methane ( $CH_4$ ), sulfur (S) and phosphorus (P) concentrations (Figure 3.13D-G).

The first two axes of the PCA computed on the physico-chemical variables associated with each sample explained 64% of the total variation. The first axis was positively correlated with the mean and maximal temperature and mean  $\Sigma S$  and negatively correlated with pH while the second axis was positively correlated with methane concentration. The

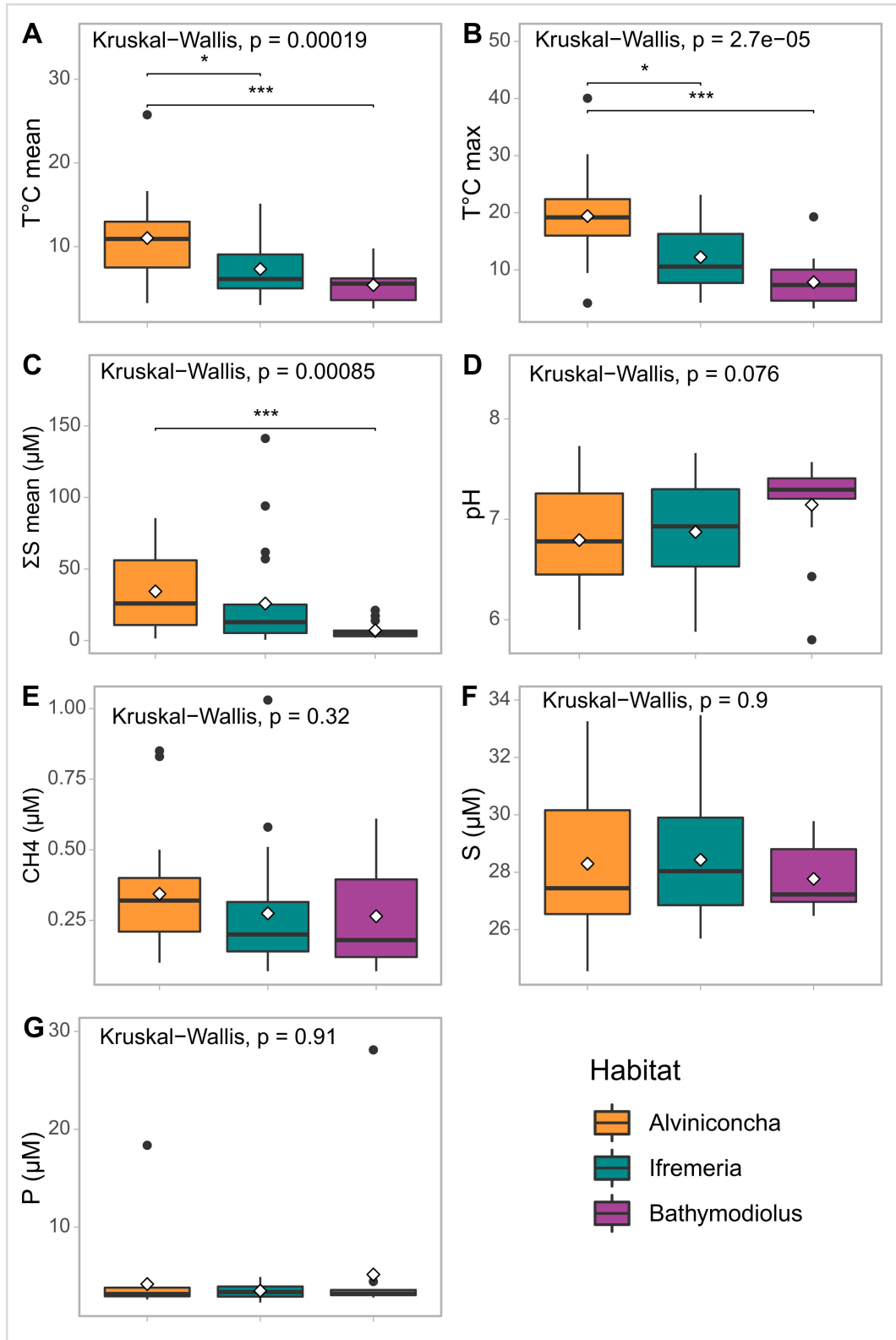


Figure 3.13 – Physico-chemical measures by habitat: Temperature max and min (A-B),  $H_2S$  mean (C), pH (D),  $CH_4$  (E), S and P (F-G). White rhombus indicates the average. Kruskal-Wallis test results and level of significance of the post-hoc Nemenyi and Dunn test: \*  $p$  value <0.05; \*\*  $p$  value <0.01; \*\*\*  $p$  value <0.001.

### 3.3 Results

third axis explained 15.2% of the variation and was mainly correlated with sulfur. Consistent with the previous observations, the PCA highlights an environmental gradient from the *Bathymodiolus* to the *Alviniconcha* samples with *Ifremeria* samples in between (Figure 3.14A). The *Bathymodiolus* habitat was characterized by lower temperature and  $\Sigma S$  and a higher pH. However, large variations were observed in the physico-chemical conditions among *Alviniconcha* samples, resulting in a full overlap between the ellipses of the *Ifremeria* and *Bathymodiolus* samples and the ellipse of the *Alviniconcha* samples. When looking at the differences between basins, there was a large variability in the physico-chemical conditions reported in the Lau Basin as a result of the large variability in temperature among the Tui Malila samples (South of the Lau Basin) and in methane concentrations among samples from Mangatolo vent field (North of the Lau Basin) (Figure 3.14B). Samples from the vent fields of the Lau Basin (i.e. Tui Malila, Tow Cam, Mangatolo, Fatu Kapa and Phoenix) showed slightly greater  $\Sigma S$  concentrations compared to the Manus Basin vent fields (i.e. Pacmanus and Susu), although samples from Fatu kapa (Futuna Volcanic Arc) showed a great variability in sulfur concentration (Figure 3.14D). Similar patterns were observed in the analysis without methane and the Woodlark Basin samples were included in the Manus Basin ellipse (see Appendix C.1).

**Spatial and environmental drivers of faunal composition** In the dbRDA, the forward selection procedure selected only two physico-chemical variables, i.e. the maximal temperature (T.max) and the sulfur (S), and two spatial variables, i.e. the depth and the latitude (Lat.dec). According to the sampling design of the present study, latitude was correlated with the longitude. As methane was not retained by the forward selection, the analysis included samples for which no methane concentration was available – the forward selection kept the same variables when performed with the data set that did not include methane.

The selected model explained 16.67% of the total inertia in the structure of macrofaunal assemblages (Figure 3.15). The dbRDA was significant ( $p < 0.001$ ) as were the first two axes which explained 8.1 and 3.9% of the variation respectively ( $p < 0.001$ ). The latitude divided macrofaunal assemblages along the first axis, separating the eastern from the



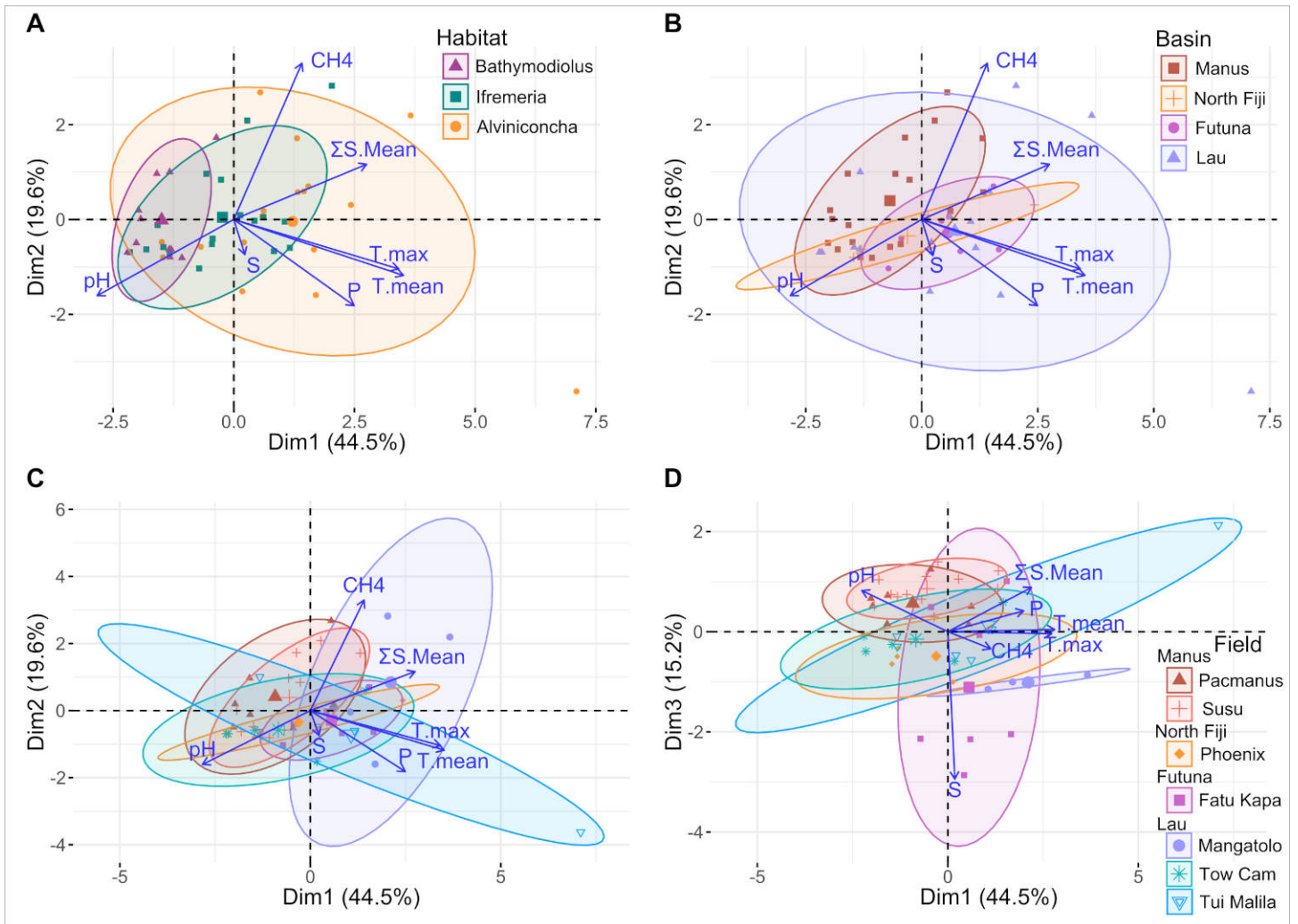


Figure 3.14 – PCA based on scaled physico-chemical data. The first three graphs show axes one and two with ellipses constructed by habitat (A), basin (B) and field (C). The fourth graph displays axes one and three with ellipses produced by field (D).

### 3.4 Discussion

western basins (Lau/Futuna/North Fiji vs Woodlark/Manus), while the maximum temperature partitioned the habitats along the second axis from low (i.e. *Bathymodiolus* habitat) to moderate (i.e. *Alviniconcha* habitat) diffused flow areas. The third axis, also significant ( $p < 0.05$ ), explained 3% of the variation and was correlated with the depth which separated the Woodlark Basin from the others. For the variation partitioning analysis, all components were significant ( $p < 0.001$ ) and explained very similar proportions of the variation in benthic assemblages. Physico-chemical variables alone (i.e. T.max and S) explained 3.1% of the variation while spatial variables (i.e. depth and latitude) explained 4%. The interactions between the two categories of variables, i.e. the spatial structure of the physico-chemical conditions, explained 2.7% of the variation. Residuals represented 90.1% of the variation (Figure 3.15). Similar patterns were observed with the analyses carried out on the dataset with methane values (see Appendix C.2).

## 3.4 Discussion

So far, most studies on southwestern back-arc basins communities focused on megafauna (Galkin, 1997; Podowski *et al.*, 2009, 2010; Kim et Hammerstrom, 2012; Sen *et al.*, 2013, 2016). The few studies that considered the entire macrofaunal community (i.e. dominant engineer species and the associated smaller macrofauna) were carried out at the Manus (Collins *et al.*, 2012; Van Audenhaege *et al.*, 2019) or the Lau/North Fiji Basins (Desbruyères *et al.*, 1994). In this study, we assessed the  $\gamma$  diversity and identified patterns of  $\alpha$  and  $\beta$  diversity of vent macrofaunal communities at different spatial scales within three iconic habitats of the southwestern Pacific back-arc basins: assemblages dominated by the large mobile gastropods *Alviniconcha* and *Ifremeria* and mussel beds of *Bathymodiolus*. Using a set of spatial and physico-chemical variables, we explored the factors that structure observed biodiversity patterns. Faunal assemblages were highly structured along the hydrothermal diffuse flow gradient from high (i.e. *Alviniconcha* habitat) to low temperature (i.e. *Bathymodiolus* habitat) diffused flow areas and along a geographical gradient, dividing the

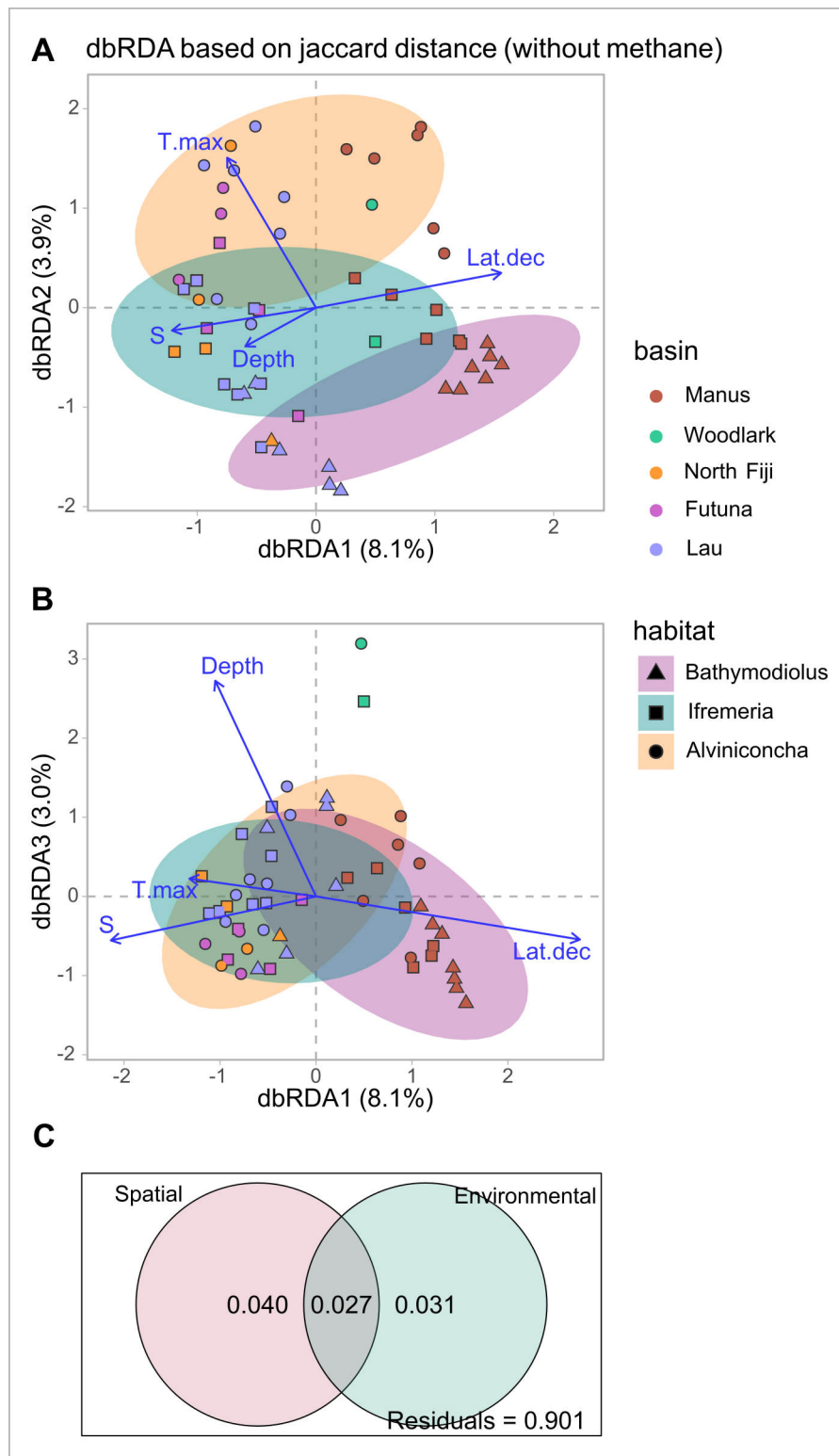


Figure 3.15 – dbRDA axes 1 and 2 (A) and 1 and 3 (B) and variance partitioning (C) based on square root of Jaccard dissimilarities and environmental data without methane.

### 3.4 Discussion

assemblages in the western basins (i.e. the Manus and Woodlark Basins) from the eastern ones (i.e. the Lau and North Fiji Basins) and the Futuna Volcanic Arc.

#### 3.4.1 Regional scale diversity and taxonomic issues

Quantifying and assessing regional and local biodiversity requires a good taxonomic resolution that is currently unavailable in the western back-arc basins, a region where biological classification regularly undergoes changes and new species descriptions are regularly published. Indeed many species are undescribed or are still under description while some families do not have any species described to date (e.g. the Capitellidae, Nereididae, Dorvilleidae). Two species of Phyllodocidae have been described very recently (Pearson et Rouse, 2022) but were not yet known at the time we identified the specimens. In addition, species identification by ecologists based on morphological characteristics can lead to wrong classifications. Indeed, original taxonomic descriptions do not always mention species morphological plasticity or ontogenic changes, perhaps because descriptions are based on a small number of individuals whereas morphological variability may be high for some species. In this study, we used two complementary methods to reach optimal taxonomic resolution, i.e. morphological identification and Cytochrome Oxidase I gene barcoding, as cryptic species are common among vent environments (Johnson *et al.*, 2008; Matabos *et al.*, 2008b, 2011; Plouviez *et al.*, 2009, 2019). However, because barcode data was incomplete, many taxa could not be identified down to species level (i.e. 43%). In addition, we were forced to downgrade the information for taxa where cryptic species spatially overlapped among basins (e.g. the polychaetes *Archinome*, *Amphisamytha* and the *Lepidonotopodium* and *Levensteiniella* polynoids but also crabs for which barcode data are incomplete) and for others where we had no genetic information (e.g. the copepods). This species list is therefore likely to evolve, but it is the most accurate we have so far.

Polychaetes and gastropods were dominant in terms of number of taxa. These are also the groups for which a greater identification and molecular barcoding effort has been made.

However, there are likely to be even more species among Polychaetes as many taxa remained at the genus level while COI barcoding highlighted several species. Chabert's study based on COI barcoding detected at least six species of *Amphisamytha* with several species from the Lau and Manus Basins, and another six species among Phyllodocidae Chabert (2021). The very diverse polynoid family includes at least 11 additional species in the region among the three most diverse vents genera: five species in the genus *Branchinotogluma*, four species in the genera *Levensteiniella* and *Lepidonotopodium* and two species in the genus *Branchipolynoe* which is a mussel commensal Chabert (2021). In addition, the family Siboglinidae includes at least two species, and the genus *Archinome* at least three Chabert (2021). Crustacean diversity was also likely underestimated as the *Austrinograea* crab genus comprised more than three morphologically distinct species from this area (Guinot et Segonzac, 2018). Copepods, although very abundant, were not identified at the species level in this study, yet this group is highly diversified. As an example, eighteen species were reported from *Alviniconcha*, *Bathymodiolus* and *Ifremeria* habitats in the ABE vent field from the Lau basin (Diaz-Recio Lorenzo *et al.*, 2021).

With the above mentioned taxonomic descriptions issues in mind, a total of 114 taxa were identified in this study among *Alviniconcha*, *Bathymodiolus* and *Ifremeria* habitats. This number is an obvious underestimation of the biodiversity associated with the southwestern basins. Of these, 96 were identified in the *Bathymodiolus* habitat, which is higher than observed in mussel beds (i.e. *B. thermophilus*) along the mid-ocean Southern East Pacific Rise (SEPR), where 61 taxa were identified (Matabos *et al.*, 2011).

### **3.4.2 Community structure through habitat type**

The three engineer species (i.e. *Alviniconcha*, *Ifremeria* and *Bathymodiolus*), by providing habitat and food increase the number of local ecological niches that can be colonised by smaller mobile macrofaunal species and contribute to enhance local diversity (Van Dover *et al.* 2002; Govenar et Fisher 2007). Species richness, measured as the number of species in a sample or the expected number of species based on rarefaction method, was significantly lower

### 3.4 Discussion

in the *Alviniconcha* habitat compared to the *Ifremeria* and *Bathymodiolus* habitats. This habitat was dominated in abundance by copepod species that were not identified taxonomically, hence introducing a potential bias in biodiversity assessment. However, Diaz-Recio Lorenzo *et al.* (2021) observed that the copepod community in the *Alviniconcha* habitat in which the vent endemic copepod *Stygiopontius lauensis* (Dirivultidae) constituted over 90% of the total abundance, was less diverse than the one in the *Bathymodiolus* habitat characterised by more generalist species. Few vent gastropods colonised this habitat compared to the *Ifremeria* and *Bathymodiolus* ones. Periostracal hairs of *Alviniconcha* individuals may keep these limpets from settling on the shells. By contrast, Dirivultidae copepods, could crawl between these hairs to feed on bacterial mats that develop on the shell hairs or in the mucus produced by *Alviniconcha* species (Sigwart et Chen, 2018), using their "siphon-like" mouth (Diaz-Recio Lorenzo *et al.*, 2021). Conversely, the *Ifremeria* and *Bathymodiolus* habitats had a higher species richness and more species in common. Interestingly, *in situ* videos recorded during the CHUBACARC cruise, using autonomous camera systems over several days in the three habitats, showed that *Alviniconcha* gastropods are much more mobile than *Ifremeria* gastropods and *Bathymodiolus* mussels (M. Matabos, unpublished data). This higher mobility could prevent the creation of stable ecological niches available for the colonisation by smaller macrofaunal species and result in higher environmental variations. Regarding the limpets, *S. tollmanni* was more abundant on *Ifremeria* individuals' shells than *Bathymodiolus* ones. Conversely *L. schrolli*, although very abundant in both habitats was found in higher number in mussel beds. Biotic interactions such as competition for space among these limpets (i.e. engineer species shell surface) (Mullineaux *et al.*, 2003; Govenar *et al.*, 2005), resource partitioning (Levesque *et al.*, 2003; Lelièvre *et al.*, 2018) and/or abiotic factors including physico-chemical conditions (e.g. temperature, sulphides, dissolved oxygen concentration; Tunnicliffe, 1991; Sarrazin *et al.*, 1997; Mills *et al.*, 2007; Matabos *et al.*, 2008a), that structure the habitat, could explain these differences.

Over a third of identified taxa are common to all three habitats (i.e. 39%), suggesting

a large number of ubiquitous species and that the associated smaller macrofaunal species are not exclusive to a given megafaunal species but are rather specific to local microhabitats that can be present in different assemblages as was previously observed on the EPR (Mills *et al.*, 2007; Matabos *et al.*, 2008a). In addition, the spatial organization of the different habitats is not always clear. In some cases, there was an overlap in the distribution of the engineer species at the scale of the sampling area, as can be seen from the proportions of each engineer species in the different samples. Furthermore, habitat organization was not only in the horizontal plane but could also be vertical where *Ifremeria* individuals would be found beneath *Alviniconcha* specimens, creating transition zones between habitats that could also account for the large number of species in common. Finally, sampling protocols can also influence this large species pool, with suction collection sometimes adding many species (e.g. PH3), even doubling the species richness in some cases (e.g. MG4). Depending on the community configuration, suction could have deviated from the target community and add species not truly representative of the habitat sampled. This might explain the very rich MG4 *Alviniconcha* habitat sample combined with *Ifremeria* individuals from a crevasse. On the other hand, PH3 was a very small mussel bed sample. Both PH3 and MG4 were surrounded by *Eochionelasmus ohtai* cirripeds (see appendix D.3) that constitute a low-temperature community characterised by a different species composition than the *Alviniconcha* habitat (Collins *et al.*, 2012). The other small isolated mussel bed, PM9 sample, was very diverse with rather well represented species. Species richness was above the average for this sample (i.e. 29 for a mean of 25), and interestingly comprised only a few individuals of the mostly very abundant *L. schrolli*. This suggest that this species could outcompete others when present in high abundance as was previously observed for gastropods along the EPR and the Mid-Atlantic Ridge (Matabos *et al.*, 2008a; Sarrazin *et al.*, in press). Alternatively, the quantity of sediment collected could also increase the number of species by adding infauna such as polychaetes.

Except for species only collected in the Woodlark Basin, the few species unique to the *Alviniconcha* or *Ifremeria* habitats seemed more related to their rarity (i.e. low occurrence

### 3.4 Discussion

and low abundance) than to the habitat itself. In the case of *Ifremeria* habitat unique species appeared to be specific to the Woodlark Basin (i.e. *Peltospiridae* n. sp. A, *Shinkailepas* aff. *tufari* W and *Symmetronphalus* aff. *hageni* W). These are genera that could have been found in mussels or even in *Alviniconcha* but the absence of mussels in the Woodlark Basin and very few samples of *Alviniconcha* may explain why they only appear in the *Ifremeria* habitat. The *Bathymodiolus* habitat, on the other hand, comprised a large number of unique species (i.e almost a quarter). These taxa were essentially genera or families also reported from the sessile barnacle *E. othai* habitat associated with temperature close to ambient (e.g. *Vulcanolepas* stalk barnacle, *Nereis* or Terebellidae Polychaetes) (Collins *et al.*, 2012), or even in periphery. They included *Actiniaria* cnidarians, *Chiridota* or Ophioridae echinoderms, *Munidopsis* squat lobsters, *Phymorhynchus* gastropods, *Ophryotrocha* dorvilleids and *Nicomache* maldanids, also very abundant among *Vulcanolepas* thickets from the Woodlark Basin (Boulart *et al.*, 2022).

The distribution of *Alviniconcha* and *Ifremeria* gastropods and *Bathymodiolus* mussels along the hydrothermal diffuse flow gradient from high to low diffused flow areas was already reported in the literature (Desbruyères *et al.*, 1994; Podowski *et al.*, 2010; Kim et Hammerstrom, 2012). Temperature, sulphide concentrations, geological and biological controls were all suggested to contribute to the Lau Basin megafauna zonation (Desbruyères *et al.*, 1994; Henry *et al.*, 2008; Podowski *et al.*, 2009; Kim et Hammerstrom, 2012; Diaz-Rocio Lorenzo *et al.*, 2021). Our results supported the temperature gradient from the *Alviniconcha* to the *Bathymodiolus* habitats in our samples but not the link with  $\Sigma S$ . Indeed, highest values were recorded among the *Ifremeria* habitat (SU4-5 and KL1), while *Alviniconcha* is commonly reported to have the highest concentrations (Podowski *et al.*, 2009, 2010; Diaz-Rocio Lorenzo *et al.*, 2021). However, these are some exceptional values, the concentration of  $\Sigma S$  tends to be somewhat higher in the *Alviniconcha* habitat. This reflects the strong environmental heterogeneity that can be found in *Ifremeria* habitats.

Presence-absence community composition analysis showed that associated macrofauna assemblages are also structured according to the habitat along this temperature gradient.



While *Bathymodiolus* assemblages were well separated from the two others, an overlap was observed between the *Ifremeria* and the *Alviniconcha* habitats community compositions. This can also be the result of the overlap of engineer species as highlighted by the various proportions of the dominant species in the samples. The main process driving changes in diversity along the three habitats was species replacement which may result from environmental filtering along the local diffuse flow environmental gradient (Alfaro-Lucas *et al.*, 2020). Environmental heterogeneity is high within a site and species distribute along the gradient resulting from the mixing between vent fluid and seawater according to environmental conditions, leading to a high  $\beta$  diversity due to species being replaced by others. However, this is not the case between *Alviniconcha* and *Bathymodiolus* or *Ifremeria* from the Manus Basin, where species richness difference is the dominant component of the observed  $\beta$  diversity. This could be a results of sampling bias, as some *Alviniconcha* gastropods and *Bathymodiolus* mussels, mainly from the Manus Basin, were also mixed with other megafauna habitat-building/engineer species such as the alvinellid worms *Paralvinella* that lives in mucus tubes (i.e. PM10) or the siboglinid *Oasisia* tube-dwelling polychaete (i.e. PM5) that could have introduced other species. Alternatively, this could be a consequence of under-estimation of the diversity of the *Alviniconcha* habitat, which will minimise the proportion of species replacement. This habitat depicted the highest mean and maximum temperature, high sulphide concentration and the highest variability in physico-chemical conditions. Species that colonise these habitat must be tolerant to high sulphur concentration, high temperatures and also environmental variability, mobile species such as copepods or small polynoidea like *Branchinotogluma* species for instance, might be better adapted to this habitat.

However, the environment explains a relatively low proportion of the variation in the assemblage. One explanation is that the variables considered in this study were not sufficient to properly characterise the environment or that this latter was poorly characterised using our methodological approach. For instance, we did not consider iron, which is an important compound. Iron and pH affect the bioavailability or toxicity of sulphide (Luther *et al.*, 2001;

### 3.4 Discussion

Le Bris *et al.*, 2003; Matabos *et al.*, 2008a). In addition, we used single point measurements that are probably not sufficient to fully describe the local conditions in terms of spatial heterogeneity and temporal variability. Indeed, physico-chemical conditions are highly variables at the centimeter scale in vent habitats and require temporal and multiple spatial measurements to be properly characterised (Le Bris *et al.*, 2005; Lee *et al.*, 2015; Van Audenhaege *et al.*, 2022). Due to the 3D structure of the habitat and the shells of megafauna, environmental conditions may vary depending on the location of the organism on the shell as was previously observed within *Alvinella pompejana* habitat (Le Bris *et al.*, 2005). Finally, in addition to the horizontal and vertical environmental heterogeneity, small-scale temporal fluctuation occurs as well (Johnson *et al.*, 1988; Lee *et al.*, 2015; Van Audenhaege *et al.*, 2022). This small-scale spatio-temporal variability could strongly impact the species distributions. On the other hand, species distribution could be controlled by the physico-chemical conditions experienced by the organisms at the individual scale (Bates *et al.*, 2005). Some hydrothermal vent species observed in each habitat define by the large engineer species may occupy specific micro-habitats that differ from the general surrounding physico-chemical environment described in this study. Finally, physico-chemical conditions are not the only factors that can structure communities. Biotic interactions can strongly influence species distribution. Diaz-Recio Lorenzo *et al.* (2021) suggested that megafauna enhance their local environment by decreasing  $\Sigma S$  through endosymbiotic process. The shape shell characteristics, with crevasses as on *Ifremeria* or smoother as on *Bathymodiolus*, or biotic interactions such as facilitation, space competition or predation could also structure the assemblages. Although extreme environmental conditions (e.g. upper limit of thermal tolerance) may control the presence or absence of a given species, abiotic and biotic factors are also expected to modulate the relative densities of the different species. A smaller scale analysis (e.g. within a basin) of community composition using abundance data would provide a better understanding of potential species interactions.

### 3.4.3 Biogeography

Analysis of communities composition based on presence-absence data highlighted a split between the western basins (i.e. Manus/Woodlark) and the eastern basins (i.e. North Fiji/ Lau) and the Futuna Volcanic Arc. Previous studies already reported a biogeographical break between the eastern and western basins in this region, both at the population scale within a species or among species within a genus. Geographic divergence between populations from the Manus Basin and the North Fiji/Lau Basins occurs within various phyla, including gastropods such as the provannids *Ifremeria nautilei* (Thaler *et al.*, 2011; Tran Lu Y *et al.*, 2022) and *Provanna* (Poitrimol *et al.*, 2022), as well as the *Symmetromphalus*, *Lepetodrilus* and *Shinkailepas* limpets (Plouviez *et al.*, 2019; Poitrimol *et al.*, 2022), crustaceans including *Rimicaris* spp. shrimps (Thaler *et al.*, 2014) and *Austinaugraea* crabs (Lee *et al.*, 2019) and the stalked barnacles *Vulcanolepas* (Chan et Chang, 2018; Chan *et al.*, 2019). The present study confirms the occurrence of a geographic split in terms of community diversity and composition. Species replacement appeared to be the main process driving biodiversity changes along the back-arc basins, mainly in the *Bathymodiolus* and *Ifremeria* habitats and to a lesser extent in the *Alviniconcha* habitat. This could be explained by the occurrence of species restricted to the eastern or western basin (e.g. the polynoids *Branchinotogluma* aff. *marianus* A from the East vs. *B.* aff. *marianus* B from the West or *B.* aff. *trifurcus* or *B. trifurcus*, but also *Bruceilla globulus* or Peltospinidae n. spp. from the East). In the *Alviniconcha* habitat, the richness difference component was more important. While this could be a consequence of our taxonomic resolution as discussed above, the harsher environmental conditions existing in this habitat could enhance the nestedness where only a subset of species are adapted to cope with the local environmental conditions.

Tectonic history and ocean circulation are part of the processes that explain biogeographic patterns in hydrothermal vent fauna along mid-ocean ridges (Van Dover, 2002; Matabos *et al.*, 2011; Matabos et Jollivet, 2019; Watanabe *et al.*, 2019). The isolation of the Manus Basin by the New Guinea archipelago forming a physical barrier limits exchanges with

### 3.4 Discussion

others basins (Thaler *et al.*, 2011). This barrier can account for the high level of endemism reported in that basin. Similarly a number of species are only found in the eastern basins (e.g. *Bruceiella globulus*, *Peltospiridae* n. spp., *Branchinotogluma trifurcus* and *B. aff. marianus* A ). The barrier efficiency will depend on species life history traits of the associated fauna, such as larval dispersal behaviour and life span, with connectivity between the eastern and western basins being limited for species with short planktonic larval duration (Mitarai *et al.*, 2016). Specimens from these three assemblages could include a significant number of species with lower dispersal ability, unable to cross the potential barrier between the North Fiji Basin and the Woodlark Basin. Alternatively, this break may also reflect a data gap and limited sampling effort between these two basins. Indeed, no information is available regarding active sites and associated fauna in the intermediate Vanuatu (i.e. New Hebrides) and Solomon areas while they may have an important role connecting eastern and western basins (Mitarai *et al.*, 2016). Indeed Poitrimol *et al.* (2022) showed that phylogeographic patterns can strongly vary among taxa, with some species being able to connect across the full geographical gradient. Further sampling is needed in intermediate sites to test for the occurrence of a continuum in faunal composition along the southwestern back-arc basins. The presence of 'phantom sites' have already been suggested along the mid-Atlantic ridge to account for connectivity observed over large distances (Breusing *et al.*, 2016). Hydrothermal vents are dynamic environments with sites or field becoming inactive or being reactivated as observed during the CHUBACARC cruise (S. Hourdez, pers. comm.) as well as sites being regularly discovered in the region (e.g. Boulart *et al.*, 2022) resulting in a constant evolution of the current distribution map of active sites over time.

Interestingly, faunal assemblages in the Woodlark Basin, although represented by a few samples, differed from all other locations. Assemblages from the very deep La Scala vent field included some endemic limpet species (i.e. *Shinkailepas* aff. *tufari* W, *Symmetromphalus* aff. *hageni* W and *Peltospiridae* n. sp. A), species widely distributed across basins (e.g. *Thermopolynoe branchiata* polynoids, *Rimicaris variabilis* shrimps, *Lepetodrilus schrolli* and *Shinkailepas tollmanni* limpets), or others only shared with the Manus basins assemblages

(e.g. *Paralvinella hessleri*, *Branchinotogluma* aff. *marianus* B). Woodlark was the deepest visited basin during the cruise, La Scala vent site being located at 3,388 m depth against 2,716 m for the next deepest site located in the Lau Basin (i.e. Tow Cam). While depth could be an important factor in structuring biodiversity and species distribution as suggested in our multivariate analyses (Desbruyères *et al.*, 2001; Watanabe *et al.*, 2019), the particularity of the Woodlark Basin is more likely to reside in its intermediate geographical positioning between the Manus Basin and the eastern basins and the Futuna Volcanic Arc, supporting the biological stepping-stone role of this basin as suggested by Boulart *et al.* (2022) and Poitrimol *et al.* (2022).

To conclude, faunal assemblages were structured at different spatial scales, among habitats along the hydrothermal diffuse flow environmental gradient from high to low temperature conditions, among vent fields within a basin and across the different back-arc basins, species being replaced by others along both spatial end environmental gradients. At global scale several processes are involved, including geological events and current geographic barriers driving colonisation and speciation. Macrofaunal species associated with the three targeted habitats seem to be composed of a large number of species with lower dispersal capacity that does not allow effective connectivity between the eastern and western areas. This result has a major implication in terms of biodiversity conservation issues, especially in this region highly targeted for its mineral resources. The isolation and high level of endemism of the Manus Basin and the particularity of the Woodlark Basin make them potentially highly vulnerable to mining, with a risk of significant loss of biodiversity.

---

## Discussion générale et perspectives

---

Cette thèse avait pour objectif principal de décrire la distribution de la biodiversité des bassins arrière-arc du sud-ouest du Pacifique (i.e. les bassins de Manus et Woodlark à l'ouest, et ceux de Nord-Fidji et de Lau et de l'arc volcanique de Futuna à l'est) à différentes échelles spatiales, en lien avec les caractéristiques physico-chimiques de l'habitat et les traits d'histoire de vie des espèces. Trois habitats caractéristiques des zones de diffusion actives de la région et leur macrofaune associée ont été ciblés : les agrégations de gastéropodes *Alviniconcha* et *Ifremeria* et les moulières à *Bathymodiolus*.

Dans un premier temps, la mise en œuvre d'une approche de barcode moléculaire sur le gène mitochondrial *Cox1* a mis en évidence la présence d'espèces cryptiques chez les gastéropodes *Shinkailepas tufari* et *Symmetromphalus hageni* à l'échelle du sud-ouest Pacifique. Bien que reflétant l'histoire tectonique des bassins (Kojima *et al.*, 2006; Plouviez *et al.*, 2019), les patrons phylogéographiques décrits variaient fortement entre les différents taxons de gastéropodes étudiés (Chapitre 1), suggérant que les espèces ont pu évoluer en sélectionnant des stratégies de dispersion contrastées, voire opposées. Dans un second temps, l'étude de la structure des populations et la biologie de la reproduction de deux espèces de gastéropodes emblématiques de la zone d'étude (i.e. *Lepetodrilus schrolli* et *Shinkailepas tollmanni*) a montré

que ces espèces avaient une gamétogénèse et un recrutement continu, traits communs à de nombreuses espèces hydrothermales (Chapitre 2) (Lutz *et al.*, 1986; Eckelbarger et Watling, 1995), mais présentaient pourtant des patrons phylogéographiques contrastés, suggérant des potentiels de dispersion distincts. Aucune influence des conditions environnementales sur le recrutement ou la gamétogénèse n'a pu être démontrée, suggérant que l'hétérogénéité des habitats n'impacte pas ces deux caractéristiques démographiques dans la gamme de variation échantillonnée. Enfin, l'analyse des assemblages faunistiques associées aux trois habitats a révélé une structuration à différentes échelles spatiales : entre les habitats le long du gradient de dilution du fluide hydrothermal, entre les champs d'un même bassin et entre les différents bassins (Chapitre 3). Une partition de la diversité  $\beta$  montre que le principal mécanisme responsable de ces changements est un remplacement des espèces le long de ces différents gradients.

De manière générale, les conditions environnementales expliquent peu la variabilité observée, que ce soit celle constatée à l'échelle des assemblages faunistiques ou celle des caractéristiques biologiques des populations de *L. schrolli* et *S. tollmanni*. Différentes hypothèses peuvent être proposées pour expliquer ce rôle mineur de l'environnement physico-chimique régulièrement mis en avant pour expliquer la distribution des espèces de la mégafaune (Luther *et al.*, 2001; Podowski *et al.*, 2010). D'abord, ce constat peut être la conséquence de notre capacité limitée à mesurer correctement les conditions environnementales à l'échelle des organismes. En effet, les outils de mesures utilisés ne permettent pas de caractériser les conditions environnementales au contact direct des organismes. Bien que cela soit possible pour la sonde de température, le risque de boucher la canule de prélèvement d'eau ne le permet pas pour la caractérisation de la chimie du fluide. Il est donc nécessaire de relever la sonde d'environ 1 cm. L'environnement très variable à l'échelle du cm dans les communautés hydrothermales se traduit pas une zonation de la macrofaune très différente à quelques centimètres d'écart que nous ne sommes pas en mesure d'appréhender correctement (Le Bris *et al.*, 2005; Lee *et al.*, 2019; Van Audenhaege *et al.*, 2022). Les conditions environnementales sont

certainement contrastées entre (1) les zones occupées par les individus situés sur le substrat, directement en contact avec le fluide hydrothermal, (2) les surfaces des coquilles d'*Ifremeria* ou des moules sous l'influence du fluide colonisées par différents espèces de gastéropodes (e.g. les patelles *Shinkailepas tollmanni*, *Lepetodrilus schrolli*, le complexe d'espèces cryptiques *Symmetromphalus hageni* ou encore les *Peltospiridae* n. spp. et *Bathyacmaea becki*), (3) l'ombilic ou l'ouverture péristomiale des deux grands Provannidae *Ifremeria* ou *Alviniconcha* où sont présentes certaines polychètes (e.g. *Amphisamytha* spp.), (4) le milieu des agrégations des gastéropodes ou des moulières, dans les byssus, ou (5) l'intérieur des coquilles (e.g. *Branchipolynoe*, polynoidae commensal des moules). Il y a donc un mélange d'espèces qui ont des préférences et tolérances physico-chimiques différentes et qui colonisent des microhabitats pouvant être présents dans les différents habitats définis par la mégafaune (Mills *et al.*, 2007; Matabos *et al.*, 2008a). De plus, les conditions sont très variables dans l'espace pour une même communauté le long du gradient de mélange (de l'ordre de la dizaine de centimètres au mètre; Podowski *et al.*, 2009). Les différents points de mesures de température et de sulfure total réalisés dans les différents habitats échantillonnés témoignent bien de cette variabilité. Cette multitude de microhabitats dans les structures tridimensionnelles formées par les espèces ingénieuses est donc mal représenté dans nos analyses.

Par ailleurs, les conditions environnementales sont très variables dans le temps, de l'échelle de la seconde (i.e. en lien avec la turbulence) jusqu'à plusieurs années (i.e. en lien avec les modifications du flux). Les mesures ponctuelles réalisées ne sont donc pas forcément représentatives des conditions environnementales dominantes qui définissent la niche écologique des différentes espèces. Lors de la mission Chubacarc des boutons connectés ont été déployés au niveau d'une moulière et dans un agrégat d'*Ifremeria* dans le champ de Tow Cam (bassin de Lau) et dans un agrégat d'*Alviniconcha* dans le champ de Fatu Kapa (arc volcanique de Futuna). Ces boutons ont mesuré la température toutes les minutes pendant plusieurs heures ou même plusieurs jours à différents endroits en surface de l'habitat. Ces données ont montré le rôle prépondérant de la marée dans la variabilité temporelle de la



température à l'échelle de l'habitat, ainsi qu'une forte variabilité spatiale au sein même de celui-ci (Matabos M., comm. pers.). Le développement de ce type de capteurs automatisés pour mesurer des paramètres chimiques clés seraient utiles. Toutefois de tels systèmes de boutons connectés ne font des mesures qu'au niveau de la surface des coquilles au contact direct du fluide, et il serait intéressant de mettre en place ce genre de système au sein même de l'habitat formé par les espèces ingénieuses, afin d'avoir une meilleure représentation des conditions environnementales sur la verticale et donc mieux représenter la diversité des micro-habitats et leur caractéristiques physico-chimiques. La faible proportion de variabilité expliquée par l'environnement peut également résulter d'une caractérisation insuffisante de l'environnement chimique en termes d'éléments mesurés ou en termes de formes chimiques des divers éléments, notamment du sulfure. Ainsi, le sulfure sera très toxique pour les invertébrés s'il se trouve majoritairement sous forme  $H_2S$  alors qu'il sera biodisponible pour les organismes chimiosynthétique sous forme  $HS^-$ . La forme dominante des sulfures et donc le degré de toxicité va dépendre de la valeur du pH et de la concentration en fer qui va favoriser la formation de sulfure de fer qui précipite, réduisant ainsi la proportion de sulfures sous forme toxique (Luther *et al.*, 2001; Le Bris *et al.*, 2003; Matabos *et al.*, 2008a). La concentration en  $H_2S$  sera plus élevée lorsque les valeurs de pH et les concentrations en fer sont faibles, rendant le fluide plus toxique. De ce fait, prendre en considération la concentration en fer permettrait une meilleure appréhension de la composition exacte du fluide. Une collaboration avec les géochimistes du projet CERBERUS permettra d'approfondir la caractérisation de l'environnement pour de futures analyses. Il pourrait également être pertinent de prendre en considération la nature des environnements géologiques (basalte vs. andésite) qui influence la distribution des communautés dans le bassin de Lau (Podowski *et al.*, 2010).

Enfin, l'échelle à laquelle nous faisons les analyses ainsi que l'utilisation de données de type présence-absence pour l'étude de la structure des communautés limitent la quantité d'informations disponibles quant au rôle des conditions environnementales. Travailler à une échelle plus petite, à l'échelle des bassins est (i.e. Lau, Nord Fidji et Futuna), ouest

(i.e. Manus et Woodlark) ou même d'un seul bassin, permettrait d'avoir une meilleure appréhension du rôle de l'environnement sur les assemblages faunistiques, qui à grande échelle spatiale vont davantage être structuré par les processus historiques. D'autre part, prendre en compte les données d'abondances à ces échelles permettrait de mieux appréhender le rôle de l'environnement sur la composition des communautés. En effet, si les conditions environnementales extrêmes peuvent exclure certaines espèces d'un habitat, ces conditions combinées aux interactions biotiques comme la facilitation, la prédation ou la compétition pour l'espace et/ou les ressources sont également susceptibles de moduler la présence/absence ou les densités relatives des différentes espèces (Micheli *et al.*, 2002; Mullineaux *et al.*, 2003; Sancho *et al.*, 2005).

Une séparation des bassins est et ouest a été mise en évidence à différents niveaux d'organisation de la biodiversité, de la diversité génétique (Chapitre 1) à la diversité des communautés (Chapitre 3). Si cette scission entre l'est et l'ouest avait déjà été observée pour la diversité génétique de plusieurs taxons (e.g. le gastéropode *Ifremeria nautilei*, la crevette *Rimicaris variabilis* ou le crabe *Austinograea alayseae*; Thaler *et al.*, 2011, 2014; Lee *et al.*, 2019; Tran Lu Y *et al.*, 2022), elle n'avait pas encore été montrée à l'échelle des communautés. Plusieurs hypothèses peuvent être avancées pour expliquer cette rupture dans la biodiversité à l'échelle de la région sud-ouest Pacifique. Tout d'abord, l'histoire géologique et les barrières hydrographiques entre les bassins du sud-ouest Pacifique peuvent jouer un rôle important. L'ouverture des différents bassins initiée il y a environ 10 Ma pourrait avoir conduit à une colonisation progressive des différentes dorsales et à un isolement des espèces par vicariance entre l'est et l'ouest, notamment au moment de l'ouverture du bassin nord fidjien qui a débuté il y a 10-12 Ma et s'est déroulée en plusieurs étapes (Ruellan et Lagabriele, 2005) créant davantage de distance avec le bassin de Woodlark. D'autre part, la faune observée aujourd'hui est le reflet d'évènements passés. La distribution actuelle des sites n'est pas forcément celle d'il y a quelques dizaines, centaines ou milliers d'années. On peut imaginer que certains sites se sont éteints, limitant la dispersion des espèces créant ainsi de la structure génétique à l'échelle de la région,

ou si ces sites sont sur sénescence cela pourrait impacter la structure des communautés. En effet, certains champs, comme Kilo Moana (i.e. dans le bassin de Lau) ou White Lady (i.e. dans le bassin Nord-Fidjien), encore très actifs il y a une quinzaine d'années (Breusing *et al.*, 2020) étaient sur le déclin voire même inactifs en 2019 lors de la mission CHUBACARC (S. Hourdez, comm. pers.). D'autre part, la structure de la biodiversité va également dépendre des traits d'histoire de vie des espèces telles que la reproduction et la biologie larvaire, qui affectent la dispersion des larves. La capacité de dispersion des espèces avec les courants va dépendre de la fécondité (i.e. nombre de larves), de la durée de vie larvaire planctonique, du comportement des larves et de la profondeur à laquelle elles se dispersent (Hilário *et al.*, 2015). La connectivité entre les bassins est et ouest étant limitée pour les espèces présentant des durées larvaires planctoniques courtes (Mitarai *et al.*, 2016), la petite faune associée aux différents habitats pourrait inclure de nombreuses espèces n'ayant pas des capacités dispersives suffisantes pour passer cette barrière potentielle entre les bassins nord fidjien et Woodlark, structurant ainsi la biodiversité dans la région. Enfin, cette rupture observée dans la biodiversité peut également refléter un manque de données entre les bassins de Woodlark et Nord-Fidji. Par exemple, l'échantillonnage à Woodlark a permis d'apporter des informations essentielles pour caractériser la biodiversité dans la région. Ce bassin pourrait ainsi constituer un centre de dispersion à l'origine de la biodiversité hydrothermale actuelle et une zone de connections pour la dispersion de la faune dans la région (Boulart *et al.*, 2022; Poitrimol *et al.*, 2022). Toutefois, il manque encore des informations dans d'autres zones clés. En effet, environ 2 000 km séparent les champs de La Scala à Woodlark et Phoenix dans le bassin nord Fidjien. Il n'existe aujourd'hui aucune information sur de potentiels sites actifs, et donc la faune associée, dans les zones du Vanuatu (ou Nouvelle-Hébrides) et des îles Salomon, alors que ceux-ci pourraient pourtant jouer un rôle important dans la connectivité des bassins est et ouest (Mitarai *et al.*, 2016). Ce sont donc des secteurs qu'il faudrait cibler lors de futures campagnes océanographiques pour mieux caractériser la biodiversité dans la région.

Comprendre la connectivité au sein et entre les bassins est essentielle dans cette

région ciblée pour l'exploitation de ses ressources minérales (Boschen *et al.*, 2013). En effet, la résilience des communautés à une perturbation dépend fortement, entre autres, de la capacité des espèces à recoloniser des sites et donc de la distance entre sites, de la disponibilité de l'habitat et de la dispersion larvaire. La connectivité entre les différents bassins est fortement variable selon les espèces (Chapitre 1). Celles-ci semblent avoir des potentiels de dispersion très variables et ce même entre espèces phylogénétiquement proches. Alors que certaines vont être capables de se disperser sur de longues distances (e.g. *Shinkailepas tollmanni*) et donc potentiellement recoloniser facilement des sites après une perturbation, d'origine naturelle ou anthropiques, d'autres (e.g. les complexes d'espèces *Shinkailepas tufari* ou *Symmetromphalus hageni*) vont avoir plus de difficultés à maintenir leurs populations. Une telle divergence dans les patrons de connectivité des espèces hydrothermales, même au sein d'un même genre, a déjà été observée le long des dorsales médio-océaniques telles que la dorsale Est Pacifique (Plouviez *et al.*, 2009; Matabos *et al.*, 2011) ou médio-Atlantique (Faure *et al.*, 2007; Teixeira *et al.*, 2011). Ceci peut s'expliquer par des différences de traits d'histoire de vie des espèces, notamment en termes de reproduction et de biologie larvaire. Dans cette étude, il semble y avoir un nombre important de petites espèces de la faune benthique avec des capacités de dispersion insuffisantes pour coloniser l'ensemble des bassins de la région. Plusieurs espèces n'ont été trouvées que dans les bassins de l'est, d'autres exclusivement à Manus et/ou Woodlark. Cependant l'étude la reproduction et de la structure démographique de deux espèces présentant des patrons phylogéographiques contrastés (i.e. *Shinkailepas tollmanni* et *Lepetodrilus schrolli*) a montré une gamétogénèse et un recrutement continus, caractéristiques communes aux deux espèces. Un point clef ne serait donc pas les patrons de reproduction et de recrutement mais la seule biologie larvaire non appréhendée dans notre étude. Une autre hypothèse, liée à la fragmentation et l'instabilité de l'habitat hydrothermal, peut-être la disponibilité en habitat, également importante pour la résilience des communautés puisqu'elle influence le succès de recrutement et le taux de survie des populations locale à l'échelle des métapopulations (Mullineaux *et al.*, 2018). En effet, la disponibilité des larves dépend du taux

d'occupation d'une espèce. Celui-ci résulte de leur succès de colonisation mais aussi de la disponibilité et de la fréquence d'occupation des habitats. Ainsi une espèce à forte occupation et avec une forte fécondité produira plus de larves dans le temps et dans l'espace, augmentant ses chances de dispersion (Vrijenhoek, 2010). Les moulières étant absentes de Woodlark et peu nombreuses au nord Fidji et à Futuna, où seulement quelques individus isolés ont été observés contrairement aux grandes moulières qui se développent dans les bassins de Lau et Manus, les espèces associées à cet habitat auront donc plus de mal à maintenir leur population à large échelle et seront donc potentiellement moins résilientes face aux perturbations. Les habitats à *Bathymodiolus* soutiennent une part importante de la diversité spécifique de la région, et une perte importante de ces habitats, dans des zones telles que Manus et Lau, pourrait fortement impacter la biodiversité régionale. Enfin, le taux d'endémisme est important dans le bassin de Manus (Chapitre 1, Chapitre 2, Chabert, 2021), dont les communautés semblent fortement dépendre des apports larvaires provenant du bassin de Woodlark. Ce bassin étant considéré comme un système stable de dorsale (Boulart *et al.*, 2022), les espèces pourraient être moins résilientes dans cette zone car potentiellement moins sujettes aux perturbations naturelles (e.g. séismes, éruptions volcaniques). Une perte importante d'habitats dans cette zone pourrait fortement impacter la connectivité entre Manus et les autres bassins de l'est. Ainsi les bassins de Manus et Woodlark apparaissent comme des zones particulièrement vulnérables à l'exploitation minière, avec une perte potentielle importante de biodiversité associée.

Enfin, le bassin de Manus partage des espèces échantillonnées dans les bassins arrière-arc du nord-ouest Pacifique bien que ces bassins appartiennent à une province biogéographique distincte (Chapitre 1). Préciser la connectivité entre les bassins sud-ouest et le nord-ouest restent à éclaircir pour pouvoir véritablement évaluer l'impact que pourrait avoir l'exploitation minière sur la biodiversité à l'échelle du Pacifique Ouest.

La biodiversité hydrothermale des bassins arrière-arc du sud-ouest Pacifique est complexe, et nous n'avons traité qu'une partie de celle-ci dans le cadre de cette thèse. Le couplage de deux méthodes d'identification taxonomique, sur la base des descriptions

morphologiques des espèces (i.e. morpho-espèces) et par barcode moléculaire, a permis d'obtenir une meilleure estimation de la diversité spécifique. Néanmoins, nous savons que celle-ci demeure sous-estimée. Afin de ne pas créer artificiellement de patrons de distribution biaisés de la diversité, nous avons choisi d'adopter un comportement conservateur pour certains taxons pour lesquels nous savions que plusieurs espèces étaient présentes mais pour lesquelles nous n'avions pas d'information suffisante à l'échelle de la région pour proprement décrire leur distribution. Même si la résolution taxonomique que nous avons utilisée reste perfectible, surtout pour certains taxons très abondants, nous avons des raisons de penser qu'une meilleure résolution taxonomique pour ces groupes ne changerait pas fondamentalement les patrons que nous avons observés. À titre d'exemple, pour les copépodes non identifiés à l'espèce dans notre étude, Diaz-Recio Lorenzo *et al.* (2021) ont montré que leur richesse spécifique était plus importante dans l'habitat à *Bathymodiolus* que dans celui à *Alviniconcha*, conformément à ce que nous avons décrit. À l'inverse, travailler au niveau du genre ou de la famille a vraisemblablement limité notre capacité à démontrer les différences entre les bassins est et ouest, et sans doute même entre les bassins de Manus et de Woodlark, d'autant plus que l'effort d'échantillonnage pour ce bassin est faible. Il reste un travail de zoologie important à réaliser dans le sud-ouest Pacifique dans la mesure où beaucoup d'espèces ne sont pas encore décrites. Sans compter le nombre potentiellement important d'espèces cryptiques (Chapitre 1), certaines familles ne possèdent encore aucune espèce décrite. Cet effort est essentiel pour bien décrire la biodiversité à l'échelle de la région et être en mesure de mieux comprendre les processus évolutifs et écologiques à l'origine de sa distribution, ou sa sensibilité face aux futures pressions anthropiques.



---

## Bibliographie

---

- ALFARO-LUCAS, J. M., PRADILLON, F., ZEPELLI, D., MICHEL, L. N., MARTINEZ-ARBIZU, P., TANAKA, H., FOVIAUX, M. et SARRAZIN, J. (2020). High environmental stress and productivity increase functional diversity along a deep-sea hydrothermal vent gradient. *Ecology*, 101(11):e03144.
- ANDERSON, M., CRIST, T., CHASE, J., VELLEND, M., INOUE, B., FREESTONE, A., SANDERS, N., CORNELL, H., COMITA, L., DAVIES, K., HARRISON, S., KRAFT, N., STEGEN, J. et SWENSON, N. (2011). Navigating the multiple meanings of  $\beta$  diversity : a roadmap for the practicing ecologist. *Ecology Letters*, 14(1):19–28.
- BACHRATY, C., LEGENDRE, P. et DESBRUYÈRES, D. (2009). Biogeographic relationships among deep-sea hydrothermal vent faunas at global scale. *Deep Sea Research Part I: Oceanographic Research Papers*, 56(8):1371–1378.
- BANDELT, H., FORSTER, P. et RÖHL, A. (1999). Median-joining networks for inferring intraspecific phylogenies. *Molecular Biology and Evolution*, 16(1):37–48.
- BASELGA, A. (2010). Partitioning the turnover and nestedness components of beta diversity. *Global Ecology and Biogeography*, 19(1):134–143.
- BASELGA, A. (2012). The relationship between species replacement, dissimilarity derived from nestedness, and nestedness. *Global Ecology and Biogeography*, 21(12):1223–1232.
- BATES, A. (2008). Size- and sex-based habitat partitioning by *Lepetodrilus fucensis* near hydrothermal vents on the Juan de Fuca Ridge, Northeast Pacific. *Canadian Journal of Fisheries and Aquatic Sciences*, 65(11):2332–2341.



- BATES, A., TUNNICLIFFE, V. et LEE, R. (2005). Role of thermal conditions in habitat selection by hydrothermal vent gastropods. *Marine Ecology Progress Series*, 305:1–15.
- BAYER, S., MULLINEAUX, L., WALLER, R. et SOLOW, A. (2011). Reproductive traits of pioneer gastropod species colonizing deep-sea hydrothermal vents after an eruption. *Marine Biology*, 158(1):181–192.
- BEAULIEU, S., BAKER, E. et GERMAN, C. (2015). Where are the undiscovered hydrothermal vents on oceanic spreading ridges? *Deep Sea Research Part II : Topical Studies in Oceanography*, 121:202–212.
- BEAULIEU, S., BAKER, E., GERMAN, C. et MAFFEI, A. (2013). An authoritative global database for active submarine hydrothermal vent fields. *Geochemistry, Geophysics, Geosystems*, 14(11): 4892–4905.
- BEAULIEU, S. et SZAFRAŃSKI, K. (2020). InterRidge global database of active submarine hydrothermal vent fields version 3.4.
- BECK, L. (1992a). *Symmetromphalus hageni* sp. n., a new neomphalid gastropod (Prosobranchia : Neomphalidae) from hydrothermal vents at the Manus Back-Arc Basin (Bismarck Sea, Papua New Guinea). *Annalen des Naturhistorischen Museums in Wien. Serie B für Botanik und Zoologie*, 93(B):243–257.
- BECK, L. (1992b). Two new neritacean limpets (Gastropoda : Prosobranchia : Neritacea : Phenacolepadidae) from active hydrothermal vents at Hydrothermal Field 1 "Wienerwald" in the Manus Back-Arc Basin (Bismarck Sea, Papua-New Guinea). *Annalen des Naturhistorischen Museums in Wien. Serie B für Botanik und Zoologie*, 93(B):259–275.
- BECK, L. (1993). Morphological and anatomical studies on a new lepetodrilacean limpet (Gastropoda, Prosobranchia) from hydrothermal vents at the Manus Back-Arc Basin (Bismarck Sea, Papua New Guinea). *Annalen des Naturhistorischen Museums in Wien. Serie B für Botanik und Zoologie*, 94/95(B):167–179.
- BEINART, R., SANDERS, J., FAURE, B., SYLVA, S., LEE, R., BECKER, E., GARTMAN, A., LUTHER, G., SEEWALD, J., FISHER, C. et GIRGUIS, P. (2012). Evidence for the role of endosymbionts in regional-scale habitat partitioning by hydrothermal vent symbioses. *Proceedings of the National Academy of Sciences*, 109(47):E3241–E3250.
- BERG, C. (1985). Reproductive strategies of mollusks from abyssal hydrothermal vent communities. *Bulletin of the Biological Society of Washington*, 6:185–197.

## BIBLIOGRAPHIE

- BEVIS, M., TAYLOR, F., SCHUTZ, B., RECY, J., ISACKS, B. L., HELU, S., SINGH, R., KENDRICK, E., STOWELL, J., TAYLOR, B. et CALMANTLI, S. (1995). Geodetic observations of very rapid convergence and back-arc extension at the Tonga arc. *Nature*, 374(6519):249–251.
- BHATTACHARYA, C. (1967). A simple method of resolution of a distribution into gaussian components. *Biometrics*, 23(1):115–135.
- BOSCHEN, R., ROWDEN, A., CLARK, M. et GARDNER, J. (2013). Mining of deep-sea seafloor massive sulfides : A review of the deposits, their benthic communities, impacts from mining, regulatory frameworks and management strategies. *Ocean & Coastal Management*, 84:54–67.
- BOSCHEN-ROSE, R., CLARK, M., ROWDEN, A. et GARDNER, J. (2021). Assessing the ecological risk to deep-sea megafaunal assemblages from seafloor massive sulfide mining using a functional traits sensitivity approach. *Ocean & Coastal Management*, 210:105656.
- BOTH, R., CROOK, K., TAYLOR, B., BROGAN, S., CHAPPELL, B., FRANKEL, E., LIU, L., SINTON, J. et TIFFIN, D. (1986). Hydrothermal chimneys and associated fauna in the Manus Back-Arc Basin, Papua New Guinea. *Eos, Transactions American Geophysical Union*, 67(21):489–490.
- BOULART, C., ROUXEL, O., SCALABRIN, C., LE MEUR, P., PELLETER, E., POITRIMOL, C., THIÉBAUT, E., MATABOS, M., CASTEL, J., TRAN LU Y, A., MICHEL, L., CATHALOT, C., CHÉRON, S., BOISSIER, A., GERMAIN, Y., GUYADER, V., ARNAUD-HAOND, S., BONHOMME, F., BROQUET, T., CUEFF-GAUCHARD, V., LE LAYEC, V., L'HARIDON, S., MARY, J., LE PORT, A.-S., TASIEMSKI, A., KUAMA, D., HOURDEZ, S. et JOLLIVET, D. (2022). Active hydrothermal vents in the Woodlark Basin may act as dispersing centres for hydrothermal fauna. *Communications Earth & Environment*, 3(1):1–16.
- BREUSING, C., BIASTOCH, A., DREWS, A., METAXAS, A., JOLLIVET, D., VRIJENHOEK, R., BAYER, T., MELZNER, F., SAYAVEDRA, L., PETERSEN, J., DUBILIER, N., SCHILHABEL, M., ROSENSTIEL, P. et REUSCH, T. (2016). Biophysical and population genetic models predict the presence of “Phantom” stepping stones connecting Mid-Atlantic Ridge vent ecosystems. *Current Biology*, 26(17):2257–2267.
- BREUSING, C., JOHNSON, S., MITARAI, S., BEINART, R. et TUNNICLIFFE, V. (2021). Differential patterns of connectivity in Western Pacific hydrothermal vent metapopulations : A comparison of biophysical and genetic models. *Evolutionary Applications*, 00:1–14.
- BREUSING, C., JOHNSON, S., TUNNICLIFFE, V., CLAGUE, D., VRIJENHOEK, R. et BEINART, R. (2020). Allopatric and sympatric drivers of speciation in *Alviniconcha* hydrothermal vent snails. *Molecular Biology and Evolution*, 37(12):3469–3484.

- BURGESS, S., NICKOLS, K., GRIESEMER, C., BARNETT, L., DEDRICK, A., SATTERTHWAITE, E., YAMANE, L., MORGAN, S., WHITE, J. et BOTSFORD, L. (2014). Beyond connectivity : how empirical methods can quantify population persistence to improve marine protected-area design. *Ecological Applications*, 24(2):257–270.
- BÉZOS, A., ESCRIG, S., LANGMUIR, C., MICHAEL, P. et ASIMOW, P. (2009). Origins of chemical diversity of back-arc basin basalts : A segment-scale study of the Eastern Lau Spreading Center. *Journal of Geophysical Research : Solid Earth*, 114(B6).
- CARDINALE, B., DUFFY, J., GONZALEZ, A., HOOPER, D., PERRINGS, C., VENAIL, P., NARWANI, A., MACE, G., TILMAN, D., WARDLE, D., KINZIG, A., DAILY, G., LOREAU, M., GRACE, J., LARIGAUDERIE, A., SRIVASTAVA, D. et NAEEM, S. (2012). Biodiversity loss and its impact on humanity. *Nature*, 486(7401):59–67.
- CARVALHO, J., CARDOSO, P. et GOMES, P. (2012). Determining the relative roles of species replacement and species richness differences in generating beta-diversity patterns. *Global Ecology and Biogeography*, 21(7):760–771.
- CASTEL, J., HOURDEZ, S., PRADILLON, F., DAGUIN-THIÉBAUT, C., BALLENGHIEN, M., RUAULT, S., CORRE, E., TRAN LU Y, A., MARY, J., GAGNAIRE, P.-A., BONHOMME, F., BREUSING, C., BROQUET, T. et JOLLIVET, D. (2022). Inter-specific genetic exchange despite strong divergence in deep-sea hydrothermal vent gastropods of the genus *Alviniconcha*. *Genes*, 13(6):985.
- CHABERT, A. (2021). Diversity of western pacific Back-arc Basins invertebrates reevaluated through a barcode approach - Results on decapods and polychaetes. *Dissertations, Theses and Masters Projects*.
- CHAN, B. et CHANG, Y.-W. (2018). A new deep-sea scalpelliform barnacle, *Vulcanolepas buckeridgei* sp. nov. (Eolepadidae : Neolepadinae) from hydrothermal vents in the Lau Basin. *Zootaxa*, 4407(1):117.
- CHAN, B., CHEN, H.-N., RODRIGUEZ MORENO, P. A. et CORBARI, L. (2016). Diversity and biogeography of the little known deep-sea barnacles of the genus *Waikalasma* Buckeridge, 1983 (Balanomorpha : Chionelasmatoidea) in the Southwest Pacific, with description of a new species. *Journal of Natural History*, 50(47-48):2961–2984.
- CHAN, B., JU, S.-J. et KIM, S.-J. (2019). A new species of hydrothermal vent stalked barnacle *Vulcanolepas* (Scalpelliforms : Eolepadidae) from the North Fiji Basin, Southwestern Pacific Ocean. *Zootaxa*, 4563(1):135–148.

## BIBLIOGRAPHIE

- CHASE, J. et MYERS, J. (2011). Disentangling the importance of ecological niches from stochastic processes across scales. *Philosophical Transactions of the Royal Society B : Biological Sciences*, 366(1576):2351–2363.
- CHEN, C., OGURA, T., HIRAYAMA, H., WATANABE, H., MIYAZAKI, J. et OKUTANI, T. (2016). First seep-dwelling *Desbruyeresia* (Gastropoda : Abyssochrysoidea) species discovered from a serpentinite-hosted seep in the Southeastern Mariana Forearc. *Molluscan Research*, 36(4): 277–284.
- CHEN, C., WATANABE, H., NAGAI, Y., TOYOFUKU, T., XU, T., SUN, J., QIU, J.-W. et SASAKI, T. (2019a). Complex factors shape phenotypic variation in deep-sea limpets. *Biology Letters*, 15(10):20190504.
- CHEN, C., WATANABE, H. et OHARA, Y. (2018). A very deep *Provanna* (Gastropoda : Abyssochrysoidea) discovered from the Shinkai Seep Field, Southern Mariana Forearc. *Journal of the Marine Biological Association of the United Kingdom*, 98(3):439–447.
- CHEN, C., WATANABE, H. et SASAKI, T. (2019b). Four new deep-sea provannid snails (Gastropoda : Abyssochrysoidea) discovered from hydrocarbon seep and hydrothermal vents in Japan. *Royal Society Open Science*, 6(7):190393.
- CHEVALDONNÉ, P., JOLLIVET, D., VANGRIESHEIM, A. et DESBRUYÈRES, D. (1997). Hydrothermal-vent alvinellid polychaete dispersal in the eastern Pacific. 1. Influence of vent site distribution, bottom currents, and biological patterns. *Limnology and Oceanography*, 42(1):67–80.
- CHILDRESS, J. J. et FISHER, C. R. (1992). The biology of hydrothermal vent animals : physiology, biochemistry, and autotrophic symbioses. [No source information available], pages 337–441.
- CHOW, V. (1987). Patterns of growth and energy allocation in northern California populations of *Littorina* (Gastropoda : Prosobranchia). *Journal of Experimental Marine Biology and Ecology*, 110(1):69–89.
- CLARK, M., ALTHAUS, F., SCHLACHER, T., WILLIAMS, A., BOWDEN, D. et ROWDEN, A. (2016). The impacts of deep-sea fisheries on benthic communities : a review. *ICES Journal of Marine Science*, 73(suppl\_1):i51–i69.
- CLARKE, K. R. et WARWICK, R. (2001). Change in marine communities. *An approach to statistical analysis and interpretation*, 2:1–68.
- COLLIN, R. (2004). Phylogenetic effects, the loss of complex characters, and the evolution of development in Calyptraeid gastropods. *Evolution*, 58(7):1488–1502.

- COLLINS, P., KENNEDY, R. et VAN DOVER, C. L. (2012). A biological survey method applied to seafloor massive sulphides (SMS) with contagiously distributed hydrothermal-vent fauna. *Marine Ecology Progress Series*, 452:89–107.
- COMTET, T. et DESBRUYÈRES, D. (1998). Population structure and recruitment in mytilid bivalves from the Lucky Strike and Menez Gwen hydrothermal vent fields (37°17'N and 37°50'N on the Mid-Atlantic Ridge). *Marine Ecology Progress Series*, 163:165–177.
- CONNELLY, D., COPLEY, J., MURTON, B. J., STANSFIELD, K., TYLER, P. A., GERMAN, C., VAN DOVER, C., AMON, D., FURLONG, M., GRINDLAY, N., HAYMAN, N., HÜHNERBACH, V., JUDGE, M., LE BAS, T., MCPHAIL, S., MEIER, A., NAKAMURA, K.-I., NYE, V., PEBODY, M., PEDERSEN, R., PLOUVIEZ, S., SANDS, C., SEARLE, R., STEVENSON, P., TAWS, S. et WILCOX, S. (2012). Hydrothermal vent fields and chemosynthetic biota on the world's deepest seafloor spreading centre. *Nature Communications*, 3(1):620.
- COPLEY, J. et YOUNG, C. (2006). Seasonality and zonation in the reproductive biology and population structure of the shrimp *Alvinocaris stactophila* (Caridea : Alvinocarididae) at a Louisiana Slope cold seep. *Marine Ecology Progress Series*, 315:199–209.
- COTTE, L., CHAVAGNAC, V., PELLETER, E., LAËS-HUON, A., CATHALOT, C., DULAQUAIS, G., RISO, R. D., SARRADIN, P.-M. et WAELES, M. (2020). Metal partitioning after in situ filtration at deep-sea vents of the Lucky Strike hydrothermal field (EMSO-Azores, Mid-Atlantic Ridge, 37°N). *Deep Sea Research Part I: Oceanographic Research Papers*, 157:103204.
- CRIST, T., VEECH, J., GERING, J. et SUMMERVILLE, K. (2003). Partitioning species diversity across landscapes and regions : a hierarchical analysis of  $\alpha$ ,  $\beta$ , and  $\gamma$  diversity. *The American Naturalist*, 162(6):734–743.
- CUVELIER, D., SARRADIN, P.-M., SARRAZIN, J., COLAÇO, A., COPLEY, J. T., DESBRUYÈRES, D., GLOVER, A. G., SANTOS, R. S. et TYLER, P. A. (2011). Hydrothermal faunal assemblages and habitat characterisation at the eiffel tower edifice (lucky strike, mid-atlantic ridge). *Marine Ecology*, 32(2):243–255.
- CUVELIER, D., SARRAZIN, J., COLAÇO, A., COPLEY, J., DESBRUYÈRES, D., GLOVER, A., TYLER, P. et SERRÃO SANTOS, R. (2009). Distribution and spatial variation of hydrothermal faunal assemblages at Lucky Strike (Mid-Atlantic Ridge) revealed by high-resolution video image analysis. *Deep Sea Research Part I: Oceanographic Research Papers*, 56(11):2026–2040.
- DE QUEIROZ, K. (2007). Species concepts and species delimitation. *Systematic Biology*, 56(6): 879–886.

## BIBLIOGRAPHIE

- DESBRUYÈRES, D., ALAYSE-DANET, A.-M., OHTA, S. et THE SCIENTIFIC PARTIES OF BIOLAU AND STARMER CRUISES (1994). Deep-sea hydrothermal communities in Southwestern Pacific back-arc basins (the North Fiji and Lau Basins) : Composition, microdistribution and food web. *Marine Geology*, 116(1):227–242.
- DESBRUYÈRES, D., ALMEIDA, A., BISCOITO, M., COMTET, T., KHRIPOUNOFF, A., LE BRIS, N., SARRADIN, P. M. et SEGONZAC, M. (2000). A review of the distribution of hydrothermal vent communities along the northern Mid-Atlantic Ridge : dispersal vs. environmental controls. *Island, Ocean and Deep-Sea Biology*, 152:201–216.
- DESBRUYÈRES, D., BISCOITO, M., CAPRAIS, J.-C., COLAÇO, A., COMTET, T., CRASSOUS, P., FOUQUET, Y., KHRIPOUNOFF, A., LE BRIS, N., OLU, K., RISO, R., SARRADIN, P.-M., SEGONZAC, M. et VANGRIESHEIM, A. (2001). Variations in deep-sea hydrothermal vent communities on the Mid-Atlantic Ridge near the Azores plateau. *Deep Sea Research Part I : Oceanographic Research Papers*, 48(5):1325–1346.
- DESBRUYÈRES, D., HASHIMOTO, J. et FABRI, M.-C. (2006a). Composition and biogeography of hydrothermal vent communities in Western Pacific Back-Arc Basins. In CHRISTIE, D., FISHER, C., LEE, S.-M. et GIVENS, S., éditeurs : *Geophysical Monograph Series*, volume 166, pages 215–234. American Geophysical Union, Washington D. C.
- DESBRUYÈRES, D., SEGONZAC, M. et BRIGHT, M. (2006b). *Handbook of deep-sea hydrothermal vent fauna*. Art & Publishing, Linz, second compl. rev. ed édition.
- DIAZ-RECIO LORENZO, C., ter BRUGGEN, D., LUTHER, G., GARTMAN, A. et GOLLNER, S. (2021). Copepod assemblages along a hydrothermal stress gradient at diffuse flow habitats within the ABE vent site (Eastern Lau Spreading Center, Southwest Pacific). *Deep Sea Research Part I : Oceanographic Research Papers*, 173:103532.
- DICK, G. (2019). The microbiomes of deep-sea hydrothermal vents : distributed globally, shaped locally. *Nature Reviews Microbiology*, 17(5):271–283.
- DONVAL, J.-P., CHARLOU, J.-L. et LUCAS, L. (2008). Analysis of light hydrocarbons in marine sediments by headspace technique : Optimization using design of experiments. *Chemometrics and Intelligent Laboratory Systems*, 94(2):89–94.
- DOYLE, J. et DOYLE, J. (1987). A rapid DNA isolation procedure for small quantities of fresh leaf tissue. *Phytochemical Bulletin*, 19:11–15.

- DRAY, S., BAUMAN, D., BLANCHET, G., BORCARD, D., CLAPPE, S., GUENARD, G., JOMBART, T., LAROCQUE, G., LEGENDRE, P., MADI, N. et WAGNER, H. H. (2021). *adespatial : Multivariate Multiscale Spatial Analysis*. R package version 0.3-14.
- DUBILIER, N., BERGIN, C. et LOTT, C. (2008). Symbiotic diversity in marine animals : the art of harnessing chemosynthesis. *Nature Reviews Microbiology*, 6(10):725–740.
- ECKELBARGER, K. et WATLING, L. (1995). Role of phylogenetic constraints in determining reproductive patterns in deep-Sea invertebrates. *Invertebrate Biology*, 114(3):256–269.
- FAURE, B., CHEVALDONNÉ, P., PRADILLON, F., THIÉBAUT, E. et JOLLIVET, D. (2007). Spatial and temporal dynamics of reproduction and settlement in the Pompeii worm *Alvinella pompejana* (Polychaeta : Alvinellidae). *Marine Ecology Progress Series*, 348:197–211.
- FOLMER, O., BLACK, M., HOEH, W., LUTZ, R. et VRIJENHOEK, R. (1994). DNA primers for amplification of mitochondrial cytochrome c oxidase subunit I from diverse metazoan invertebrates. *Molecular marine biology and biotechnology*, 3(5):294–299.
- FRETTER, V. (1988). New Archaeogastropod limpets from hydrothermal vents; superfamily Lepetodrilacea II. Anatomy. *Philosophical Transactions of the Royal Society of London. Series B, Biological Sciences*, 319(1192):33–82.
- FU, Y. et LI, W. (1993). Statistical tests of neutrality of mutations. *Genetics*, 133(3):693–709.
- FUKUMORI, H., YAHAGI, T., WARÉN, A. et KANO, Y. (2019). Amended generic classification of the marine gastropod family Phenacolepadidae : transitions from snails to limpets and shallow-water to deep-sea hydrothermal vents and cold seeps. *Zoological Journal of the Linnean Society*, 185(3):636–655.
- GABE, M. (1968). Techniques histologiques.
- GALKIN, S. (1997). Megafauna associated with hydrothermal vents in the Manus Back-Arc Basin (Bismarck Sea). *Marine Geology*, 142(1):197–206.
- GAMFELDT, L., LEFCHECK, J., BYRNES, J., CARDINALE, B., DUFFY, J. et GRIFFIN, J. (2015). Marine biodiversity and ecosystem functioning : what's known and what's next? *Oikos*, 124(3):252–265.
- GEBRUK, A., GALKIN, S., VERESHCHAKA, A., MOSKALEV, L. I. et SOUTHWARD, A. (1997). Ecology and biogeography of the hydrothermal vent fauna of the Mid-Atlantic Ridge. In BLAXTER, J., SOUTHWARD, A., GEBRUK, A., SOUTHWARD, E. et TYLER, P., éditeurs : *Advances in Marine Biology*, volume 32 de *The Biogeography of the Oceans*, pages 93–144. Academic Press.

## BIBLIOGRAPHIE

- GERMAN, C. et SEYFRIED, W. (2014). Hydrothermal Processes. *In Treatise on Geochemistry*, volume 8, pages 191–233. Elsevier, Oxford, second edition édition.
- GIGUÈRE, T. et TUNNICLIFFE, V. (2021). Beta diversity differs among hydrothermal vent systems : Implications for conservation. *PLoS ONE*, 16(8):e0256637.
- GIRARD, F., SARRAZIN, J., ARNAUBEC, A., CANNAT, M., SARRADIN, P.-M., WHEELER, B. et MATABOS, M. (2020). Currents and topography drive assemblage distribution on an active hydrothermal edifice. *Progress in Oceanography*, 187:102397.
- GOLLNER, S., KAISER, S., MENZEL, L., JONES, D. O. B., BROWN, A., MESTRE, N., VAN OEVELEN, D., MENOT, L., COLAÇO, A., CANALS, M., CUVELIER, D., DURDEN, J., GEBRUK, A., EGHO, G., HAECKEL, M., MARCON, Y., MEVENKAMP, L., MORATO, T., PHAM, C., PURSER, A., SANCHEZ-VIDAL, A., VANREUSEL, A., VINK, A. et MARTINEZ ARBIZU, P. (2017). Resilience of benthic deep-sea fauna to mining activities. *Marine Environmental Research*, 129:76–101.
- GOTELLI, N. et COLWELL, R. (2001). Quantifying biodiversity : procedures and pitfalls in the measurement and comparison of species richness. *Ecology Letters*, 4(4):379–391.
- GOVENAR, B., LE BRIS, N., GOLLNER, S., GLANVILLE, J., APERGHIS, A., HOURDEZ, S. et FISHER, C. (2005). Epifaunal community structure associated with *Riftia pachyptila* aggregations in chemically different hydrothermal vent habitats. *Marine Ecology Progress Series*, 305:67–77.
- GRAY, J. (2000). The measurement of marine species diversity, with an application to the benthic fauna of the Norwegian continental shelf. *Journal of Experimental Marine Biology and Ecology*, 250(1):23–49.
- GUINOT, D. et SEGONZAC, M. (2018). A review of the brachyuran deep-sea vent community of the western Pacific, with two new species of *Austinograea* Hessler & Martin, 1989 (Crustacea, Decapoda, Brachyura, Bythograeidae) from the Lau and North Fiji Back-Arc Basins. *Zoosystema*, 40(1):1.
- GUSTAFSON, R. G. et LUTZ, R. A. (1994). *Molluscan life history traits at deep-sea hydrothermal vents and cold methane/sulfide seeps*. Columbia University Press New York.
- HALL, R. (2002). Cenozoic geological and plate tectonic evolution of SE Asia and the SW Pacific : computer-based reconstructions, model and animations. *Journal of Asian Earth Sciences*, 20(4):353–431.
- HALL, T. (1999). BioEdit : a user-friendly biological sequence alignment editor and analysis program for Windows 95/98/NT. *In Nucleic Acids Symp. Ser.*, volume 41, pages 95–98.



- HALPERN, B., FRAZIER, M., POTAPENKO, J., CASEY, K., KOENIG, K., LONGO, C., LOWNDES, J., ROCKWOOD, R., SELIG, E., SELKOE, K. et WALBRIDGE, S. (2015). Spatial and temporal changes in cumulative human impacts on the world's ocean. *Nature Communications*, 6:7615.
- HALPERN, B., WALBRIDGE, S., SELKOE, K., KAPPEL, C., MICHELI, F., D'AGROSA, C., BRUNO, J., CASEY, K., EBERT, C., FOX, H., FUJITA, R., HEINEMANN, D., LENIHAN, H., MADIN, E., PERRY, M., SELIG, E., SPALDING, M., STENECK, R. et WATSON, R. (2008). A global map of human impact on marine ecosystems. *Science*, 319(5865):948–952.
- HANNINGTON, M., JONASSON, I., HERZIG, P. et PETERSEN, S. (1995). Physical and chemical processes of seafloor mineralization at Mid-Ocean Ridges. *In Seafloor Hydrothermal Systems : Physical, Chemical, Biological, and Geological Interactions*, pages 115–157. American Geophysical Union (AGU).
- HARPENDING, H. (1994). Signature of ancient population growth in a low-resolution mitochondrial DNA mismatch distribution. *Human Biology*, 66(4):591–600.
- HASZPRUNAR, G. (1989). New slit-limpets (Scissurellacea and Fissurellacea) from hydrothermal vents. Part 2. Anatomy and relationships. *Contributions in science*, 408:1–17.
- HESS, M., BECK, F., GENSLER, H., KANO, Y., KIEL, S. et HASZPRUNAR, G. (2008). Microanatomy, shell structure and molecular phylogeny of *Leptogyra*, *Xyleptogyra* and *Leptogyropsis* (Gastropoda : Neomphalida : Melanodrymiidae) from sunken wood. *Journal of Molluscan Studies*, 74(4):383–401.
- HENRY, M., CHILDRESS, J. et FIGUEROA, D. (2008). Metabolic rates and thermal tolerances of chemoautotrophic symbioses from Lau Basin hydrothermal vents and their implications for species distributions. *Deep Sea Research Part I : Oceanographic Research Papers*, 55(5):679–695.
- HESSLER, R., SMITHEY, W., BOUDRIAS, M., KELLER, C., LUTZ, R. et CHILDRESS, J. (1988). Temporal change in megafauna at the Rose Garden hydrothermal vent (Galapagos Rift; eastern tropical Pacific). *Deep Sea Research Part A. Oceanographic Research Papers*, 35(10):1681–1709.
- HILL, M. (1973). Diversity and evenness : a unifying notation and its consequences. *Ecology*, 54(2):427–432.
- HILÁRIO, A., METAXAS, A., GAUDRON, S., HOWELL, K. L., MERCIER, A., MESTRE, N., ROSS, R., THURNHERR, A. et YOUNG, C. (2015). Estimating dispersal distance in the deep sea : challenges and applications to marine reserves. *Frontiers in Marine Science*, 2.

## BIBLIOGRAPHIE

- HOAGLAND, P., BEAULIEU, S., TIVEY, M., EGGERT, R., GERMAN, C., GLOWKA, L. et LIN, J. (2010). Deep-sea mining of seafloor massive sulfides. *Marine Policy*, 34(3):728–732.
- HOURDEZ, S. et JOLLIVET, D. (2019). CHUBACARC cruise, L'Atalante R/V.
- IPBES (2019). Global assessment report on biodiversity and ecosystem services of the Intergovernmental Science-Policy Platform on Biodiversity and Ecosystem Services.
- IVES, A. et CARPENTER, S. (2007). Stability and diversity of ecosystems. *Science*, 317(5834):58–62.
- JANNASCH, H. et MOTTL, M. (1985). Geomicrobiology of deep-sea hydrothermal vents. *Science*, 229(4715):717–725.
- JOHNSON, K., CHILDRESS, J. et BEEHLER, C. (1988). Short-term temperature variability in the Rose Garden hydrothermal vent field : an unstable deep-sea environment. *Deep Sea Research Part A. Oceanographic Research Papers*, 35(10):1711–1721.
- JOHNSON, S., WARÉN, A., LEE, R., KANO, Y., KAIM, A., DAVIS, A., STRONG, E. et VRIJENHOEK, R. (2010). *Rubyspira*, new genus and two new species of bone-eating deep-sea snails with ancient habits. *The Biological Bulletin*, 219(2):166–177.
- JOHNSON, S., WARÉN, A., TUNNICLIFFE, V., VAN DOVER, C., WHEAT, C., SCHULTZ, T. et VRIJENHOEK, R. (2015). Molecular taxonomy and naming of five cryptic species of *Alviniconcha* snails (Gastropoda : Abysochrysoidea) from hydrothermal vents. *Systematics and Biodiversity*, 13(3):278–295.
- JOHNSON, S., WARÉN, A. et VRIJENHOEK, R. (2008). DNA barcoding of *Lepetodrilus* limpets reveals cryptic species. *Journal of Shellfish Research*, 27(1):43–51.
- JOHNSON, S., YOUNG, C., JONES, W., WARÉN, A. et VRIJENHOEK, R. (2006). Migration, isolation, and speciation of hydrothermal vent limpets (Gastropoda; Lepetodrilidae) across the blanco transform fault. *The Biological Bulletin*, 210(2):140–157.
- JOLLIVET, D., EMPIS, A., BAKER, M., HOURDEZ, S., COMTET, T., JOUIN-TOULMOND, C., DESBRUYÈRES, D. et TYLER, P. (2000). Reproductive biology, sexual dimorphism, and population structure of the deep sea hydrothermal vent scale-worm, *Branchipolynoe seepensis* (Polychaeta : Polynoidae). *Journal of the Marine Biological Association of the United Kingdom*, 80(1):55–68.
- JOLLIVET, D., LALLIER, F., BARNAY, A., BIENVENU, N., BONNIVARD, E., BRIAND, P., CAMBON-BONAVITA, M., COMTET, T., COSSON, R. et DAGUIN, C. (2004). The BIOSPEEDO cruise : a

- new survey of hydrothermal vents along the South East Pacific Rise from 7° 24' S to 21° 33' S. *InterRidge News*, 13:20–26.
- JOLLY, M., VIARD, E., WEINMAYR, G., GENTIL, F., THIÉBAUT, E. et JOLLIVET, D. (2003). Does the genetic structure of *Pectinaria koreni* (Polychaeta : Pectinariidae) conform to a source–sink metapopulation model at the scale of the Baie de Seine? *Helgoland Marine Research*, 56(4): 238–246.
- JOSEFSON, A. (2009). Additive partitioning of estuarine benthic macroinvertebrate diversity across multiple spatial scales. *Marine Ecology Progress Series*, 396:283–292.
- JUNIPER, S. et TUNNICLIFFE, V. (1997). Crustal accretion and the hot vent ecosystem. *Philosophical Transactions of the Royal Society of London. Series A : Mathematical, Physical and Engineering Sciences*, 355(1723):459–474.
- KAKEE, T. (2020). Deep-sea mining legislation in Pacific Island countries : From the perspective of public participation in approval procedures. *Marine Policy*, page 103881.
- KASSAMBARA, A. et MUNDT, F. (2020). *factoextra : Extract and Visualize the Results of Multivariate Data Analyses*. R package version 1.0.7.
- KELLEY, D., BAROSS, J. et DELANEY, J. (2002). Volcanoes, fluids, and life at Mid-Ocean Ridge spreading centers. *Annual Review of Earth and Planetary Sciences*, 30(1):385–491.
- KELLY, N. et METAXAS, A. (2007). Influence of habitat on the reproductive biology of the deep-sea hydrothermal vent limpet *Lepetodrilus fucensis* (Vetigastropoda : Mollusca) from the Northeast Pacific. *Marine Biology*, 151(2):649–662.
- KELLY, N. et METAXAS, A. (2008). Population structure of two deep-sea hydrothermal vent gastropods from the Juan de Fuca Ridge, NE Pacific. *Marine Biology*, 153(3):457–471.
- KIM, S. et HAMMERSTROM, K. (2012). Hydrothermal vent community zonation along environmental gradients at the Lau back-arc spreading center. *Deep Sea Research Part I : Oceanographic Research Papers*, 62:10–19.
- KNOWLTON, N. (1993). Sibling Species in the sea. *Annual Review of Ecology and Systematics*, 24:189–216.
- KOJIMA, S. et WATANABE, H. (2015). Vent fauna in the Mariana Trough. In ISHIBASHI, J.-I., OKINO, K. et SUNAMURA, M., éditeurs : *Subseafloor Biosphere Linked to Hydrothermal Systems : TAIGA Concept*, pages 313–323. Springer Japan, Tokyo.

## BIBLIOGRAPHIE

- KOJIMA, S., WATANABE, H., TSUCHIDA, S., FUJIKURA, K., ROWDEN, A., TAKAI, K. et MIURA, T. (2006). Phylogenetic relationships of a tube worm (*Lamellibrachia juni*) from three hydrothermal vent fields in the South Pacific. *Journal of the Marine Biological Association of the United Kingdom*, 86(6):1357–1361.
- KONN, C., DONVAL, J. P., GUYADER, V., ROUSSEL, E., FOURRÉ, E., JEAN-BAPTISTE, P., PELLETER, E., CHARLOU, J. L. et FOUQUET, Y. (2018). Organic, gas, and element geochemistry of hydrothermal fluids of the newly discovered extensive hydrothermal area in the Wallis and Futuna region (SW Pacific). *Geofluids*, 2018:e7692839.
- KOSCHINSKY, A. (2014). Hydrothermal vent fluids (Seafloor). In HARFF, J., MESCHEDÉ, M., PETERSEN, S. et THIEDE, J., éditeurs : *Encyclopedia of Marine Geosciences*, pages 1–8. Springer Netherlands, Dordrecht.
- KUMAR, S., STECHER, G., LI, M., KNYAZ, C. et TAMURA, K. (2018). MEGA X : Molecular Evolutionary Genetics Analysis across computing platforms. *Molecular Biology and Evolution*, 35(6):1547–1549.
- LALOU, C. (1991). Deep-sea hydrothermal venting : A recently discovered marine system. *Journal of Marine Systems*, 1(4):403–440.
- LAMING, S., HOURDEZ, S., CAMBON-BONAVITA, M.-A. et PRADILLON, F. (2020). Classical and computed tomographic anatomical analyses in a not-so-cryptic *Alviniconcha* species complex from hydrothermal vents in the SW Pacific. *Frontiers in Zoology*, 17:1–27.
- LANDE, R. (1996). Statistics and partitioning of species diversity, and similarity among multiple communities. *Oikos*, 76(1):5.
- LE BRIS, N., SARRADIN, P.-M. et CAPRAIS, J.-C. (2003). Contrasted sulphide chemistries in the environment of 13°N EPR vent fauna. *Deep Sea Research Part I : Oceanographic Research Papers*, 50(6):737–747.
- LE BRIS, N., YÜCEL, M., DAS, A., SIEVERT, S., LOKABHARATHI, P. et GIRGUIS, P. (2019). Hydrothermal energy transfer and organic carbon production at the deep seafloor. *Frontiers in Marine Science*, 5.
- LE BRIS, N., ZBINDEN, M. et GAILL, F. (2005). Processes controlling the physico-chemical micro-environments associated with Pompeii worms. *Deep Sea Research Part I : Oceanographic Research Papers*, 52(6):1071–1083.

- LEE, R. W., ROBERT, K., MATABOS, M., BATES, A. E. et JUNIPER, S. K. (2015). Temporal and spatial variation in temperature experienced by macrofauna at Main Endeavour hydrothermal vent field. *Deep Sea Research Part I : Oceanographic Research Papers*, 106:154–166.
- LEE, W.-K., KIM, S.-J., HOU, B., VAN DOVER, C. et JU, S.-J. (2019). Population genetic differentiation of the hydrothermal vent crab *Austinograea alayseae* (Crustacea : Bythograeidae) in the Southwest Pacific Ocean. *PLoS ONE*, 14(4):e0215829.
- LEGENDRE, P. (2014). Interpreting the replacement and richness difference components of beta diversity. *Global Ecology and Biogeography*, 23(11):1324–1334.
- LEGENDRE, P. et GALLAGHER, E. (2001). Ecologically meaningful transformations for ordination of species data. *Oecologia*, 129(2):271–280.
- LEGENDRE, P. et LEGENDRE, L. (2012). *Numerical ecology*. Elsevier.
- LEIBOLD, M. A., HOLYOAK, M., MOUQUET, N., AMARASEKARE, P., CHASE, J. M., HOOPES, M. F., HOLT, R. D., SHURIN, J. B., LAW, R., TILMAN, D., LOREAU, M. et GONZALEZ, A. (2004). The metacommunity concept : a framework for multi-scale community ecology. *Ecology Letters*, 7(7):601–613.
- LELIÈVRE, Y., SARRAZIN, J., MARTICORENA, J., SCHAAL, G., DAY, T., LEGENDRE, P., HOURDEZ, S. et MATABOS, M. (2018). Biodiversity and trophic ecology of hydrothermal vent fauna associated with tubeworm assemblages on the Juan de Fuca Ridge. *Biogeosciences*, 15(9):2629–2647.
- LENIHAN, H., MILLS, S., MULLINEAUX, L., PETERSON, C., FISHER, C. et MICHELI, F. (2008). Biotic interactions at hydrothermal vents : Recruitment inhibition by the mussel *Bathymodiolus thermophilus*. *Deep Sea Research Part I : Oceanographic Research Papers*, 55(12):1707–1717.
- LEPRIEUR, F., TEDESCO, P., HUGUENY, B., BEAUCHARD, O., DÜRR, H., BROSSE, S. et OBERDORFF, T. (2011). Partitioning global patterns of freshwater fish beta diversity reveals contrasting signatures of past climate changes. *Ecology Letters*, 14(4):325–334.
- LEVESQUE, C., JUNIPER, S. et MARCUS, J. (2003). Food resource partitioning and competition among alvinellid polychaetes of Juan de Fuca Ridge hydrothermal vents. *Marine Ecology Progress Series*, 246:173–182.
- LEVIN, L. et LE BRIS, N. (2015). The deep ocean under climate change. *Science*, 350(6262):766–768.
- LIBRADO, P. et ROZAS, J. (2009). DnaSP v5 : a software for comprehensive analysis of DNA polymorphism data. *Bioinformatics*, 25(11):1451–1452.

## BIBLIOGRAPHIE

- LILLIEFORS, H. (1967). On the kolmogorov-smirnov test for normality with mean and variance unknown. *Journal of the American Statistical Association*, 62(318):399–402.
- LIN, H.-C., CHEANG, C.-C., CORBARI, L. et CHAN, B. (2020). Trans-Pacific genetic differentiation in the deep-water stalked barnacle *Scalpellum stearnsii* (Cirripedia : Thoracica : Scalpellidae). *Deep Sea Research Part I : Oceanographic Research Papers*, 164:103359.
- LINSE, K., NYE, V., COPLEY, J. et CHEN, C. (2019). On the systematics and ecology of two new species of *Provanna* (Gastropoda : Provannidae) from deep-sea hydrothermal vents in the Caribbean Sea and Southern Ocean. *Journal of Molluscan Studies*, 85(4):425–438.
- LONSDALE, P. (1977). Clustering of suspension-feeding macrobenthos near abyssal hydrothermal vents at oceanic spreading centers. *Deep Sea Research*, 24(9):857–863.
- LOREAU, M., NAEEM, S., INCHAUSTI, P., BENGTSSON, J., GRIME, J. P., HECTOR, A., HOOPER, D. U., HUSTON, M. A., RAFFAELLI, D., SCHMID, B., TILMAN, D. et WARDLE, D. A. (2001). Biodiversity and ecosystem functioning : current knowledge and future challenges. *Science*, 294(5543): 804–808.
- LUTHER, G., ROZAN, T., TAILLEFERT, M., NUZZIO, D., DI MEO, C., SHANK, T., LUTZ, R. et CARY, S. (2001). Chemical speciation drives hydrothermal vent ecology. *Nature*, 410(6830):813–816.
- LUTZ, R., BOUCHET, P., JABLONSKI, D., TURNER, R. et WARÉN, A. (1986). Larval ecology of mollusks at deep-sea hydrothermal vents. *American Malacological Bulletin*, 4(1):49–54.
- MAGURRAN, A., BAILLIE, S., BUCKLAND, S., DICK, J., ELSTON, D., SCOTT, E., SMITH, R., SOMERFIELD, P. et WATT, A. (2010). Long-term datasets in biodiversity research and monitoring : assessing change in ecological communities through time. *Trends in Ecology & Evolution*, 25(10):574–582.
- MAGURRAN, A. E. (1988). *Ecological diversity and its measurement*. Princeton university press.
- MAHLKE, J., DEVEY, C., HOERNLE, K. et GARBE-SCHÖNBERG, D. (2011). Geochemistry of volcanic rocks from the Woodlark Basin. In [Poster] In : *EGU General Assembly 2011, 03.04.-08.04.2011, Vienna, Austria; p. 12864* ., page 12864, Göttingen. Copernicus.
- MARSH, L., COPLEY, J., HUVENNE, V., LINSE, K., REID, W., ROGERS, A., SWEETING, C. et TYLER, P. (2012). Microdistribution of faunal assemblages at deep-sea hydrothermal vents in the Southern Ocean. *PLoS ONE*, 7(10):e48348.

- MARTICORENA, J., MATABOS, M., SARRAZIN, J. et RAMIREZ-LLODRA, E. (2020). Contrasting reproductive biology of two hydrothermal gastropods from the Mid-Atlantic Ridge : implications for resilience of vent communities. *Marine Biology*, 167(8):109.
- MATABOS, M. et JOLLIVET, D. (2019). Revisiting the *Lepetodrilus elevatus* species complex (Vetigastropoda : Lepetodrilidae), using samples from the Galápagos and Guaymas hydrothermal vent systems. *Journal of Molluscan Studies*, 85(1):154–165.
- MATABOS, M., LE BRIS, N., PENDLEBURY, S. et THIÉBAUT, E. (2008a). Role of physico-chemical environment on gastropod assemblages at hydrothermal vents on the East Pacific Rise (13°N/EPR). *Journal of the Marine Biological Association of the United Kingdom*, 88(5):995–1008.
- MATABOS, M., PLOUVIEZ, S., HOURDEZ, S., DESBRUYÈRES, D., LEGENDRE, P., WARÉN, A., JOLLIVET, D. et THIÉBAUT, E. (2011). Faunal changes and geographic crypticism indicate the occurrence of a biogeographic transition zone along the southern East Pacific Rise : Biogeographic transition zone along the southern EPR. *Journal of Biogeography*, 38(3):575–594.
- MATABOS, M. et THIÉBAUT, E. (2010). Reproductive biology of three hydrothermal vent peltospirid gastropods (*Nodopelta heminoda*, *N. subnoda* and *Peltoospira operculata*) associated with Pompeii worms on the East Pacific Rise. *Journal of Molluscan Studies*, 76(3):257–266.
- MATABOS, M., THIÉBAUT, E., LE GUEN, D., SADOSKY, F., JOLLIVET, D. et BONHOMME, F. (2008b). Geographic clines and stepping-stone patterns detected along the East Pacific Rise in the vetigastropod *Lepetodrilus elevatus* reflect species crypticism. *Marine Biology*, 153(4):545–563.
- MCHUGH, D. et ROUSE, G. (1998). Life history evolution of marine invertebrates : New views from phylogenetic systematics. *Trends in Ecology & Evolution*, 13(5):182–186.
- METAXAS, A. (2011). Spatial patterns of larval abundance at hydrothermal vents on seamounts : evidence for recruitment limitation. *Marine Ecology Progress Series*, 437:103–117.
- MICHELI, E., PETERSON, C., MULLINEAUX, L., FISHER, C., MILLS, S., SANCHO, G., JOHNSON, G. et LENIHAN, H. (2002). Predation structures communities at deep-sea hydrothermal vents. *Ecological Monographs*, 72(3):365–382.
- MILLS, S., MULLINEAUX, L. et TYLER, P. (2007). Habitat associations in gastropod species at East Pacific Rise hydrothermal vents (9°50'N). *The Biological Bulletin*, 212(3):185–194.

## BIBLIOGRAPHIE

- MITARAI, S., WATANABE, H., NAKAJIMA, Y., SHCHEPETKIN, A. et MCWILLIAMS, J. (2016). Quantifying dispersal from hydrothermal vent fields in the western Pacific Ocean. *Proceedings of the National Academy of Sciences*, 113(11):2976–2981.
- MITTELSTAEDT, E., ESCARTÍN, J., GRACIAS, N., OLIVE, J.-A., BARREYRE, T., DAVAILLE, A., CANNAT, M. et GARCIA, R. (2012). Quantifying diffuse and discrete venting at the Tour Eiffel vent site, Lucky Strike hydrothermal field. *Geochemistry, Geophysics, Geosystems*, 13(4).
- MOALIC, Y., DESBRUYÈRES, D., DUARTE, C., ROZENFELD, A., BACHRATY, C. et ARNAUD-HAOND, S. (2012). Biogeography revisited with network theory : retracing the history of hydrothermal vent communities. *Systematic Biology*, 61(1):127.
- MULLINEAUX, L., ADAMS, D., MILLS, S. et BEAULIEU, S. (2010). Larvae from afar colonize deep-sea hydrothermal vents after a catastrophic eruption. *Proceedings of the National Academy of Sciences*, 107(17):7829–7834.
- MULLINEAUX, L., FISHER, C., PETERSON, C. et SCHAEFFER, S. (2000). Tubeworm succession at hydrothermal vents : use of biogenic cues to reduce habitat selection error? *Oecologia*, 123(2): 275–284.
- MULLINEAUX, L., METAXAS, A., BEAULIEU, S., BRIGHT, M., GOLLNER, S., GRUPE, B., HERRERA, S., KELLNER, J., LEVIN, L., MITARAI, S., NEUBERT, M., THURNHERR, A., TUNNICLIFFE, V., WATANABE, H. et WON, Y.-J. (2018). Exploring the ecology of deep-sea hydrothermal vents in a metacommunity framework. *Frontiers in Marine Science*, 5:49.
- MULLINEAUX, L., MILLS, S. et GOLDMAN, E. (1998). Recruitment variation during a pilot colonization study of hydrothermal vents (9°50'N, East Pacific Rise). *Deep Sea Research Part II: Topical Studies in Oceanography*, 45(1):441–464.
- MULLINEAUX, L., PETERSON, C., MICHELI, F. et MILLS, S. (2003). Successional mechanism varies along a gradient in hydrothermal fluid flux at deep-sea vents. *Ecological Monographs*, 73(4): 523–542.
- NAKAGAWA, S. et TAKAI, K. (2008). Deep-sea vent chemoautotrophs : diversity, biochemistry and ecological significance. *FEMS Microbiology Ecology*, 65(1):1–14.
- NAKAMURA, M., WATANABE, H., SASAKI, T., ISHIBASHI, J., FUJIKURA, K. et MITARAI, S. (2014). Life history traits of *Lepetodrilus nux* in the Okinawa Trough, based upon gametogenesis, shell size, and genetic variability. *Marine Ecology Progress Series*, 505:119–130.



- OGURA, T., WATANABE, H., CHEN, C., SASAKI, T., KOJIMA, S., ISHIBASHI, J.-I. et FUJIKURA, K. (2018). Population history of deep-sea vent and seep *Provanna* snails (Mollusca : Abyssochrysoidea) in the northwestern Pacific. *PeerJ*, 6:e5673.
- OKSANEN, J., BLANCHET, F. G., FRIENDLY, M., KINDT, R., LEGENDRE, P., MCGLINN, D., MINCHIN, P. R., O'HARA, R. B., SIMPSON, G. L., SOLYMOS, P., STEVENS, M. H. H., SZOECES, E. et WAGNER, H. (2020). *vegan : Community Ecology Package*. R package version 2.5-7.
- PAULUS, E. (2021). Shedding light on deep-sea biodiversity—A highly vulnerable habitat in the face of anthropogenic change. *Frontiers in Marine Science*, 8.
- PAULY, D. et CADDY, J. (1985). *A modification of Bhattacharya's method for the analysis of mixtures of normal distributions*, volume 781. FAO.
- PEARSON, K. et ROUSE, G. (2022). Vampire Worms; A revision of *Galapagomystides* (Phyllodoceidae, Annelida), with the description of three new species. *Zootaxa*, 5128(4):451–485.
- PERES-NETO, P., LEGENDRE, P., DRAY, S. et BORCARD, D. (2006). Variation partitioning of species data matrices : estimation and comparison of fractions. *Ecology*, 87(10):2614–2625.
- PERFIT, M. et CHADWICK, W. (1998). Magmatism at mid-ocean ridges : Constraints from volcanological and geochemical investigations. *Geophysical Monograph-American Geophysical Union*, 106:59–116.
- PETERSEN, J., ZIELINSKI, F., PAPE, T., SEIFERT, R., MORARU, C., AMANN, R., HOURDEZ, S., GIRGUIS, P., WANKEL, S., BARBE, V., PELLETIER, E., FINK, D., BOROWSKI, C., BACH, W. et DUBILIER, N. (2011). Hydrogen is an energy source for hydrothermal vent symbioses. *Nature*, 476(7359): 176–180.
- PETERSEN, S., KRÄTSCHHELL, A., AUGUSTIN, N., JAMIESON, J., HEIN, J. et HANNINGTON, M. (2016). News from the seabed – Geological characteristics and resource potential of deep-sea mineral resources. *Marine Policy*, 70:175–187.
- PLOUVIEZ, S., FAURE, B., LE GUEN, D., LALLIER, F., BIERNE, N. et JOLLIVET, D. (2013). A new barrier to dispersal trapped old genetic clines that escaped the easter microplate tension zone of the pacific vent mussels. *PLoS ONE*, 8(12):e81555.
- PLOUVIEZ, S., LABELLA, A., WEISROCK, D., VON MEIJENFELDT, F., BALL, B., NEIGEL, J. et VAN DOVER, C. (2019). Amplicon sequencing of 42 nuclear loci supports directional gene flow

## BIBLIOGRAPHIE

- between South Pacific populations of a hydrothermal vent limpet. *Ecology and Evolution*, 9(11):6568–6580.
- PLOUVIEZ, S., SHANK, T., FAURE, B., DAGUIN-THIÉBAUT, C., VIARD, F., LALLIER, F. et JOLLIVET, D. (2009). Comparative phylogeography among hydrothermal vent species along the East Pacific Rise reveals vicariant processes and population expansion in the South. *Molecular Ecology*, 18(18):3903–3917.
- PODANI, J., RICOTTA, C. et SCHMERA, D. (2013). A general framework for analyzing beta diversity, nestedness and related community-level phenomena based on abundance data. *Ecological Complexity*, 15:52–61.
- PODANI, J. et SCHMERA, D. (2011). A new conceptual and methodological framework for exploring and explaining pattern in presence – absence data. *Oikos*, 120(11):1625–1638.
- PODOWSKI, E., MA, S., LUTHER III, G., WARDROP, D. et FISHER, C. (2010). Biotic and abiotic factors affecting distributions of megafauna in diffuse flow on andesite and basalt along the Eastern Lau Spreading Center, Tonga. *Marine Ecology Progress Series*, 418:25–45.
- PODOWSKI, E. L., MOORE, T. S., ZELNIO, K. A., LUTHER, G. W. et FISHER, C. R. (2009). Distribution of diffuse flow megafauna in two sites on the Eastern Lau Spreading Center, Tonga. *Deep Sea Research Part I: Oceanographic Research Papers*, 56(11):2041–2056.
- POITRIMOL, C., THIÉBAUT, E., DAGUIN-THIÉBAUT, C., LE PORT, A.-S., BALLENGHIEN, M., TRAN LU Y, A., JOLLIVET, D., HOURDEZ, S. et MATABOS, M. (2022). Contrasted phylogeographic patterns of hydrothermal vent gastropods along Southwest Pacific : Woodlark basin, a possible contact zone and/or stepping-stone. *PLoS ONE*, 17(10):e0275638.
- PRADILLON, F., LE BRIS, N., SHILLITO, B., YOUNG, C. et GAILL, F. (2005). Influence of environmental conditions on early development of the hydrothermal vent polychaete *Alvinella pompejana*. *Journal of Experimental Biology*, 208(8):1551–1561.
- PRADILLON, F., SHILLITO, B., YOUNG, C. et GAILL, F. (2001). Developmental arrest in vent worm embryos. *Nature*, 413(6857):698–699.
- PRIMACK, R., MILLER-RUSHING, A., CORLETT, R., DEVICTOR, V., JOHNS, D., LOYOLA, R., HASS, B., PAKEMAN, R. J. et PEJCHAR, L. (2018). Biodiversity gains? The debate on changes in local-vs global-scale species richness. *Biological Conservation*, 219:A1–A3.
- PULLANDRE, N., LAMBERT, A., BROUILLET, S. et ACHAZ, G. (2012). ABGD, Automatic Barcode Gap Discovery for primary species delimitation. *Molecular Ecology*, 21(8):1864–1877.

- R CORE TEAM (2020). *R : A Language and Environment for Statistical Computing*. R Foundation for Statistical Computing, Vienna, Austria.
- RAMIREZ-LLODRA, E. (2002). Fecundity and life-history strategies in marine invertebrates. *In Advances in Marine Biology*, volume 43, pages 87–170. Academic Press.
- RAMIREZ-LLODRA, E., BRANDT, A., DANOVARO, R., DE MOL, B., ESCOBAR, E., GERMAN, C. R., LEVIN, L. A., MARTINEZ ARBIZU, P., MENOT, L., BUHL-MORTENSEN, P., NARAYANASWAMY, B. E., SMITH, C. R., TITTENSOR, D. P., TYLER, P. A., VANREUSEL, A. et VECCHIONE, M. (2010). Deep, diverse and definitely different : unique attributes of the world's largest ecosystem. *Biogeosciences*, 7(9):2851–2899.
- RIASCOS, J. et GUZMAN, P. (2010). The ecological significance of growth rate, sexual dimorphism and size at maturity of *Littoraria zebra* and *L. variegata* (Gastropoda : Littorinidae). *Journal of Molluscan Studies*, 76(3):289–295.
- ROGERS, A. et HARPENDING, H. (1992). Population growth makes waves in the distribution of pairwise genetic differences. *Molecular Biology and Evolution*, 9(3):552–569.
- ROGERS, A., TYLER, P., CONNELLY, D., COPLEY, J., JAMES, R., LARTER, R., LINSE, K., MILLS, R., GARABATO, A., PANCOST, R., PEARCE, D., POLUNIN, N., GERMAN, C., SHANK, T., BOERSCH-SUPAN, P., ALKER, B., AQUILINA, A., BENNETT, S., CLARKE, A., DINLEY, R., GRAHAM, A., GREEN, D., HAWKES, J., HEPBURN, L., HILARIO, A., HUVENNE, V., MARSH, L., RAMIREZ-LLODRA, E., REID, W., ROTERMAN, C., SWEETING, C., THATJE, S. et ZWIRGLMAIER, K. (2012). The discovery of new deep-sea hydrothermal vent communities in the Southern Ocean and implications for biogeography. *PLOS Biology*, 10(1):e1001234.
- ROSENZWEIG, M. (1995). *Species diversity in space and time*. Cambridge university press.
- ROUX, C., FRAÏSSE, C., ROMIGUIER, J., ANCIAUX, Y., GALTIER, N. et BIERNE, N. (2016). Shedding light on the grey zone of speciation along a continuum of genomic divergence. *PLOS Biology*, 14(12):e2000234.
- RSTUDIO TEAM (2020). *RStudio : Integrated Development Environment for R*. RStudio, PBC, Boston, MA.
- RUELLAN, E. et LAGABRIELLE, Y. (2005). Subductions et ouvertures océaniques dans le Sud-Ouest Pacifique. *Géomorphologie : relief, processus, environnement*, 11(2):121–142.
- SADOSKY, F., THIÉBAUT, E., JOLLIVET, D. et SHILLITO, B. (2002). Recruitment and population structure of the vetigastropod *Lepetodrilus elevatus* at 13°N hydrothermal vent sites on East Pacific Rise. *Cahiers de biologie marine*, 43(3/4):399–402.

## BIBLIOGRAPHIE

- SAMADI, S., QUÉMÉRÉ, E., LORION, J., TILLIER, A., von COSEL, R., LOPEZ, P., CRUAUD, C., COULOUX, A. et BOISSELIER-DUBAYLE, M.-C. (2007). Molecular phylogeny in mytilids supports the wooden steps to deep-sea vents hypothesis. *Comptes Rendus Biologies*, 330(5): 446–456.
- SANCHO, G., FISHER, C., MILLS, S., MICHELI, E., JOHNSON, G., LENIHAN, H., PETERSON, C. et MULLINEAUX, L. (2005). Selective predation by the zoarcid fish *Thermarces cerberus* at hydrothermal vents. *Deep Sea Research Part I : Oceanographic Research Papers*, 52(5):837–844.
- SARRAZIN, J. et JUNIPER, K. (1998). The use of video imagery to gather biological information at deep-sea hydrothermal vents. *Cahiers de biologie marine*, 39(3-4):255–258.
- SARRAZIN, J. et JUNIPER, S. (1999). Biological characteristics of a hydrothermal edifice mosaic community. *Marine Ecology Progress Series*, 185:1–19.
- SARRAZIN, J., JUNIPER, S., MASSOTH, G. et LEGENDRE, P. (1999). Physical and chemical factors influencing species distributions on hydrothermal sulfide edifices of the Juan de Fuca Ridge, northeast Pacific. *Marine Ecology Progress Series*, 190:89–112.
- SARRAZIN, J., PORTAIL, M., LEGRAND, E., CATHALOT, C., LAES, A., LAHAYE, N., SARRADIN, P. M. et HUSSON, B. (2020). Endogenous versus exogenous factors : What matters for vent mussel communities? *Deep Sea Research Part I : Oceanographic Research Papers*, 160:103260.
- SARRAZIN, J., ROBIGO, V., JUNIPER, S. et DELANEY, J. (1997). Biological and geological dynamics over four years on a high-temperature sulfide structure at the Juan de Fuca Ridge hydrothermal observatory. *Marine Ecology Progress Series*, 153:5–24.
- SASAKI, T., WARÉN, A., KANO, Y., OKUTANI, T. et FUJIKURA, K. (2010). Gastropods from recent hot vents and cold seeps : systematics, diversity and life strategies. In KIEL, S., éditeur : *The Vent and Seep Biota*, volume 33, pages 169–254. Springer Netherlands, Dordrecht.
- SCHELLART, W., LISTER, G. et TOY, V. (2006). A Late Cretaceous and Cenozoic reconstruction of the Southwest Pacific region : Tectonics controlled by subduction and slab rollback processes. *Earth-Science Reviews*, 76(3):191–233.
- SCHNEIDER, C., RASBAND, W. et ELICEIRI, K. (2012). NIH Image to ImageJ : 25 years of image analysis. *Nature Methods*, 9(7):671–675.
- SEN, A., BECKER, E., PODOWSKI, E., WICKES, L., MA, S., MULLAUGH, K., HOURDEZ, S., LUTHER, G. et FISHER, C. (2013). Distribution of mega fauna on sulfide edifices on the Eastern Lau

- Spreading Center and Valu Fa Ridge. *Deep Sea Research Part I : Oceanographic Research Papers*, 72:48–60.
- SEN, A., KIM, S., MILLER, A., HOVEY, K., HOURDEZ, S., LUTHER, G. et FISHER, C. (2016). Peripheral communities of the Eastern Lau Spreading Center and Valu Fa Ridge : community composition, temporal change and comparison to near-vent communities. *Marine Ecology*, 37(3):599–617.
- SHANK, T., FORNARI, D., VON DAMM, K., LILLEY, M., HAYMON, R. et LUTZ, R. (1998). Temporal and spatial patterns of biological community development at nascent deep-sea hydrothermal vents (9°50'N, East Pacific Rise). *Deep Sea Research Part II : Topical Studies in Oceanography*, 45(1):465–515.
- SIGWART, J. et CHEN, C. (2018). Comparative oxygen consumption of Gastropod holobionts from deep-sea hydrothermal vents in the Indian Ocean. *The Biological Bulletin*, 235(2):102–112.
- SOCOLAR, J., GILROY, J., KUNIN, W. et EDWARDS, D. (2016). How should beta-diversity inform biodiversity conservation? *Trends in Ecology & Evolution*, 31(1):67–80.
- STRONG, J., ANDONEGI, E., BIZSEL, K., DANOVARO, R., ELLIOTT, M., FRANCO, A., GARCES, E., LITTLE, S., MAZIK, K., MONCHEVA, S., PAPADOPOULOU, N., PATRÍCIO, J., QUEIRÓS, A., SMITH, C., STEFANOVA, K. et SOLAUN, O. (2015). Marine biodiversity and ecosystem function relationships : The potential for practical monitoring applications. *Estuarine, Coastal and Shelf Science*, 161:46–64.
- SWEETMAN, A., THURBER, A., SMITH, C., LEVIN, L., MORA, C., WEI, C., GOODAY, A., JONES, D., REX, M., YASUHARA, M., INGELS, J., RUHL, H., FRIEDER, C., DANOVARO, R., WÜRZBERG, L., BACO, A., GRUPE, B., PASULKA, A., MEYER, K., DUNLOP, K., HENRY, L.-A. et ROBERTS, J. (2017). Major impacts of climate change on deep-sea benthic ecosystems. *Elementa : Science of the Anthropocene*, 5:4.
- TAYLOR, B., GOODLIFFE, A., MARTINEZ, F. et HEY, R. (1995). Continental rifting and initial sea-floor spreading in the Woodlark basin. *Nature*, 374(6522):534–537.
- TEIXEIRA, S., CAMBON-BONAVITA, M.-A., SERRÃO, E., DESBRUYÉRES, D. et ARNAUD-HAOND, S. (2011). Recent population expansion and connectivity in the hydrothermal shrimp *Rimicaris exoculata* along the Mid-Atlantic Ridge : Genetic diversity of a hydrothermal vent shrimp. *Journal of Biogeography*, 38(3):564–574.
- THALER, A. et AMON, D. (2019). 262 Voyages beneath the sea : a global assessment of macro- and megafaunal biodiversity and research effort at deep-sea hydrothermal vents. *PeerJ*, 7:e7397.

## BIBLIOGRAPHIE

- THALER, A., PLOUVIEZ, S., SALEU, W., ALEI, F., JACOBSON, A., BOYLE, E., SCHULTZ, T., CARLSSON, J. et VAN DOVER, C. (2014). Comparative population structure of two deep-sea hydrothermal-vent-associated decapods (*Chorocaris* sp. 2 and *Munidopsis lauensis*) from Southwestern Pacific back-arc basins. *PLoS ONE*, 9(7):e101345.
- THALER, A., ZELNIO, K., SALEU, W., SCHULTZ, T., CARLSSON, J., CUNNINGHAM, C., VRIJENHOEK, R. et VAN DOVER, C. (2011). The spatial scale of genetic subdivision in populations of *Ifremeria nautiliei*, a hydrothermal-vent gastropod from the southwest Pacific. *BMC Evolutionary Biology*, 11(1):372.
- THIÉBAUT, E., HUTHER, X., SHILLITO, B., JOLLIVET, D. et GAILL, F. (2002). Spatial and temporal variations of recruitment in the tube worm *Riftia pachyptila* on the East Pacific Rise (9°50'N and 13°N). *Marine Ecology Progress Series*, 234:147–157.
- THRUSH, S., HALLIDAY, J., HEWITT, J. et LOHRER, A. (2008). The effects of habitat loss, fragmentation, and community homogenization on resilience in estuaries. *Ecological Applications*, 18(1):12–21.
- TRAN LU Y, A., RUALT, S., DAGUIN-THIÉBAUT, C., CASTEL, J., BIERNE, N., BROQUET, T., WINCKER, P., PERDEREAU, A., ARNAUD-HAOND, S., GAGNAIRE, P.-A., JOLLIVET, D., HOURDEZ, S. et BONHOMME, F. (2022). Subtle limits to connectivity revealed by outlier loci within two divergent metapopulations of the deep-sea hydrothermal gastropod *Ifremeria nautiliei*. *Molecular Ecology*, 31(10):2796–2813.
- TUNNICLIFFE, V. (1991). The biology of hydrothermal vents : ecology and evolution. *Oceanogr Mar Biol Annu Rev*, 29:319–407.
- TUNNICLIFFE, V. et FOWLER, C. (1996). Influence of sea-floor spreading on the global hydrothermal vent fauna. *Nature*, 379(6565):531–533.
- TYLER, P., CAMPOS-CREASEY, L. et GILES, L. (1994). Environmental control of quasi-continuous and seasonal reproduction in deep-sea benthic invertebrates. In YOUNG, C. et ECKELBARGER, K., éditeurs : *Reproduction, larval biology, and recruitment of the deep-sea benthos*, pages 158–178. Columbia University Press.
- TYLER, P., PENDLEBURY, S., MILLS, S., MULLINEAUX, L., ECKELBARGER, K., BAKER, M. et YOUNG, C. (2008). Reproduction of gastropods from vents on the East Pacific Rise and the Mid-Atlantic Ridge. *Journal of Shellfish Research*, 27(1):107–118.
- TYLER, P. et YOUNG, C. (1999). Reproduction and dispersal at vents and cold seeps. *Journal of the Marine Biological Association of the United Kingdom*, 79(2):193–208.

- VAN AUDENHAEGE, L., FARIÑAS-BERMEJO, A., SCHULTZ, T. et VAN DOVER, C. (2019). An environmental baseline for food webs at deep-sea hydrothermal vents in Manus Basin (Papua New Guinea). *Deep Sea Research Part I: Oceanographic Research Papers*, 148:88–99.
- VAN AUDENHAEGE, L., MATABOS, M., BRIND'AMOUR, A., DRUGMAND, J., LAËS-HUON, A., SARRADIN, P.-M. et SARRAZIN, J. (2022). Long-term monitoring reveals unprecedented stability of a vent mussel assemblage on the Mid-Atlantic Ridge. *Progress in Oceanography*, 204:102791.
- VAN DER HEIJDEN, K., PETERSEN, J., DUBILIER, N. et BOROWSKI, C. (2012). Genetic connectivity between North and South Mid-Atlantic Ridge chemosynthetic bivalves and their symbionts. *PLOS ONE*, 7(7):e39994.
- VAN DOVER, C. (2000). *The ecology of deep-sea hydrothermal vents*. Princeton University Press.
- VAN DOVER, C. (2002). Evolution and biogeography of deep-sea vent and seep invertebrates. *Science*, 295(5558):1253–1257.
- VAN DOVER, C. (2011). Mining seafloor massive sulphides and biodiversity : what is at risk? *ICES Journal of Marine Science*, 68(2):341–348.
- VAN DOVER, C., COLAÇO, A., COLLINS, P., CROOT, P., METAXAS, A., MURTON, B., SWADDLING, A., BOSCHEN-ROSE, R., CARLSSON, J., CUYVERS, L., FUKUSHIMA, T., GARTMAN, A., KENNEDY, R., KRIETE, C., MESTRE, N., MOLODTSOVA, T., MYHRVOLD, A., PELLETER, E., POPOOLA, S., QIAN, P.-Y., SARRAZIN, J., SHARMA, R., SUH, Y., SYLVAN, J., TAO, C., TOMCZAK, M. et VERMILYE, J. (2020). Research is needed to inform environmental management of hydrothermally inactive and extinct polymetallic sulfide (PMS) deposits. *Marine Policy*, 121:104183.
- VAN DOVER, C. L., ARNAUD-HAOND, S., GIANNI, M., HELMREICH, S., HUBER, J. A., JAECKEL, A. L., METAXAS, A., PENDLETON, L. H., PETERSEN, S., RAMIREZ-LLODRA, E., STEINBERG, P. E., TUNNICLIFFE, V. et YAMAMOTO, H. (2018). Scientific rationale and international obligations for protection of active hydrothermal vent ecosystems from deep-sea mining. *Marine Policy*, 90:20–28.
- VAN DOVER, C. L., HUMPHRIS, S. E., FORNARI, D., CAVANAUGH, C. M., COLLIER, R., GOFFREDI, S. K., HASHIMOTO, J., LILLEY, M. D., REYSENBACH, A. L., SHANK, T. M., VON DAMM, K. L., BANTA, A., GALLANT, R. M., GÖTZ, D., GREEN, D., HALL, J., HARMER, T. L., HURTADO, L. A., JOHNSON, P., MCKINESS, Z. P., MEREDITH, C., OLSON, E., PAN, I. L., TURNIPSEED, M., WON, Y., YOUNG, C. R. et VRIJENHOEK, R. C. (2001). Biogeography and ecological setting of Indian Ocean hydrothermal vents. *Science*, 294(5543):818–823.

## BIBLIOGRAPHIE

- VISMANN, B. (1991). Sulfide tolerance : Physiological mechanisms and ecological implications. *Ophelia*, 34(1):1–27.
- VRIJENHOEK, R. (2009). Cryptic species, phenotypic plasticity, and complex life histories : Assessing deep-sea faunal diversity with molecular markers. *Deep Sea Research Part II : Topical Studies in Oceanography*, 56(19):1713–1723.
- VRIJENHOEK, R., FELDMAN, R., LUTZ, R., CRADDOCK, C. et HASHIMOTO, J. (1997). Genetic characterization of *Lepetodrilus limpets* from hydrothermal vents in the Mariana Trough. *Deep-sea research special volume. Deep sea research in subduction zones, spreading centres and backarc basins*, pages 111–116.
- VRIJENHOEK, R. C. (2010). Genetic diversity and connectivity of deep-sea hydrothermal vent metapopulations. *Molecular Ecology*, 19(20):4391–4411.
- VUILLEMIN, R., LE ROUX, D., DORVAL, P., BUCAS, K., SUDREAU, J., HAMON, M., LE GALL, C. et SARRADIN, P. (2009). CHEMINI : A new in situ CHEMical MINIaturized analyzer. *Deep Sea Research Part I : Oceanographic Research Papers*, 56(8):1391–1399.
- WARÉN, A. et BOUCHET, P. (1993). New records, species, genera, and a new family of gastropods from hydrothermal vents and hydrocarbon seeps. *Zoologica Scripta*, 22(1):1–90.
- WARÉN, A. et BOUCHET, P. (2001). Gastropoda and Monoplacophora from hydrothermal vents and seeps; new taxa and records. *The Veliger*, 44:116–231.
- WARÉN, A. et PONDER, W. (1991). New species, anatomy, and systematic position of the hydrothermal vent and hydrocarbon seep gastropod family Provannidae fam.n. (Caenogastropoda). *Zoologica Scripta*, 20(1):27–56.
- WATANABE, H., CHEN, C. et CHAN, B. (2021). A new deep-sea hot vent stalked barnacle from the Mariana Trough with notes on the feeding ecology of *Vulcanolepas*. *Marine Biodiversity*, 51(1):9.
- WATANABE, H. et KOJIMA, S. (2015). Vent fauna in the Okinawa Trough. In ISHIBASHI, J.-I., OKINO, K. et SUNAMURA, M., éditeurs : *Subseafloor Biosphere Linked to Hydrothermal Systems : TAIGA Concept*, pages 449–459. Springer Japan, Tokyo.
- WATANABE, H., SHIGENO, S., FUJIKURA, K., MATSUI, T., KATO, S. et YAMAMOTO, H. (2019). Faunal composition of deep-sea hydrothermal vent fields on the Izu–Bonin–Mariana Arc, northwestern Pacific. *Deep Sea Research Part I : Oceanographic Research Papers*, 149:103050.



- WHITTAKER, R. (1960). Vegetation of the Siskiyou Mountains, Oregon and California. *Ecological Monographs*, 30(3):279–338.
- WHITTAKER, R. (1972). Evolution and measurement of species diversity. *TAXON*, 21(2-3):213–251.
- WILLIAMS, S., SMITH, L., HERBERT, D., MARSHALL, B., WARÉN, A., KIEL, S., DYAL, P., LINSE, K., VILVENS, C. et KANO, Y. (2013). Cenozoic climate change and diversification on the continental shelf and slope : evolution of gastropod diversity in the family Solariellidae (Trochoidea). *Ecology and Evolution*, 3(4):887–917.
- WON, Y., YOUNG, C., LUTZ, R. et VRIJENHOEK, R. (2002). Dispersal barriers and isolation among deep-sea mussel populations (Mytilidae : Bathymodiolus) from eastern Pacific hydrothermal vents : barriers to gene flow of deep-sea hydrothermal vent mussels. *Molecular Ecology*, 12(1): 169–184.
- YAHAGI, T., FUKUMORI, H., WARÉN, A. et KANO, Y. (2019). Population connectivity of hydrothermal-vent limpets along the northern Mid-Atlantic Ridge (Gastropoda : Neritimorpha : Phenacolepadidae). *Journal of the Marine Biological Association of the United Kingdom*, 99(1):179–185.
- YAHAGI, T., THALER, A., VAN DOVER, C. et KANO, Y. (2020). Population connectivity of the hydrothermal-vent limpet *Shinkailepas tollmanni* in the Southwest Pacific (Gastropoda : Neritimorpha : Phenacolepadidae). *PLoS ONE*, 15(9):e0239784.
- YAHAGI, T., WATANABE, H., KOJIMA, S. et KANO, Y. (2017). Do larvae from deep-sea hydrothermal vents disperse in surface waters? *Ecology*, 98(6):1524–1534.
- YOUNG, C., SEWELL, M., TYLER, P. et METAXAS, A. (1997). Biogeographic and bathymetric ranges of Atlantic deep-sea echinoderms and ascidians : the role of larval dispersal. *Biodiversity & Conservation*, 6(11):1507–1522.
- ZAL, E., JOLLIVET, D., CHEVALDONNÉ, P. et DESBRUYÈRES, D. (1995). Reproductive biology and population structure of the deep-sea hydrothermal vent worm *Paralvinella grasslei* (Polychaeta : Alvinellidae) at 13°N on the East Pacific Rise. *Marine Biology*, 122(4):637–648.
- ZHANG, S. et ZHANG, S. (2017). A new species of the genus *Phymorhynchus* (Neogastropoda : Raphitomidae) from a hydrothermal vent in the Manus Back-Arc Basin. *Zootaxa*, 4300(3):441.

---

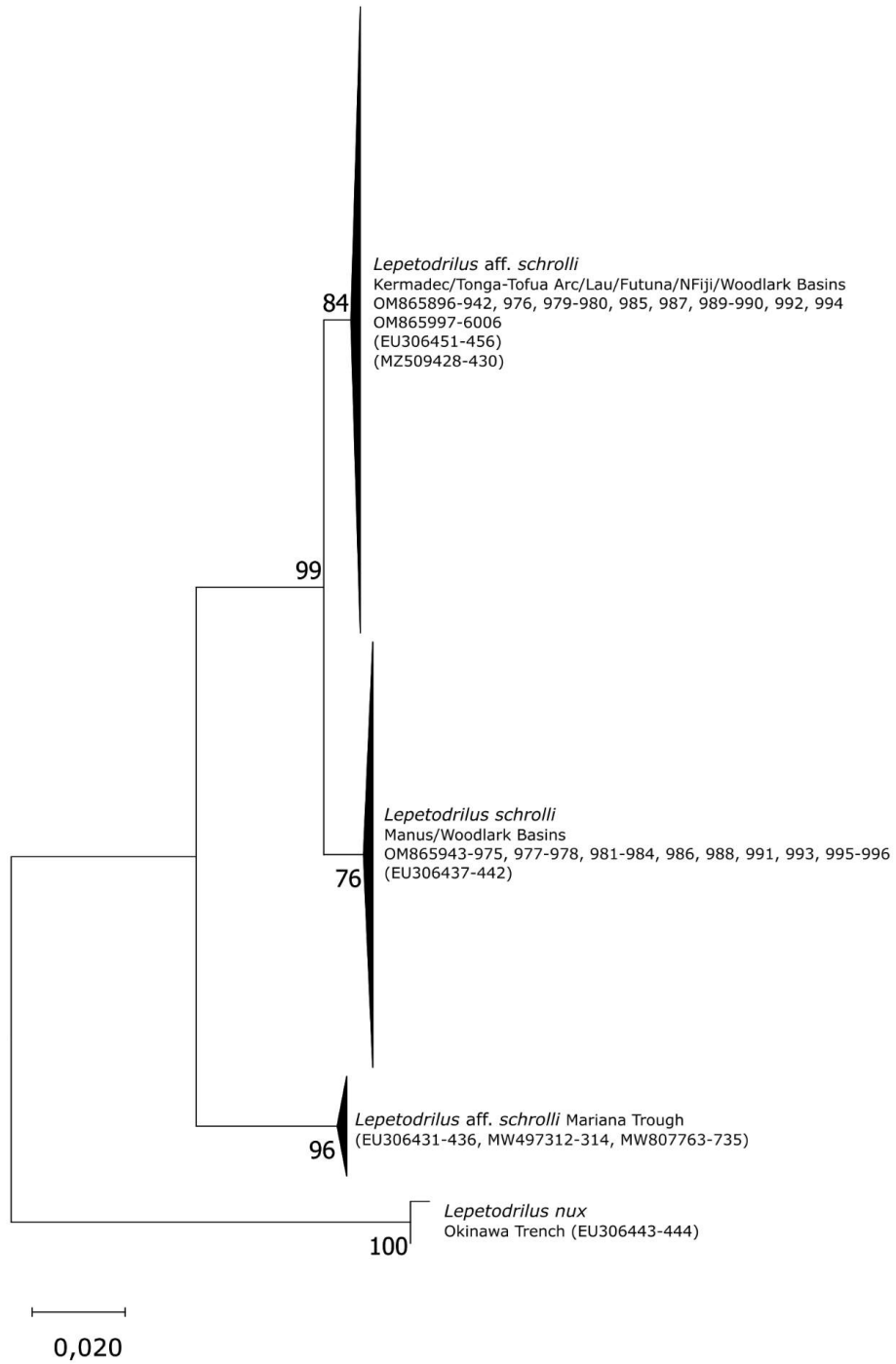
Annexes du chapitre 1

---

**A.1 *Cox1* Maximum Likelihood trees inferred from *Cox1* sequences from *Lepetodrilus* (A), *Symmetromphalus* and *Lamellomphalus* (B), *Shinkailepas* (C) and *Desbruyeresia* and *Provanna* (D) within their genus or family**

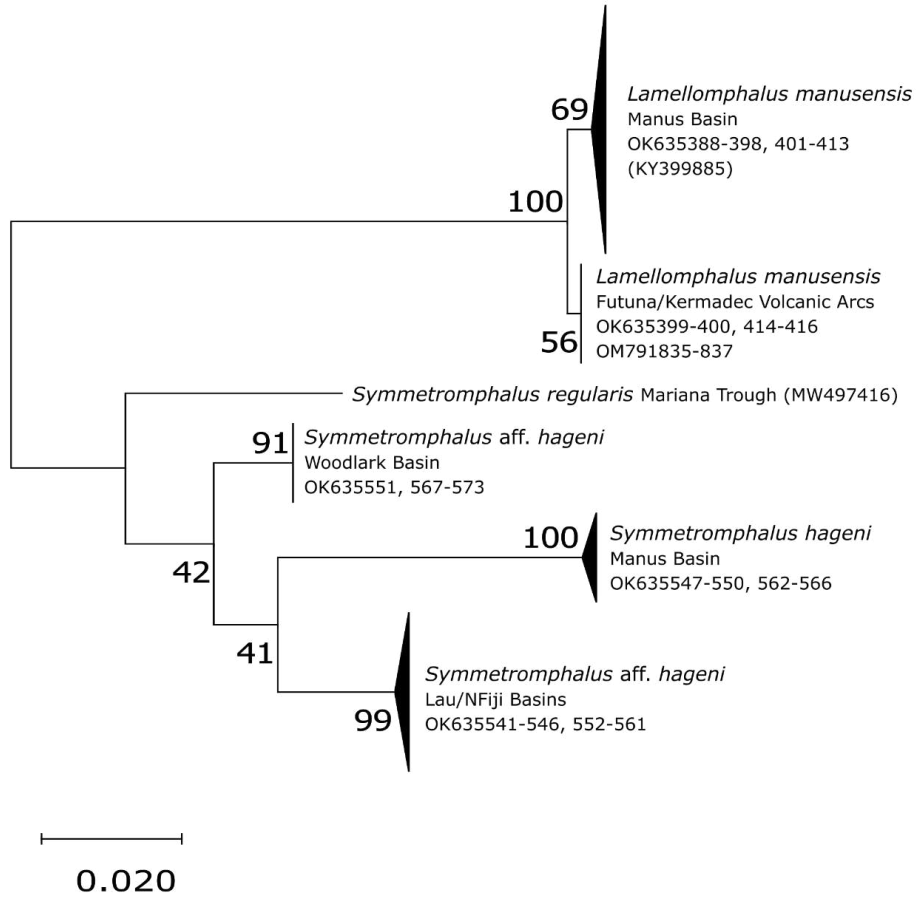
Number at nodes indicates the proportion of occurrences in 1000 bootstraps. Genbank accession numbers of the present study and published sequences are indicated. Published sequences are in brackets. See NJ trees for sequence lengths.

A

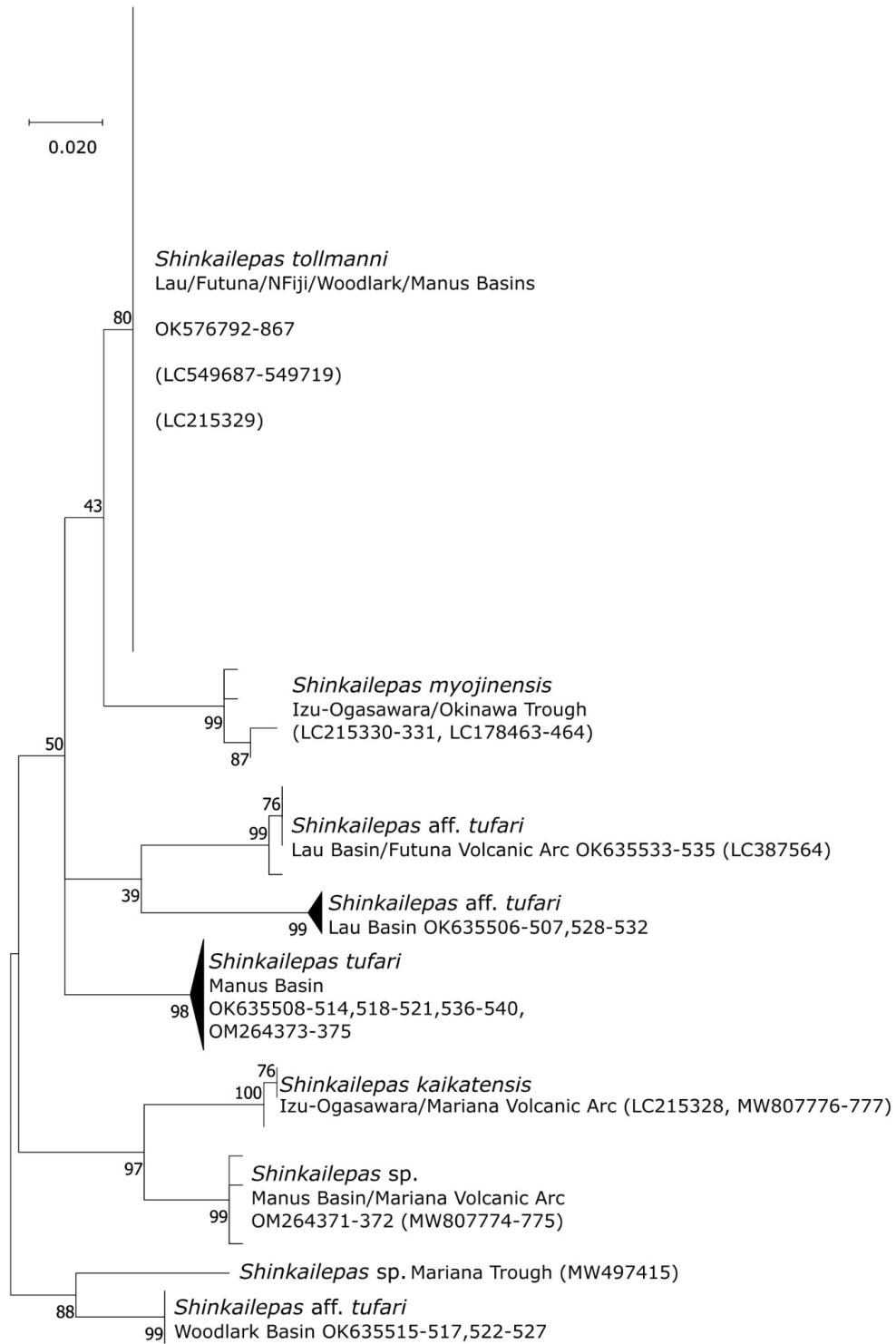


A.1 *Cox1* Maximum Likelihood trees inferred from *Cox1* sequences from *Lepetodrilus* (A), *Symmetromphalus* and *Lamellomphalus* (B), *Shinkailepas* (C) and *Desbruyeresia* and *Provanna* (D) within their genus or family

B

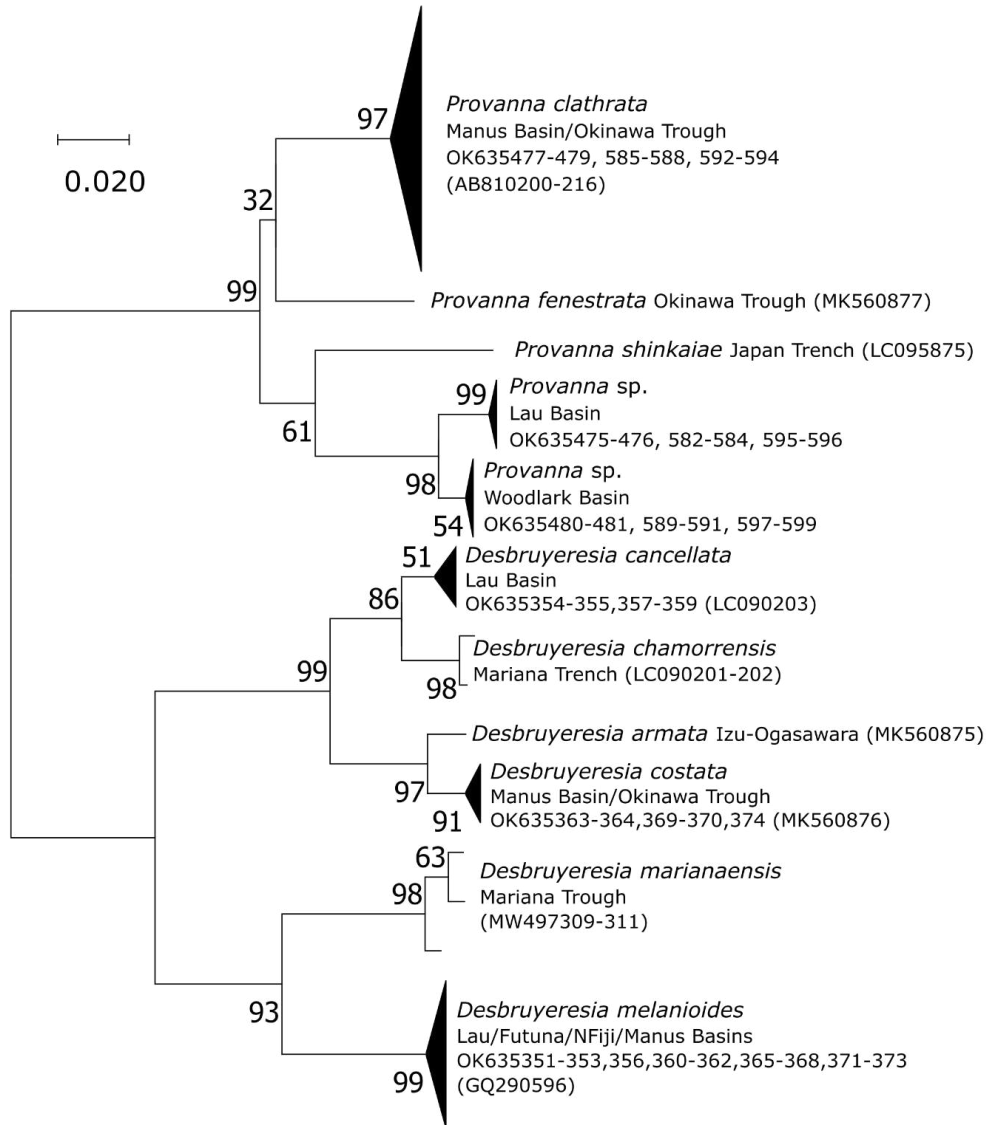


C



A.1 *Cox1* Maximum Likelihood trees inferred from *Cox1* sequences from *Lepetodrilus* (A), *Symmetromphalus* and *Lamellomphalus* (B), *Shinkailepas* (C) and *Desbruyeresia* and *Provanna* (D) within their genus or family

D





- B.1 Illustrations of *Lepetodrilus schrolli* and *Shinkailepas tollmanni* and the different shell measurements**
- B.2 Size-frequency histograms of *Lepetodrilus schrolli***
- B.3 Oocytes size-frequency histograms of *Lepetodrilus schrolli***
- B.4 Size-frequency histograms of *Shinkailepas tollmanni***



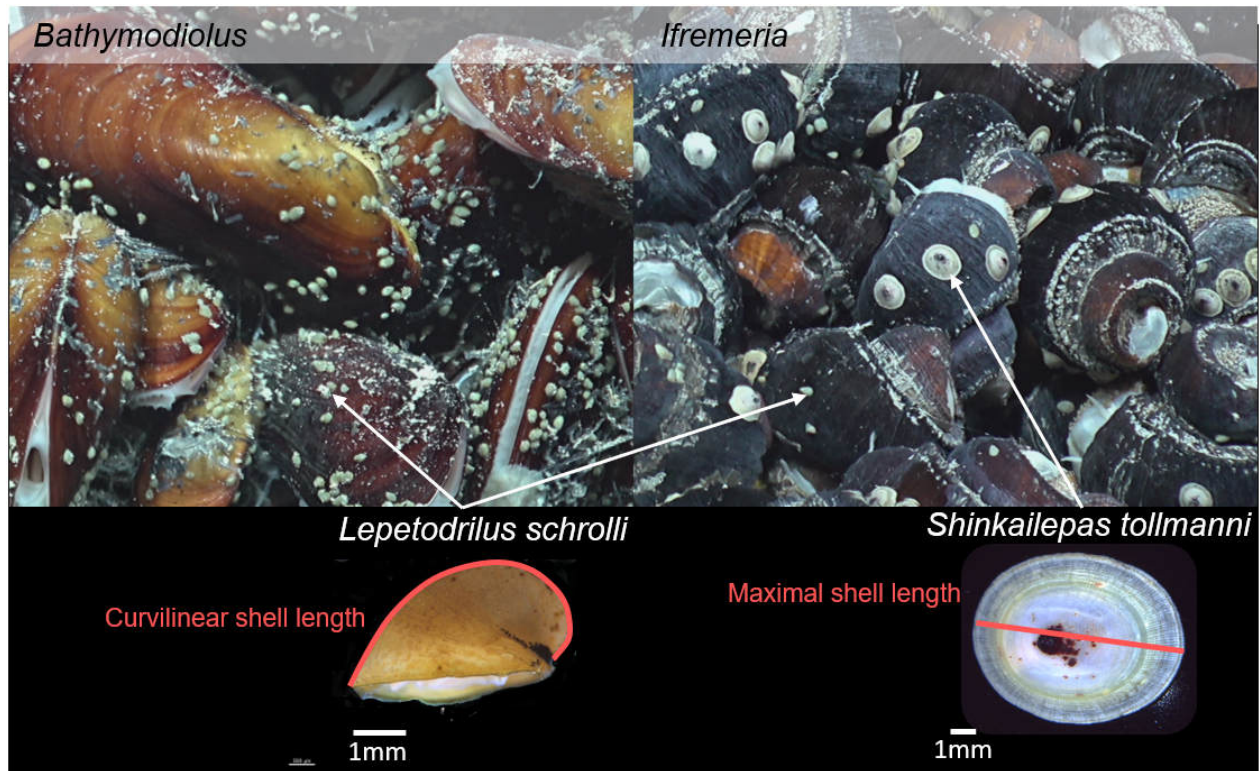


FIGURE B.1 – Illustrations of *Lepetodrilus schrolli* and *Shinkailepas tollmanni* inhabiting the complex three-dimensional habitat formed by *Bathymodiolus* and *Ifremeria* and the different shell measurements (in pink).

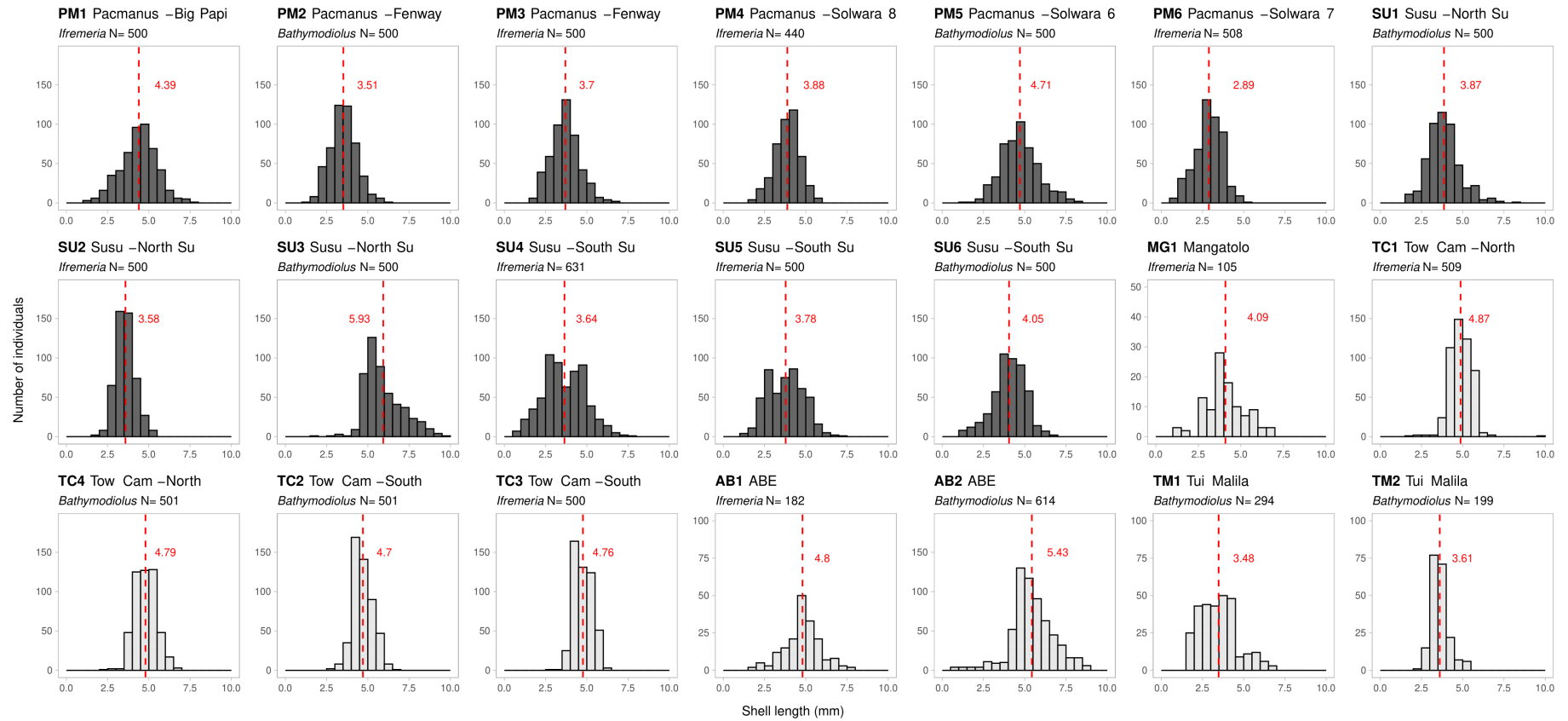


FIGURE B.2 – Size-frequency histograms of the curvilinear shell length of *Lepetodrilus schrolli* for each sample from the Manus (in black) and Lau Basins (in grey). N = number of measured individuals. The mean is indicated in red.

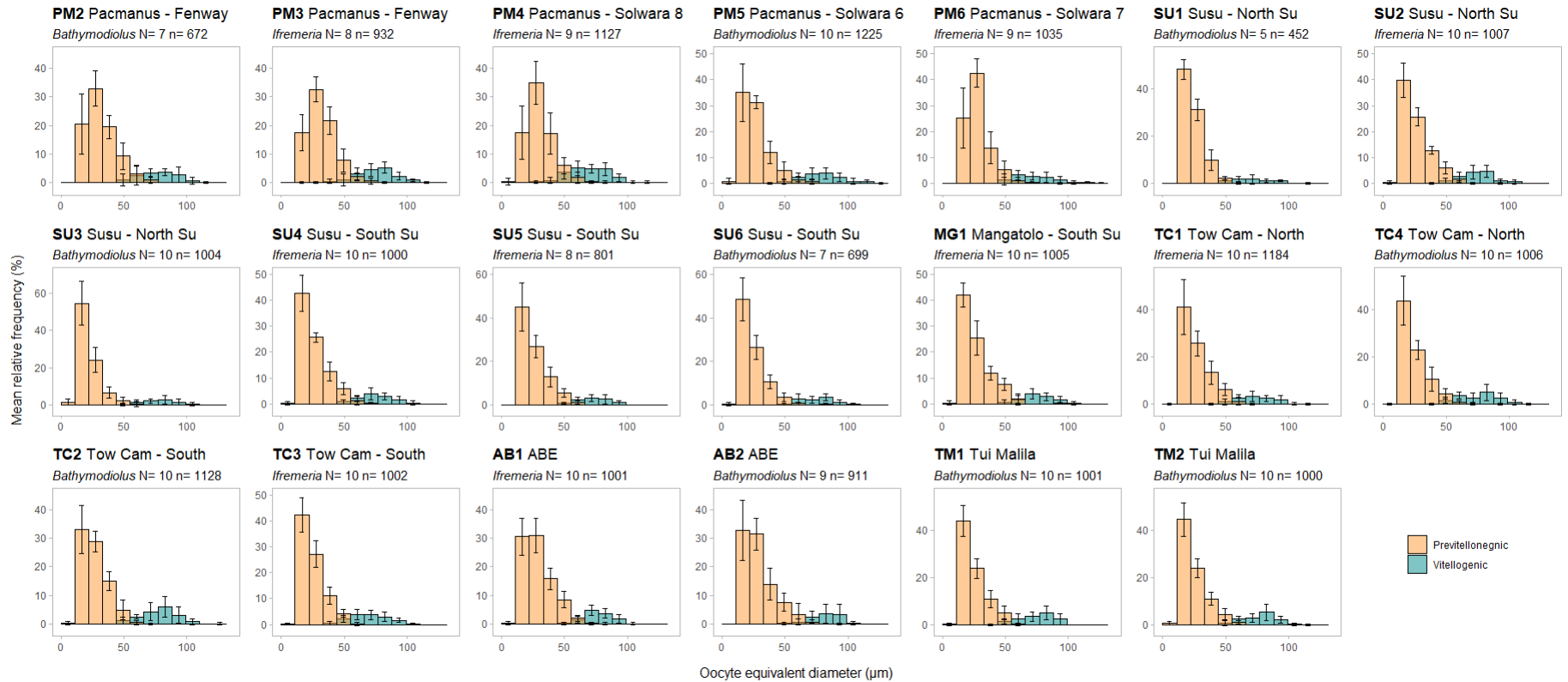


FIGURE B.3 – Mean oocytes size-frequency histograms of *Lepetodrilus shcrolli* females for each sample. N = number of females n= number of oocytes measured.

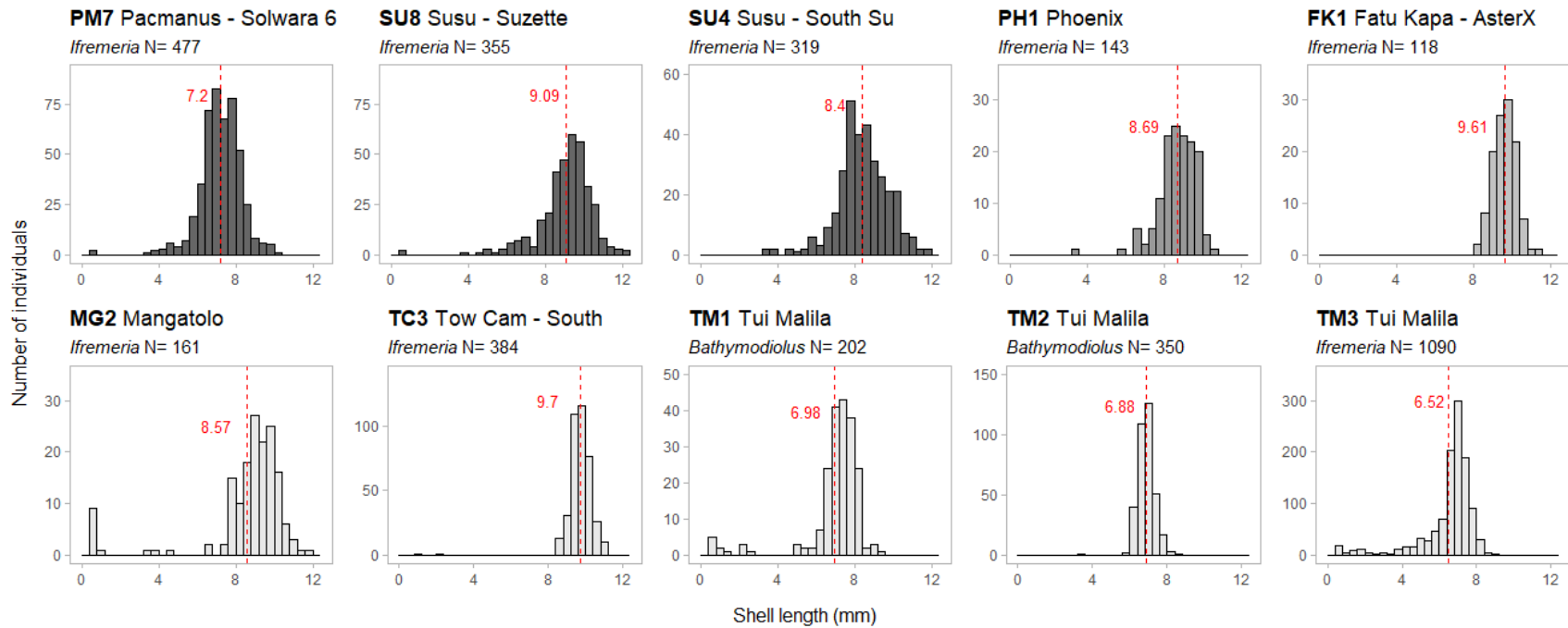


FIGURE B.4 – Size-frequency histograms of the maximal shell length of *Shinkailepas tollmanni* for each sample from the Manus Basin (in black), the North Fiji Basin (in dark grey), the Futuna Volcanic Arc (grey) and the Lau Basin (light grey). N = number of measured individuals. The mean is indicated in red.



## ANNEXE C

---

### Annexes du chapitre 3

---

**C.1 PCA based on scaled physico-chemical datas (without Methane)**

**C.2 dbRDA and variance partitioning**

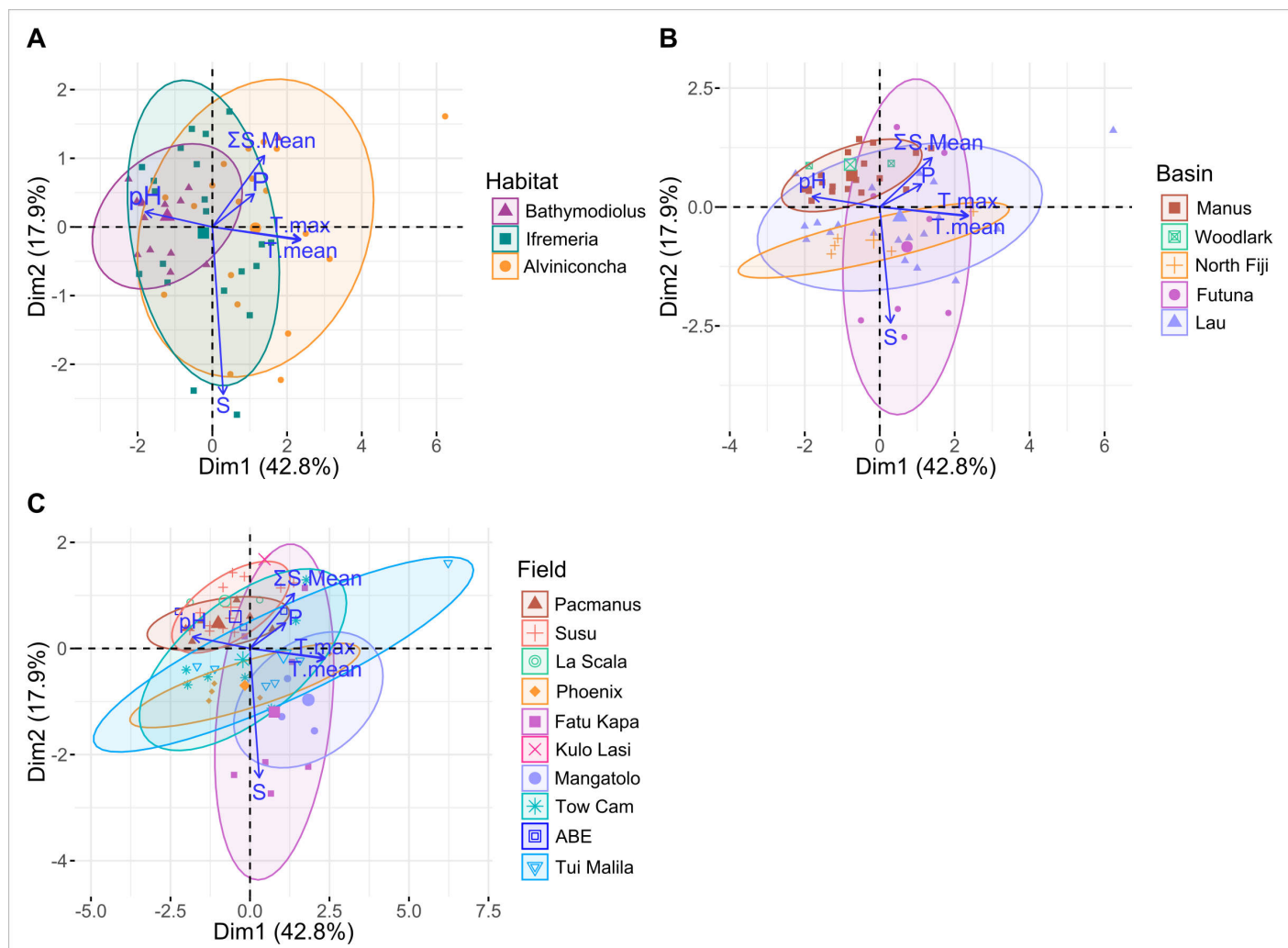


FIGURE C.1 – PCA based on scaled physico-chemical datas (without Methane). Graphs show axes one and two with ellipses constructed by habitat (A), basin (B) and field (C).

C.2 dbRDA and variance partitioning

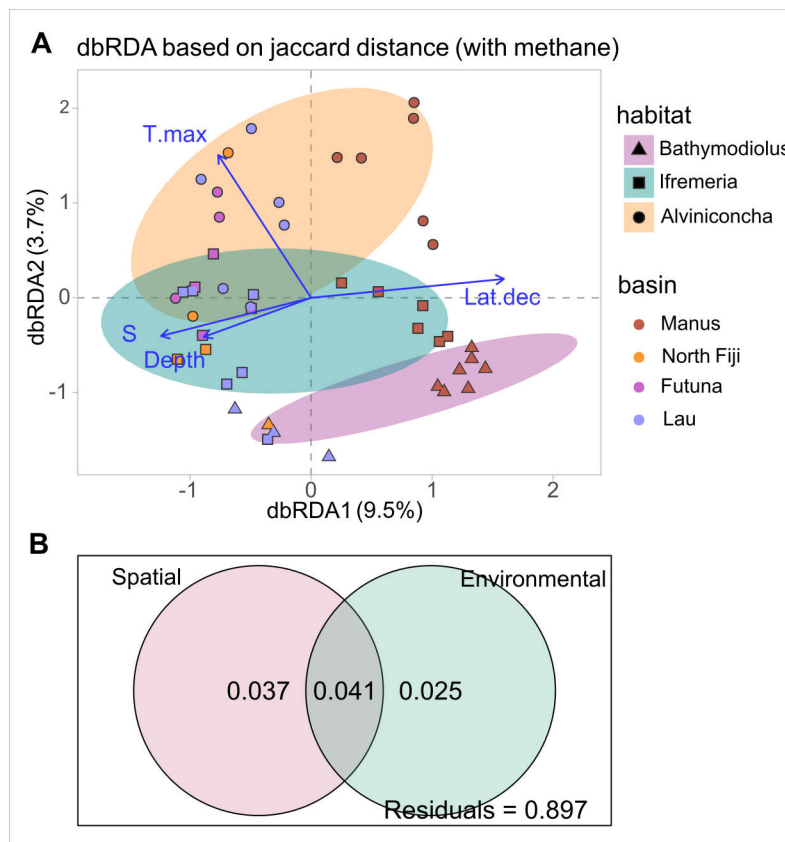


FIGURE C.2 – dbRDA (A) and variance partitioning (B) based on square root of Jaccard dissimilarities and environmental datas with methane.





## ANNEXE D

---

### Annexes générales

---

#### **D.1 Description du champ hydrothermal La Scala**

# communications

## earth & environment

ARTICLE


<https://doi.org/10.1038/s43247-022-00387-9>

OPEN

# Active hydrothermal vents in the Woodlark Basin may act as dispersing centres for hydrothermal fauna

Cédric Boulart <sup>1✉</sup>, Olivier Rouxel <sup>2</sup>, Carla Scalabrin <sup>2</sup>, Pierre Le Meur<sup>3</sup>, Ewan Pelleter<sup>2</sup>, Camille Poitrimol<sup>1,4</sup>, Eric Thiébaud<sup>1</sup>, Marjolaine Matabos <sup>4</sup>, Jade Castel<sup>1</sup>, Adrien Tran Lu Y<sup>5,6</sup>, Loic N. Michel<sup>4</sup>, Cécile Cathalot<sup>2</sup>, Sandrine Chéron<sup>2</sup>, Audrey Boissier<sup>2</sup>, Yoan Germain<sup>2</sup>, Vivien Guyader<sup>2</sup>, Sophie Arnaud-Haond<sup>7</sup>, François Bonhomme<sup>5</sup>, Thomas Broquet <sup>1</sup>, Valérie Cueff-Gauchard<sup>8</sup>, Victor Le Layec<sup>1,6</sup>, Stéphane L'Haridon<sup>8</sup>, Jean Mary<sup>1</sup>, Anne-Sophie Le Port<sup>1</sup>, Aurélie Tasiemski<sup>9</sup>, Darren C. Kuama<sup>10</sup>, Stéphane Hourdez<sup>6</sup> & Didier Jollivet<sup>1</sup>

Here we report the discovery of a high-temperature hydrothermal vent field on the Woodlark Ridge, using ship-borne multibeam echosounding and Remotely Operated Vehicle (ROV) exploration. La Scala Vent Field comprises two main active areas and several inactive zones dominated by variably altered basaltic rocks, indicating that an active and stable hydrothermal circulation has been maintained over a long period of time. The Pandora Site, at a depth of 3380 m, is mainly composed of diffuse vents. The Corto site, at a depth of 3360 m, is characterized by vigorous black smokers (temperature above 360 °C). The striking features of this new vent field are the profusion of stalked barnacles *Vulcanolepas* sp. nov., the absence of mussels and the scarcity of the gastropod symbiotic fauna. We suggest that La Scala Vent Field may act as a dispersing centre for hydrothermal fauna towards the nearby North Fiji, Lau and Manus basins.

<sup>1</sup>UMR 7144 AD2M CNRS-Sorbonne Université, Station Biologique de Roscoff, Place Georges Tessier, 29680 Roscoff, France. <sup>2</sup>IFREMER REM-GM, Technopôle Brest Plouzané, 29280 Plouzané, France. <sup>3</sup>GENAVIR, Technopôle Brest Plouzané, 29280 Plouzané, France. <sup>4</sup>IFREMER REM-EEP, Technopôle Brest Plouzané, 29280 Plouzané, France. <sup>5</sup>ISEM CNRS UMR 5554, Université de Montpellier 2, 34095 Montpellier Cedex 5, France. <sup>6</sup>UMR 8222 LECOB CNRS-Sorbonne Université, Observatoire Océanologique de Banyuls, Avenue du Fontaulé, 66650 Banyuls-sur-mer, France. <sup>7</sup>IFREMER UMR 248 MARBEC, Avenue Jean Monnet CS 30171, 34203 Sète, France. <sup>8</sup>Univ. Brest, Ifremer, CNRS, Laboratoire de Microbiologie des Environnements Extrêmes UMR6197, F-29280 Plouzané, France. <sup>9</sup>Univ. Lille, CNRS, Inserm, CHU Lille, Institut Pasteur de Lille, U1019-UMR9017-CIIL-Centre d'Infection et d'Immunité de Lille, Lille, France. <sup>10</sup>PNG Science and Technology Secretariat, University of Papua New Guinea, Port Moresby, Papua New Guinea. ✉email: [cedric.boulart@sb-roscoff.fr](mailto:cedric.boulart@sb-roscoff.fr)

Hydrothermal venting on the deep seafloor is the manifestation of heat and matter transfer from the lithosphere to the oceans, which modify their geochemical composition<sup>1</sup>. Upon mixing with the surrounding, cold, deep-sea water, a precipitation occurs and forms sulfide deposits on the seafloor. These hot and acidic fluids sustain diverse chemical-based ecosystems where large specialized bacterial and animal communities can thrive under extreme conditions of temperature, pressure, and pH<sup>2</sup>. Since the observation of the first active high-temperature vents more than 40 years ago<sup>3</sup>, the exploration of the deep ocean has revealed the existence of hydrothermal circulation in a wide range of geological settings from fast-spreading ridges<sup>4</sup> to ultra-slow ones<sup>5</sup> as well as in intraplate hotspots<sup>6</sup>, subduction zones<sup>7</sup>, and back-arc basins<sup>8</sup>.

Economic and societal interest in deep-sea hydrothermal vents has increased in the recent years because of the formation of massive polymetallic sulfide deposits<sup>9</sup> that are now targeted for deep-sea mining<sup>10</sup>, which may impact the deep ocean environment. The Woodlark Basin, located South of the Solomon Islands arc region in the Western Pacific Ocean, is a rather young (~5–7 Mya) oceanic basin that is subducting beneath the New Britain-San Cristobal Trench (Fig. 1). This is in fact one of the only places

on Earth where an active spreading centre expands into both continental crust to the West, and is bound by a subduction zone to the East<sup>11,12</sup>, therefore offering a wide range of geotectonic constraints for the development of seamounts and the possibility of forming high and low temperature hydrothermal venting along the axis. This may then provide a great diversity of niches for hydrothermal fauna and microbial colonization, and the potential settlement of associated fauna, provided that venting sites remain active over a long period of time.

The Woodlark Basin is characterized by an E–W active spreading axis that Goodliffe et al.<sup>13</sup> divided into five segments, numbered 1 through 5 from West to East (Fig. 1). The bathymetry shows major differences between the Eastern and Western parts, separated by the Moresby Transform Fault (TF), with a significantly shallower seafloor to the West, and a well-developed axial graben to the East<sup>14</sup>. Spreading rates vary from 38 mm yr<sup>-1</sup> in the West, to 67 mm yr<sup>-1</sup> on the Eastern part<sup>15</sup>. Hydrothermal activities are known to occur on only three segments of the ridge, which include confirmed volcanic activity on Segment 1 (Franklin Seamount<sup>11</sup>), and inferred hydrothermal venting thought to be due to punctual eruptive phases on Segment 3 and Segment 5<sup>12</sup>. Although recent exploration found consistent turbidity and redox

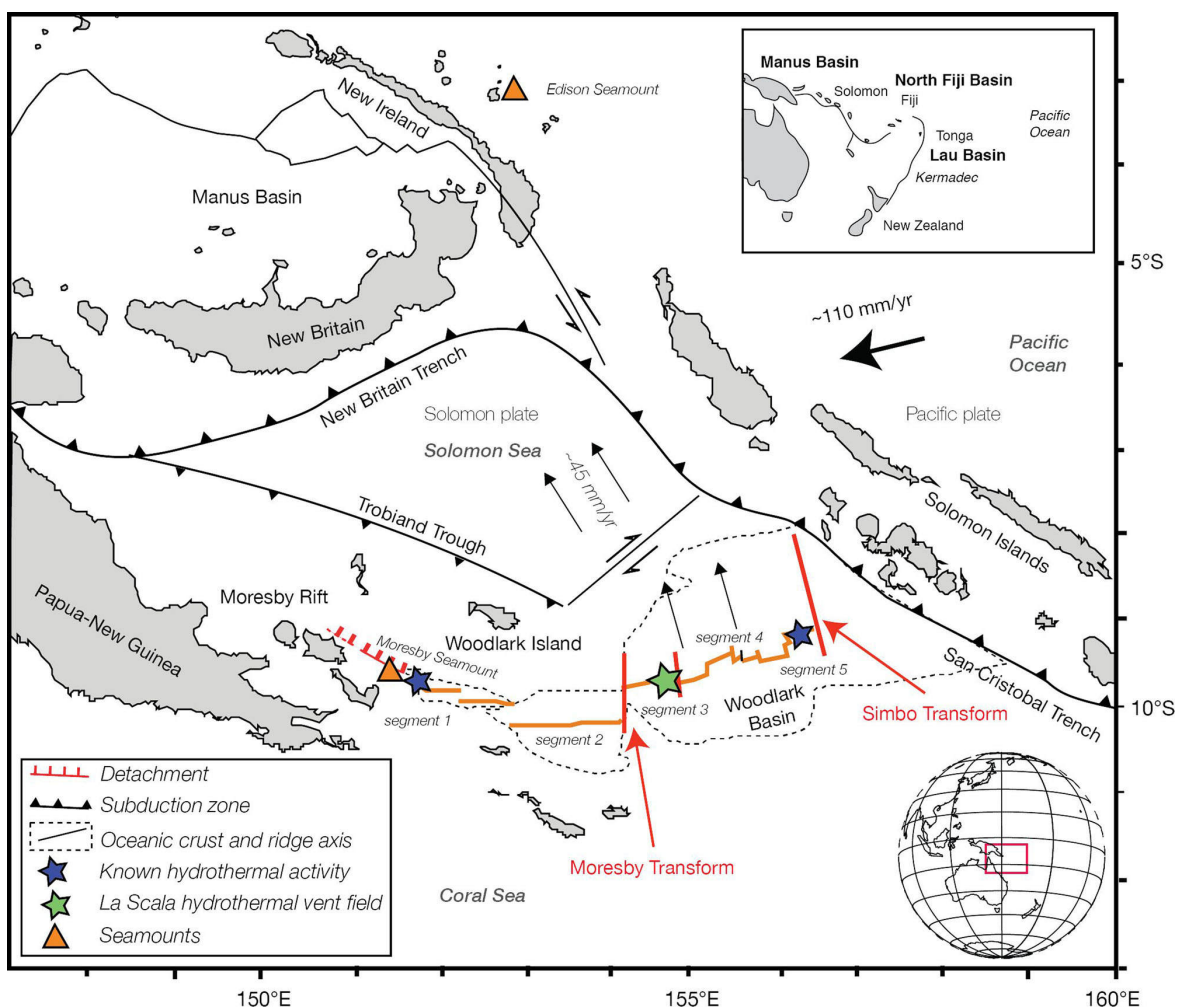


**Fig. 1 Regional map of the Woodlark Basin.** The main tectonic settings are highlighted as well as the location of the newly discovered 'La Scala' hydrothermal vent field (green star), modified from Laurila et al. (2012)<sup>12</sup>. Black arrows indicate the directions of plate motion relative to a fixed Australian plate.

potential anomalies at 2900 m below sea level (mbsl) over the eastern edge of Segment 3, Laurila et al.<sup>12</sup> concluded that “the complexity of the tectonics, i.e., frequent ridge jumps and re-orientation of the spreading axis, prevents high-temperature venting in one stable location and, hence the formation of sea-floor massive sulfide deposits”, suggesting that stable deep-sea vent communities may not be able to establish there.

Although not reported, the presence of perennial hydrothermal vent fields in the Woodlark Basin could constitute a stepping stone for hydrothermal fauna, at the intersection between the Manus Basin, the Edison Seamount, and the North Fiji and Lau basins, because of its possible link to the Northern expansion of the North Fiji basin which started about 10–11 Mya<sup>16</sup>. This spreading centre, now subducted, was presumed to bridge the older -and fossil- Solomon and South Fiji ridges that shaped the region before the collision of the Melanesian arc and the Ontong Java plateau about 18 Mya<sup>17</sup>. This collision coincides with the oldest dates of speciation events in the complex of gastropod species *Alviniconcha* which initiated 20 Mya<sup>18</sup>. The Woodlark Basin is older than the currently active spreading centres of the adjacent Lau (1–2 Ma) and North Fiji (3–4 Ma) basins, and therefore, may act as a biodiversity dispersion centre for the modern hydrothermal vent fauna at a crossroad between the Manus, North Fiji, and Lau basins.

During the CHUBACARC 2019 cruise (<https://doi.org/10.17600/18001111>), we carried out an extensive water-column survey of the eastern edge of Segment 3, using a strategy based on ship-borne acoustic survey followed by CTD-casts, to detect both thermal and chemical anomalies near the location where Laurila et al.<sup>12</sup> previously reported activity. Based on these observations, we then conducted a seafloor survey using the ROV Victor 6000 that led to the discovery of several high-temperature hydrothermal black smokers. Here, we report on the acoustic and chemical characterization of the hydrothermal plumes, the composition of endmember fluids, the geological setting of the vent fields, and the composition of the fauna associated with the newly discovered vent field we named ‘La Scala’.

## Results and discussion

**Hydrothermal plume exploration over the Eastern Woodlark Ridge.** As part of the high-resolution mapping—using the ship-borne multibeam echosounder (EM122 12 kHz)—carried out over Segment 3 (Fig. 2a), the water column imaging survey revealed the presence of echoes rooted to the seafloor in the vicinity of the ‘TVG-150’ marker<sup>15</sup>. These echoes, rising 200–300 m above the seafloor (Fig. 2b, Supplementary Fig. 1), remained visible at the same location at each passage of the ship over the area and showed the same features as the plumes previously observed in the Guaymas Basin<sup>19</sup>. During the CHUBACARC cruise, similar signals were also observed at shallower sites known to host active vents in the Manus Basin. These echoes were therefore attributed to the presence of hydrothermal plumes. It is commonly believed that deep hydrothermal plumes cannot be detected by water column acoustic imaging because of the absence of strong scatterers such as gas bubbles or droplets<sup>20</sup>. However, Ondréas et al.<sup>19</sup> showed that hydrothermal plumes down to 2000 mbsl could be identified using ship-borne multi-beam echosounding and differentiated from gas and liquid emissions. In the case of La Scala plumes, the backscattering mechanism may result from a combination of turbulence-induced temperature fluctuations within the first tens of metres of the vents and the presence of fine particles over the entire field at 100–500 m above the seafloor, which was later confirmed by the CTD surveys over the area (very strong turbidity signal and temperature anomalies >0.2 °C in the buoyant plume) and the

subsequent ROV dives. By modelling the acoustic characteristics of the hydrothermal plumes, Xu et al.<sup>21</sup> showed that particles had a predominant role in the acoustic backscatter with the height above the vents. It is worth noting that the success of this technique of detection strongly depends on the acoustic impedance difference between the hydrothermal fluid and the surrounding water, on the acoustic frequency, and on the sea state.

The subsequent CTD/tow-yo survey (Fig. 2c) first in the N–S direction and, then followed by a NE–SW transect crossing above the fluid echo showed turbidity (or nephelometry) anomalies at 2800 and 3300 mbsl i.e., at an altitude of 300–500 m above the seafloor (Fig. 3a, b), associated to manganese (Mn) anomalies (up to ~108 nM, Supplementary Data 1) and redox potential (Eh) signals. The strongest anomalies appeared to be consistent with the location of the echoes, confirming the presence of a buoyant plume.

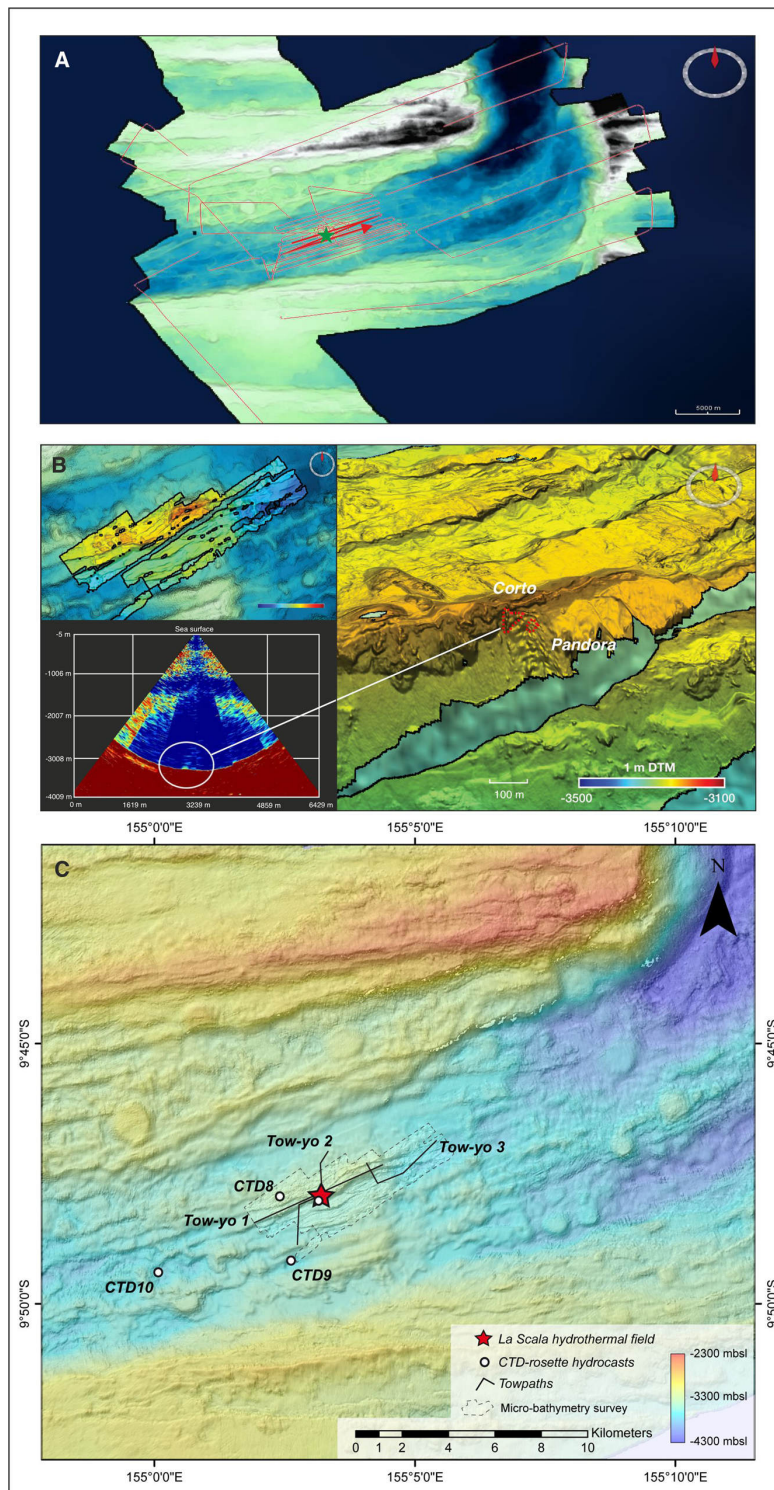
The second phase of the water column survey consisted of two vertical CTD casts (CTD-06 and CTD-07) above the strongest acoustic and chemical anomalies spotted during the MBES and the tow-yo survey. The data showed unambiguous anomalies of Eh, pH, potential temperature, density, and turbidity (Fig. 3c, d), which confirmed the presence of both buoyant and non-buoyant plumes. During CTD-06, we encountered a first turbidity anomaly (0.08 NTU) associated to an Eh signal at 2850 mbsl corresponding to a dispersing buoyant plume 500 m above seafloor. Below, a second, weaker turbidity anomaly (0.03 NTU) was found but not associated to any other chemical signal. Finally, very strong turbidity signals (up to 0.5 NTU), as well as temperature anomalies (~0.1–0.3 °C), were observed close to the seafloor (180 and 100 m above the seafloor) indicative of the presence of at least two hydrothermal plumes (Supplementary Fig. 2). The CTD-07 cast, conducted a few hours later and 60 m away from the CTD-06 location, showed a typical non-buoyant plume structure for turbidity and temperature (anomalies >0.2 °C), as well Mn varying from 34 to 265 nM. The CTD-07 vertical profile clearly indicated the presence of several black smoker-type sources spread out on the flank of the ridge, from 3300 to 3500 mbsl. These vents seem to generate a regional neutrally-buoyant plume dispersing northeastward at 2800–2850 mbsl.

Based on these exploratory results, an ROV dive close to the bottom led to the discovery of many active hydrothermal chimneys (i.e., black smoker types) and complex spires located between 3300 and 3400 mbsl, as well as a large diffuse venting area colonized by extensive communities of stalked barnacles (Fig. 4). The new vent field, discovered at coordinates 9°47S/155°03E was named ‘La Scala’, in recognition of the acoustic eyes of its discoverer.

Three additional CTD casts (CTD-08, 09, and 10, Fig. 2c) were carried out to estimate the dispersion of the plumes. While the CTD-08 profile showed some clear evidence of hydrothermal plumes dispersing at 2800–2900 mbsl, no anomalies were observed on the CTD-09 and CTD-10 profiles, located at 2.4 and 5.7 km, south and southwest of CTD-07, respectively (Supplementary Data 1). This may indicate a strong control of the dispersion of the plumes by the topography.

## Field observations of the La Scala Vent Field

La Scala Vent Field (LSVF) is located at a distance of 1.2 km North of the neovolcanic axis on the northern part of an old split axial volcanic ridge. The LSVF lies on a NE-trending talus slope and is composed of two main active areas and several zones with inactive chimneys (Fig. 2b). The first active site, named ‘Pandora’, is located Southeast of the field at 3380 mbsl and extends some 30 m by 10 m. It is characterized by predominantly diffusive vents, a few black smokers (Fig. 4a, b) and



extinct chimneys N20 aligned and colonized by an extensive coverage of stalked barnacles and patches of gastropods. The second active site of the field, named 'Corto', lies along a steeper slope at 3360 mbsl, only 15–20 m Northwest of the first site. It comprises a 50 m by 15 m sulfide zone where several 7–10 m tall, vigorous, high-temperature black smokers (Temperature

ranging from 364 to 366 °C, Table 1, Fig. 4c, d) were observed at the Southern edge.

Active hydrothermal chimneys are located on steep talus composed of hydrothermally encrusted basaltic rubble, chimneys fragments, and white blocks of hydrothermally altered volcanic rocks. Near the summit, just above the Corto site, a 30 m tall cliff

**Fig. 2 La Scala Vent Field bathymetry.** **A** Chubacarc cruise bathymetry image (20 m grid DTM (Digital Terrain Model), ship-borne MBES) corresponding to the water column acoustic surveys of the Woodlark Ridge (segment 3b). The green star locates the 'La Scala' hydrothermal field. **B** Northward 3D view of the high-resolution bathymetry image (1 m grid DTM, ROV VICTOR MBES) overlaid on the greyed 20 m grid DTM corresponding to the northern part of the old split axial volcanic ridge where LSVF is located. La Scala Vent Field including Pandora and Corto sites is delimited by the red dashed line, on the southern flank of the ridge together with the post-processed echogram of the second profile showing the echo attributed to LSVF. **C** Bathymetry of the segment 3 of the Woodlark Ridge from shipboard multibeam survey showing the location of LSVF as well as the towpaths and the CTD-hydrocasts. Note that CTD06 and CTD07 are located right above LSVF. TVG-150 spot from Laurila et al. (2012)<sup>12</sup> is not showed for clarity as it is 140 m away from LSVF.

is composed of pillow lavas topped by massive lava flows (Fig. 4e). On this same cliff, fifty metres Southwest of the second hydrothermal site, pervasive alteration zones and possibly oxidized massive sulfides exposed after a tectonic event (Fig. 4f) have been observed, indicating past hydrothermal activity in the area. Even though high-temperature chimneys could have formed during previous hydrothermal episodes, most ancient sulfide structures were probably destroyed during a collapse. Thus, at least two hydrothermal events occurred at LSVF. Based on the spreading rate ( $\sim 50 \text{ mm yr}^{-1}$ ) and the distance from the neo-volcanic axis ( $\sim 1.2 \text{ km}$ ), the maximum age of the first event of hydrothermal activity at LSVF can be estimated to be 24,000 years ago. This calculation, along with the presence of numerous inactive chimneys and altered lava, clearly indicates that an active and stable hydrothermal circulation has been maintained over a certain period of time and may not be the result of a recent and episodic volcanic eruption as previously suggested<sup>12</sup>.

#### Petrological and geochemical characteristics

Basement rocks recovered at LSVF are composed of rounded to sub-angular clasts of non-vesicular aphyric to plagioclase-pyroxene-phyric basalt (cm-size pebbles), cemented by a silica-rich matrix (quartz and cristobalite) and often coated by mm-thick iron oxyhydroxide crust. Pyrite and minor sphalerite are also identified by X-ray diffraction (XRD) confirming the importance of hydrothermal fluid circulation in basement rock alteration at LSVF. East of the vent field along the summit of the ridge crest, recovered basement rocks consisted of essentially aphyric and non-vesicular pillow lava with glassy chilled margin. Incipient to no alteration was identified. The volcanic crest is covered by thin sediment dusting composed of nanofossil-bearing clay.

Geochemical analyses of volcanic rocks show silica contents ranging from 48.4 to 48.7 wt% and low alkali contents ( $\text{Na}_2\text{O} + \text{K}_2\text{O}$ ) from 2.7 to 2.9 wt% (Supplementary Table 1). Thus, all samples from the LSVF area are tholeiitic basalt similar to mid-ocean ridge basalt (MORB) composition (Supplementary Fig. 3). Glassy pillow margins contain 9.1–9.5 wt% MgO suggestive of rather primitive melt. To our knowledge, these are the first report of basaltic rock composition along Segment 3 of the Woodlark Basin in agreement with the previous studies along Eastern Segment 4<sup>22,23</sup> and consistent with MORB composition with major element variations resulting from fractional crystallization.

#### Sulfide deposits and hydrothermal fluids

Three different types of mineralization (Fig. 4 and Supplementary Data 2) were observed and sampled during the subsequent ROV dives: (1) active high-temperature sulfide/sulfate chimneys without significant presence of sessile animals; (2) inactive black smoker chimneys; (3) massive sulfide recovered at the base of either active or inactive complex spire densely colonized by vent organisms. Mineralogical and petrological descriptions show that anhydrite is the dominant mineral in the top section of active black smoker chimney, followed by chalcopyrite, sphalerite, and pyrite towards the inner and lower section of the chimney. Multiple vigorously venting internal conduits are lined with fine

grained euhedral chalcopyrite while chimney walls are composed of mixed mineral assemblages of chalcopyrite, sphalerite, and pyrite. Inactive chimneys and massive sulfides have essentially similar characteristics to active chimney except that anhydrite is absent due to retrograde dissolution and chimney wall are consolidated by more massive pyrite/marcasite assemblages, and thinly encrusted by Fe oxyhydroxide crust.

Sulfide deposits show a wide range of copper (Cu) and zinc (Zn) concentrations reflecting the abundances of chalcopyrite versus sphalerite, while calcium (Ca), strontium (Sr), and silica (Si) reflect the abundance of anhydrite and silica respectively (Suppl. Data 3). As previously recognized<sup>24</sup>, trace elements such as cadmium (Cd) and lead (Pb) are associated with lower-temperature sphalerite-rich mineral assemblages. Average compositions are relatively similar between sulfide deposits, except for the Carioca black smoker characterized by lower Cu and higher cobalt (Co) concentration, up to 0.6 wt% in pyrite-rich samples. High Co contents in basalt-hosted sulfide chimneys have been previously inferred as reflecting a higher magmatic contribution to the hydrothermal fluid<sup>24</sup>. By comparison with average compositions of sulfide mineralization in other tectonic environments in the modern seafloor, LSVF lacks any of the geochemical features of back-arc settings (e.g., gold and Pb enrichment) and is seemingly identical to other basalt-hosted hydrothermal fields along mid-oceanic ridges.

Sulfur isotope analysis was performed on the mineral fractions of pyrite and chalcopyrite of four samples, yielding a range of  $\delta^{34}\text{S}$  values between 1.96‰ and 4.20‰, with an average of 3.03‰ (Supplementary Data 3). Slightly higher  $\delta^{34}\text{S}$  values in the Carioca black smoker indicate a seawater contribution to the hydrothermal fluid in the upflow zone. Such  $\delta^{34}\text{S}$  values are typical of sulfide mineralization from mid-oceanic ridge settings (Supplementary Fig. 4) and suggest no contribution of magmatic  $\text{SO}_2$  ( $\delta^{34}\text{S} < 0\text{‰}$ ) as encountered in back-arc basin hydrothermal systems (e.g., Lau Basin and Manus Basin). Altogether, these results are consistent with the basaltic rock composition and indicate that the magmatic activity on the ridge segment is not directly related to subduction but rather to accretion.

Hydrothermal vent fluids were recovered from three black smoker chimneys from LSVF, all showing remarkably homogeneous venting temperature of  $\sim 365 \text{ °C}$  (Table 1 and Supplementary Table 2). All recovered vent fluids have non-zero magnesium (Mg) concentrations due to significant seawater entrainment during sampling. Endmember composition of vent fluids are conventionally assumed to be devoid of Mg, because of the quantitative removal of Mg from seawater during hydrothermal interactions with basalt<sup>25,26</sup>. Calculated end-member hydrothermal fluid compositions are reported in Table 1 for all measured elements.

Homogeneous end-member compositions suggest that LSVF is fed by a deep-seated hydrothermal fluid source undergoing minor subsurface fluid mixing. The lowest pH value (3.31) was recorded in Carioca vent fluids consistent with the lowest Mg concentration of 1.6 mM, which suggests minor seawater contribution during sampling. Hence, the end-member pH value is considered to be close to 3.3 for all vents. All end-member vent fluids have

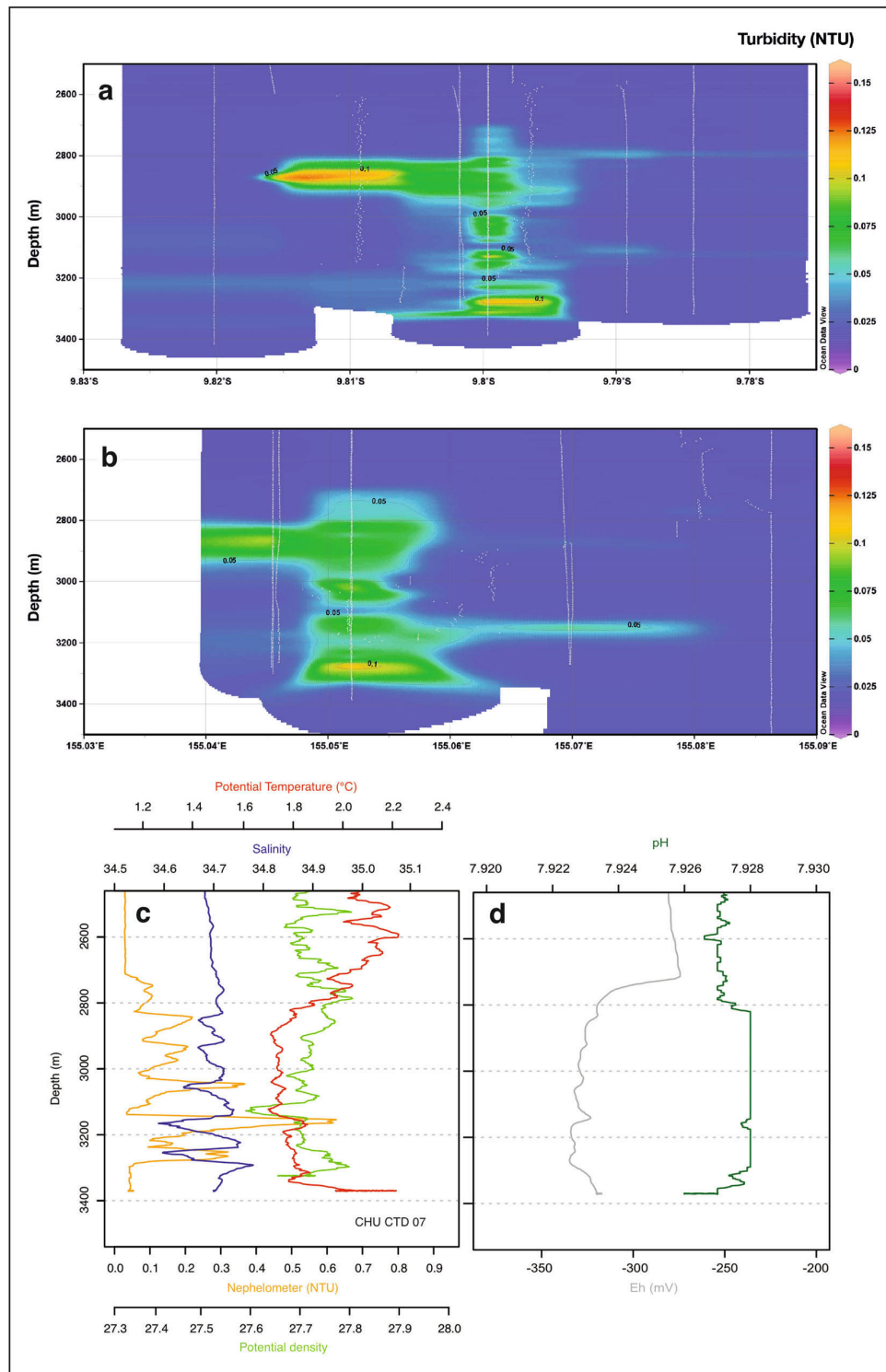


**Fig. 3 Physico-chemical characteristics of hydrothermal plumes above La Scala Vent Field.** N-S (a) and NE-SW (b) sections of turbidity anomalies above Segment 3. The section compiles data from tow-yo surveys (CTD-01 to CTD-03) and vertical casts (CTD-06 and CTD-07) (grey lines). **c, d** Nephelometry (yellow), density (light green), salinity (blue), temperature (red), Eh (grey), and pH (dark green) vertical profiles in the non-buoyant plume of ‘La Scala’ vent site (CTD-07).



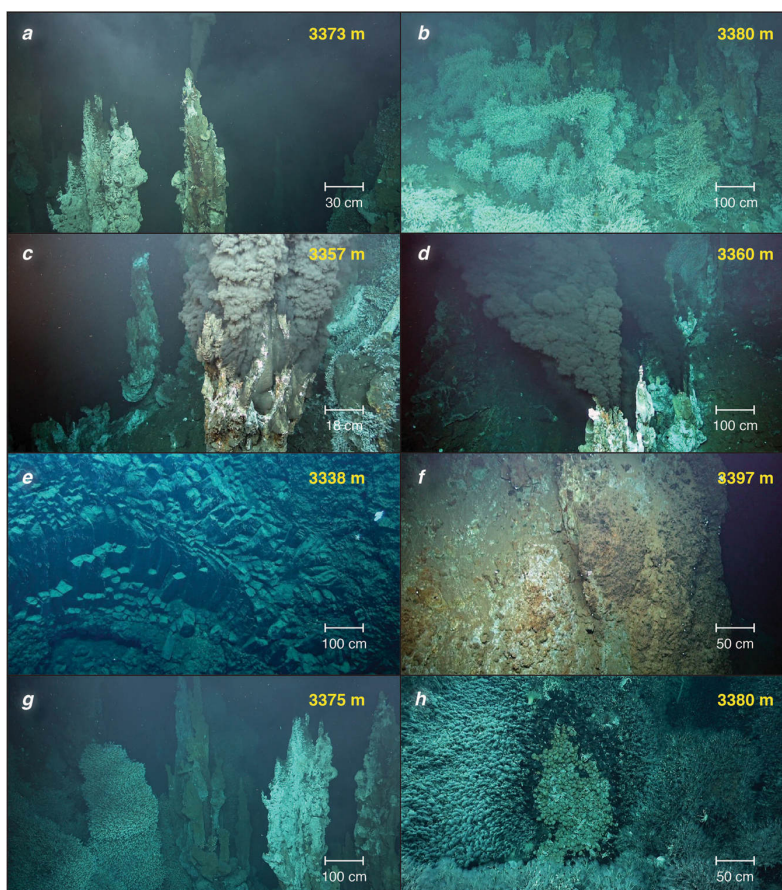


**Fig. 4 La Scala Vent Field.** **a, b** Chimney cluster ('Pandora Site'), SE of the vent field at 3380 m depth characterized by a few black smokers and predominant weakly diffusive vents. This site is surrounded by cirripeds to the West, North and East. **c, d** Second site ('Corto Site') located on the flank of a cliff controlled by a N55-60 fault. The South area at 3360 m depth is the most active of the hydrothermal field. **e** Massive prismatic lava. **f** Highly altered basalts due to past high temperature hydrothermal circulation. **g** Large colonies of *Vulcanolepas* sp. colonizing inactive chimneys. **h** A patch of *Alviniconcha* endosymbiotic gastropods surrounded by *Ifremeria nautiliei* and *Vulcanolepas* sp.

chlorinities higher than seawater suggesting they have undergone sub-critical phase separation. Alkali concentrations ( $K \approx 25.4$  mM;  $Rb \approx 15.6 \mu\text{M}$ ) are similar to most basaltic-hosted vent sites consistent with LSVF geological setting. Silica (Si), iron (Fe) and Mn concentrations are  $\approx 20$  mM,  $\approx 1.7$  mM, and  $\approx 1.0$  mM, respectively. Fe/Mn ratio of 1.7 is however lower than values expected from the vent temperature<sup>27</sup>, suggesting possible sub-surface sulfide precipitation. Endmember Cu and  $\text{H}_2\text{S}$  concentration of  $21 \mu\text{M}$  and  $4.1$  mM respectively, are also lower than typical high temperature (i.e.,  $>350$  °C) vent fluids, lending further support to this hypothesis.

#### Hydrothermal vent fauna

LSVF is characterized by several very active black smoker chimneys whose surface is occupied by a sparse population of *Rimicaris* shrimp and very large beds of a new species of stalked barnacles, *Vulcanolepas* sp. nov., that colonizes mildly active diffuse venting areas and old inactive chimneys or sulfide mounds (Fig. 4g). The dominant engineer species and their associated fauna were comparable to other Southwest Pacific vent communities but differed in relative abundance<sup>28–30</sup>. Stalked barnacles covered vast areas (c.a.  $>300$  m<sup>2</sup>) on the seafloor while large symbiotic gastropods were rare and restricted to patches smaller

than in other Western Pacific back-arc basins. Patches of small-sized gastropods *Ifremeria nautiliei* and *Alviniconcha* spp. were observed in the most active diffuse areas with temperatures varying from  $2.4$  to  $7.3$  °C (average of  $4.6 \pm 1.3$  °C) and  $2.5$ – $20.3$  °C (average  $8.5 \pm 4.4$  °C), respectively (Fig. 4h). Cirripeds *Eochinelaemus ohtai* and *Imbricaverruca* sp. were found next to *Ifremeria nautiliei* and *Alviniconcha* spp. communities (Fig. 5). Aggregations of alvinocaridid shrimp *Rimicaris variabilis*, *Branchinotogluma segonzaci* polynoids, and *Shinkailepas tufari* phenacolepadid gastropods were also observed on active chimneys (Fig. 5f). Extensive bacterial mats were also noticed at the periphery of the vents, as well as bamboo corals (Isididae), squat lobsters (Munidopsidae), brisingid starfish, crinoids, and sea anemones (Supplementary Fig. 5). Morphological identification of the benthic fauna collected and observed from videos was compiled as a list of at least 45 taxa, including 23 families and 23 genera (Supplementary Data 4). The macrofauna associated with *Vulcanolepas* sp. nov. was mainly composed of the barnacle *Imbricaverruca* sp., members of the polychaete families Ampharetidae (*Amphisamytha* cf. *vanuatuensis*), Maldanidae (*Nicomache* spp.), and Spionidae, and the provannid gastropod *Provanna* sp. (Supplementary Data 5). Many copepods and nematodes were also part of this community. Holothurians *Chiridota* sp., anemones (Actiniaria), squat lobsters, *Austinograea*

Table 1 Temperature, pH, and chemical composition of La Scala fluid endmembers.

Temp (°C)	pH (21 °C)	H <sub>2</sub> S mM	Mg mM	Cl mM	SO <sub>4</sub> mM	Na mM	S mM	K mM	Ca mM	Sr μM	Li μM	B μM	Rb μM	Cd μM	Ba μM	Si μM	Mn μM	Fe μM	Cu μM	Zn μM
Bottom SW	7.5	0.00	55.75	546	28.2	474	29.8	9.1	10.6	99	27	435	1.5	<0.1	0.08	122	<0.1	<1	<0.1	<0.1
Black smoker 6	364	>2.2	0	633.2	2.0	561	2.7	25.3	31.7	115	1163	763	15.6	0.2	9.4	20074	1019	1602	39.9	108.1
Black smoker 5	366	4.0	0	634.9	1.4	543	2.1	25.4	31.0	115	1208	749	15.6	0.1	17.1	19795	1019	1848	10.8	50.6
Black smoker 8	365	4.1	0	647.9	1.5	548	5.4	25.6	31.5	115	1198	757	15.6	0.1	14.6	20122	1028	1707	12.6	39.8

crabs and *Phymorhynchus* sp. gastropods were also found among and next to *Vulcanolepas* sp. nov. thickets. A sample collected in an *Ifremeria nautili* patch showed that the associated macrofauna was dominated by an undescribed peltospirid limpet and polynoid scaleworms, and formed the most diverse assemblage in term of species richness. *Amphysamytha* cf. *vanuatensis* and alvinellid worms (genus *Paralvinella*) were also found in *Ifremeria nautili* and *Alviniconcha* spp. communities. Copepods, bythograeid crabs (*Austinograea* sp., which is likely to represent a new species), *Rimicaris variabilis* shrimp and polychaetes were the dominant taxa found in *Alviniconcha* spp. patches.

Most of the fauna had  $\delta^{34}\text{S} < 10\text{‰}$  (Fig. 6), suggesting they primarily depend (either directly or indirectly) on chemosynthetic vent production and sulfide oxidation for their nutrition<sup>31</sup>. This was notably the case of organisms considered as peripheral fauna, or not strictly found at vents, such as *Vulcanolepas* sp. nov., anemones, or *Phymorhynchus* sp.. Brisingidae starfish, holothurians *Chiridota* sp., and carnivorous sponges had  $\delta^{34}\text{S}$  between 10 and 15‰, suggesting a mixed diet, depending on both chemosynthesis- and photosynthesis-derived organic matter<sup>31</sup>. Only the Isididae bamboo corals had a  $\delta^{34}\text{S}$  greater than 15‰, suggesting they primarily feed on exported photosynthetic production<sup>31</sup>. Overall, the dependence of organisms on vent endogenous production seemed significant, and spanned all sampled taxonomic and functional groups. Similar observations have been made in active<sup>32</sup> and inactive<sup>33</sup> hydrothermal vents from the Manus basin. In contrast, the dependence of hydrothermal fauna on exported photosynthetic matter is higher at shallower vents of the Southern Tonga arc<sup>34</sup>. The increased importance of endogenous production for deeper sites matches patterns observed in other chemosynthesis-based habitats<sup>35,36</sup>.

While  $\delta^{34}\text{S}$  values ruled out major photosynthetic contributions, the wide ranges of  $\delta^{13}\text{C}$  and  $\delta^{15}\text{N}$  measured in Woodlark fauna suggest that animal communities show considerable trophic diversity, and depend on several production mechanisms (Fig. 6). Some species had very negative  $\delta^{13}\text{C}$  (e.g., *Alviniconcha kojimai*, *Ifremeria nautili* or *Provanna* sp.), suggesting they mostly depend on sulfide oxidizers using the Calvin–Benson–Bassham (CBB) cycle for their nutrition<sup>37</sup>. Conversely, some species, such as *Alviniconcha boucheti* or *Branchinotogluma segonzaci* had very positive  $\delta^{13}\text{C}$ , suggesting they acquire most of their organic matter from sulfide oxidizers using the reverse tricarboxylic acid (rTCA) cycle<sup>37</sup>. Interestingly, many taxa had intermediate  $\delta^{13}\text{C}$  values comprised between those two end-members, suggesting a co-reliance on both bacterial metabolisms in variable proportions. Similar findings have been reported for the Manus Basin<sup>32,38</sup>. However, in Manus, communities seem to be mostly supported by the CBB cycle, particularly at the Solwara 1 site<sup>32</sup>. In Woodlark, our results suggest that inter- (and sometimes intra-) taxon differences in feeding preferences could lead to a more evenly balanced continuum of  $\delta^{13}\text{C}$  values, and therefore the importance of the two production mechanisms for the food web. Finally,  $\delta^{34}\text{S}$  of Woodlark fauna was similar to some hydrothermal vents from the Manus Basin (Solwara 1, PACMANUS), but markedly higher than other Manus sites (e.g., South Su)<sup>32</sup>. This suggests that local changes in sulfur geochemistry could influence this parameter and the way secondary consumers are locally distributed.

#### Genetic characterization of the main ecological engineer species

As other vent communities of the western Pacific back-arc basins, engineer species observed at LSVF are mainly composed of stalked barnacles, and provannid gastropods that belong to the genera *Alviniconcha* and *Ifremeria*. *Bathymodiolus* mussel beds

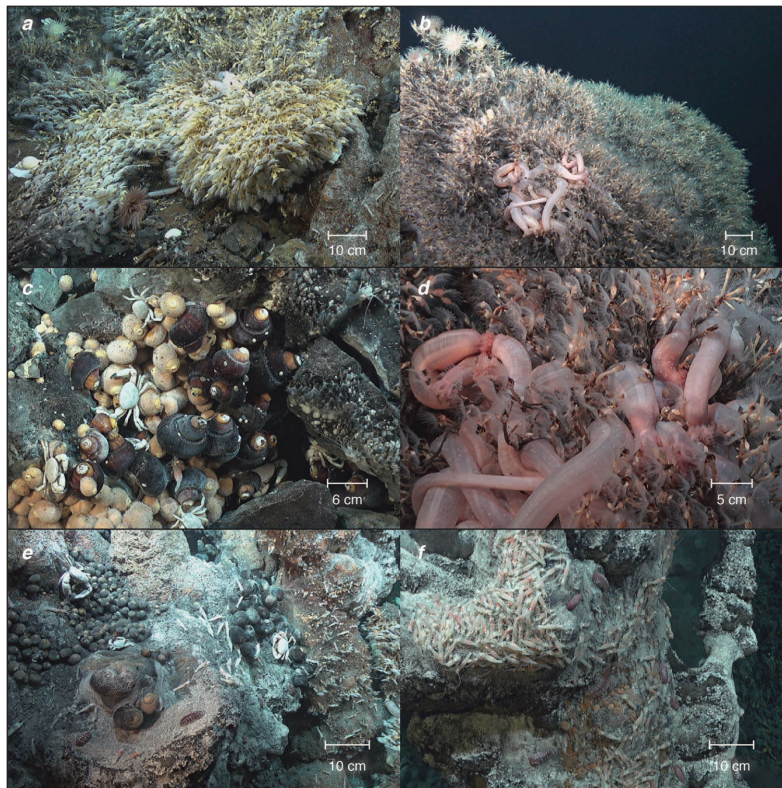


**Fig. 5 Hydrothermal fauna from La Scala Vent Field.** **a** *Vulcanolepas* sp. n. thickets, anemones and gastropod *Phymorhynchus* sp. **b** Anemones and holothurian *Chiridota* sp. in *Vulcanolepas* sp. n. thickets. **c** Aggregation of gastropods *Ifremeria nautilei* and *Alviniconcha kojimai* with *Austinograea* crabs and cirripeds *Eochionelasmus ohtai* and *Imbricaverruca* sp. (right side of the picture). **d** *Chiridota* sp. in *Vulcanolepas* sp. n. thicket. **e** Aggregation of *Alviniconcha kojimai*, polynoids, alvinocarids shrimps, and *Austinograea* crabs. **f** Aggregation of alvinocarid shrimp *Rimicaris variabilis*, polynoids *Branchinotogluma segonzaci* and gastropod *Shinkailepas tufari* on active chimney.

were surprisingly not found at Woodlark. A first genetic examination of stalked barnacles using a 658-bp fragment of the mitochondrial cytochrome c oxidase (*Cox1*) gene clearly indicated that, while falling into the *Vulcanolepas* clade (support 0.66), specimens from Woodlark form a distinct phylogenetic clade (support 0.99, within clade pairwise Jukes–Cantor distances  $0.22 \pm 0.21\%$ ) and therefore represent a new putative species (Fig. 7). This new species is surprisingly most closely related to the species found at vents on the Kermadec volcanic arc (*V. osheai*,  $6.86 \pm 0.23\%$  average Jukes–Cantor distances), and a bit more distantly to the species found at vents in the Lau Basin (*V. buckeridgei*,  $7.35 \pm 0.33\%$  average Jukes–Cantor distances) or the species *Leucolepas longa* from Lihir island<sup>39</sup>. Interestingly, for this genus, each sampled area seems to host a distinct species. *Alviniconcha* and *Ifremeria* gastropods were not numerous (distributed as small patches at the base of chimneys) and of rather small size, suggesting that they may represent genetically differentiated populations when compared to other described species elsewhere. All individuals collected at Woodlark were thus bar-coded using a 659 bp-fragment of mitochondrial *Cox1* gene to build haplotype networks and test their relationships with previously described species. For *Alviniconcha*, the use of previously published sequences yielded 5 clusters that correspond to the currently described species. *Alviniconcha* specimens collected at La Scala fall into two equally represented but distinct species, *A. boucheti* and *A. kojimai*, but are not geographically distinct from populations collected in other basins, at least using this genetic marker (Supplementary Fig. 6). *Ifremeria* specimens fall into two

main clusters separated by five fixed substitutions (divergence = 0.75%, Fig. 8): one that mainly comprises specimens from the Manus and Woodlark basins and one that comprises specimens from other basins (Lau, North Fiji, and Futuna) (Fig. 8 and Supplementary Fig. 6). Remarkably, a few specimens from Futuna and Lau however, fall into the Manus/Woodlark cluster. This suggests a possible recent migration from the Woodlark ridge to the Northern part of the Lau basin (including Futuna) following a first geographic isolation event of the Manus and Lau/North Fiji/Futuna populations in allopatry. These preliminary results clearly indicate that vent species have contrasted population histories. Some of the species are clearly endemic of the Woodlark ridge (a possible separation due to the greater depth) whereas others may use it as a stepping stone during the colonization of the present-day back-arc basins of the Western Pacific.

#### The Woodlark Ridge: A potential biological cornerstone?

The tectonic history of the western Pacific back-arc basins is complex<sup>17</sup>. The opening of some basins such as Manus, Lau, and North Fiji is recent (less than 4–3 millions years)<sup>17,40,41</sup>, and likely simultaneous, even if the formation of the North Fiji proto-basin initiated before about 10–12 Mya<sup>16</sup>. This points towards the existence of older relay-ridges for the vent fauna before their opening of the present-days basins as previously mentioned to explain the spatial distribution patterns of the symbiotic gastropod *Alviniconcha* spp<sup>18</sup>. In this context, the present-day distribution of the hydrothermal vent fauna likely results from the partition of an older hydrothermal fauna originating from ridges

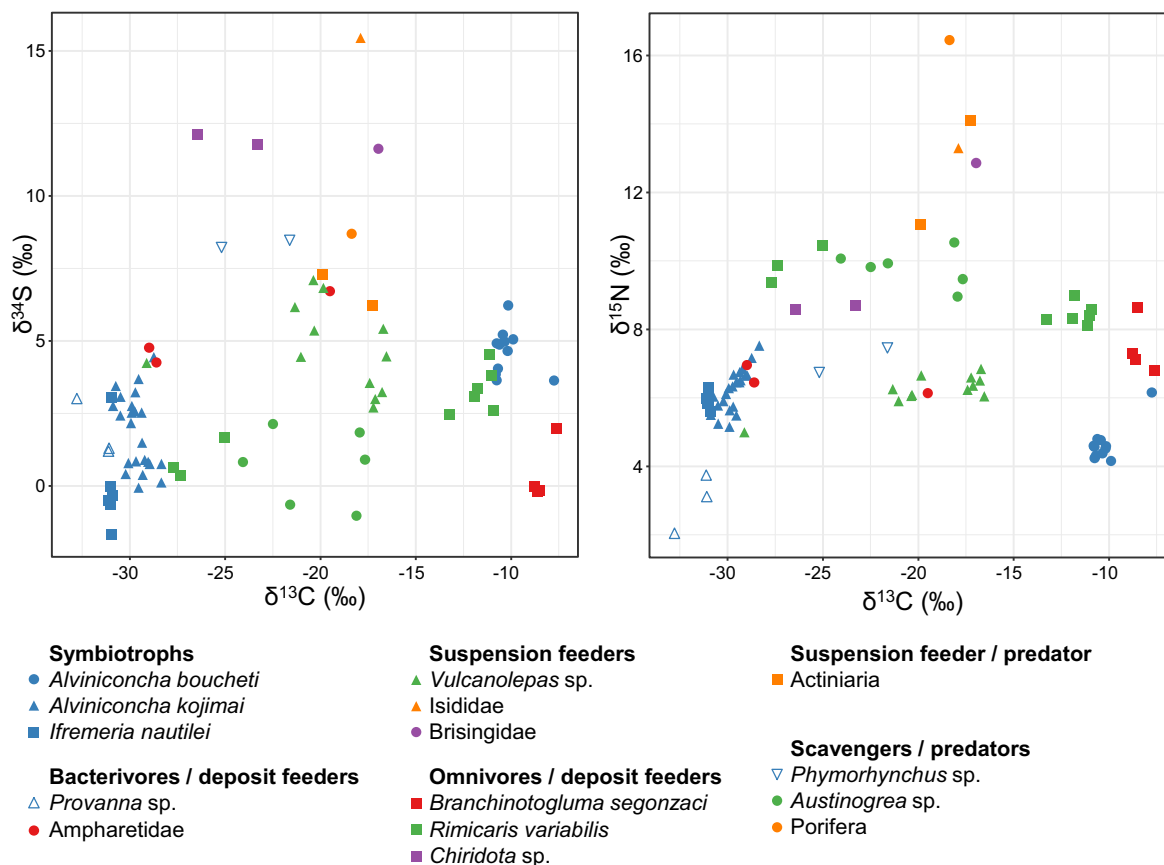
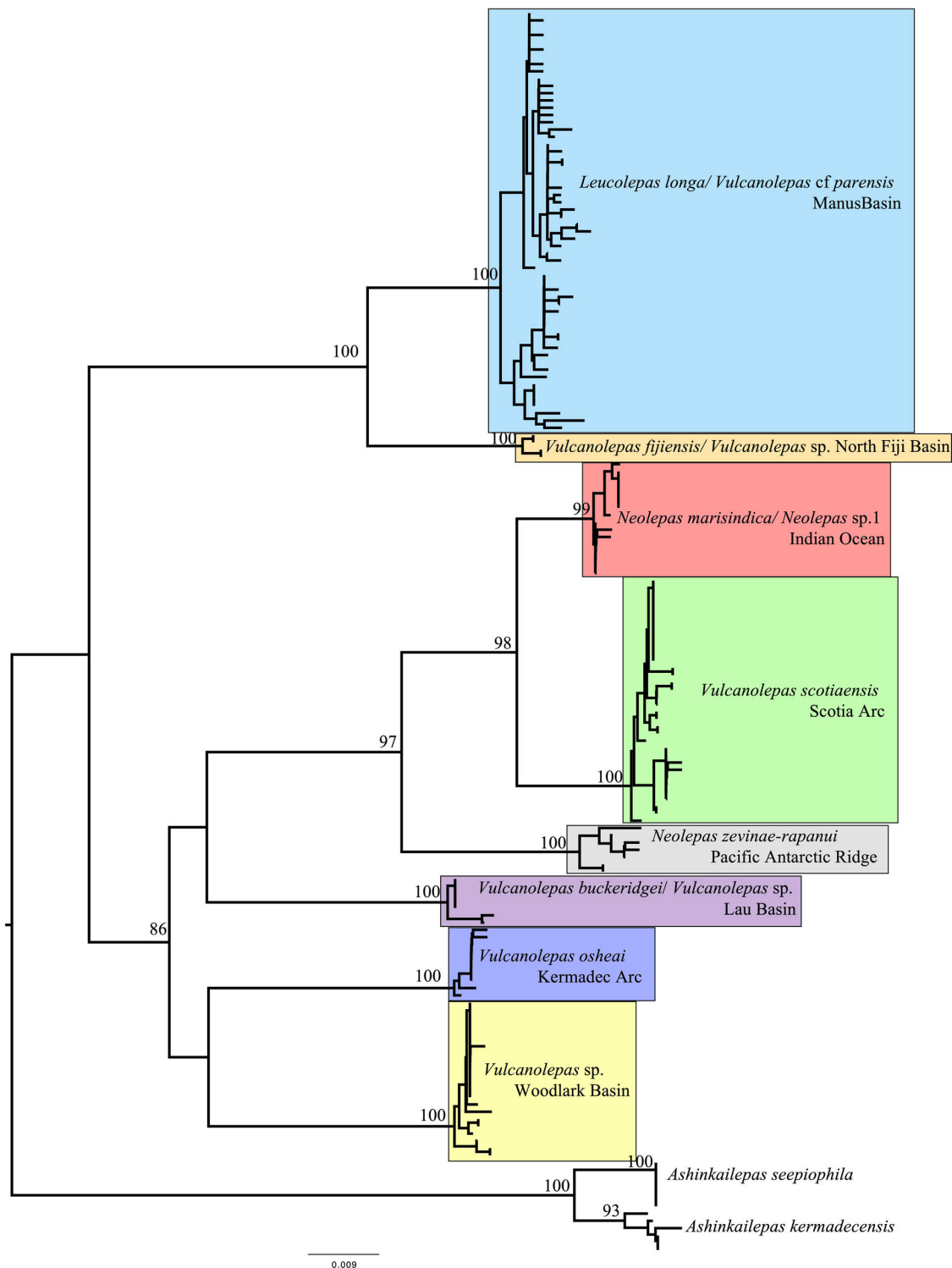


**Fig. 6 Stable isotope food web diagram of LSVF animal communities.** Stable isotope ratios of carbon vs. sulfur (left) and carbon vs. nitrogen (right) in benthic fauna from La Scala, Woodlark Basin. Blue: molluscs, red: polychaetes, green: crustaceans, orange: sponges and cnidarians, purple: echinoderms. Organisms have been assigned to functional feeding guilds according to literature data.

that have now disappeared by subduction (Fig. 9). The inactive South Fiji or Solomon ridges are relicts of such past ridge systems<sup>17</sup> and may have been transiently linked by the formation of the North Fiji proto-basin after the collision of the Melanesian arc and the Ontong Java plateau about 18 Mya. Amongst back-arc basins, the Woodlark ridge opened (about 6–7 million years<sup>17</sup>) at a time where the northern expansion of the North Fiji proto-basin became extinct, and corresponds to a region that may still contain traces of older dispersal pathways during the Oligocene (i.e., the Solomon Seaway). The Woodlark ridge could thus act as a biodiversity dispersion centre for the modern hydrothermal vent fauna and a crossroad between the Manus, North Fiji, and Lau Basins. To this extent, the discovery of the LSVF on Segment 3 of the Woodlark ridge represents an important opportunity to study the biogeography of the vent fauna associated with back-arc basins. A first examination of our list of species collected at La Scala indicates that the Woodlark assemblage is not noticeably different from other Western Pacific assemblages. It also shows that the basalt-hosted MOR vent system (such as La Scala) and its greater depth do not represent a barrier for most of the vent fauna. Although several studies highlighted genetic differentiation in populations of vent species between the Manus and Lau/Fiji basins<sup>42–44</sup>, the addition of populations sampled at Woodlark in genetic analyses will bring further insight into biogeographic patterns and the role of the Woodlark ridge in bridging populations at the regional scale. More population genetics studies using genomic tools are

currently underway. So far, the barcoding of symbiotic gastropod species reinforces the view that the Woodlark community, although deep, can be connected to much shallower populations in the Manus Basin (e.g., SuSu volcanoes located nearby, at the opening of the basin) but is also likely to act as a relay for migration between Manus and Fiji/Futuna/Lau, at least for *Ifremeria nautilei* (Fig. 8)<sup>45</sup>. Based on a more general barcoding approach, the Woodlark ridge does not seem to only represent a stepping stone but also a contact zone for some species between these basins (Poitrimol, pers. Comm.). Even if most larval dispersal trajectory modelling in the Southwestern Pacific failed to explain or only weakly explained present-day inter-basin connectivity for the deep-sea fauna even for larvae with a long pelagic duration<sup>46,47</sup>, these studies and our own genetic results pointed out the possible role of the Woodlark ridge as a biological cornerstone.

Despite faunal similarities with other Western Pacific communities in the Woodlark Basin may have specific attributes due to the greater depth (3330 mbsl) at which the vent sources are located compared to the shallower vent sites encountered elsewhere in the western Pacific (Manus Pual Ridge, Susu volcanoes, Franklin and Edison seamounts, North Fiji and Lau ridges segments). We found two new species (*Vulcanolepas* sp. nov. and *Austinograea* sp. nov.) at La Scala so far. Further examination of specimens that have been identified at the genus level as the gastropod *Desbruyeresia* or *Provanna* could yield additional new species.



The most striking features of this newly discovered vent assemblage, however, are the scarcity of the symbiotic fauna (no bathymodiolin mussels and small numbers of the large gastropods *Ifremeria nautili* and *Alviniconcha* spp.) and the astonishing profusion of stalked barnacles (*Vulcanolepas* sp. nov.) that cover most of the vent edifices and their surroundings over nearly

1000 m<sup>2</sup> of basaltic scree. Very extensive dense populations of stalked barnacles have also been observed at Haungaroa (Kermadec Arc, Hourdez, pers. obs.), at deep-sea vents discovered along the flanks of the nearby Edison seamount (near the Lihir island of New Ireland, Papua New Guinea<sup>39</sup>), along the East Scotia Ridge in the Southern Ocean<sup>48</sup> or, along the Southern East

**Fig. 7 Phylogenetic network of the LSVF stalked barnacle.** Phylogenetic position of the Woodlark stalked barnacle in the genus *Vulcanolepas*. BioNJ tree on Kimura-2-Parameter distances based on a 476 bp alignment of the mitochondrial gene *Cox1*. Numbers above branches are bootstrap values for 100 replicates. Sequences for *Ashinkailepas kermadecensis* and *A. seepiophila* used as outgroup. Accession numbers: *A. kermadecensis* (KP295001, 19, 40, 48, 53, and 61), *A. seepiophila* (KP295022, 28, 31, 46, 69, 90, and 91), *Vulcanolepas* sp. Woodlark (**MW602536-40, 602552-66**), *Vulcanolepas osheai* (**MW602550-51**, KP295005, 08, 26, 34, 36, 49, 56, and 94), *Vulcanolepas buckeridgei* (KY502196, 97, KP295009, 33, 41, 51, and 80), *Neolepas zeviniae rapanui* (KP295007, 55, 60, 63, 67, 84, and 98), *Vulcanolepas scotiaensis* (KP295013, 14, 18, 21, 35, 37, 39, 42, 45, 50, 52, 57, 58, 68, 78, 97, KF739820-38), *Neolepas marisindica/Neolepas* sp. 1 (KP295004, 30, 32, 47, 62, 64, 89, and LC350007-15), *Vulcanolepas fijiensis/Vulcanolepas* sp. (MH636381-83, MN061491), *Leucolepas longa/Vulcanolepas cf parensis* (**MW602541-49**, KP295027, 73, 76, 82, 83, 85, and JX036420-64). Accession number that appear in bold were generated for this study.

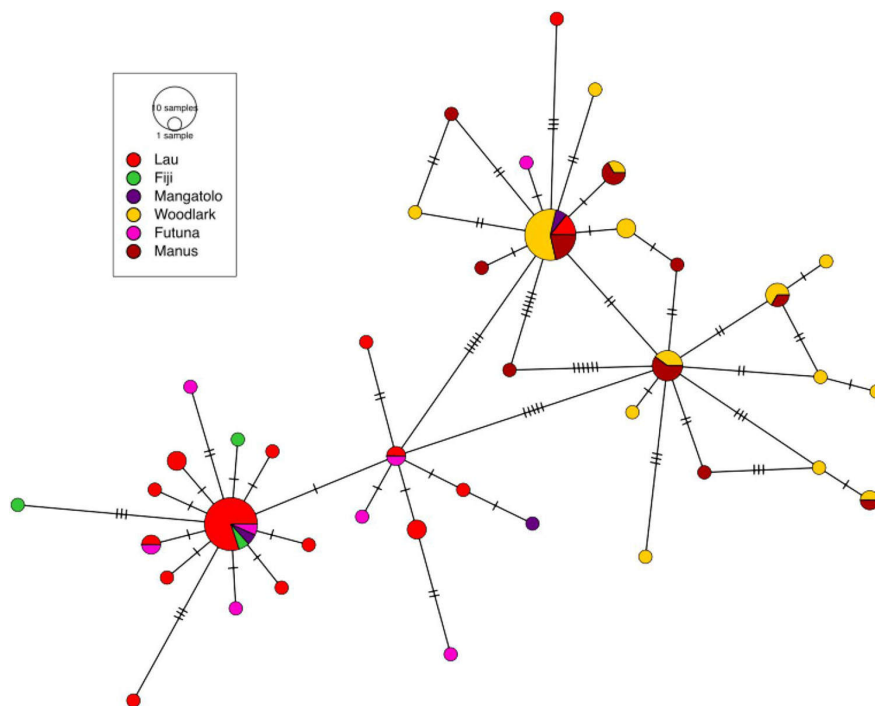


**Fig. 8 Haplotype network of the LSVF gastropod *Ifremeria*.** Haplotype network of the Woodlark *Ifremeria Cox1* gene (accession numbers: OL448876 - OL448957) with other sequences of geographically referenced individuals using the Median Joining method implemented in the software PopArt<sup>61</sup>. Purple: Woodlark Ridge, pink: Manus basin, Red: Lau basin, Green: North Fiji basin, yellow: Futuna.

Pacific Rise<sup>49</sup>. For each location, however, the stalked barnacle species are clearly different. They probably exploit the suspended particles that can disperse over large distances. This hypothesis is supported by the presence of large bacterial mats at the periphery that most likely also benefit from plume material carried from the main smokers, as observed on the mid-Atlantic ridge<sup>50</sup>. The absence of mussel beds and siboglinid worm aggregations, and the fact that symbiotic gastropods are only found in small numbers at the base of the black smoker chimneys do not seem to be attributable to the greater depth of hydrothermal sources. Dense populations of *Alviniconcha* and *Bathymodiulus* have indeed previously been observed at deeper sites (3600 mbsl) on the Mariana Trench<sup>51</sup>. Comparing the vent fauna of Mariana Trench and Mariana Trough (1470 mbsl), Fujikura (1997)<sup>52</sup> concluded that depth had no impact on the species composition of vent communities in the western Pacific. A similar situation was also depicted at the Mid-Caiman Spreading Centre where the community from the Beebe vent field was almost identical to that of the Van Damm vent site, 2000 m shallower<sup>53</sup>. Alternatively, the high number of filter-feeding species (i.e., barnacles) and the reduced, patchy distribution of symbiotic gastropods may

represent a transient state of the community where diffuse venting is prevented by focusing the hydrothermal activity into a series of black smokers exporting most of the fluid as high-velocity buoyant plumes that rise to a few tens of metres above the seafloor. This may indicate that the site has recently been reactivated by the tectonic movements that led to the collapse of part of the ridge crest where the emissions have been found, although activity in the general area probably lasted over several thousands of years.

## Materials and methods

**Bathymetry and acoustic survey.** Ship-borne multibeam data were acquired using a Kongsberg EM122 1° × 2° 12 kHz while ROV multibeam data were acquired with a RESON 7125 400 kHz 0.5° × 1°. Both datasets were processed with the GLOBE software ([doi.org/10.17882/70460](https://doi.org/10.17882/70460)) to provide 20 and 10 m grid (vessel data) and 1 m grid (ROV data) spaced digital terrain models of the surveyed area. The acoustic water column data acquired with the ship-borne 12 kHz MBES at a speed of 8 knots were characterized using the SonarScope (@Ifremer) and GLOBE softwares. Hydrothermal echoes were detected and located by visual inspection of ship-borne water-column polar echograms corresponding to the data of each ping and long-distance echograms associated to the track of the vessel. The most likely position on the seafloor and the maximum height (altitude above the seafloor) of each group of echoes attributed to rising plumes were determined. With this

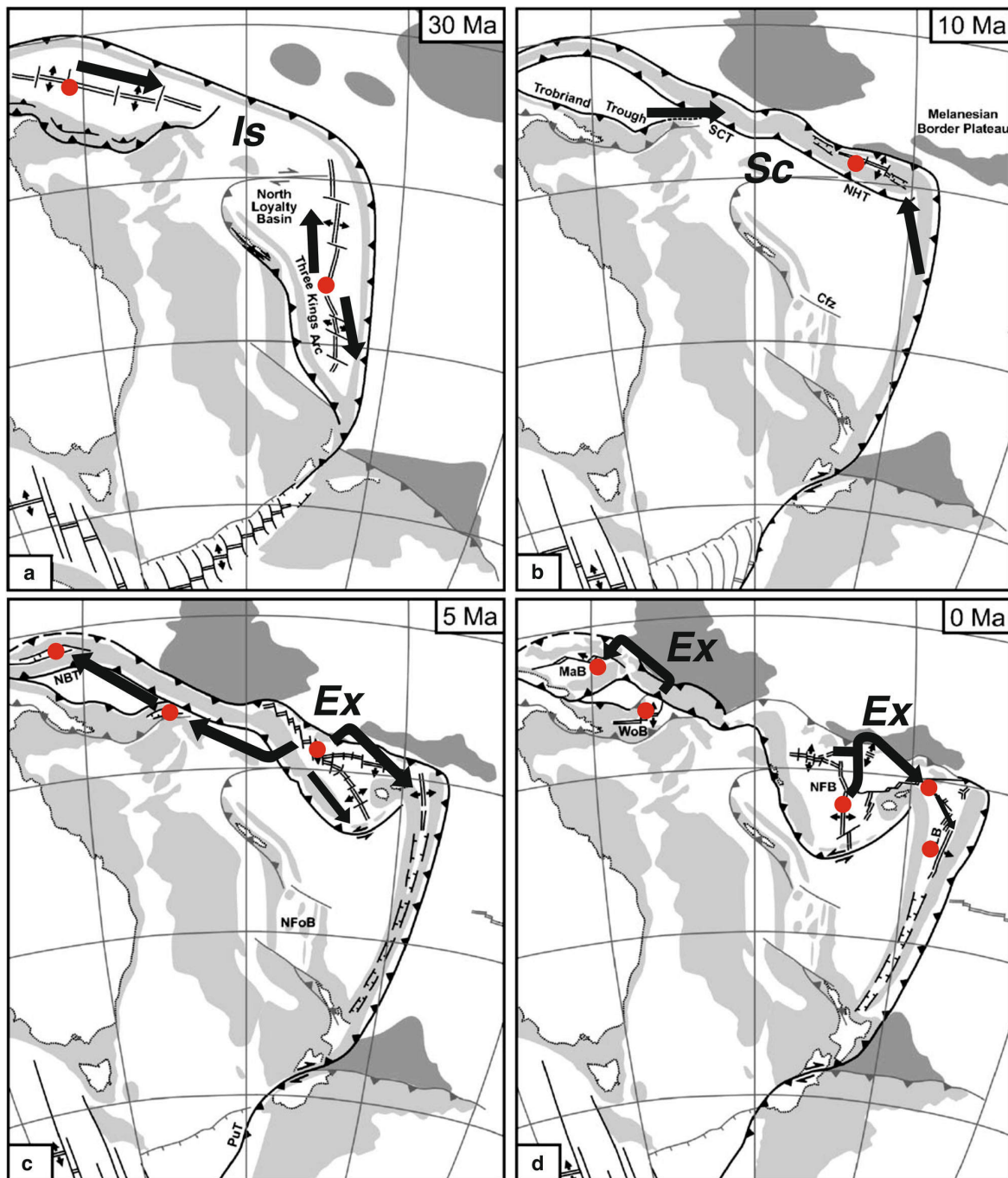


**Fig. 9 The Woodlark ridge, a potential biological cornerstone?** Scenario of the Woodlark Ridge's hypothesis as a cornerstone of the vent fauna dispersal in the western Pacific using the geotectonic reconstruction model of the Western back-arc basins adapted from Schellart et al. (2006)<sup>16</sup>. **a** Formation of the Solomon Basin and North Loyalty/South Fiji Basin with two independent ridge systems. **b** Opening of the northern branch of the North Fiji basin after the fossilization of the South Fiji basin and the opening of the Woodlark ridge about 10 Mya. **c** Expansion of the South Fiji basin together with the opening of the Lau Basin 5 Mya. **d** Present-days back arc basins with the five hydrothermally active zones, including Futuna. Red dots: active spreading centres, black arrows: putative colonization routes, **Is**: species isolation phase, **Sc**: secondary contact, and **Ex**: population expansion phase.

package, acoustic anomalies were identified, analyzed and attributed to various scatterers (large biological echoes, seafloor reflections...). Anomalies were considered as attributable to hydrothermal plumes if they were connected to the seafloor and reproducible over time, i.e., detected several times at the same location.

**Water column operations.** All operations were conducted using a 24-Niskin bottle rosette frame onto which were mounted a Seabird CTD 911+, two Turbidimeters (Seapoint Turbidity Metres), a pH sensor (AMT GmbH) and an Eh sensor (AMT GmbH), as well as an altimeter for seafloor detection. The Seasave software provided by Seabird Electronics was used for real-time data acquisition

and display of the down- and up-casts data. Niskin bottles were fired during up-casts at different levels in the water column, whenever an anomaly (T, S, turbidity and Eh) appeared in the real-time data display. The CTD-rosette was deployed in two ways, either as vertical casts or as towed casts ('tow-yos'), which consisted in lowering and raising the CTD-rosette between a constant set depth and ~100 m above the seafloor while the ship moved along a transect at a maximum speed of 1 knot. Vertical casts were stopped 5 m above the seafloor (provided by the altimeter).

Water samples were drawn from the Niskin bottles, fitted with Teflon stopcocks and sealed with Viton O-rings, both compatible with metal analyses. All subsamples were fully processed within 4 h after the CTD-rosette arrived on deck. Several types of samples were collected: (1) unfiltered water used for total dissolvable metal concentrations after acidification to pH 1.8; (2) water filtered directly from the niskin bottles using gravity flow through acid-cleaned Acropak® filters equipped with 0.45 µm Supor® Membrane. All fluid transfers from the Niskin bottles were performed under controlled conditions designed to avoid shipborne contaminations, including the use of acid-clean tubing and sampling LDPE bottles placed inside double plastic bags and protected by filling bell outlet. Each pre-cleaned LDPE bottle was rinsed 3 times with seawater sample before final filling. All samples were acidified to pH 1.8 with Optima-grade HCl inside a clean-air flow bench and analyzed back onshore for dissolved and total dissolvable metals (including Mn).

**Hydrothermal fluid sampling.** The hydrothermal fluid from each black smoker chimney was sampled in duplicate into two 750 mL syringe-style Titanium samplers manipulated by the ROV arm to estimate concentrations of end-members. In total, six samples of fluids from three chimneys were recovered immediately after removing the top of the chimney and measuring temperature with the ROV probe. Temperature was also recorded in real-time during the fluid collection using thermocouple temperature probes (NKE® probes) mounted on the sampler snorkel. Fluids were processed on board straight away after recovery using the following scheme:

- Aliquots were also transferred directly into evacuated glass bottles that contain a pre-weighed amount of Zn-acetate [ $\text{Zn}(\text{CH}_3\text{COO})_2 \cdot 2\text{H}_2\text{O}$ ] to precipitate ZnS for  $\delta^{34}\text{S}$  and  $\text{H}_2\text{S}$  concentration (i.e., total  $\text{HS}^-$ ) measurements.
- Aliquots were then collected for shipboard analysis (pH and total  $\text{HS}^-$  using either titration or Cline, method<sup>54</sup> depending on the concentration).
- The remaining fluid solutions in the Ti-samplers were then transferred into an acid cleaned 1 L HDPE bottle and homogenized before further separated into aliquots for on shore analyses: ion chromatographic analysis (major cations/anions; data not reported here); HR-ICPMS (major and trace elements); silica concentration after 100-fold dilution with ultra-pure water to prevent silica precipitation. Due to the high concentrations of metals in the hydrothermal solutions, precipitation often occurs within the titanium samplers as they cool down to ambient temperature. Those particles were found to be nearly entirely transferred into the 1 L HDPE bottle. Precipitated particles remaining in the Ti-samplers were however recovered for chemical analysis when the samplers are disassembled by rinsing with Milli-Q water and ethanol, and filtered through 0.45 µm filters. This fraction is hereafter referred to as “dregs” (not reported here).

**On shore fluid analyses.** Major and trace elements were measured by high-resolution inductively coupled plasma mass spectrometry (HR-ICPMS) Element XR operated at the French Research Institute for Exploitation of the Sea (IFREMER). Indium solution was added before analysis or mixed on-line at a final concentration of 5 ppb to correct for instrument sensitivity changes. Solutions were diluted 100-fold and introduced into the plasma torch using a quartz spray chamber system equipped with a microconcentric PFA nebulizer operating at a flow rate of about 60 µl/min. For each element, ICPMS sensitivity was calibrated using matrix matched standard solutions corresponding to seawater matrices. Anions ( $\text{Cl}$ ,  $\text{SO}_4$ ) were analyzed by ionic chromatography after appropriate dilutions.

**Sulfide analysis (XRF, XRD, HR-ICPMS,  $\delta^{34}\text{S}$ ).** Rock and sulfide samples collected during the dives were petrographically characterized directly on-board. Two types of subsamples were considered: A representative portion of the sample (referred as bulk) or mineral separates. Both sample types were dried in an air oven at 50 °C and ground to a fine powder using an agate mortar.

Mineralogical and quantitative chemical data were acquired using X-ray techniques (XRD and X-ray fluorescence) at the Laboratoire de Géochimie et Métallogénie at IFREMER. XRD analyses were conducted with a BRUKER AXS D8 Advance diffractometer. Samples were top loaded into 2.5 cm-diameter circular cavity holders, and analyses were run between 5° and 70° 2θ, in steps of 0.01° 2θ at 1 s/step (monochromatic Cu Kα radiation, 40 kV, 30 mA). Minerals were identified using the Diffrac suite EVA software.

X-ray fluorescence analyses were conducted with a wavelength dispersive X-ray fluorescence spectrometer (WD-XRF; BRUKER AXS S8 TIGER) on fusion beads

(for major elements) or compressed pellets (for trace elements). After data acquisition, the measured net peak intensities, corrected for inter-element effects, were converted into concentrations using calibration curves generated from analysis of certified geochemical standard powders (measured under identical analytical conditions). Calibrations were established using a set of certified materials obtained mainly from the Canadian Certified reference materials Project (CCRMP) (for example, CCU-1, CZN-1, Fer-1, PTC-1 or PTM-1), Geological Survey of Japan (GSJ)(JP-1), and the Centre de Recherches Pétrochimiques et Géochimiques in France (CRPG)(BE-N).

For sulfur isotopes, sample powder was digested in inverted aqua regia and then purified by elution through a cationic resin to remove any interfering matrix. The solution was analyzed by a Neptune MC-ICP-MS at Ifremer following the procedure of Craddock et al. (2008)<sup>55</sup> and calibrated against a set of internal and external standards (IAEA NZ-1, NZ-2, NZ-4, NBS 123).

All mineral samples were also analyzed for major and trace elements by HR-ICPMS at IFREMER. About 100 mg of dry powder was dissolved in a PTFE beaker on a hot plate using an acid mixture of HCl, and  $\text{HNO}_3$ . Digested samples were then further diluted 50-fold and analyzed by HR-ICPMS following similar approaches than for fluid samples described above. A set of international geo-reference materials (e.g., BHVO-2, GH, UB-N, NOD-P-1, IF-G, NIST2711) and internal standard solutions relevant to sulfide-rich samples were used to calibrate the measurements.

**Sampling and preservation of animals.** Benthic macrofauna was collected using the claw of the hydraulic arm of the ROV Victor 6000 and placed into collection boxes. The remaining fauna on the substrate was then sampled with the suction sampler of the ROV equipped with a 1 mm mesh. Three benthic communities defined by engineer species were specifically sampled over an area of about 0.5 m<sup>2</sup> (i.e., one sample for the *Vulcanolepas* community, one sample for the *Ifremeria* community and two samples for the *Alviniconcha* community). Temperature measurements were made at three locations using the ROV temperature probe prior and after sampling for *Ifremeria* and *Alviniconcha* communities. In addition, opportunistic sampling was carried out to collect organisms found on the black smokers (e.g., polynoid worms, crabs and shrimp) and peripheral area using the robotic arm and claw of the ROV. This sampling was supplemented by observations performed with the high-definition video camera of the ROV for large megafauna. Onboard, samples were sieved on a 250 µm sieve, and all organisms were sorted and preserved in 96° ethanol before their identification at the lowest taxonomic level based on morphological criteria. Some specimens of each species were also frozen at -80 °C in order to perform stable isotopes (<sup>13</sup>C, <sup>15</sup>N, and <sup>34</sup>S) analyses.

**Stable isotope analyses.** On board, animals were dissected to separate soft and non-metabolically active tissues (e.g., muscle, tegument) or, when body size was small, were used whole<sup>56</sup>. All samples were oven-dried at 60 °C for 72 h, then placed in airtight containers and kept at room temperature before further treatment once back from the expedition. They were subsequently ground to a homogeneous powder using mortar and pestle. Samples containing hard inorganic carbon parts that could not be physically removed were acidified by exposing them to HCl vapours for 48 h in an airtight container<sup>57</sup>. Stable isotope ratios measurements were performed via continuous flow—elemental analysis— isotope ratio mass spectrometry (CF-EA-IRMS) at University of Liège (Belgium), using a vario MICRO cube C-N-S elemental analyzer (Elementar Analysensysteme GMBH, Hanau, Germany) coupled to an IsoPrime100 isotope ratio mass spectrometer (Isoprime, Cheadle, United Kingdom). Isotopic ratios were expressed using the widespread δ notation<sup>58</sup>, in ‰ and relative to the international references Vienna Pee Dee Belemnite (for carbon), Atmospheric Air (for nitrogen) and Vienna Canyon Diablo Troilite (for sulfur). IAEA (International Atomic Energy Agency, Vienna, Austria) certified reference materials sucrose (IAEA-C-6;  $\delta^{13}\text{C} = -10.8 \pm 0.5\text{‰}$ ; mean ± SD), ammonium sulfate (IAEA-N-2;  $\delta^{15}\text{N} = 20.3 \pm 0.2\text{‰}$ ; mean ± SD) and silver sulfide (IAEA-S-1;  $\delta^{34}\text{S} = -0.3\text{‰}$ ) were used as primary analytical standards. Sulfanilic acid (Sigma-Aldrich;  $\delta^{13}\text{C} = -25.6 \pm 0.4\text{‰}$ ;  $\delta^{15}\text{N} = -0.13 \pm 0.4\text{‰}$ ;  $\delta^{34}\text{S} = 5.9 \pm 0.5\text{‰}$ ; means ± SD) was used as secondary analytical standard. Standard deviations on multi-batch replicate measurements of secondary and internal lab standards (amphipod crustacean muscle) analyzed interspersed with samples (one replicate of each standard every 15 analyses) were 0.2‰ for both  $\delta^{13}\text{C}$  and  $\delta^{15}\text{N}$  and 0.5‰ for  $\delta^{34}\text{S}$ .

#### Genetic analyses

**Barcoding analyses.** Genomic DNA from gastropod, barnacle and crab specimens collected from the site La Scala were extracted using a CTAB extraction procedure. Tissues were digested overnight in 600 µl of a 1% CTAB buffer solution (1.4-M NaCl, 0.2% 2-mercaptoethanol, 20 mM EDTA, 100-mM Tris-HCl pH 8 and 0.1 mg ml<sup>-1</sup> proteinase K) also containing 1% PVPP (PolyVinylPolypyrrolidone). DNA was then extracted by adding chloroform-isoamyl alcohol (24:1), precipitated with 1 ml of cold 100% ethanol, washed with 70% ethanol and resuspended in 100 µl of sterile solution of 0.1X TE (Tris EDTA pH 8.0). For shrimp, genomic DNA was extracted using E.Z.N.A. Tissue DNA kit (Omega Bio-Tek) according to the manufacturer's recommendations. For the mt *Cox1* gene,



amplifications were performed in 25 µl final volume using the 'universal' applicable primers of Folmer et al. (1994)<sup>59</sup> and the following conditions: 1× reaction buffer, 2.5 mM MgCl<sub>2</sub>, 0.12 mM of each dNTP, 0.38 µM of each primers, 1U Taq DNA polymerase (Uptitherm), 2.5 µl of template DNA and sterile H<sub>2</sub>O. Thermal cycling parameters used an initial denaturation at 94 °C for 2 min, followed by 35 cycles at 94 °C for 30 s, 50 °C for 1 min, 72 °C for 2 min and a final 5 min extension cycle. An alternative protocol was used for shrimp with specific primers for alvinocaridid shrimp<sup>60</sup>.

**Phylogenetic and haplotype networks.** A phylogenetic tree was produced to determine the position of the new pedunculate cirriped by a PhyML approach using a general time reversible model of substitutions with a Gamma distribution of the substitution rate. This latter rate, nucleotide equilibrium frequencies, and the proportion of invariant sites were optimized by the search algorithm. Node confidence was evaluated with an aLRT (SH-like) approach. Haplotype networks for the gastropods were produced using the minimum spanning method implemented in PopArt<sup>61</sup> on mtCox1 alignments of the three main symbiotic gastropod species.

**Reporting summary.** Further information on research design is available in the Nature Research Reporting Summary linked to this article.

### Data availability

The datasets generated during the current study are available at <https://doi.org/10.6084/m9.figshare.19095659>. All bathymetric data and sampling metadata from the cruise are available at <https://doi.org/10.17600/18001111>.

Received: 27 April 2021; Accepted: 11 February 2022;

Published online: 17 March 2022

### References

- German, C. R. & Von Damm, K. L. *Treatise on Geochemistry* (eds Heinrich, D. H. & Karl, K. T.) 181–222 (Pergamon, 2003).
- Van Dover, C. *The Ecology of Deep-Sea Hydrothermal Vents* (Princeton University Press, 2000).
- Spieß, F. N. et al. East Pacific rise: Hot springs and geophysical experiments. *Science* **207**, 1421–1433 (1980).
- Haymon, R. M. et al. Hydrothermal vent distribution along the East Pacific Rise crest 9° 09'–54' N and its relationship to magmatic and tectonic processes on fast-spreading mid-ocean ridges. *Earth Planetary Sci. Lett.* **104**, 513–534 (1991).
- Edmonds, H. N. et al. Discovery of abundant hydrothermal venting on the ultraslow-spreading Gakkel Ridge in the Arctic Ocean. *Nature* **421**, 252–256 (2003).
- German, C. R. et al. Hydrothermal activity and seismicity at Teahitia Seamount: Reactivation of the society islands hotspot? *Front. Mar. Sci.* **7**, 73 (2020).
- de Ronde, C. E. J. et al. Intra-oceanic subduction-related hydrothermal venting, Kermadec volcanic arc, New Zealand. *Earth Planetary Sci. Lett.* **193**, 359–369 (2001).
- Ishibashi, J. & Urabe, T. *Backarc Basins: Tectonics and Magmatism* (ed Taylor, B.) 451–495 (Springer, 1995).
- Fouquet, Y. et al. Hydrothermal activity and metallogenesis in the Lau back-arc basin. *Nature* **349**, 778–781 (1991).
- Boschen, R. E., Rowden, A. A., Clark, M. R. & Gardner, J. P. A. Mining of deep-sea seafloor massive sulfides: A review of the deposits, their benthic communities, impacts from mining, regulatory frameworks, and management strategies. *Ocean Coastal Manage.* **84**, 54–67 (2013).
- Lisitsyn, A. P. et al. Active hydrothermal activity at Franklin Seamount, Western Woodlark Sea (Papua New Guinea). *Int. Geol. Rev.* **33**, 914–929 (1991).
- Laurila, T. E. et al. Tectonic and magmatic controls on hydrothermal activity in the Woodlark Basin: Hydrothermalism in the Woodlark Basin. *Geochem. Geophys. Geosyst.* **13**, Q09006 (2012).
- Goodliffe, A. M. et al. Synchronous reorientation of the Woodlark Basin spreading center. *Earth Planetary Sci. Lett.* **146**, 233–242 (1997).
- Martínez, F., Taylor, B. & Goodliffe, A. M. Contrasting styles of seafloor spreading in the Woodlark Basin: Indications of rift-induced secondary mantle convection. *J. Geophys. Res.* **104**, 12909–12926 (1999).
- Taylor, B., Goodliffe, A., Martínez, F. & Hey, R. Continental rifting and initial sea-floor spreading in the Woodlark Basin. *Nature* **374**, 534–537 (1995).
- Schellart, W. P., Lister, G. S. & Toy, V. G. A Late Cretaceous and Cenozoic reconstruction of the Southwest Pacific region: Tectonics controlled by subduction and slab rollback processes. *Earth-Sci. Rev.* **76**, 191–233 (2006).
- Hall, R. Cenozoic geological and plate tectonic evolution of SE Asia and the SW Pacific: Computer-based reconstructions, model and animations. *J. Asian Earth Sci.* **20**, 353–431 (2002).
- Breusing, C. et al. Allopatric and sympatric drivers of speciation in Alviniconcha hydrothermal vent snails. *Mol. Biol. Evol.* **37**, 3469–3484 (2020).
- Ondreas, H., Scalabrin, C., Fouquet, Y. & Godfroy, A. Recent high-resolution mapping of Guaymas hydrothermal fields (Southern Trough). *BSGF - Earth Sci. Bull.* **189**, 6 (2018).
- Nakamura, K. et al. Water column imaging with multibeam echo-sounding in the mid-Okinawa Trough: Implications for distribution of deep-sea hydrothermal vent sites and the cause of acoustic water column anomaly. *Geochem. J.* **49**, 579–596 (2015).
- Xu, G., Jackson, D. R. & Bemis, K. G. The relative effect of particles and turbulence on acoustic scattering from deep sea hydrothermal vent plumes revisited. *J. Acoust. Soc. Am.* **141**, 1446–1458 (2017).
- Park, S.-H. et al. Petrogenesis of basalts along the eastern Woodlark spreading center, equatorial western Pacific. *Lithos* **316–317**, 122–136 (2018).
- Chadwick, J. et al. Arc lavas on both sides of a trench: Slab window effects at the Solomon Islands triple junction, SW Pacific. *Earth Planetary Sci. Lett.* **279**, 293–302 (2009).
- Fouquet, Y. et al. *Geodiversity of Hydrothermal Processes Along the Mid-Atlantic Ridge and Ultramafic-Hosted Mineralization: A New Type of Oceanic Cu-Zn-Co-Au Volcanogenic Massive Sulfide Deposit* (eds Rona, P. A., Devey, C. W., Dymont, J. & Murton, B. J.) Vol. 188, 321–367 (American Geophysical Union, 2010).
- Von Damm, K. et al. Chemistry of submarine hydrothermal solutions at 21N, East Pacific Rise. *Geochim. Cosmochim. Acta* **49**, 2197–2220 (1985).
- Seyfried, W. E. & Bischoff, J. L. Experimental seawater-basalt interaction at 300 °C, 500 bars, chemical exchange, secondary mineral formation and implications for the transport of heavy metals. *Geochim. Cosmochim. Acta* **45**, 135–147 (1981).
- Pester, N. J., Rough, M., Ding, K. & Seyfried, W. E. A new Fe/Mn geothermometer for hydrothermal systems: Implications for high-salinity fluids at 13°N on the East Pacific Rise. *Geochim. Cosmochim. Acta* <https://doi.org/10.1016/j.gca.2011.08.043> (2011).
- Podowski, E. L., Moore, T. S., Zelnio, K. A., Luther, G. W. & Fisher, C. R. Distribution of diffuse flow megafauna in two sites on the Eastern Lau Spreading Center, Tonga. *Deep Sea Res. Part I: Oceanogr. Res. Papers* **56**, 2041–2056 (2009).
- Collins, P., Kennedy, R. & Van Dover, C. A biological survey method applied to seafloor massive sulphides (SMS) with contagiously distributed hydrothermal-vent fauna. *Mar. Ecol. Prog. Ser.* **452**, 89–107 (2012).
- Desbruyères, D., Hashimoto, J. & Fabri, M.-C. Composition and biogeography of hydrothermal vent communities in Western Pacific back-arc basins. *Geophys. Monogr. Ser.* **166**, 215–234 (2006).
- Reid, W. D. K. et al. Spatial differences in East scotia ridge hydrothermal vent food webs: Influences of chemistry, microbiology, and predation on trophodynamics. *PLoS One* **8**, e65553 (2013).
- Van Audenhaege, L., Fariñas-Bermejo, A., Schultz, T. & Lee Van Dover, C. An environmental baseline for food webs at deep-sea hydrothermal vents in Manus Basin (Papua New Guinea). *Deep Sea Res. Part I: Oceanogr. Res. Papers* <https://doi.org/10.1016/j.dsr.2019.04.018> (2019).
- Erickson, K. L., Macko, S. A. & Van Dover, C. L. Evidence for a chemoautotrophically based food web at inactive hydrothermal vents (Manus Basin). *Deep-Sea Res. Part II: Top. Stud. Oceanogr.* **56**, 1577–1585 (2009).
- Comeault, A., Stevens, C. J. & Juniper, S. K. Mixed photosynthetic-chemosynthetic diets in vent obligate macroinvertebrates at shallow hydrothermal vents on Volcano 1, South Tonga Arc—evidence from stable isotope and fatty acid analyses. *Cahiers de Biologie Marine* **51**, 351–359 (2010).
- Bennett, S. A., Dover, C. V., Breier, J. A. & Coleman, M. Effect of depth and vent fluid composition on the carbon sources at two neighboring deep-sea hydrothermal vent fields (Mid-Cayman Rise). *Deep-Sea Res. Part I: Oceanogr. Res. Papers* **104**, 122–133 (2015).
- Levin, L. A. et al. Hydrothermal vents and methane seeps: Rethinking the sphere of influence. *Front. Marine Sci.* **3**, 1–23 (2016).
- Hügler, M. & Sievert, S. M. Beyond the Calvin cycle: Autotrophic carbon fixation in the ocean. *Annu. Rev. Mar. Sci.* **3**, 261–289 (2011).
- Wang, X., Li, C., Wang, M. & Zheng, P. Stable isotope signatures and nutritional sources of some dominant species from the PACManus hydrothermal area and the Desmos caldera. *PLoS One* **13**, e0208887 (2018).
- Tunncliffe, V. & Southward, A. J. Growth and breeding of a primitive stalked barnacle *Leucopelas longus* (Cirripedia: Scalpellomorpha: Eolepadidae: Neolepadinae) inhabiting a volcanic seamount off Papua New Guinea. *J. Mar. Biol. Ass.* **84**, 121–132 (2004).
- Auzende, J. M., Pelletier, B. & Lafoy, Y. Twin active spreading ridges in the North Fiji Basin (southwest Pacific). *Geology* **22**, 63–66 (1994).
- Parson, L. M. & Wright, I. C. The Lau-Havre-Taupo back-arc basin: A southward-propagating, multi-stage evolution from rifting to spreading. *Tectonophysics* **263**, 1–22 (1996).

42. Thaler, A. D. et al. Comparative population structure of two deep-sea hydrothermal-vent-associated decapods (*Chorocaris* sp. 2 and *Munidopsis lausensis*) from Southwestern Pacific back-arc basins. *PLoS One* **9**, e101345 (2014).
43. Lee, W.-K., Kim, S.-J., Hou, B. K., Van Dover, C. L. & Ju, S.-J. Population genetic differentiation of the hydrothermal vent crab *Austinochroa alaysea* (Crustacea: Bythograeidae) in the Southwest Pacific Ocean. *PLoS One* **14**, e0215829 (2019).
44. Plouviez, S. et al. Amplicon sequencing of 42 nuclear loci supports directional gene flow between South Pacific populations of a hydrothermal vent limpet. *Ecol. Evol.* <https://doi.org/10.1002/ece3.5235> (2019).
45. Tran Lu Y, A. et al. Fine-scale genomic patterns of connectivity in the deep sea hydrothermal gastropod *Ifremeria nautilei* over its species range using outlier scans and demo-genetic inferences. *Mol. Ecol.* (In Revision).
46. Yearsley, J. M. & Sigwart, J. D. Larval transport modeling of deep-sea invertebrates can aid the search for undiscovered populations. *PLoS One* **6**, e23063 (2011).
47. Mitarai, S., Watanabe, H., Nakajima, Y., Shchepetkin, A. F. & McWilliams, J. C. Quantifying dispersal from hydrothermal vent fields in the western Pacific Ocean. *Proc. Natl Acad. Sci. USA* **113**, 2976–2981 (2016).
48. Marsh, L. et al. Microdistribution of faunal assemblages at deep-sea hydrothermal vents in the southern ocean. *PLoS One* **7**, e48348 (2012).
49. Jollivet, D. et al. The Biospeedo cruise: A new survey of hydrothermal vents along the south East Pacific Rise from 7°24' S to 21°33' S. *InterRidge News* **13**, 20–26 (2005).
50. Girard, F. et al. Currents and topography drive assemblage distribution on an active hydrothermal edifice. *Prog. Oceanogr.* **187**, 102397 (2020).
51. Hessler, R. R. & Lonsdale, P. F. Biogeography of Mariana Trough hydrothermal vent communities. *Deep Sea Res. Part A. Oceanogr. Res. Papers* **38**, 185–199 (1991).
52. Fujikura, K. Biology and earth scientific investigation by the submersible 'Shinkai 6500' system of deep-sea hydrothermal and lithosphere in the Mariana back-arc basin. *JAMSTEC J. Deep Sea Res.* **13**, 1–20 (1997).
53. Connelly, D. P. et al. Hydrothermal vent fields and chemosynthetic biota on the world's deepest seafloor spreading centre. *Nat. Commun.* **3**, 620 (2012).
54. Cline, J. D. Spectrophotometric determination of hydrogen sulfide in natural waters. *Limnol. Oceanogr.* **14**, 454–458 (1969).
55. Craddock, P. R., Rouxel, O. J., Ball, L. A. & Bach, W. Sulfur isotope measurement of sulfate and sulfide by high-resolution MC-ICP-MS. *Chem. Geol.* **253**, 102–113 (2008).
56. Mateo, M. A., Serrano, O., Serrano, L. & Michener, R. H. Effects of sample preparation on stable isotope ratios of carbon and nitrogen in marine invertebrates: Implications for food web studies using stable isotopes. *Oecologia* **157**, 105–115 (2008).
57. Hedges, J. I. & Stern, J. H. Carbon and nitrogen determinations of carbonate-containing solids. *Limnol. Oceanogr.* **29**, 657–663 (1984).
58. Coplen, T. B. Guidelines and recommended terms for expression of stable-isotope-ratio and gas-ratio measurement results: Guidelines and recommended terms for expressing stable isotope results. *Rapid Commun. Mass Spectrom.* **25**, 2538–2560 (2011).
59. Folmer, O., Black, M., Hoeh, W., Lutz, R. & Vrijenhoek, R. DNA primers for amplification of mitochondrial cytochrome c oxidase subunit I from diverse metazoan invertebrates. *Mol. Mar. Biol. Biotechnol.* **3**, 294–299 (1994).
60. Methou, P., Michel, L. N., Segonzac, M., Cambon-Bonavita, M.-A. & Pradillon, F. Integrative taxonomy revisits the ontogeny and trophic niches of *Rimicaris* vent shrimps. *R. Soc. Open Sci.* **7**, 200837 (2020).
61. Leigh, J. W. & Bryant, D. Popart: Full-feature software for haplotype network construction. *Methods Ecol. Evol.* **6**, 1110–1116 (2015).

### Acknowledgements

We are deeply grateful to the captain and crew of the French Research Vessel L'Atalante and to the team in charge of the ROV 6000 Victor without whom nothing would have been possible. We also thank Delphine Pierre (Ifremer CTDI) and Emilie Hardouin (Genavir) for their assistance in the production of the High-Resolution Bathymetric Chart of the Woodlark Ridge, as well as Anne-Sophie Alix (Ifremer GM) with the Geographic Information System. We finally thank Claire Daguin-Thiébaud, Stéphanie

Ruault and Marion Ballenghien (Station Biologique de Roscoff) for their assistance in the molecular analyses. This work benefited from access to the Bigenouest genomic platform at Station Biologique de Roscoff. The authors would also like to dedicate this article to Jean-Marie Auzende who spent a large part of his life exploring the oceanic ridges of the Western Pacific to better understand the plate dynamics in this region. Finally, we thank the three anonymous reviewers for the useful comments in improving the manuscript. Ship time was supported by the French Oceanographic Fleet while scientific work was funded through the ANR 'CERBERUS' (contract number ANR-17-CE02-0003).

### Author contributions

The cruise was led by D.J. and S.H. as co-principal investigators. They also acquired the genetic data on specimens collected during the cruise. C.B. is the coordinator of the present article and was responsible for the water column survey; O.R. was responsible for the geochemical analysis of the rocks and mineralization as well as the geochemical composition of the water column; C.S. was responsible for the acquisition of bathymetry and the processing of the acoustic data (ship and ROV); P.L.M. participated in the pre-treatment of the bathymetry data on board and produced the high-resolution bathymetric map; E.P. (not onboard) helped in the interpretation of the geological structures and geochemical composition of the fluids observed during the surveys; C.C. (not onboard) was responsible for the fluid sampling equipment and helped in the data processing from the CTD; C.P., E.T., and M.M. (not onboard) were responsible for the description of the fauna and the ecology of the sites; J.C. (not onboard) and A.T.L.Y. participated in the genetic analyses of the targeted fauna collected at LSVF. S.C. (not onboard) and A.B. (not onboard) produced the X-ray data; Y.G. carried out the analyses for the isotopic composition of fluids and mineralization; V.G. was in charge of hydrothermal fluids analysis (IC); L.M. investigated the isotopic ratios across the food web; S.A.-H., F.B., T.B., V.C.-G., V.L.L., S.L'.H., J.M., A.-S.L.P., A.T., and D.C. Kuama participated and contributed to the sampling and data acquisition during the CHU-BACARC Cruise (doi: 10.17600/18001111) during which the La Scala Vent field was discovered.

### Competing interests

The authors declare no competing interests.

### Additional information

**Supplementary information** The online version contains supplementary material available at <https://doi.org/10.1038/s43247-022-00387-9>.

**Correspondence** and requests for materials should be addressed to Cédric Boulart.

**Peer review information** *Communications Earth & Environment* thanks the anonymous reviewers for their contribution to the peer review of this work. Primary Handling Editors: Maria-Luce Frezzotti and Clare Davis.

**Reprints and permission information** is available at <http://www.nature.com/reprints>






**Publisher's note** Springer Nature remains neutral with regard to jurisdictional claims in published maps and institutional affiliations.



**Open Access** This article is licensed under a Creative Commons Attribution 4.0 International License, which permits use, sharing, adaptation, distribution and reproduction in any medium or format, as long as you give appropriate credit to the original author(s) and the source, provide a link to the Creative Commons license, and indicate if changes were made. The images or other third party material in this article are included in the article's Creative Commons license, unless indicated otherwise in a credit line to the material. If material is not included in the article's Creative Commons license and your intended use is not permitted by statutory regulation or exceeds the permitted use, you will need to obtain permission directly from the copyright holder. To view a copy of this license, visit <http://creativecommons.org/licenses/by/4.0/>.

© The Author(s) 2022

## Active hydrothermal vents in the Woodlark Basin may act as dispersing centres for hydrothermal fauna

Cédric Boulart <sup>1✉</sup>, Olivier Rouxel <sup>2</sup>, Carla Scalabrin <sup>2</sup>, Pierre Le Meur<sup>3</sup>, Ewan Pelleter<sup>2</sup>, Camille Poitrimol<sup>1,4</sup>, Eric Thiébaud<sup>1</sup>, Marjolaine Matabos <sup>4</sup>, Jade Castel<sup>1</sup>, Adrien Tran Lu Y<sup>5,6</sup>, Loic N. Michel<sup>4</sup>, Cécile Cathalot<sup>2</sup>, Sandrine Chéron<sup>2</sup>, Audrey Boissier<sup>2</sup>, Yoan Germain<sup>2</sup>, Vivien Guyader<sup>2</sup>, Sophie Arnaud-Haond<sup>7</sup>, François Bonhomme<sup>5</sup>, Thomas Broquet <sup>1</sup>, Valérie Cueff-Gauchard<sup>8</sup>, Victor Le Layec<sup>1,6</sup>, Stéphane L'Haridon<sup>8</sup>, Jean Mary<sup>1</sup>, Anne-Sophie Le Port<sup>1</sup>, Aurélie Tasiemski<sup>9</sup>, Darren C. Kuama<sup>10</sup>, Stéphane Hourdez<sup>6</sup> & Didier Jollivet<sup>1</sup>

Here we report the discovery of a high-temperature hydrothermal vent field on the Woodlark Ridge, using ship-borne multibeam echosounding and Remotely Operated Vehicle (ROV) exploration. La Scala Vent Field comprises two main active areas and several inactive zones dominated by variably altered basaltic rocks, indicating that an active and stable hydrothermal circulation has been maintained over a long period of time. The Pandora Site, at a depth of 3380 m, is mainly composed of diffuse vents. The Corto site, at a depth of 3360 m, is characterized by vigorous black smokers (temperature above 360 °C). The striking features of this new vent field are the profusion of stalked barnacles *Vulcanolepas* sp. nov., the absence of mussels and the scarcity of the gastropod symbiotic fauna. We suggest that La Scala Vent Field may act as a dispersing centre for hydrothermal fauna towards the nearby North Fiji, Lau and Manus basins.

<sup>1</sup>UMR 7144 AD2M CNRS-Sorbonne Université, Station Biologique de Roscoff, Place Georges Tessier, 29680 Roscoff, France. <sup>2</sup>IFREMER REM-GM, Technopôle Brest Plouzané, 29280 Plouzané, France. <sup>3</sup>GENAVIR, Technopôle Brest Plouzané, 29280 Plouzané, France. <sup>4</sup>IFREMER REM-EEP, Technopôle Brest Plouzané, 29280 Plouzané, France. <sup>5</sup>ISEM CNRS UMR 5554, Université de Montpellier 2, 34095 Montpellier Cedex 5, France. <sup>6</sup>UMR 8222 LECOB CNRS-Sorbonne Université, Observatoire Océanologique de Banyuls, Avenue du Fontaulé, 66650 Banyuls-sur-mer, France. <sup>7</sup>IFREMER UMR 248 MARBEC, Avenue Jean Monnet CS 30171, 34203 Sète, France. <sup>8</sup>Univ. Brest, Ifremer, CNRS, Laboratoire de Microbiologie des Environnements Extrêmes UMR6197, F-29280 Plouzané, France. <sup>9</sup>Univ. Lille, CNRS, Inserm, CHU Lille, Institut Pasteur de Lille, U1019-UMR9017-CIIL-Centre d'Infection et d'Immunité de Lille, Lille, France. <sup>10</sup>PNG Science and Technology Secretariat, University of Papua New Guinea, Port Moresby, Papua New Guinea. ✉email: [cedric.boulart@sb-roscoff.fr](mailto:cedric.boulart@sb-roscoff.fr)

Hydrothermal venting on the deep seafloor is the manifestation of heat and matter transfer from the lithosphere to the oceans, which modify their geochemical composition<sup>1</sup>. Upon mixing with the surrounding, cold, deep-sea water, a precipitation occurs and forms sulfide deposits on the seafloor. These hot and acidic fluids sustain diverse chemical-based ecosystems where large specialized bacterial and animal communities can thrive under extreme conditions of temperature, pressure, and pH<sup>2</sup>. Since the observation of the first active high-temperature vents more than 40 years ago<sup>3</sup>, the exploration of the deep ocean has revealed the existence of hydrothermal circulation in a wide range of geological settings from fast-spreading ridges<sup>4</sup> to ultra-slow ones<sup>5</sup> as well as in intraplate hotspots<sup>6</sup>, subduction zones<sup>7</sup>, and back-arc basins<sup>8</sup>.

Economic and societal interest in deep-sea hydrothermal vents has increased in the recent years because of the formation of massive polymetallic sulfide deposits<sup>9</sup> that are now targeted for deep-sea mining<sup>10</sup>, which may impact the deep ocean environment. The Woodlark Basin, located South of the Solomon Islands arc region in the Western Pacific Ocean, is a rather young (~5–7 Mya) oceanic basin that is subducting beneath the New Britain-San Cristobal Trench (Fig. 1). This is in fact one of the only places

on Earth where an active spreading centre expands into both continental crust to the West, and is bound by a subduction zone to the East<sup>11,12</sup>, therefore offering a wide range of geotectonic constraints for the development of seamounts and the possibility of forming high and low temperature hydrothermal venting along the axis. This may then provide a great diversity of niches for hydrothermal fauna and microbial colonization, and the potential settlement of associated fauna, provided that venting sites remain active over a long period of time.

The Woodlark Basin is characterized by an E–W active spreading axis that Goodliffe et al.<sup>13</sup> divided into five segments, numbered 1 through 5 from West to East (Fig. 1). The bathymetry shows major differences between the Eastern and Western parts, separated by the Moresby Transform Fault (TF), with a significantly shallower seafloor to the West, and a well-developed axial graben to the East<sup>14</sup>. Spreading rates vary from 38 mm yr<sup>-1</sup> in the West, to 67 mm yr<sup>-1</sup> on the Eastern part<sup>15</sup>. Hydrothermal activities are known to occur on only three segments of the ridge, which include confirmed volcanic activity on Segment 1 (Franklin Seamount<sup>11</sup>), and inferred hydrothermal venting thought to be due to punctual eruptive phases on Segment 3 and Segment 5<sup>12</sup>. Although recent exploration found consistent turbidity and redox

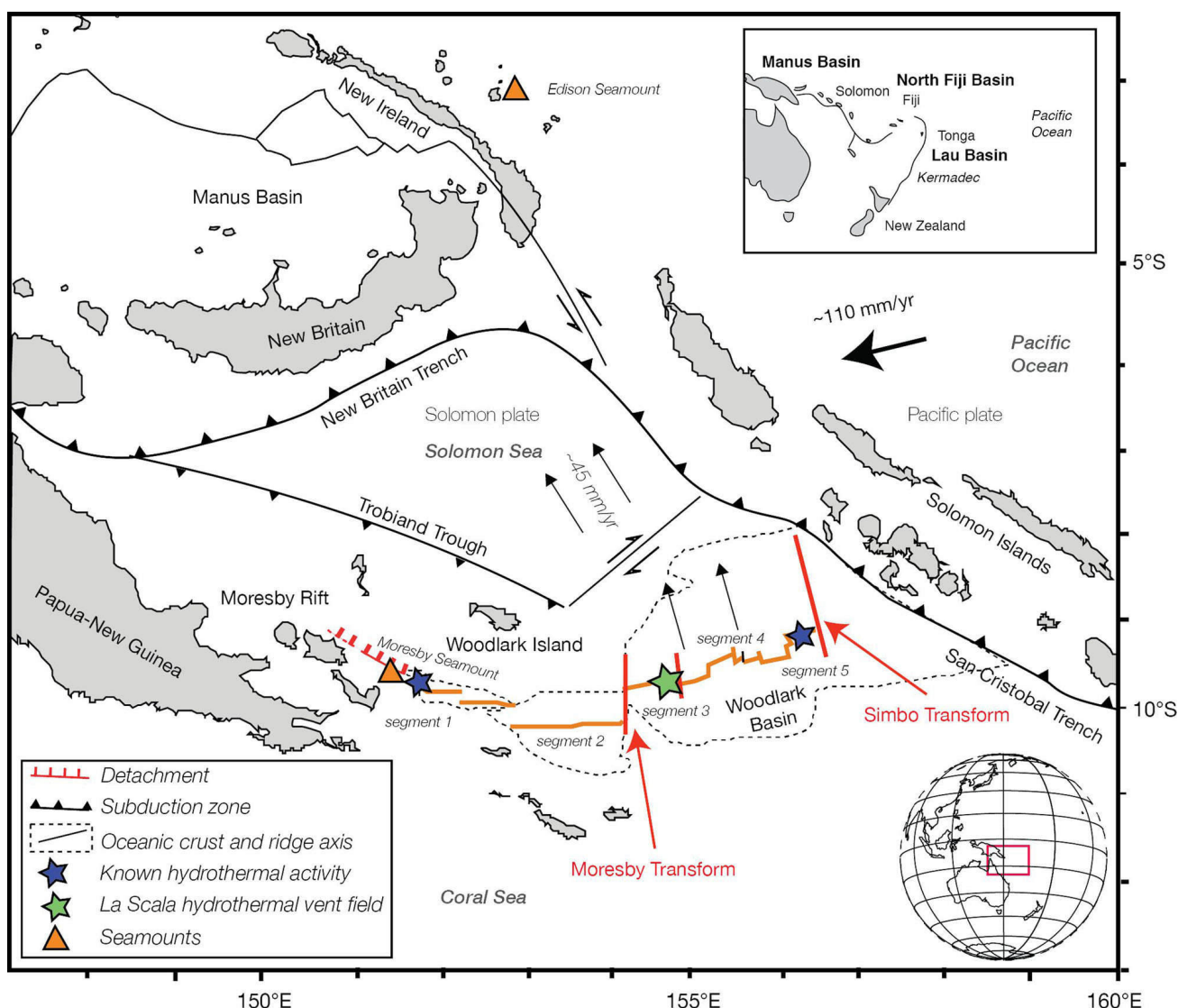


**Fig. 1 Regional map of the Woodlark Basin.** The main tectonic settings are highlighted as well as the location of the newly discovered ‘La Scala’ hydrothermal vent field (green star), modified from Laurila et al. (2012)<sup>12</sup>. Black arrows indicate the directions of plate motion relative to a fixed Australian plate.

potential anomalies at 2900 m below sea level (mbsl) over the eastern edge of Segment 3, Laurila et al.<sup>12</sup> concluded that “the complexity of the tectonics, i.e., frequent ridge jumps and re-orientation of the spreading axis, prevents high-temperature venting in one stable location and, hence the formation of seafloor massive sulfide deposits”, suggesting that stable deep-sea vent communities may not be able to establish there.

Although not reported, the presence of perennial hydrothermal vent fields in the Woodlark Basin could constitute a stepping stone for hydrothermal fauna, at the intersection between the Manus Basin, the Edison Seamount, and the North Fiji and Lau basins, because of its possible link to the Northern expansion of the North Fiji basin which started about 10–11 Mya<sup>16</sup>. This spreading centre, now subducted, was presumed to bridge the older -and fossil- Solomon and South Fiji ridges that shaped the region before the collision of the Melanesian arc and the Ontong Java plateau about 18 Mya<sup>17</sup>. This collision coincides with the oldest dates of speciation events in the complex of gastropod species *Alviniconcha* which initiated 20 Mya<sup>18</sup>. The Woodlark Basin is older than the currently active spreading centres of the adjacent Lau (1–2 Ma) and North Fiji (3–4 Ma) basins, and therefore, may act as a biodiversity dispersion centre for the modern hydrothermal vent fauna at a crossroad between the Manus, North Fiji, and Lau basins.

During the CHUBACARC 2019 cruise (<https://doi.org/10.17600/18001111>), we carried out an extensive water-column survey of the eastern edge of Segment 3, using a strategy based on ship-borne acoustic survey followed by CTD-casts, to detect both thermal and chemical anomalies near the location where Laurila et al.<sup>12</sup> previously reported activity. Based on these observations, we then conducted a seafloor survey using the ROV Victor 6000 that led to the discovery of several high-temperature hydrothermal black smokers. Here, we report on the acoustic and chemical characterization of the hydrothermal plumes, the composition of endmember fluids, the geological setting of the vent fields, and the composition of the fauna associated with the newly discovered vent field we named ‘La Scala’.

## Results and discussion

**Hydrothermal plume exploration over the Eastern Woodlark Ridge.** As part of the high-resolution mapping—using the ship-borne multibeam echosounder (EM122 12 kHz)—carried out over Segment 3 (Fig. 2a), the water column imaging survey revealed the presence of echoes rooted to the seafloor in the vicinity of the ‘TVG-150’ marker<sup>15</sup>. These echoes, rising 200–300 m above the seafloor (Fig. 2b, Supplementary Fig. 1), remained visible at the same location at each passage of the ship over the area and showed the same features as the plumes previously observed in the Guaymas Basin<sup>19</sup>. During the CHUBACARC cruise, similar signals were also observed at shallower sites known to host active vents in the Manus Basin. These echoes were therefore attributed to the presence of hydrothermal plumes. It is commonly believed that deep hydrothermal plumes cannot be detected by water column acoustic imaging because of the absence of strong scatterers such as gas bubbles or droplets<sup>20</sup>. However, Ondréas et al.<sup>19</sup> showed that hydrothermal plumes down to 2000 mbsl could be identified using ship-borne multi-beam echosounding and differentiated from gas and liquid emissions. In the case of La Scala plumes, the backscattering mechanism may result from a combination of turbulence-induced temperature fluctuations within the first tens of metres of the vents and the presence of fine particles over the entire field at 100–500 m above the seafloor, which was later confirmed by the CTD surveys over the area (very strong turbidity signal and temperature anomalies >0.2 °C in the buoyant plume) and the

subsequent ROV dives. By modelling the acoustic characteristics of the hydrothermal plumes, Xu et al.<sup>21</sup> showed that particles had a predominant role in the acoustic backscatter with the height above the vents. It is worth noting that the success of this technique of detection strongly depends on the acoustic impedance difference between the hydrothermal fluid and the surrounding water, on the acoustic frequency, and on the sea state.

The subsequent CTD/tow-yo survey (Fig. 2c) first in the N–S direction and, then followed by a NE–SW transect crossing above the fluid echo showed turbidity (or nephelometry) anomalies at 2800 and 3300 mbsl i.e., at an altitude of 300–500 m above the seafloor (Fig. 3a, b), associated to manganese (Mn) anomalies (up to ~108 nM, Supplementary Data 1) and redox potential (Eh) signals. The strongest anomalies appeared to be consistent with the location of the echoes, confirming the presence of a buoyant plume.

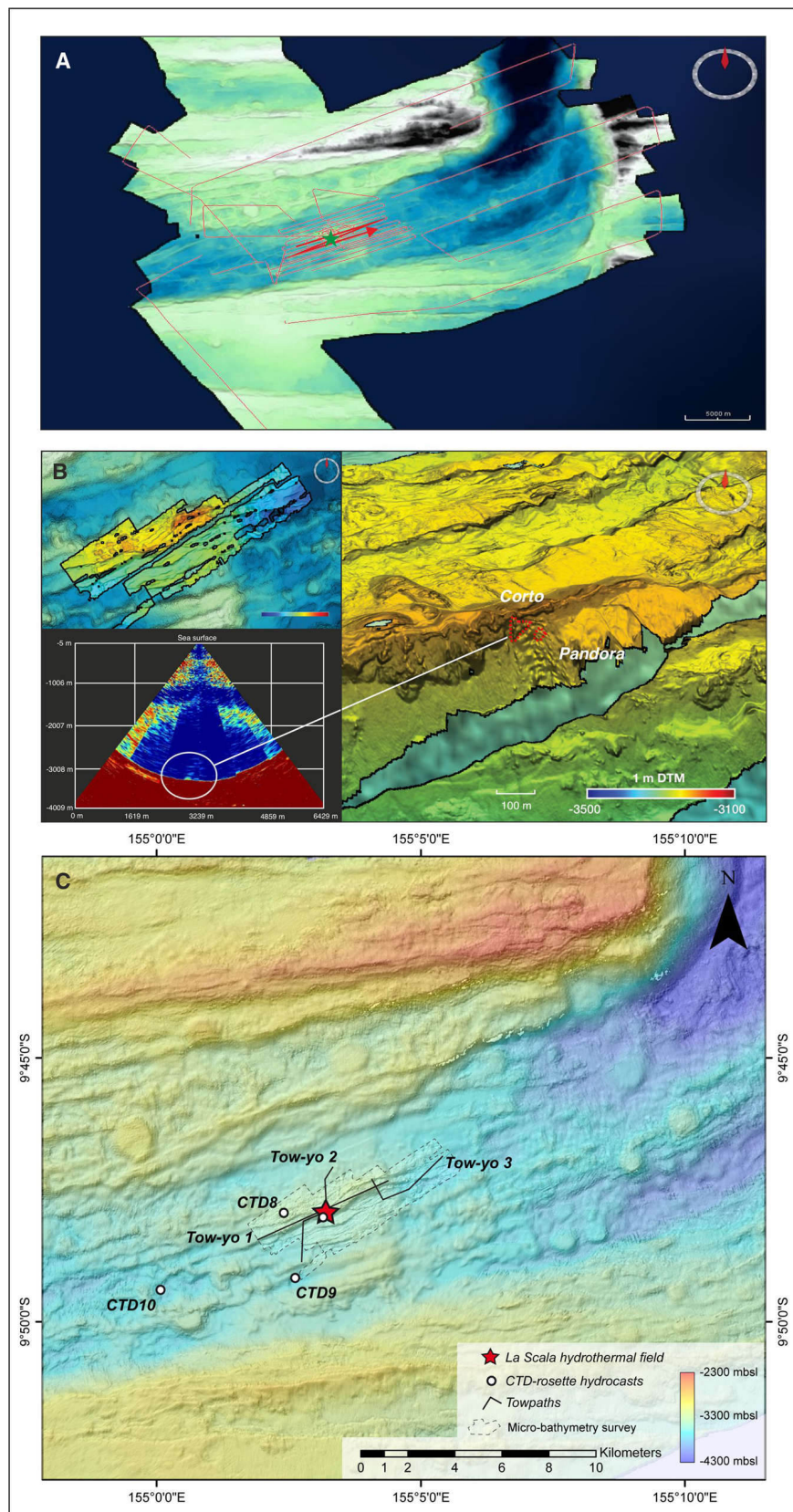
The second phase of the water column survey consisted of two vertical CTD casts (CTD-06 and CTD-07) above the strongest acoustic and chemical anomalies spotted during the MBES and the tow-yo survey. The data showed unambiguous anomalies of Eh, pH, potential temperature, density, and turbidity (Fig. 3c, d), which confirmed the presence of both buoyant and non-buoyant plumes. During CTD-06, we encountered a first turbidity anomaly (0.08 NTU) associated to an Eh signal at 2850 mbsl corresponding to a dispersing buoyant plume 500 m above seafloor. Below, a second, weaker turbidity anomaly (0.03 NTU) was found but not associated to any other chemical signal. Finally, very strong turbidity signals (up to 0.5 NTU), as well as temperature anomalies (~0.1–0.3 °C), were observed close to the seafloor (180 and 100 m above the seafloor) indicative of the presence of at least two hydrothermal plumes (Supplementary Fig. 2). The CTD-07 cast, conducted a few hours later and 60 m away from the CTD-06 location, showed a typical non-buoyant plume structure for turbidity and temperature (anomalies >0.2 °C), as well Mn varying from 34 to 265 nM. The CTD-07 vertical profile clearly indicated the presence of several black smoker-type sources spread out on the flank of the ridge, from 3300 to 3500 mbsl. These vents seem to generate a regional neutrally-buoyant plume dispersing northeastward at 2800–2850 mbsl.

Based on these exploratory results, an ROV dive close to the bottom led to the discovery of many active hydrothermal chimneys (i.e., black smoker types) and complex spires located between 3300 and 3400 mbsl, as well as a large diffuse venting area colonized by extensive communities of stalked barnacles (Fig. 4). The new vent field, discovered at coordinates 9°47S/155°03E was named ‘La Scala’, in recognition of the acoustic eyes of its discoverer.

Three additional CTD casts (CTD-08, 09, and 10, Fig. 2c) were carried out to estimate the dispersion of the plumes. While the CTD-08 profile showed some clear evidence of hydrothermal plumes dispersing at 2800–2900 mbsl, no anomalies were observed on the CTD-09 and CTD-10 profiles, located at 2.4 and 5.7 km, south and southwest of CTD-07, respectively (Supplementary Data 1). This may indicate a strong control of the dispersion of the plumes by the topography.

## Field observations of the La Scala Vent Field

La Scala Vent Field (LSVF) is located at a distance of 1.2 km North of the neovolcanic axis on the northern part of an old split axial volcanic ridge. The LSVF lies on a NE-trending talus slope and is composed of two main active areas and several zones with inactive chimneys (Fig. 2b). The first active site, named ‘Pandora’, is located Southeast of the field at 3380 mbsl and extends some 30 m by 10 m. It is characterized by predominantly diffusive vents, a few black smokers (Fig. 4a, b) and



extinct chimneys N20 aligned and colonized by an extensive coverage of stalked barnacles and patches of gastropods. The second active site of the field, named 'Corto', lies along a steeper slope at 3360 mbsl, only 15–20 m Northwest of the first site. It comprises a 50 m by 15 m sulfide zone where several 7–10 m tall, vigorous, high-temperature black smokers (Temperature

ranging from 364 to 366 °C, Table 1, Fig. 4c, d) were observed at the Southern edge.

Active hydrothermal chimneys are located on steep talus composed of hydrothermally encrusted basaltic rubble, chimneys fragments, and white blocks of hydrothermally altered volcanic rocks. Near the summit, just above the Corto site, a 30 m tall cliff

**Fig. 2 La Scala Vent Field bathymetry.** **A** Chubacarc cruise bathymetry image (20 m grid DTM (Digital Terrain Model), ship-borne MBES) corresponding to the water column acoustic surveys of the Woodlark Ridge (segment 3b). The green star locates the ‘La Scala’ hydrothermal field. **B** Northward 3D view of the high-resolution bathymetry image (1 m grid DTM, ROV VICTOR MBES) overlaid on the greyed 20 m grid DTM corresponding to the northern part of the old split axial volcanic ridge where LSVF is located. La Scala Vent Field including Pandora and Corto sites is delimited by the red dashed line, on the southern flank of the ridge together with the post-processed echogram of the second profile showing the echo attributed to LSVF. **C** Bathymetry of the segment 3 of the Woodlark Ridge from shipboard multibeam survey showing the location of LSVF as well as the towpaths and the CTD-hydrocasts. Note that CTD06 and CTD07 are located right above LSVF. TVG-150 spot from Laurila et al. (2012)<sup>12</sup> is not showed for clarity as it is 140 m away from LSVF.

is composed of pillow lavas topped by massive lava flows (Fig. 4e). On this same cliff, fifty metres Southwest of the second hydrothermal site, pervasive alteration zones and possibly oxidized massive sulfides exposed after a tectonic event (Fig. 4f) have been observed, indicating past hydrothermal activity in the area. Even though high-temperature chimneys could have formed during previous hydrothermal episodes, most ancient sulfide structures were probably destroyed during a collapse. Thus, at least two hydrothermal events occurred at LSVF. Based on the spreading rate ( $\sim 50 \text{ mm yr}^{-1}$ ) and the distance from the neo-volcanic axis ( $\sim 1.2 \text{ km}$ ), the maximum age of the first event of hydrothermal activity at LSVF can be estimated to be 24,000 years ago. This calculation, along with the presence of numerous inactive chimneys and altered lava, clearly indicates that an active and stable hydrothermal circulation has been maintained over a certain period of time and may not be the result of a recent and episodic volcanic eruption as previously suggested<sup>12</sup>.

### Petrological and geochemical characteristics

Basement rocks recovered at LSVF are composed of rounded to sub-angular clasts of non-vesicular aphyric to plagioclase-pyroxene-phyric basalt (cm-size pebbles), cemented by a silica-rich matrix (quartz and cristobalite) and often coated by mm-thick iron oxyhydroxide crust. Pyrite and minor sphalerite are also identified by X-ray diffraction (XRD) confirming the importance of hydrothermal fluid circulation in basement rock alteration at LSVF. East of the vent field along the summit of the ridge crest, recovered basement rocks consisted of essentially aphyric and non-vesicular pillow lava with glassy chilled margin. Incipient to no alteration was identified. The volcanic crest is covered by thin sediment dusting composed of nanofossil-bearing clay.

Geochemical analyses of volcanic rocks show silica contents ranging from 48.4 to 48.7 wt% and low alkali contents ( $\text{Na}_2\text{O} + \text{K}_2\text{O}$ ) from 2.7 to 2.9 wt% (Supplementary Table 1). Thus, all samples from the LSVF area are tholeiitic basalt similar to mid-ocean ridge basalt (MORB) composition (Supplementary Fig. 3). Glassy pillow margins contain 9.1–9.5 wt% MgO suggestive of rather primitive melt. To our knowledge, these are the first report of basaltic rock composition along Segment 3 of the Woodlark Basin in agreement with the previous studies along Eastern Segment 4<sup>22,23</sup> and consistent with MORB composition with major element variations resulting from fractional crystallization.

### Sulfide deposits and hydrothermal fluids

Three different types of mineralization (Fig. 4 and Supplementary Data 2) were observed and sampled during the subsequent ROV dives: (1) active high-temperature sulfide/sulfate chimneys without significant presence of sessile animals; (2) inactive black smoker chimneys; (3) massive sulfide recovered at the base of either active or inactive complex spire densely colonized by vent organisms. Mineralogical and petrological descriptions show that anhydrite is the dominant mineral in the top section of active black smoker chimney, followed by chalcopyrite, sphalerite, and pyrite towards the inner and lower section of the chimney. Multiple vigorously venting internal conduits are lined with fine

grained euhedral chalcopyrite while chimney walls are composed of mixed mineral assemblages of chalcopyrite, sphalerite, and pyrite. Inactive chimneys and massive sulfides have essentially similar characteristics to active chimney except that anhydrite is absent due to retrograde dissolution and chimney wall are consolidated by more massive pyrite/marcasite assemblages, and thinly encrusted by Fe oxyhydroxide crust.

Sulfide deposits show a wide range of copper (Cu) and zinc (Zn) concentrations reflecting the abundances of chalcopyrite versus sphalerite, while calcium (Ca), strontium (Sr), and silica (Si) reflect the abundance of anhydrite and silica respectively (Suppl. Data 3). As previously recognized<sup>24</sup>, trace elements such as cadmium (Cd) and lead (Pb) are associated with lower-temperature sphalerite-rich mineral assemblages. Average compositions are relatively similar between sulfide deposits, except for the Carioca black smoker characterized by lower Cu and higher cobalt (Co) concentration, up to 0.6 wt% in pyrite-rich samples. High Co contents in basalt-hosted sulfide chimneys have been previously inferred as reflecting a higher magmatic contribution to the hydrothermal fluid<sup>24</sup>. By comparison with average compositions of sulfide mineralization in other tectonic environments in the modern seafloor, LSVF lacks any of the geochemical features of back-arc settings (e.g., gold and Pb enrichment) and is seemingly identical to other basalt-hosted hydrothermal fields along mid-oceanic ridges.

Sulfur isotope analysis was performed on the mineral fractions of pyrite and chalcopyrite of four samples, yielding a range of  $\delta^{34}\text{S}$  values between 1.96‰ and 4.20‰, with an average of 3.03‰ (Supplementary Data 3). Slightly higher  $\delta^{34}\text{S}$  values in the Carioca black smoker indicate a seawater contribution to the hydrothermal fluid in the upflow zone. Such  $\delta^{34}\text{S}$  values are typical of sulfide mineralization from mid-oceanic ridge settings (Supplementary Fig. 4) and suggest no contribution of magmatic  $\text{SO}_2$  ( $\delta^{34}\text{S} < 0\text{‰}$ ) as encountered in back-arc basin hydrothermal systems (e.g., Lau Basin and Manus Basin). Altogether, these results are consistent with the basaltic rock composition and indicate that the magmatic activity on the ridge segment is not directly related to subduction but rather to accretion.

Hydrothermal vent fluids were recovered from three black smoker chimneys from LSVF, all showing remarkably homogeneous venting temperature of  $\sim 365^\circ\text{C}$  (Table 1 and Supplementary Table 2). All recovered vent fluids have non-zero magnesium (Mg) concentrations due to significant seawater entrainment during sampling. Endmember composition of vent fluids are conventionally assumed to be devoid of Mg, because of the quantitative removal of Mg from seawater during hydrothermal interactions with basalt<sup>25,26</sup>. Calculated end-member hydrothermal fluid compositions are reported in Table 1 for all measured elements.

Homogeneous end-member compositions suggest that LSVF is fed by a deep-seated hydrothermal fluid source undergoing minor subsurface fluid mixing. The lowest pH value (3.31) was recorded in Carioca vent fluids consistent with the lowest Mg concentration of 1.6 mM, which suggests minor seawater contribution during sampling. Hence, the end-member pH value is considered to be close to 3.3 for all vents. All end-member vent fluids have

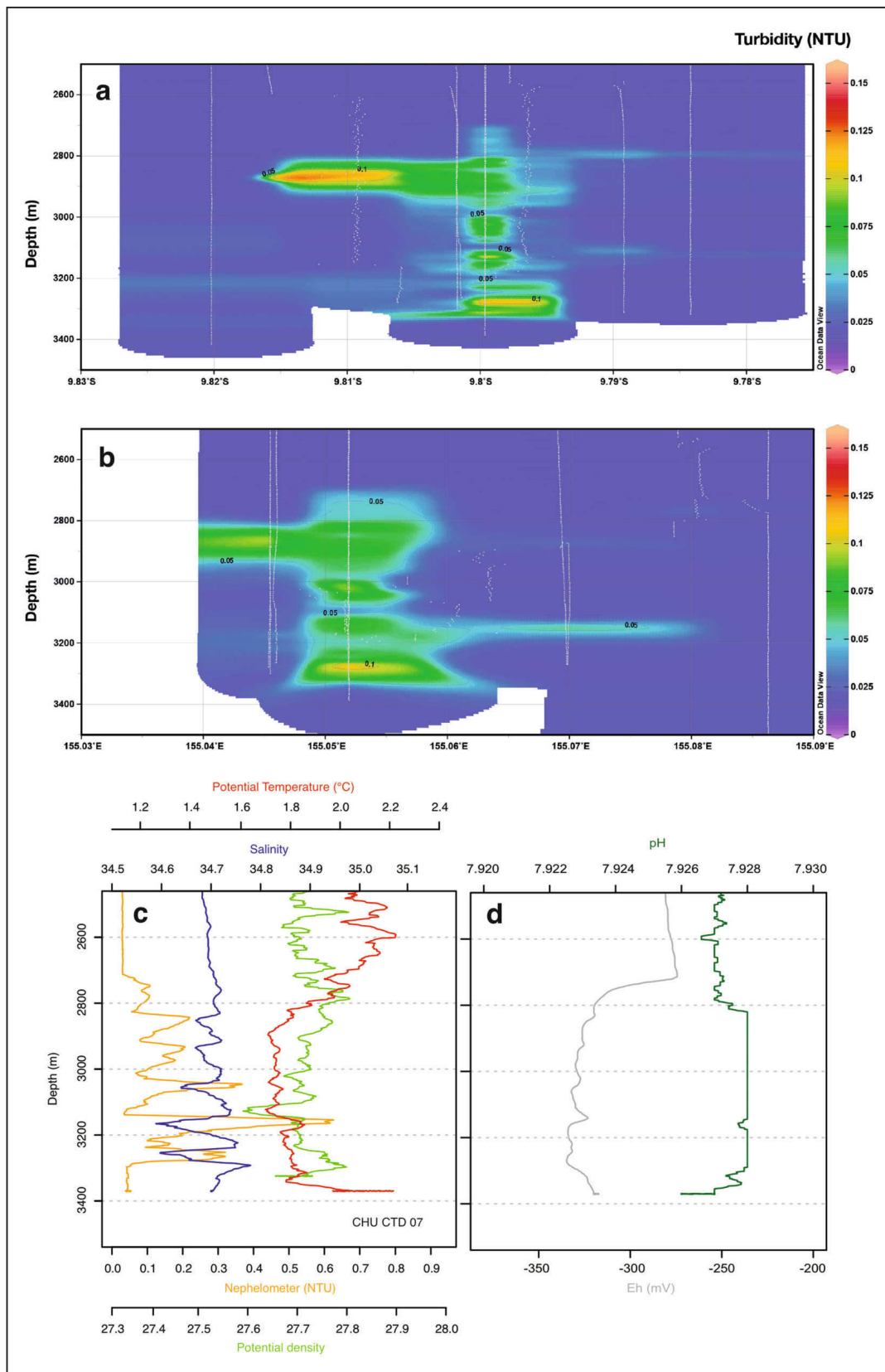


**Fig. 3 Physico-chemical characteristics of hydrothermal plumes above La Scala Vent Field.** N-S (a) and NE-SW (b) sections of turbidity anomalies above Segment 3. The section compiles data from tow-yo surveys (CTD-01 to CTD-03) and vertical casts (CTD-06 and CTD-07) (grey lines). **c, d** Nephelometry (yellow), density (light green), salinity (blue), temperature (red), Eh (grey), and pH (dark green) vertical profiles in the non-buoyant plume of 'La Scala' vent site (CTD-07).



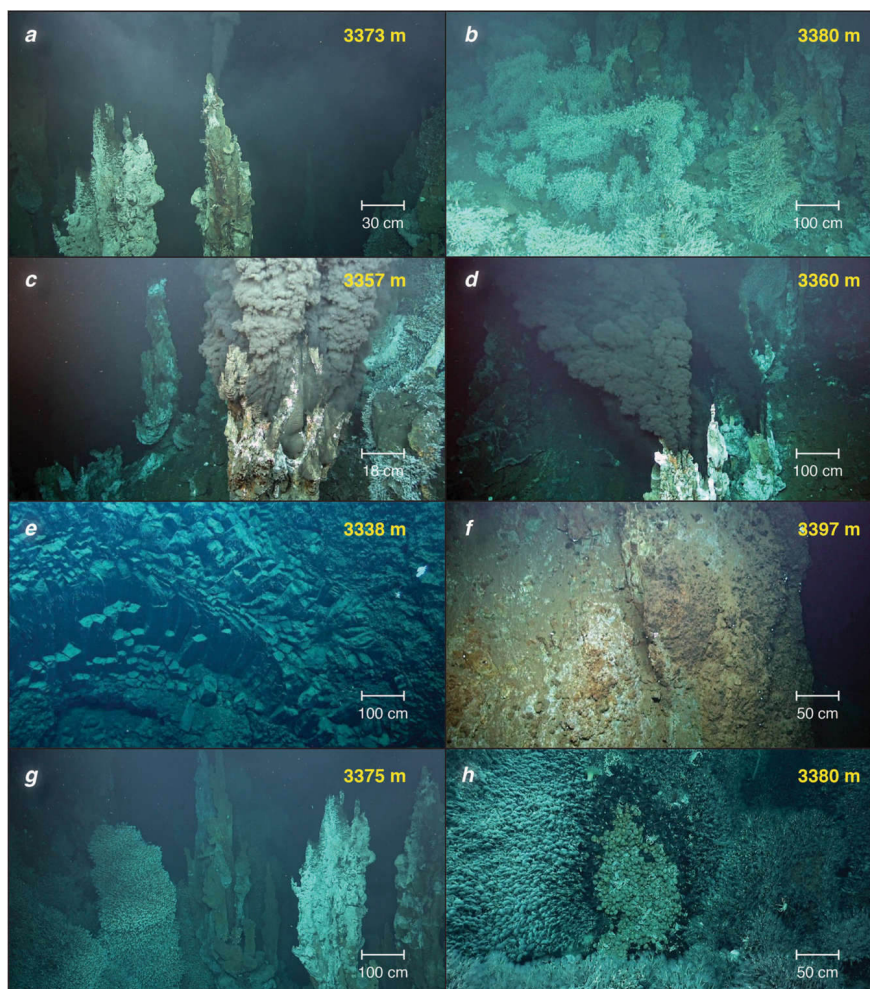


**Fig. 4 La Scala Vent Field.** **a, b** Chimney cluster ('Pandora Site'), SE of the vent field at 3380 m depth characterized by a few black smokers and predominant weakly diffusive vents. This site is surrounded by cirripeds to the West, North and East. **c, d** Second site ('Corto Site') located on the flank of a cliff controlled by a N55-60 fault. The South area at 3360 m depth is the most active of the hydrothermal field. **e** Massive prismatic lava. **f** Highly altered basalts due to past high temperature hydrothermal circulation. **g** Large colonies of *Vulcanolepas* sp. colonizing inactive chimneys. **h** A patch of *Alviniconcha* endosymbiotic gastropods surrounded by *Ifremeria nautilei* and *Vulcanolepas* sp.

chlorinities higher than seawater suggesting they have undergone sub-critical phase separation. Alkali concentrations ( $K \approx 25.4 \text{ mM}$ ;  $Rb \approx 15.6 \mu\text{M}$ ) are similar to most basaltic-hosted vent sites consistent with LSVF geological setting. Silica (Si), iron (Fe) and Mn concentrations are  $\approx 20 \text{ mM}$ ,  $\approx 1.7 \text{ mM}$ , and  $\approx 1.0 \text{ mM}$ , respectively. Fe/Mn ratio of 1.7 is however lower than values expected from the vent temperature<sup>27</sup>, suggesting possible sub-surface sulfide precipitation. Endmember Cu and  $\text{H}_2\text{S}$  concentration of  $21 \mu\text{M}$  and  $4.1 \text{ mM}$  respectively, are also lower than typical high temperature (i.e.,  $>350^\circ\text{C}$ ) vent fluids, lending further support to this hypothesis.

#### Hydrothermal vent fauna

LSVF is characterized by several very active black smoker chimneys whose surface is occupied by a sparse population of *Rimicaris* shrimp and very large beds of a new species of stalked barnacles, *Vulcanolepas* sp. nov., that colonizes mildly active diffuse venting areas and old inactive chimneys or sulfide mounds (Fig. 4g). The dominant engineer species and their associated fauna were comparable to other Southwest Pacific vent communities but differed in relative abundance<sup>28–30</sup>. Stalked barnacles covered vast areas (c.a.  $>300 \text{ m}^2$ ) on the seafloor while large symbiotic gastropods were rare and restricted to patches smaller

than in other Western Pacific back-arc basins. Patches of small-sized gastropods *Ifremeria nautilei* and *Alviniconcha* spp. were observed in the most active diffuse areas with temperatures varying from  $2.4$  to  $7.3^\circ\text{C}$  (average of  $4.6 \pm 1.3^\circ\text{C}$ ) and  $2.5$ – $20.3^\circ\text{C}$  (average  $8.5 \pm 4.4^\circ\text{C}$ ), respectively (Fig. 4h). Cirripeds *Eochinelasmus ohtai* and *Imbricaverruca* sp. were found next to *Ifremeria nautilei* and *Alviniconcha* spp. communities (Fig. 5). Aggregations of alvinocaridid shrimp *Rimicaris variabilis*, *Branchinotogluma segonzaci* polynoids, and *Shinkailepas tufari* phenacolepadid gastropods were also observed on active chimneys (Fig. 5f). Extensive bacterial mats were also noticed at the periphery of the vents, as well as bamboo corals (Isididae), squat lobsters (Munidopsidae), brisingid starfish, crinoids, and sea anemones (Supplementary Fig. 5). Morphological identification of the benthic fauna collected and observed from videos was compiled as a list of at least 45 taxa, including 23 families and 23 genera (Supplementary Data 4). The macrofauna associated with *Vulcanolepas* sp. nov. was mainly composed of the barnacle *Imbricaverruca* sp., members of the polychaete families Ampharetidae (*Amphisamytha* cf. *vanuatuensis*), Maldanidae (*Nicomache* spp.), and Spionidae, and the provannid gastropod *Provanna* sp. (Supplementary Data 5). Many copepods and nematodes were also part of this community. Holothurians *Chiridota* sp., anemones (Actiniaria), squat lobsters, *Austinograea*

**Table 1** Temperature, pH, and chemical composition of La Scala fluid endmembers.

	Temp (°C)	pH (21 °C)	H <sub>2</sub> S mM	Mg mM	Cl mM	SO <sub>4</sub> mM	Na mM	S mM	K mM	Ca mM	Sr μM	Li μM	B μM	Rb μM	Cd μM	Ba μM	Si μM	Mn μM	Fe μM	Cu μM	Zn μM
Bottom SW		7.5	0.00	55.75	546	28.2	474	29.8	9.1	10.6	99	27	435	1.5	<0.1	0.08	122	<0.1	<1	<0.1	<0.1
Black smoker 6	364	<4.31	>2.2	0	633.2	2.0	561	2.7	25.3	31.7	115	1163	763	15.6	0.2	9.4	2007.4	1019	1602	39.9	108.1
Black smoker 5	366	3.3	4.0	0	634.9	1.4	543	2.1	25.4	31.0	115	1208	749	15.6	0.1	17.1	19795	1019	1848	10.8	50.6
Black smoker 8	365	3.3	4.1	0	647.9	1.5	548	5.4	25.6	31.5	115	1198	757	15.6	0.1	14.6	20122	1028	1707	12.6	39.8

crabs and *Phymorhynchus* sp. gastropods were also found among and next to *Vulcanolepas* sp. nov. thickets. A sample collected in an *Ifremeria nautiliei* patch showed that the associated macrofauna was dominated by an undescribed peltospirid limpet and polynoid scaleworms, and formed the most diverse assemblage in term of species richness. *Amphysamytha* cf. *vanuatensis* and alvinellid worms (genus *Paralvinella*) were also found in *Ifremeria nautiliei* and *Alviniconcha* spp. communities. Copepods, bythograeid crabs (*Austinograea* sp., which is likely to represent a new species), *Rimicaris variabilis* shrimp and polychaetes were the dominant taxa found in *Alviniconcha* spp. patches.

Most of the fauna had  $\delta^{34}\text{S} < 10\text{‰}$  (Fig. 6), suggesting they primarily depend (either directly or indirectly) on chemosynthetic vent production and sulfide oxidation for their nutrition<sup>31</sup>. This was notably the case of organisms considered as peripheral fauna, or not strictly found at vents, such as *Vulcanolepas* sp. nov., anemones, or *Phymorhynchus* sp.. Brisingidae starfish, holothurians *Chiridota* sp., and carnivorous sponges had  $\delta^{34}\text{S}$  between 10 and 15‰, suggesting a mixed diet, depending on both chemosynthesis- and photosynthesis-derived organic matter<sup>31</sup>. Only the Isididae bamboo corals had a  $\delta^{34}\text{S}$  greater than 15‰, suggesting they primarily feed on exported photosynthetic production<sup>31</sup>. Overall, the dependence of organisms on vent endogenous production seemed significant, and spanned all sampled taxonomic and functional groups. Similar observations have been made in active<sup>32</sup> and inactive<sup>33</sup> hydrothermal vents from the Manus basin. In contrast, the dependence of hydrothermal fauna on exported photosynthetic matter is higher at shallower vents of the Southern Tonga arc<sup>34</sup>. The increased importance of endogenous production for deeper sites matches patterns observed in other chemosynthesis-based habitats<sup>35,36</sup>.

While  $\delta^{34}\text{S}$  values ruled out major photosynthetic contributions, the wide ranges of  $\delta^{13}\text{C}$  and  $\delta^{15}\text{N}$  measured in Woodlark fauna suggest that animal communities show considerable trophic diversity, and depend on several production mechanisms (Fig. 6). Some species had very negative  $\delta^{13}\text{C}$  (e.g., *Alviniconcha kojimai*, *Ifremeria nautiliei* or *Provanna* sp.), suggesting they mostly depend on sulfide oxidizers using the Calvin–Benson–Bassham (CBB) cycle for their nutrition<sup>37</sup>. Conversely, some species, such as *Alviniconcha boucheti* or *Branchinotogluma segonzaci* had very positive  $\delta^{13}\text{C}$ , suggesting they acquire most of their organic matter from sulfide oxidizers using the reverse tricarboxylic acid (rTCA) cycle<sup>37</sup>. Interestingly, many taxa had intermediate  $\delta^{13}\text{C}$  values comprised between those two end-members, suggesting a co-reliance on both bacterial metabolisms in variable proportions. Similar findings have been reported for the Manus Basin<sup>32,38</sup>. However, in Manus, communities seem to be mostly supported by the CBB cycle, particularly at the Solwara 1 site<sup>32</sup>. In Woodlark, our results suggest that inter- (and sometimes intra-) taxon differences in feeding preferences could lead to a more evenly balanced continuum of  $\delta^{13}\text{C}$  values, and therefore the importance of the two production mechanisms for the food web. Finally,  $\delta^{34}\text{S}$  of Woodlark fauna was similar to some hydrothermal vents from the Manus Basin (Solwara 1, PACMANUS), but markedly higher than other Manus sites (e.g., South Su)<sup>32</sup>. This suggests that local changes in sulfur geochemistry could influence this parameter and the way secondary consumers are locally distributed.

### Genetic characterization of the main ecological engineer species

As other vent communities of the western Pacific back-arc basins, engineer species observed at LSVF are mainly composed of stalked barnacles, and provannid gastropods that belong to the genera *Alviniconcha* and *Ifremeria*. *Bathymodiolus* mussel beds

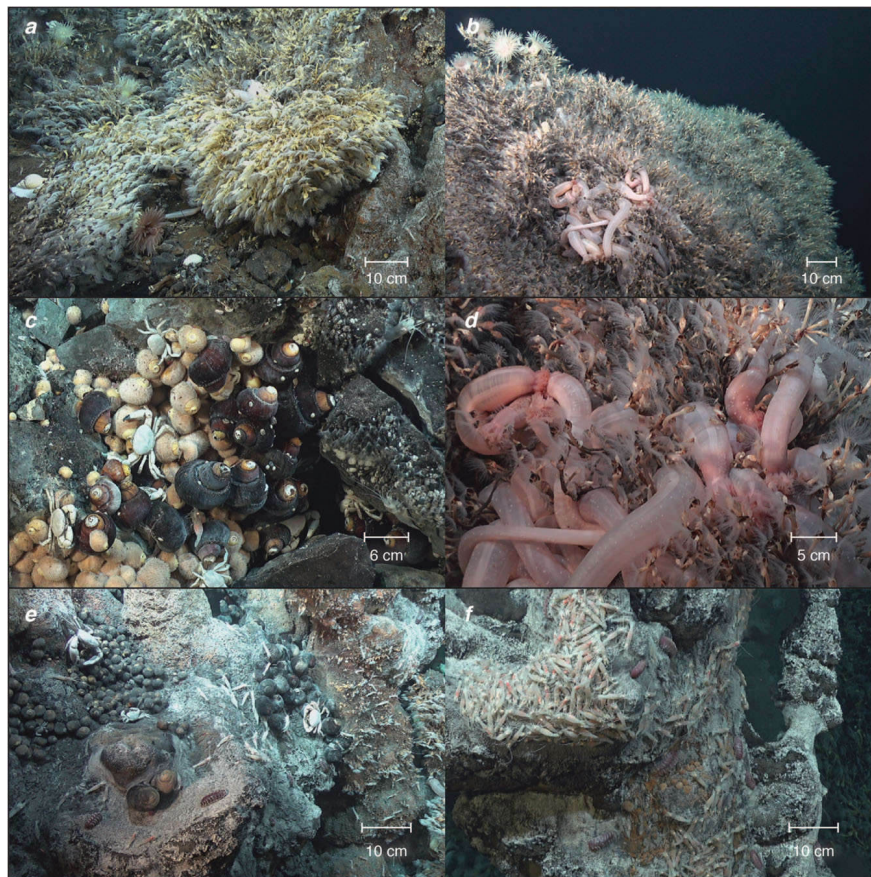


**Fig. 5 Hydrothermal fauna from La Scala Vent Field.** **a** *Vulcanolepas* sp. n. thickets, anemones and gastropod *Phymorhynchus* sp. **b** Anemones and holothurian *Chiridota* sp. in *Vulcanolepas* sp. n. thickets. **c** Aggregation of gastropods *Ifremeria nautilei* and *Alviniconcha kojimai* with *Austinograea* crabs and cirripeds *Eochionelasmus ohtai* and *Imbricaverruca* sp. (right side of the picture). **d** *Chiridota* sp. in *Vulcanolepas* sp. n. thicket. **e** Aggregation of *Alviniconcha kojimai*, polynoids, alvinocarids shrimps, and *Austinograea* crabs. **f** Aggregation of alvinocarid shrimp *Rimicaris variabilis*, polynoids *Branchinotogluma segonzaci* and gastropod *Shinkailepas tufari* on active chimney.

were surprisingly not found at Woodlark. A first genetic examination of stalked barnacles using a 658-bp fragment of the mitochondrial cytochrome c oxidase (*Cox1*) gene clearly indicated that, while falling into the *Vulcanolepas* clade (support 0.66), specimens from Woodlark form a distinct phylogenetic clade (support 0.99, within clade pairwise Jukes–Cantor distances  $0.22 \pm 0.21\%$ ) and therefore represent a new putative species (Fig. 7). This new species is surprisingly most closely related to the species found at vents on the Kermadec volcanic arc (*V. osheai*,  $6.86 \pm 0.23\%$  average Jukes–Cantor distances), and a bit more distantly to the species found at vents in the Lau Basin (*V. buckeridgei*,  $7.35 \pm 0.33\%$  average Jukes–Cantor distances) or the species *Leucolepas longa* from Lihir island<sup>39</sup>. Interestingly, for this genus, each sampled area seems to host a distinct species. *Alviniconcha* and *Ifremeria* gastropods were not numerous (distributed as small patches at the base of chimneys) and of rather small size, suggesting that they may represent genetically differentiated populations when compared to other described species elsewhere. All individuals collected at Woodlark were thus bar-coded using a 659 bp-fragment of mitochondrial *Cox1* gene to build haplotype networks and test their relationships with previously described species. For *Alviniconcha*, the use of previously published sequences yielded 5 clusters that correspond to the currently described species. *Alviniconcha* specimens collected at La Scala fall into two equally represented but distinct species, *A. boucheti* and *A. kojimai*, but are not geographically distinct from populations collected in other basins, at least using this genetic marker (Supplementary Fig. 6). *Ifremeria* specimens fall into two

main clusters separated by five fixed substitutions (divergence = 0.75%, Fig. 8): one that mainly comprises specimens from the Manus and Woodlark basins and one that comprises specimens from other basins (Lau, North Fiji, and Futuna) (Fig. 8 and Supplementary Fig. 6). Remarkably, a few specimens from Futuna and Lau however, fall into the Manus/Woodlark cluster. This suggests a possible recent migration from the Woodlark ridge to the Northern part of the Lau basin (including Futuna) following a first geographic isolation event of the Manus and Lau/North Fiji/Futuna populations in allopatry. These preliminary results clearly indicate that vent species have contrasted population histories. Some of the species are clearly endemic of the Woodlark ridge (a possible separation due to the greater depth) whereas others may use it as a stepping stone during the colonization of the present-day back-arc basins of the Western Pacific.

### The Woodlark Ridge: A potential biological cornerstone?

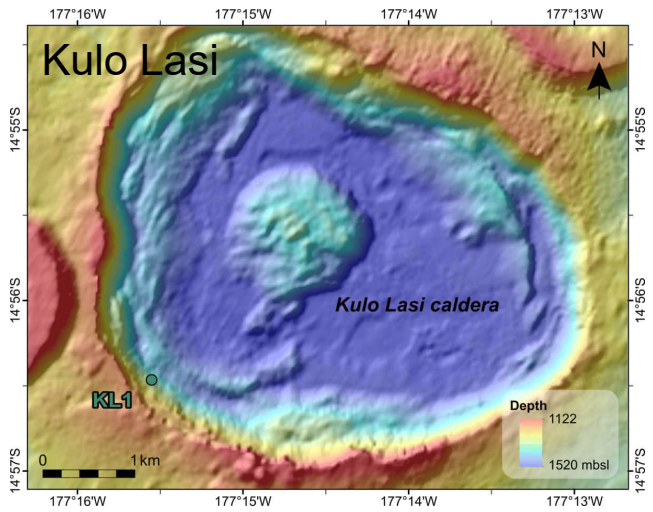
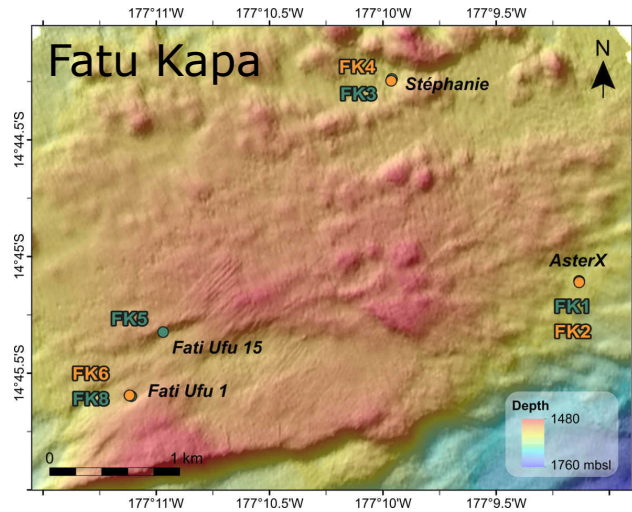
The tectonic history of the western Pacific back-arc basins is complex<sup>17</sup>. The opening of some basins such as Manus, Lau, and North Fiji is recent (less than 4–3 millions years)<sup>17,40,41</sup>, and likely simultaneous, even if the formation of the North Fiji proto-basin initiated before about 10–12 Mya<sup>16</sup>. This points towards the existence of older relay-ridges for the vent fauna before their opening of the present-days basins as previously mentioned to explain the spatial distribution patterns of the symbiotic gastropod *Alviniconcha* spp<sup>18</sup>. In this context, the present-day distribution of the hydrothermal vent fauna likely results from the partition of an older hydrothermal fauna originating from ridges

## **D.2 Cartes des champs échantillonnées**

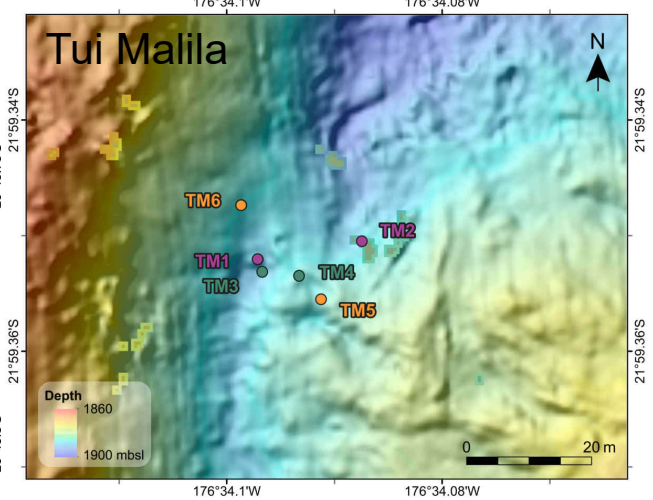
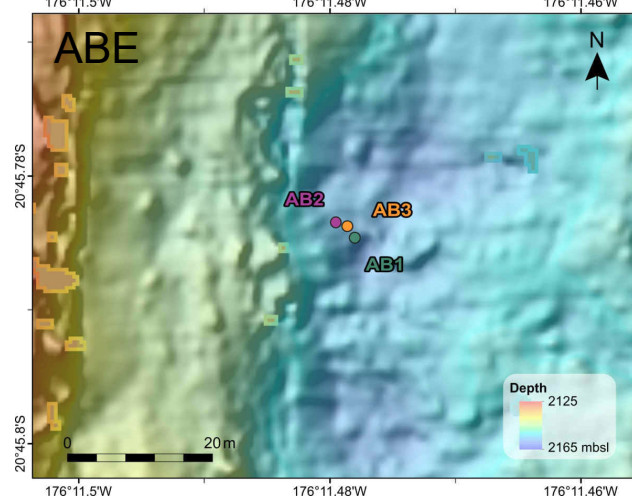
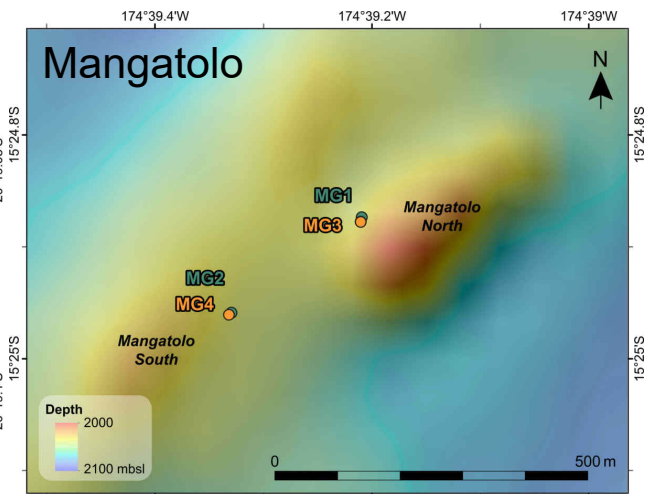
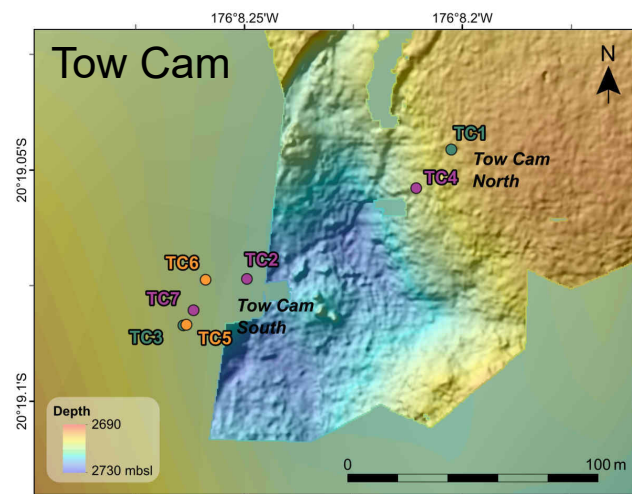
# Basin: Futuna

## Habitat

- *Alviniconcha*
- *Bathymodiolus*
- *Ifremeria*



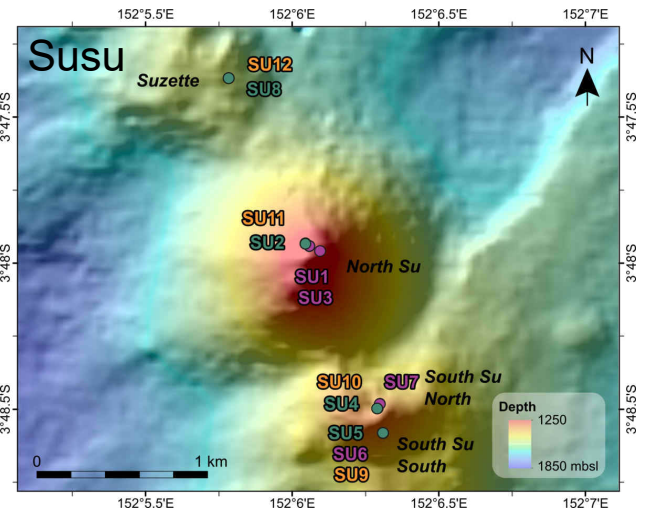
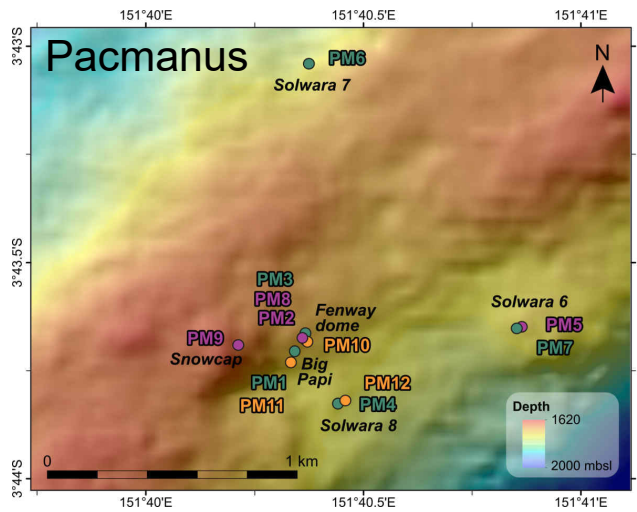
# Basin: Lau



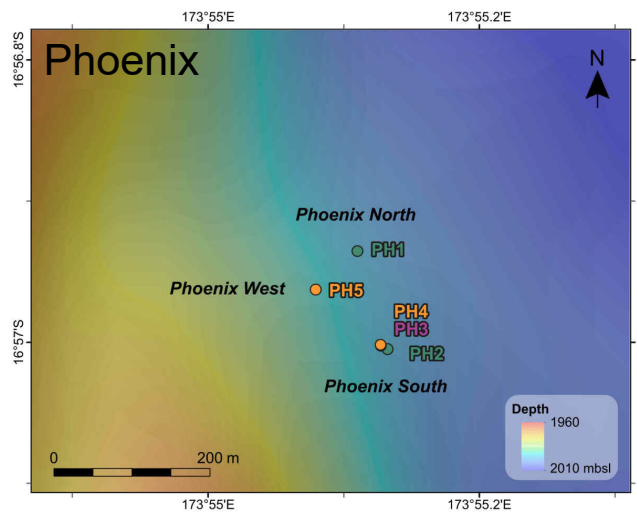
# Basin: Manus

## Habitat

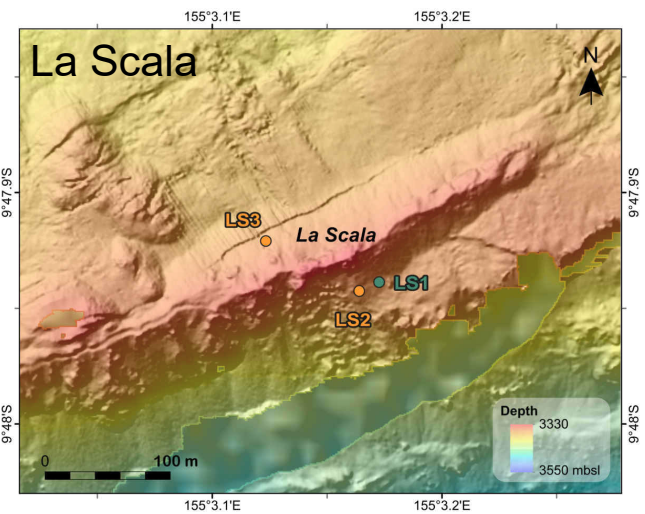
- *Alviniconcha*
- *Bathymodiolus*
- *Ifremeria*



# Basin: North Fiji



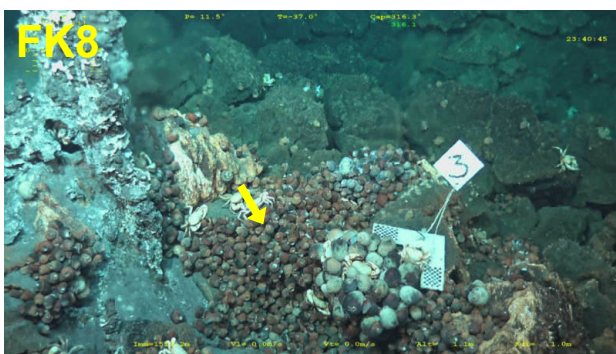
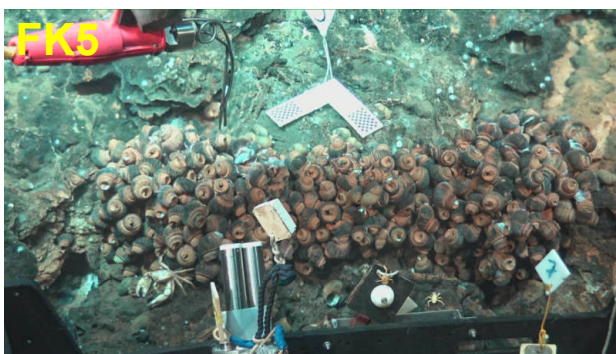
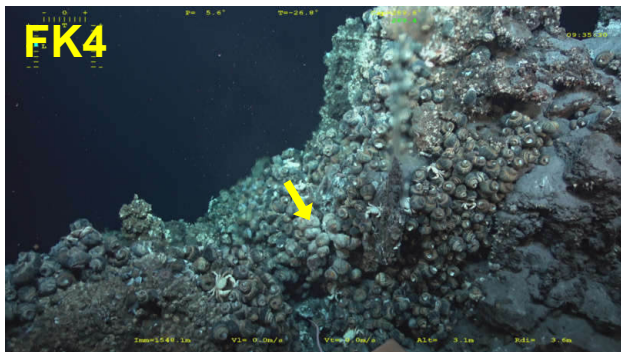
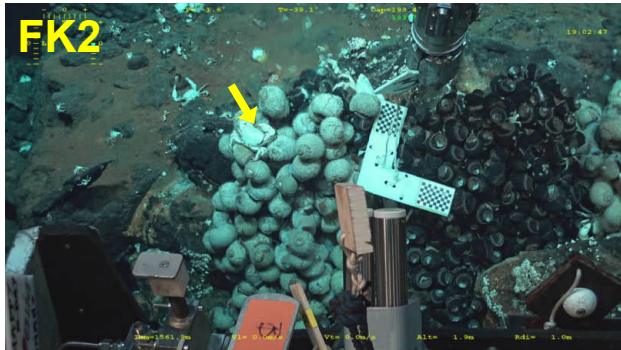
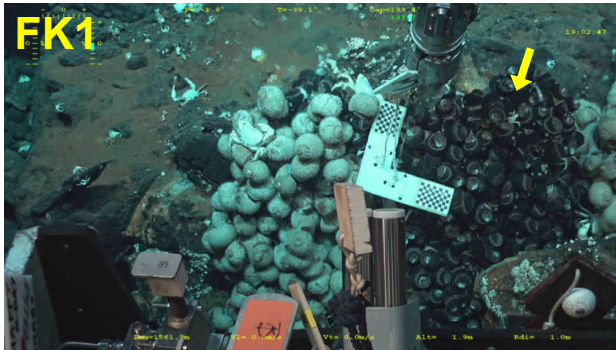
# Basin: Woodlark



### **D.3 Photos des habitats échantillonnées**

# Basin: Futuna

## Field: Fatu Kapa



## Field: Kulo Lasi

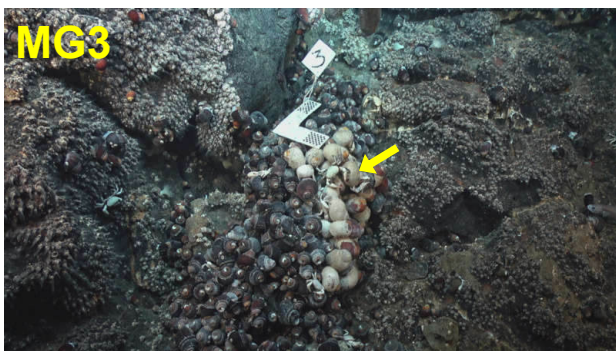
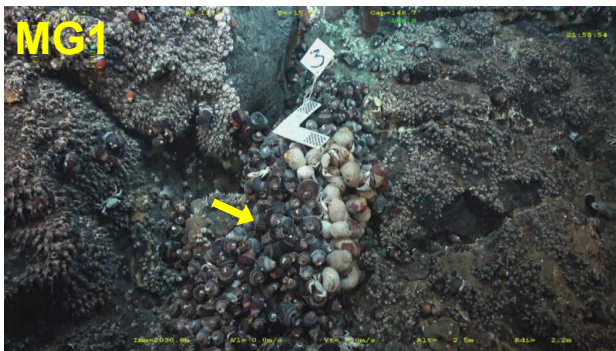




Basin: Lau  
Field: ABE

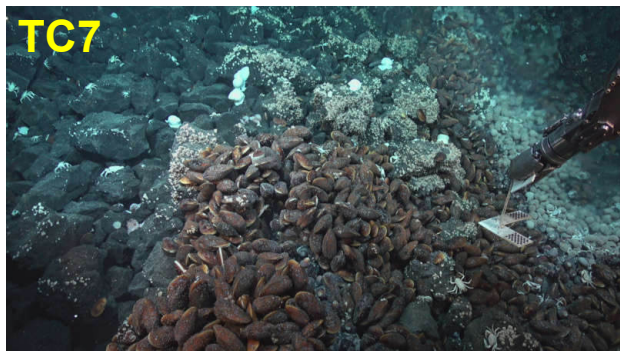
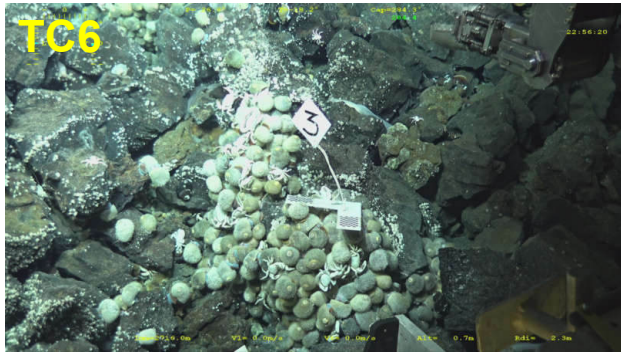
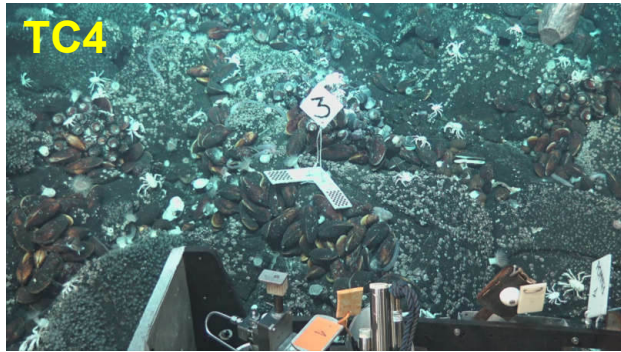
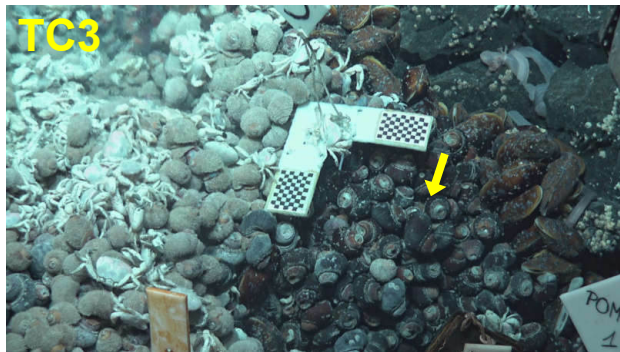
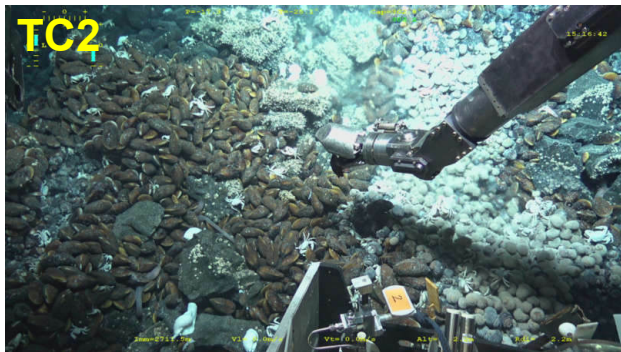
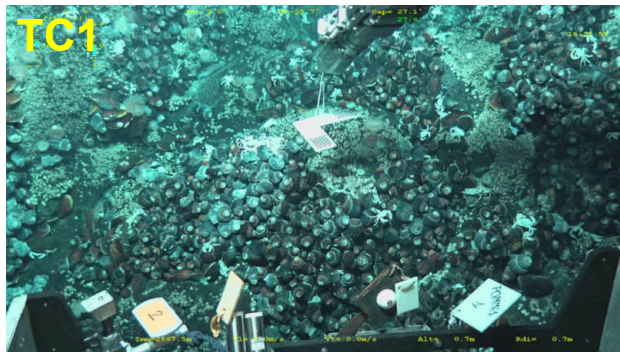


Field: Mangatolo

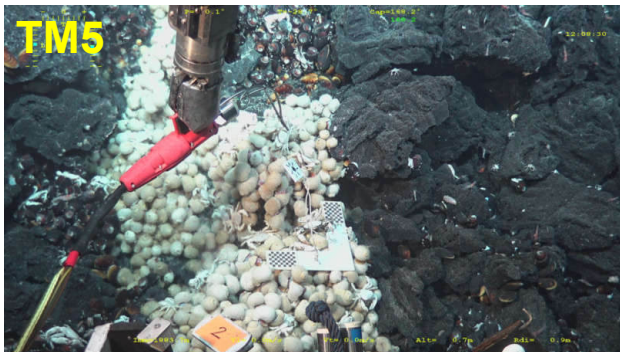
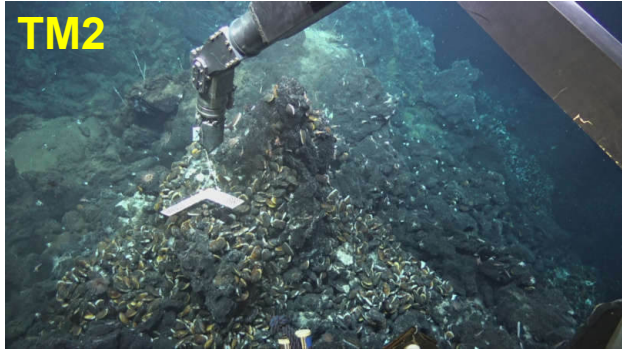
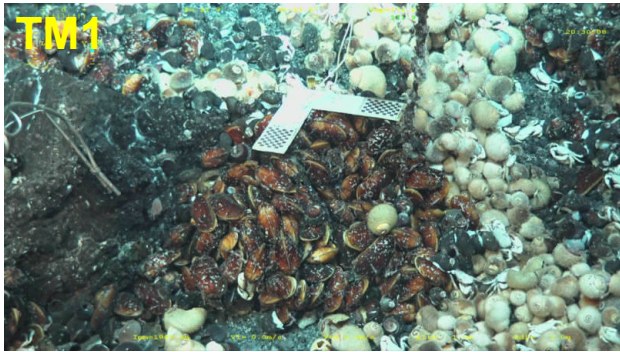


# Basin: Lau

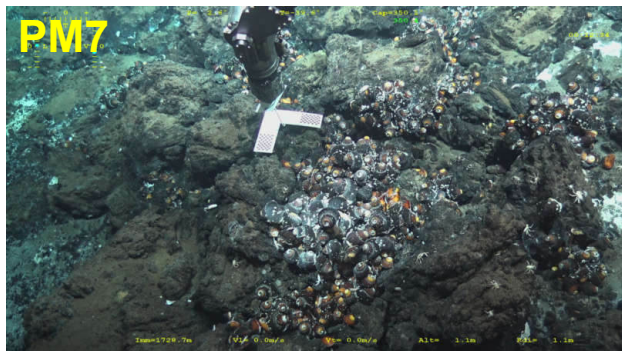
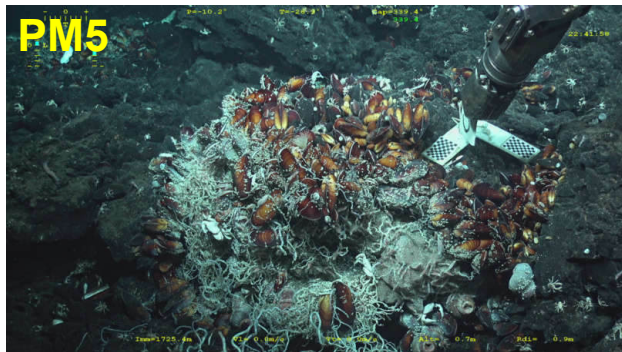
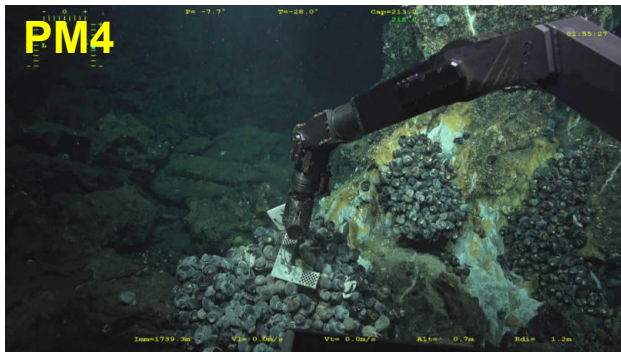
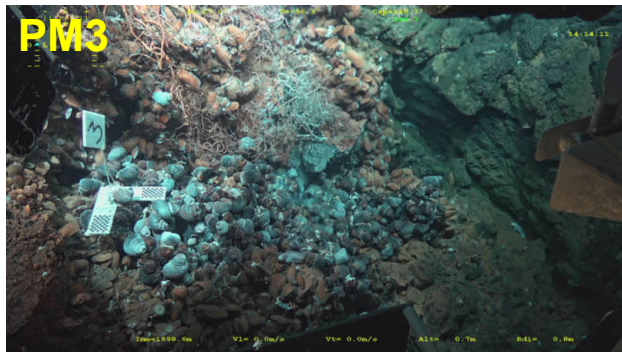
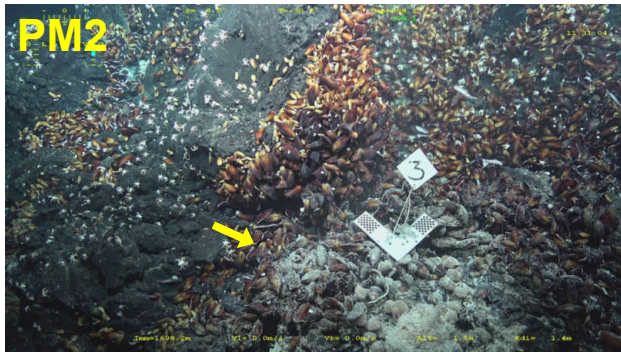
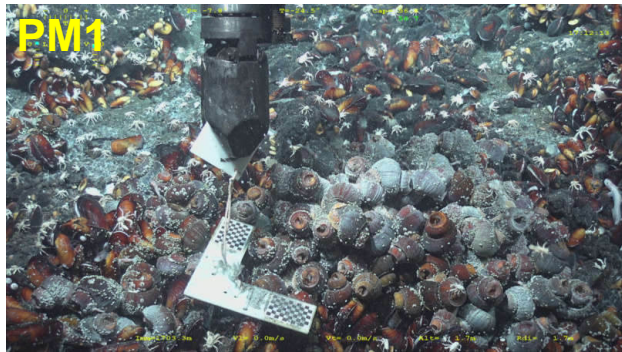
## Field: Tow Cam



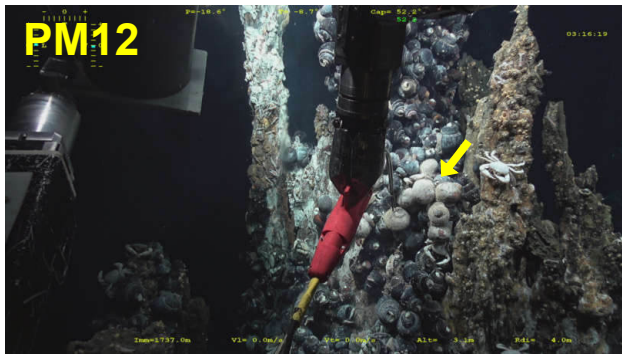
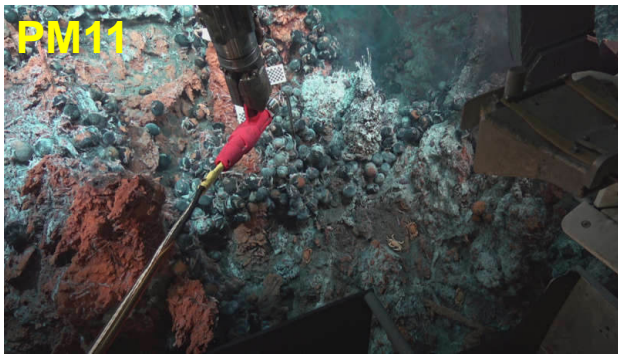
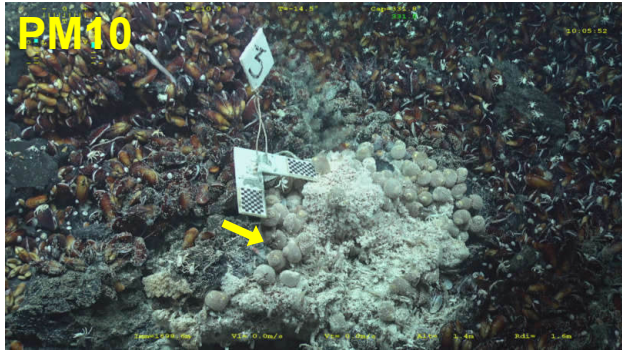
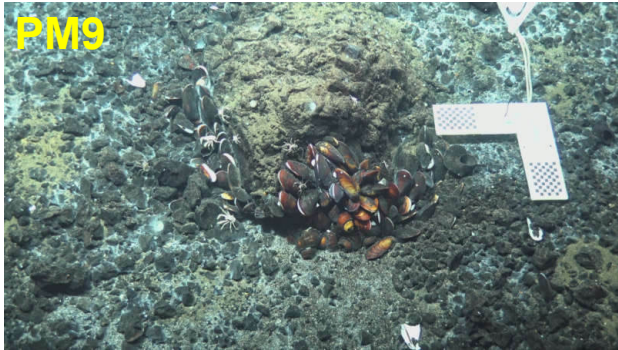
**Basin: Lau**  
**Field: Tui Malila**



# Basin: Manus Field: Pacmanus

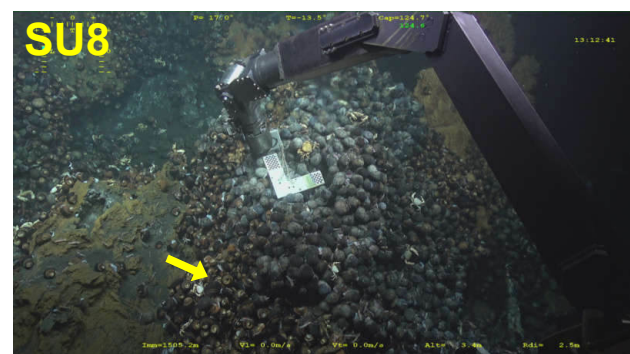
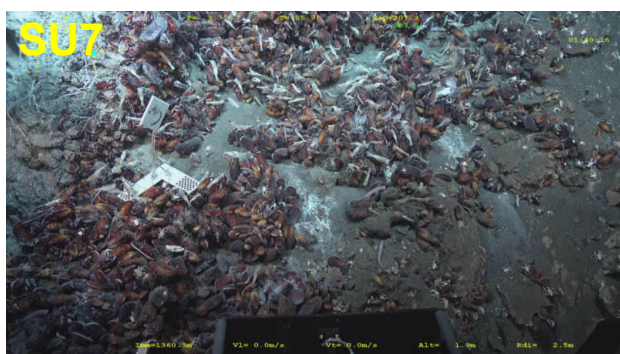
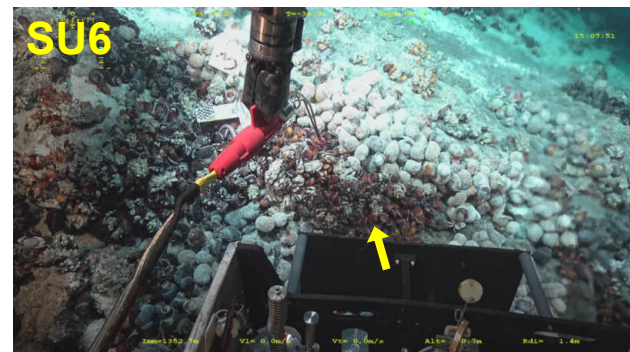
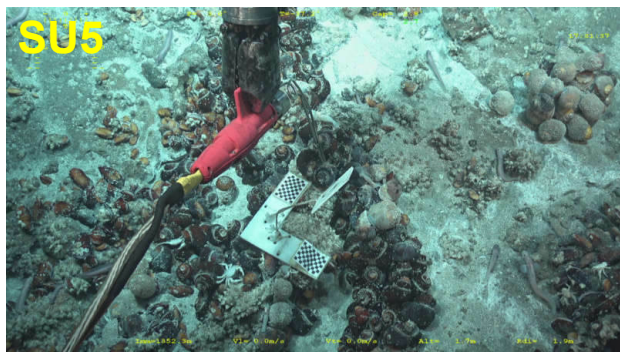
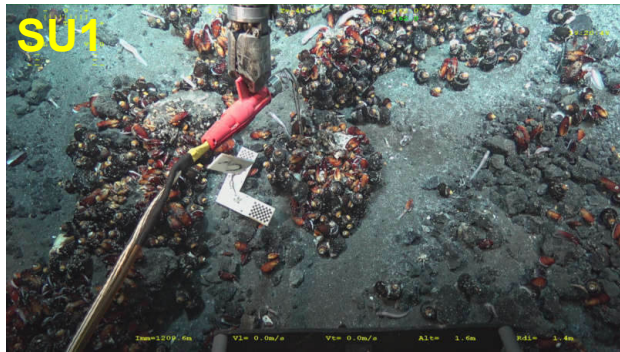


**Basin: Manus**  
**Field: Pacmanus**

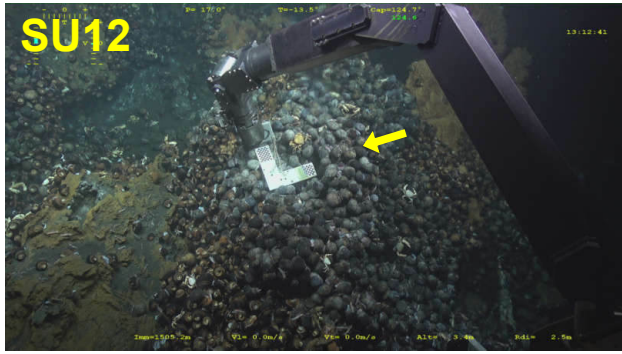
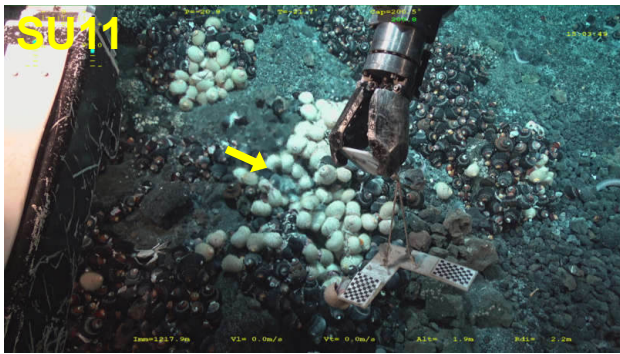
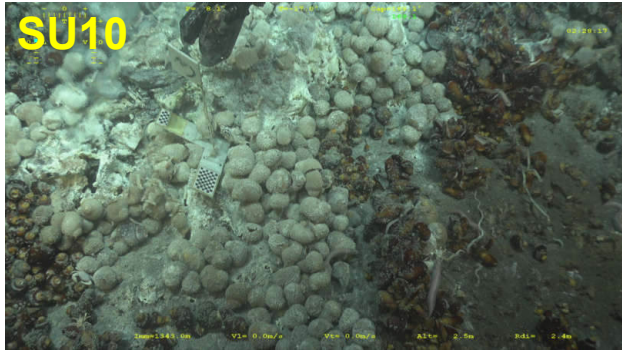
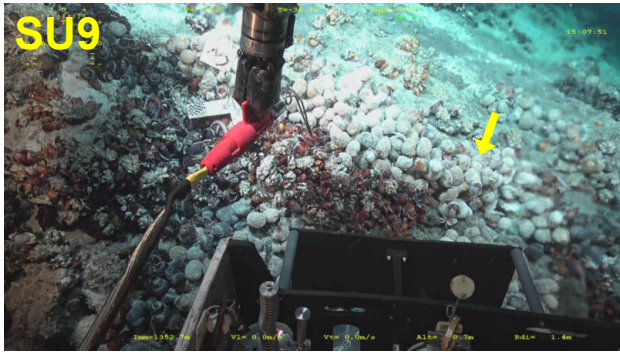


# Basin: Manus

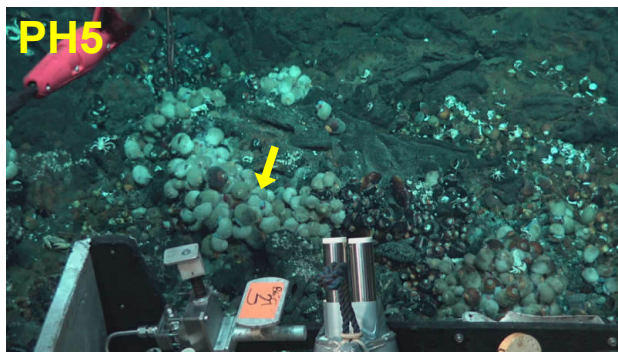
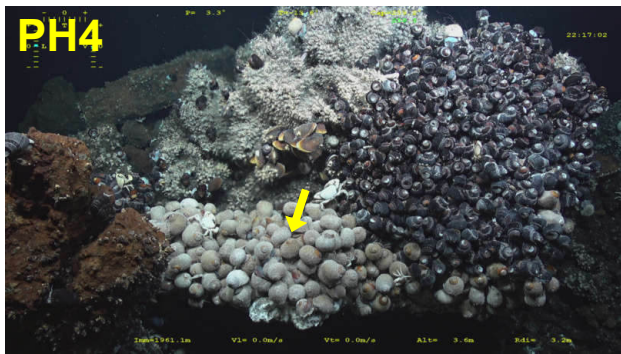
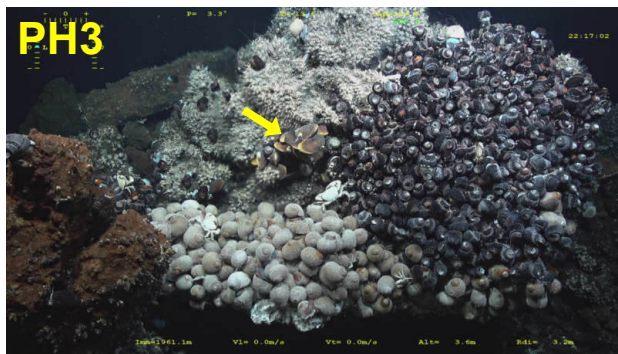
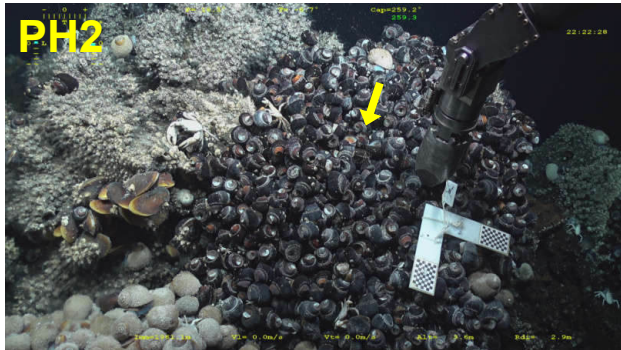
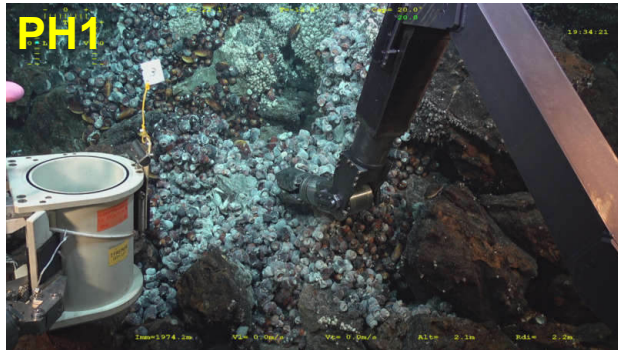
## Field: Susu



# Basin: Manus Field: Susu



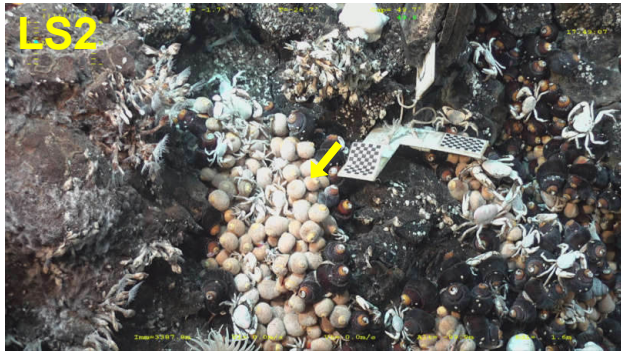
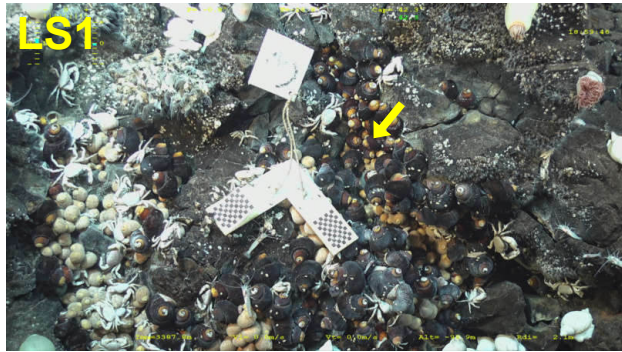
# Basin: North Fiji Field: Phoenix





# Basin: Woodlark

## Field: La Scala



*D.4 Numéros de plongée, de boîte et d'aspirateur pour chaque échantillon*

## **D.4 Numéros de plongée, de boîte et d'aspirateur pour chaque échantillon**

TABLE D.4 – Chubacarc dive, box and suction numbers for each sample.

Basin	Field	Site	Hab.	Sample	Dive ID	Biobox number	Suction number	
Manus	Pacmanus	Big Papi	I	PM1	733	733_GBT3	-	
			A	PM11	733	733_GBT2	733_ASPI2	
		Fenway	A	PM10	733	733_GBT8	-	
			B	PM2	733	733_GBT5	-	
			I	PM3	733	733_GBT7	-	
			B	PM8	734	734_GBT1	734_ASPI5	
		Snow Cap	B	PM9	733	733_GBT1	733_ASPI1	
		Solwara 6	B	PM5	734	734_GBT2	734_ASPI6	
			I	PM7	734	734_GBT4	734_ASPI8	
		Solwara 7	I	PM6	734	734_GBT5	734_ASPI3	
		Solwara 8	A	PM12	733	733_GBT9	733_ASPI7	
			I	PM4	733	733_GBT11	733_ASPI6	
		Susu	North Su	B	SU1	736	736_GBT7	736_ASPI3
				A	SU11	736	736_GBT10	-
				I	SU2	736	736_GBT8	736_ASPI7
				B	SU3	736	736_GBT9	736_ASPI6
			South Su North	A	SU10	737	737_GBT7	-
				I	SU4	737	737_GBT4	737_ASPI4
B	SU7			737	737_GBT3	737_ASPI8		
South Su South	I		SU5	737	737_GBT8	737_ASPI2		
	B		SU6	737	737_GBT9	737_ASPI1		
	A		SU9	737	737_GBT10	-		
Suzette	A		SU12	736	736_GBT3	-		
	I		SU8	736	736_GBT4	736_ASPI2		
Woodlark	La Scala	La Scala	I	LS1	738	738_GBT9	738_ASPI1	
			A	LS2	738	738_GBT10	-	
			A	LS3	739	739_GBT10	-	

#### D.4 Numéros de plongée, de boîte et d'aspirateur pour chaque échantillon

Basin	Field	Site	Hab.	sample	Dive ID	Biobox number	Suction number		
North Fiji	Phoenix	Phoenix North	I	PH1	724	724_PBT6	724_ASPI6		
		Phoenix South	I	PH2	724	724_GBT1	724_ASPI4		
			B	PH3	724	724_GBT3	724_ASPI3		
			A	PH4	724	724_GBT4	724_ASPI1		
		Phoenix West	A	PH5	724	724_PBT4	724_ASPI7		
Futuna	Fatu Kapa	AsterX	I	FK1	727	727_GBT3	727_ASPI2		
			A	FK2	727	727_GBT2	727_ASPI1		
		Fati Ufu 1	A	FK6	728	728_GBT2	-		
			I	FK8	728	728_GBT4	728_ASPI1		
		Fati Ufu 15	I	FK5	728	728_GBT3	728_ASPI5		
		Stephanie	I	FK3	727	727_GBT5	-		
			A	FK4	727	727_GBT4	-		
		Kulo Lasi	Kulo Lasi	I	KL1	729	729_GBT2	729_ASPI4	
		Lau	ABE	ABE	I	AB1	731	731_GBT2	731_ASPI1
					B	AB2	731	731_GBT1	731_ASPI2
A	AB3				731	731_GBT3	731_ASPI3		
Mangatolo	Mangatolo North		I	MG1	726	726_GBT2	726_ASPI1		
			A	MG3	726	726_GBT4	726_ASPI2		
			Mangatolo South	I	MG2	726	726_PBT4	726_ASPI5	
				A	MG4	726	726_PBT6	726_ASPI6	
Tow Cam	Tow Cam North		I	TC1	721	721_GBT2	721_ASPI2		
			B	TC4	721	721_PBT3	721_ASPI6		
	Tow Cam South		B	TC2	721	721_GBT4	721_ASPI1		
			I	TC3	721	721_GBT5	-		
			A	TC5	721	721_GBT6	721_ASPI4/5		
			A	TC6	721	721_GBT1	721_ASPI3		
			B	TC7	730	730_GBT2/3	-		
Tui Malila	Tui Malila		B	TM1	722	722_GBT8	722_ASPI8		
			B	TM2	722	722_GBT2	722_ASPI1		
			I	TM3	722	722_GBT6	-		
			I	TM4	722	722_GBT3	-		
			A	TM5	722	722_GBT5	-		
		A	TM6	722	722_GBT1	722_ASPI2			



---

## Abstract

---

Hydrothermal environments are being targeted by mining industries for their mineral resources, rich in metals that include rare earth elements used in the construction of high-tech equipment. Although exploitation has not yet started, such activity could have significant impacts on ecosystems and their biodiversity. While we now have a good knowledge of the processes structuring hydrothermal biodiversity in continuous mid-ocean ridge systems, this information is still lacking in the fragmented back-arc systems of the western Pacific, primary target of mining companies. Understanding how biodiversity is structured and the processes involved is yet essential to assess communities' resilience to disturbances and thus inform relevant and efficient management and conservation measures. In this context, this PhD thesis aims at describing the distribution of biodiversity in the back-arc basins of the South West Pacific (i.e. the Manus and Woodlark Basins in the West and the North Fiji and Lau Basins and the Futuna Volcanic Arc in the East) at different spatial scales, and in relation with the physico-chemical characteristics of the habitat and species' life history traits. The macrofauna associated with three habitats characteristic of the active diffusion zones in this region was targeted: the *Alviniconcha* and *Ifremeria* gastropod aggregations and the *Bathymodiolus* mussel beds. First, the molecular barcoding of the mitochondrial gene *Cox1* has revealed the presence of several cryptic species in gastropods. Although reflecting the tectonic history of the basins, the observed phylogeographic patterns were highly variable between the studied gastropod taxa, suggesting that species may have evolved by selecting contrasting, even opposing, dispersal strategies. This diversity in strategies may have been favoured as a result of habitat fragmentation and instability. Second, the study of population structure and reproductive biology of two emblematic gastropod species in the study area (i.e. *Lepetodrilus schrolli* and *Shinkailepas tollmanni*) showed that both species have a continuous gametogenesis and recruitment, traits shared by many hydrothermal vent species. Environmental conditions did not influence recruitment or gametogenesis, suggesting that habitat heterogeneity does not impact these two demographic traits. Finally, faunal assemblages associated with the three targeted habitats were structured at different spatial scales: between habitats along the dilution gradient of the hydrothermal fluid, between fields in the same basin and between different basins.  $\beta$  diversity partitioning indicated that species replacement along the different gradients was the main mechanism responsible for these changes. Similarly, environmental conditions only explained a little amount of the observed variability. This may be a consequence of our limited ability to properly characterise environmental conditions at the organism level, the existence of micro-habitats or an important role of biotic relationships. The separation between the eastern and western basins was observed at different levels of biodiversity organisation: from genetic diversity within species to specific diversity of communities. The Woodlark Basin thus appears to be an area linking the eastern basins and the Manus Basin.

**Keywords :** Back-arc basins, *Bathymodiolus*, *Ifremeria*, community ecology, population biology, biodiversity.

---

## Résumé

---

Les environnements hydrothermaux sont ciblés par les industriels dans le but d'exploiter les métaux qui les composent, notamment des terres rares utilisées dans la fabrication de produits de haute technologie. Bien que l'exploitation de ces minerais n'ait pas encore commencée, une telle activité pourrait avoir des impacts considérables sur les écosystèmes hydrothermaux et leur biodiversité. Si les processus structurant la biodiversité hydrothermale commencent à être bien compris le long des systèmes continus de dorsales médio-océaniques, ils sont encore mal connus au sein des systèmes fragmentés que sont les bassins arrière-arc de l'ouest Pacifique, cible première des entreprises minières. Comprendre comment est structurée la biodiversité et les processus impliqués est pourtant indispensable pour évaluer le degré de résilience des communautés face à des perturbations et mettre en place des mesures adaptées et efficaces de gestion et de protection de ces écosystèmes. Dans ce contexte, cette thèse a pour objectif de décrire la distribution de la biodiversité des bassins arrière-arc du sud-ouest du Pacifique (i.e. les bassins de Manus et Woodlark à l'ouest et ceux de Nord-Fidji et de Lau et l'arc-volcanique de Futuna à l'est) à différentes échelles spatiales, et ses liens avec les caractéristiques chimiques de l'habitat et les traits d'histoire de vie des espèces. La macrofaune associée à trois habitats caractéristiques des zones de diffusion actives de la région a été ciblée : les agrégations de gastéropodes *Alviniconcha* et *Ifremeria* et les moulières à *Bathymodiolus*. Dans un premier temps, la mise en œuvre d'une approche de barcode moléculaire sur le gène mitochondrial *Cox1* a mis en évidence la présence de plusieurs espèces cryptiques chez les gastéropodes. Bien que reflétant l'histoire tectonique des bassins, les patrons phylogéographiques décrits variaient fortement entre les différents taxons de gastéropodes étudiés, suggérant que les espèces ont pu évoluer en sélectionnant des stratégies de dispersion contrastées, voire opposées. Cette diversité de stratégie a pu être favorisée par la fragmentation et l'instabilité de l'habitat. Dans un second temps, l'étude de la structure des populations et la biologie de la reproduction de deux espèces de gastéropodes emblématiques de la zone d'étude (i.e. *Lepetodrilus schrolli* et *Shinkailepas tollmanni*) a montré que celles-ci avaient une gamétogénèse et un recrutement continu, traits communs à de nombreuses espèces hydrothermales. Aucune influence des conditions environnementales sur le recrutement ou la gamétogénèse n'a pu être démontrée, suggérant que l'hétérogénéité des habitats n'impacte pas ces deux caractéristiques démographiques. Enfin, l'analyse des assemblages faunistiques associés aux trois habitats a révélé une structuration à différentes échelles spatiales : entre les habitats le long du gradient de dilution du fluide hydrothermal, entre les champs d'un même bassin et entre les différents bassins. Une partition de la diversité  $\beta$  montre que le principal mécanisme responsable de ces changements est un remplacement des espèces le long des différents gradients. Comme pour l'étude de la biologie des populations de *L. schrolli* et *S. tollmanni*, les conditions environnementales expliquent peu la variabilité observée. Cela peut être la conséquence de notre faible capacité à mesurer correctement les conditions environnementales à l'échelle des organismes, de l'existence de micro-habitats ou d'un rôle important des relations biotiques. La séparation entre les bassins de l'est et celui de Manus est observée à différents niveaux d'organisation de la biodiversité : de la diversité génétique au sein des espèces jusqu'à la diversité spécifique des communautés. Le bassin de Woodlark apparaît alors être une zone de connexion entre les bassins Est et le bassin de Manus.

**Mots clés :** Bassins arrière-arc, *Bathymodiolus*, *Ifremeria*, biodiversité, biologie des populations, écologie des communautés.